

**Pathogen defense mechanisms against *Verticillium longisporum* in *Brassica napus* L. – investigation on the role of sulfur-containing compounds**

Von der Naturwissenschaftlichen Fakultät der  
Gottfried Wilhelm Leibniz Universität Hannover

zur Erlangung des Grades  
Doktorin der Naturwissenschaften (Dr. rer. nat.)

genehmigte Dissertation

von

Sofia Isabell Rupp, Diplom-Biologin

2020

Referentin: Prof. Dr. rer. nat. Jutta Papenbrock

Korreferent: Prof. Dr. rer. hort. Edgar Maiß

Tag der Promotion: 04.06.2020

*für Hasi Carrell & meine Familie*



## Content

## Content

<b>Summary</b> .....	<b>I</b>
<b>Zusammenfassung</b> .....	<b>II</b>
<b>Abbreviations</b> .....	<b>III</b>
<b>1. Introduction</b> .....	<b>1</b>
<b>1.1 Crop plants and their threat from fungal pathogens</b> .....	<b>1</b>
<b>1.2 Sulfur in nature and the meaning of sulfur fertilization to strengthen the plant against pathogenic infestation</b> .....	<b>3</b>
1.2.1 Biogeochemical cycle of sulfur in nature .....	3
1.2.2 Transport and metabolism of sulfur: from root to shoot .....	3
1.2.3 Sulfur fertilization – long story short of “Sulfur-Induced Resistance” or “Sulfur-Enhanced Resistance” .....	6
<b>1.3 The Brassicaceae: a family with many important crop plants</b> .....	<b>6</b>
1.3.1 The important crop plant <i>Brassica napus</i> .....	7
1.3.2 Evolutionary history and origin of <i>B. napus</i> .....	9
<b>1.4 The plant root as battleground for fungal pathogens</b> .....	<b>10</b>
1.4.1 The vascular system of plants.....	10
1.4.2 The xylem as a niche for vascular wilt pathogens .....	11
1.4.3 The genus <i>Verticillium</i> ssp. ....	12
1.4.4 <i>Verticillium longisporum</i> : the causal agent of <i>Verticillium</i> stem striping .....	12
1.4.5 Evolutionary history and origin: hybridization with fatal consequences .....	15
<b>1.5 Plant defense mechanisms – when plants make a counterattack</b> .....	<b>18</b>
1.5.1 Sulfur-containing defense compounds – SDCs.....	18
<i>Glucosinolates: the mustard oil bombs</i> .....	20
<i>Glutathione: a versatile protector</i> .....	22
<i>Hydrogen sulfide: a foul-smelling affair with benefits</i> .....	23
1.5.2 The second line of defense – the pathogen-induced mechanisms ....	24
<b>1.6 Through time and defense – does timing matter?</b> .....	<b>28</b>
1.6.1 Tick-tock: circadian clocks and diurnal rhythms of plants .....	28
<b>1.7 Aims of the thesis</b> .....	<b>32</b>
<b>2. Material and methods</b> .....	<b>33</b>
<b>2.1 Plant material</b> .....	<b>33</b>
2.1.1 Plant seed surface sterilisation .....	33
2.1.2 Blake-Kalff medium.....	34
2.1.3 Cultivation of <i>Brassica napus</i> in climatic chambers.....	35
<b>2.2 <i>Verticillium longisporum</i> strain</b> .....	<b>35</b>
2.2.1 <i>Verticillium longisporum</i> growth and cultivation.....	35
2.2.2 Preparation of <i>Verticillium longisporum</i> spore stock solutions.....	36

## Content

<b>2.3</b>	<b>Various inoculation procedures of <i>Brassica napus</i> with <i>Verticillium longisporum</i> .....</b>	<b>36</b>
2.3.1	Inoculation of 16 d old <i>B. napus</i> plants (previous fertilization with different sulfur supply) with mycelium-spore mixture of <i>V. longisporum</i> .....	36
2.3.2	Inoculation of 16 d old <i>B. napus</i> plants (previous fertilization with different sulfur supply) with different dilutions of mycelium-spore mixture of <i>V. longisporum</i> .....	37
2.3.3	Inoculation of 7 d old <i>B. napus</i> seedlings with mycelium-spore mixture of <i>V. longisporum</i> .....	37
2.3.4	Inoculation of 7 d old <i>B. napus</i> seedlings with spore solution of <i>V. longisporum</i> .....	37
<b>2.4</b>	<b>General experimental design: the definition of different time-points of inoculation (TPIs).....</b>	<b>38</b>
<b>2.5</b>	<b>Preliminary inoculation experiments of <i>Brassica napus</i> with <i>Verticillium longisporum</i> under diurnal rhythmic and with different sulfur supply ....</b>	<b>39</b>
2.5.1	Preliminary experiment I: inoculation of 7 d old plants with mycelium-spore mixture and subsequent cultivation in sand/soil mixture .....	39
2.5.2	Pre-experiment II: inoculation of 16 d old plants (previous fertilization with different sulfur supply) with mycelium-spore mixture and subsequent cultivation in sand .....	41
2.5.3	Pre-experiment IIIa: inoculation of 16 d old plants (previous fertilization with different sulfur supply) with different dilutions of mycelium-spore mixtures and subsequent cultivation in sand.....	43
2.5.4	Pre-experiment IIIb: inoculation of 16 d old plants (previous fertilization with different sulfur supply) with diluted mycelium-spore mixture and subsequent cultivation in sand .....	44
2.5.5	Pre-experiment IV: inoculation of 7 d old plants with spore solution and subsequent cultivation in sand .....	45
<b>2.6</b>	<b>Main experiment: inoculation of <i>Brassica napus</i> with <i>Verticillium longisporum</i> under diurnal rhythmic and with different sulfur supply....</b>	<b>45</b>
2.6.1	Experimental design: different time-points of inoculation of 7 d old plants with mycelium-spore mixture and different sulfur supply .....	45
<b>2.7</b>	<b>Analytical methods .....</b>	<b>47</b>
2.7.1	DNA-extraction .....	47
2.7.2	Real-time quantitative PCR.....	47
2.7.3	Elemental analysis via ICP-OES.....	49
2.7.4	Glucosinolate analysis via HPLC .....	51
2.7.5	Thiol (cysteine and glutathione) analysis via HPLC.....	54
2.7.6	Histology: Staining of the plant hypocotyl with toluidine blue.....	55
2.7.7	Histology: Staining of fungal mycelium with cotton blue .....	57
<b>2.8</b>	<b>Statistical analysis .....</b>	<b>58</b>
<b>2.9</b>	<b>Necessary additional notes to the used climatic chambers, biological replicates and amount of plant material .....</b>	<b>59</b>
2.9.1	Climatic chambers from Johnson Controls.....	59
2.9.2	Biological replicates and amount of plant material .....	59

## Content

<b>3.</b>	<b>Results .....</b>	<b>61</b>
<b>3.1</b>	<b>Pre-experiment I: inoculation of 7 d old plants with mycelium-spore mixture and subsequent cultivation in sand/soil mixture.....</b>	<b>61</b>
3.1.1	Detection and verification of the infection with <i>V. longisporum</i> in mycelium-spore inoculated <i>B. napus</i> plants potted in sand/soil.....	61
3.1.2	The occurrence of occlusions in the xylem of mycelium-spore inoculated plants potted in sand/soil.....	62
3.1.3	Elemental analysis: levels of sulfur, calcium, potassium and iron in mock- and mycelium-spore inoculated plants potted in sand/soil .....	66
3.1.4	The content of indolic, aliphatic and benzylic glucosinolates in mock- and mycelium-spore inoculated plants potted in sand/soil.....	70
<b>3.2</b>	<b>Pre-experiment II: inoculation of 16 d old plants (previous fertilization with different sulfur supply) with mycelium-spore mixture and subsequent cultivation in sand .....</b>	<b>79</b>
3.2.1	Detection and verification of the infection with <i>V. longisporum</i> in mycelium-spore inoculated <i>B. napus</i> plants potted in sand .....	79
3.2.2	Elemental analysis: levels of sulfur, calcium, potassium and iron in mock- and mycelium-spore inoculated plants potted in sand .....	80
<b>3.3</b>	<b>Pre-experiment IIIa: inoculation of 16 d old plants (previous fertilization with different sulfur supply) with different dilutions of mycelium-spore mixtures and subsequent cultivation in sand .....</b>	<b>85</b>
3.3.1	Detection and verification of the infection with <i>V. longisporum</i> in different dilutions of mycelium-spore mixture inoculated <i>B. napus</i> plants potted in sand.....	85
<b>3.4</b>	<b>Pre-experiment IIIb: inoculation of 16 d old plants (previous fertilization with different sulfur supply) with diluted mycelium-spore mixture and subsequent cultivation in sand .....</b>	<b>87</b>
3.4.1	Detection and verification of the infection with <i>V. longisporum</i> in 1:10 dilution of mycelium-spore mixture inoculated <i>B. napus</i> plants potted in sand.....	87
<b>3.5</b>	<b>Pre-experiment IV: inoculation of 7 d old plants with spore solution and subsequent cultivation in sand .....</b>	<b>90</b>
3.5.1	Detection and verification of the infection with <i>V. longisporum</i> in spore solution inoculated <i>B. napus</i> plants potted in sand.....	90
<b>3.6</b>	<b>Selection of the experimental design .....</b>	<b>92</b>
<b>3.7</b>	<b>Results of the main experiment: inoculation of <i>Brassica napus</i> with <i>Verticillium longisporum</i> under diurnal rhythmic and with different sulfur supply.....</b>	<b>95</b>
3.7.1	First run: detection and verification of the infection with <i>V. longisporum</i> in <i>B. napus</i> .....	95
3.7.2	First run: stunting of <i>B. napus</i> plants infected with the <i>V. longisporum</i> strain VL43 under artificial inoculation.....	97
3.7.3	First run: the influence of different TPIs and different sulfur supply on the occurrence of occlusions in the xylem of <i>B. napus</i> infected with <i>V. longisporum</i> strain VL43 .....	100
3.7.4	First run: levels of sulfur, calcium, potassium and iron at different TPIs in mock- and mycelium-spore inoculated plants under different sulfur supply .....	102

## Content

3.7.5	First run: levels of indolic, aliphatic and benzylic GSLs in mock- and mycelium-spore inoculated plants at different TPIs under different sulfur supply .....	105
3.7.6	First run: levels of cysteine and glutathione in mock- and mycelium-spore inoculated plants at different TPIs under different sulfur supply .....	112
3.7.7	Second run: detection and verification of the infection with <i>V. longisporum</i> in <i>B. napus</i> .....	113
3.7.8	Second run: stunting of <i>B. napus</i> plants infected with the <i>V. longisporum</i> strain VL43 under artificial inoculation.....	116
3.7.9	Second run: the influence of different TPIs and different sulfur supply on the occurrence of occlusions in the xylem of <i>B. napus</i> infected with <i>V. longisporum</i> strain VL43 .....	119
3.7.10	Second run: levels of sulfur, calcium, potassium and iron at different TPIs in mock- and mycelium-spore inoculated plants under different sulfur supply.....	121
3.7.11	Second run: levels of indolic, aliphatic and benzylic GSLs in mock- and mycelium-spore inoculated plants at different TPIs under different sulfur supply .....	124
3.7.12	Second run: levels of cysteine and glutathione in mock- and mycelium-spore inoculated plants at different TPIs under different sulfur supply .....	131
<b>4.</b>	<b>Discussion .....</b>	<b>133</b>
<b>4.1</b>	<b>Thick as thieves - the many faces of sulfur in fungal pathogen defense mechanisms .....</b>	<b>135</b>
4.1.1	An important supporting role - glucosinolates as sulfur-containing defense compounds.....	136
4.1.2	Onlookers or main actors? - The role of cysteine and glutathione ...	140
<b>4.2</b>	<b>Highway of plant response - influence of fungal infection on nutrient element content of <i>B. napus</i> .....</b>	<b>141</b>
<b>4.3</b>	<b>Don't mess with <i>B. napus</i>: occlusions as a mechanical barrier against the spread of <i>V. longisporum</i>.....</b>	<b>142</b>
<b>4.4</b>	<b>Time to kill - importance of diurnal rhythmic in the defense against <i>V. longisporum</i>.....</b>	<b>144</b>
<b>4.5</b>	<b>Inoculation system with mycelium-spore mixture - creation of ballpark figures? .....</b>	<b>151</b>
<b>4.6</b>	<b>Conclusion and outlook.....</b>	<b>151</b>
4.6.1	What lies beneath? - A critical conclusion .....	151
4.6.2	Out and look - an outlook.....	152
<b>5.</b>	<b>References .....</b>	<b>154</b>
<b>6.</b>	<b>Appendix .....</b>	<b>194</b>
	<b>Danksagung .....</b>	<b>213</b>
	<b>Lebenslauf.....</b>	<b>215</b>



## Summary

Reduction in atmospheric sulfur deposition and the use of low-sulfur fertilizers in an intensified agriculture have led to a widespread nutrient disturbance in the crop production. Sulfur deficiency was observed and in parallel a higher susceptibility to biotic stresses. Sulfur-enhanced defense compounds were postulated. Recently, the spread of fungal pathogens such as *Verticillium longisporum*, a soil borne pathogenic fungus was observed resulting in high yield losses in the plant family Brassicaceae. This pathogen preferably infects the high sulfur-demanding crop species *Brassica napus* L. by entering through the roots and spreading via the xylem. Defense response of plants are linked to sulfur-containing compounds including glucosinolates (GSLs), whereby abiotic and biotic stress factors can cause increased synthesis rates. A number of biological processes such as innate immunity in plants are under circadian control. Therefore, pathogens seem to carry out their attacks at specific time periods during the day.

In this thesis a possible influence of sufficient and deficient sulfur fertilization of *B. napus* plants on the course of infection with *V. longisporum* is investigated. Besides, the susceptibility of the host plant to the fungal pathogen, which may be dependent on the time of infection was examined. For this purpose, the plants were infected at different time points. When a successful infection was detected by using qPCR, subsequent analyses were focused on GSLs, cysteine, glutathione and elemental nutrients. Higher levels of *V. longisporum*-DNA were found in plants infected one hour before sunset and at early night indicating a higher susceptibility. Increased amounts of the benzylic GSL gluconasturtiin were observed in infected plants whereby severely infected plants displayed higher levels regardless of sulfur supply in comparison with the corresponding control plants. Higher contents of indolic and aliphatic GSLs were also found in infected plants. Based on the ability of plants to form mechanical barriers in the xylem for the purpose to protect themselves from further invasion of pathogens, histological cross sections of hypocotyls were prepared. It was observed that the occurrence of occlusions may be influenced by the time of infection, but not by the different sulfur levels. In order to draw final conclusions regarding the interaction of sulfur-containing compounds and the time of infection, it is necessary to perform additional analyses of the circadian clock genes involved.

**Keywords:** *Brassica napus*, *Verticillium longisporum*, sulfur, sulfur-containing compounds, glucosinolates, gluconasturtiin, defense, diurnal, hypocotyl, xylem, occlusions

## Zusammenfassung

Die Verringerung der Schwefelablagerung in der Atmosphäre und die Verwendung von schwefelarmen Düngemitteln in einer intensivierten Landwirtschaft haben zu einem weit verbreiteten Defizit an Nährstoffen in Kulturpflanzen geführt. Es wurden Schwefelmangel und eine gleichzeitig höhere Anfälligkeit gegenüber biotischem Stress beobachtet. Eine durch Schwefel gesteigerte Abwehrfähigkeit wurde postuliert. Kürzlich wurde die Ausbreitung von Pilzpathogenen, wie dem im Boden lebenden Pilz *Verticillium longisporum*, beobachtet, der zu hohen Ertragsverlusten bei der Kultivierung von Nutzpflanzen aus der Familie der Brassicaceae führt. Dieser Erreger infiziert vorzugsweise die auf höhere Schwefelmengen angewiesene Kulturpflanze *Brassica napus* L., indem er durch die Wurzeln eindringt und sich über das Xylem ausbreitet. Die Abwehrreaktion von Pflanzen ist mit schwefelhaltigen Verbindungen, einschließlich Glucosinolaten (GSLs), korreliert, wobei abiotische und biotische Stressfaktoren zu erhöhten Syntheseraten führen können. Eine Reihe von biologischen Prozessen, wie die angeborene Immunität in Pflanzen, steht unter circadianer Kontrolle. Daher scheinen Pathogene ihre Angriffe zu bestimmten Zeitpunkten während des Tages durchzuführen.

In dieser Arbeit wird ein möglicher Einfluss von ausreichender und mangelhafter Schwefeldüngung auf den Infektionsverlauf von *V. longisporum* in *B. napus* untersucht. Zudem wurde die Anfälligkeit der Wirtspflanze gegenüber dem Pilz untersucht, die vom Infektionszeitpunkt abhängen kann. Zu diesem Zweck wurden die Pflanzen zu verschiedenen Zeitpunkten infiziert. Wenn eine erfolgreiche Infektion mittels qPCR festgestellt wurde, konzentrierten sich die nachfolgenden Analysen auf GSLs, Cystein, Glutathion und elementare Nährstoffe. Höhere Konzentrationen von *V. longisporum*-DNA wurden in Pflanzen gefunden, die eine Stunde vor Sonnenuntergang und in der frühen Nacht infiziert wurden, was auf eine höhere Anfälligkeit hinweist. In infizierten Pflanzen wurden erhöhte Mengen von dem benzylichen GSL Gluconasturtiin beobachtet, wobei stark infizierte Pflanzen im Vergleich zu den entsprechenden Kontrollpflanzen, unabhängig von der Schwefelversorgung, höhere Gehalte aufwiesen. Ebenfalls wurden höhere Mengen an indolischen und aliphatischen GSLs in infizierten Pflanzen gefunden. Basierend auf der Fähigkeit von Pflanzen, mechanische Barrieren im Xylem zu bilden, um sich vor einem weiteren Eindringen von Pathogenen zu schützen, wurden vom Hypokotyl histologische Querschnitte angefertigt. Es wurde beobachtet, dass das Auftreten von Verstopfungen durch den Zeitpunkt der Infektion beeinflusst werden kann, jedoch nicht durch die unterschiedlichen Schwefelgaben. Um endgültige Rückschlüsse auf die Wechselwirkung zwischen schwefelhaltigen Verbindungen und dem Infektionszeitpunkt ziehen zu können, müssen zusätzliche Analysen der beteiligten circadianen Uhr-Gene durchgeführt werden.

**Schlüsselwörter:** *Brassica napus*, *Verticillium longisporum*, Schwefel, schwefelhaltige Verbindungen, Glucosinolate, Gluconasturtiin, Abwehr, diurnal, Hypokotyl, Xylem, Verstopfungen

## Abbreviations

AGSL	aliphatic glucosinolate
APK	adenosine 5'-phosphosulfate kinase
APR	adenosine 5'-phosphosulfate reductase
APS	adenosine 5'-phosphosulfate
<i>A. thaliana</i>	<i>Arabidopsis thaliana</i>
ATPS	adenosine triphosphate sulfurylase
BGSL	benzylic glucosinolate
BK	Blake-Kalff
<i>B. napus</i>	<i>Brassica napus</i>
bp	base pair
Ca	calcium
CCA1	CIRCADIAN CLOCK ASSOCIATED 1
CDB	Czapek-Dox broth
°C	degree Celsius
d	day
dpi	day post-inoculation
DW	dry weight
ETI	effector-triggered immunity
EtOH	ethanol
ETS	effector-triggered susceptibility
Fe	iron
Fig.	figure
FW	fresh weight
GSL	glucosinolate
g	gram
GSH	glutathione
h	hour
H <sub>2</sub> O <sub>2</sub>	hydrogen peroxide
HPLC	high performance liquid chromatography
HR	hypersensitive reaction
H <sub>2</sub> S	hydrogen sulfide
ICP-OES	inductively coupled plasma optical emission spectrometry
IGSL	indolic glucosinolate
ITS	internal transcribed spacer
JA	jasmonic acid
K	potassium
LHY	LATE ELONGATED HYPOCOTY

## Abbreviations

LRR	leucine rich repeat
mg	milligram
min	minute
mL	millilitre
mM	millimole
MAMP	microbe-associated molecular pattern
N	nitrogen
NB	nucleotide binding
NB-LRR	nucleotide-binding-leucine-rich repeat receptor
ng	nanogram
nmol	nanomole
NPR1	natriuretic peptide receptor 1
OAS	O-acetylserine
OASTL	O-acetylserine (thiol) lyase
OSR	oilseed rape
P	phosphorus
PAMP	pathogen-associated molecular pattern
PAPS	3'-phosphoadenosine 5'-phosphosulfate
PCD	programmed cell death
PDB	potato dextrose broth
PRR	transmembrane-pattern recognition receptor
PTI	pathogen-associated molecular pattern-triggered immunity
qPCR	real-time quantitative polymerase chain reaction
ROS	reactive oxygen species
RNS	reactive nitrogen species
RT	room temperature
S	sulfur
S <sup>0</sup>	elemental sulfur
S <sup>2-</sup>	sulfide
SA	salicylic acid
SAR	systemic acquired resistance
SAT	serine acetyltransferase
SD	standard deviation
SDC	sulfur-containing defense compounds
sec	second
SED	sulfur-enhanced defense
SiR	sulfite reductase
SIR	sulfur-induced resistance

## Abbreviations

SO <sub>3</sub> <sup>2-</sup>	sulfite
SO <sub>4</sub> <sup>2-</sup>	sulfate
SOT	sulfotransferase
SRP	sulfur-rich protein
SULTR	sulfate transporter
+S	sufficient sulfur supply
-S	deficient sulfur supply
TOC1	TIMING OF CAB 1
TPI	time-point of inoculation
<i>V. albo-atrum</i>	<i>Verticillium albo-atrum</i>
<i>V. dahliae</i>	<i>Verticillium dahliae</i>
<i>V. longisporum</i>	<i>Verticillium longisporum</i>
VL	<i>Verticillium longisporum</i>
VL43	<i>Verticillium longisporum</i> strain 43
v/v	volume per volume
w/v	weight per volume
µg	microgram
µl	microlitre
µm	micrometre
µM	micromole

# 1. Introduction

## 1.1 Crop plants and their threat from fungal pathogens

Agricultural crops provide food, feed for livestock, oil, biodiesel and other important raw materials for human consumption and use. Already at the beginning of agriculture about 10,000 years ago, a number of pests threatened the crop plants production. These harmful organisms are mainly insects, nematodes, snails, weeds and specific plant pathogens such as viruses, bacteria and fungi. **Figure 1.1** shows biotic and abiotic factors responsible for crop losses. It is estimated that since the 21st century the group of plant pathogens are responsible for 16% (related to tonnage production) of annual crop failure. The pathogenic fungi play with a participation of 70-80% the biggest role in this group. Furthermore, animal pests are to be mentioned with 18% and weeds with 36% participation in crop failures. Abiotic factors are responsible for 32% (Oerke, 2006).

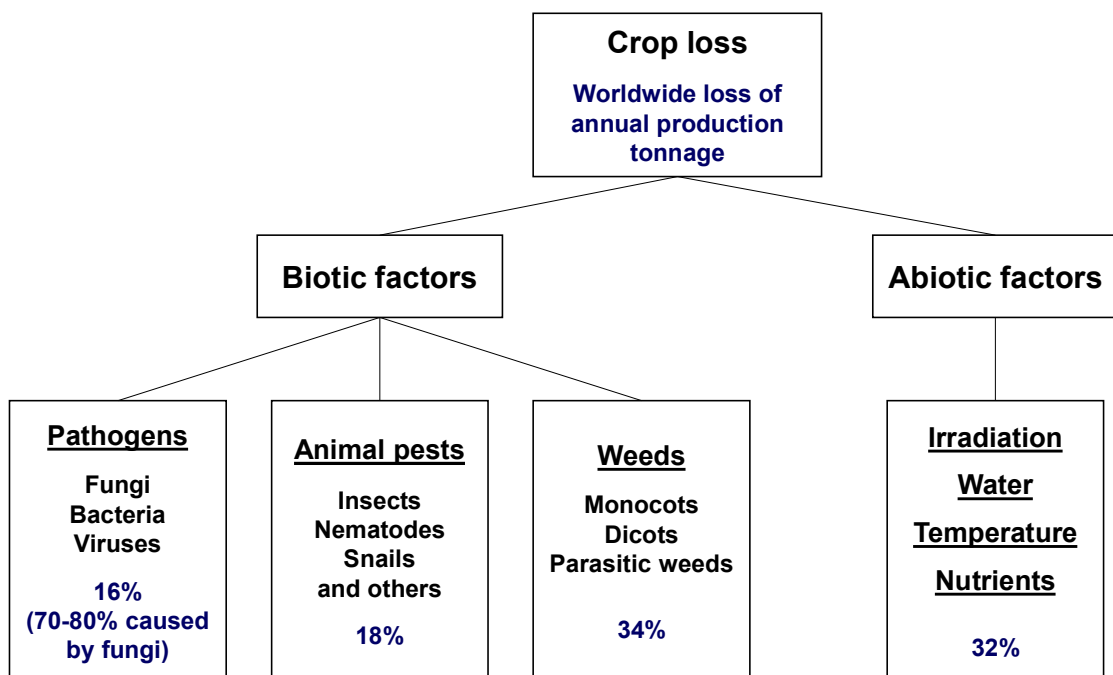


**Figure 1.1: Crop loss factors and estimated worldwide loss of annual production tonnage (%) since the beginning of the 21st century.** Biotic factors: pathogens cause 16% crop loss, with fungi accounting for 70-80% of it; animal pests cause 18% and weeds 34% crop loss; abiotic factors cause 32% crop loss. Data from Oerke (2006).

Human history is riddled with numerous crop damage due to biotic factors, for instance, the potato blight caused by *Phytophthora infestans* in Ireland (1845 to 1849) (Gray, 1995), maize leaf blight caused by *Cochliobolus heterostrophus* in the United States (1970) (Tatum, 1971) and the coffee rust caused by *Hemileia vastatrix* in Brazil (1970)

## Introduction

(Schieber, 1975). These are just some of the worst crop plants catastrophes of the past, which shut down food production, cost millions of human lives and led to migration to other countries. And all of them were triggered by fungal pathogens. However, new challenges have emerged in the world of today: global warming and over-exploitation of arable land are factors that may favor the spread of certain plant pathogens or even contribute to the emergence of new plant pathogens (Baker *et al.*, 2000; Etterson and Shaw, 2001; Jahn *et al.*, 2001; Sanghera *et al.*, 2011; Juroszek and von Tiedemann, 2013). Furthermore global warming will influence the growth and development of both crops and pathogens (Siebold and von Tiedemann, 2013). In addition, symptoms and susceptibility of host plants may increase due to increasing humidity and temperature (McElrone *et al.*, 2003). In the last 15 years, the number of identified fungal plant pathogens has more than quadrupled (Fisher *et al.*, 2012). However, this is not only due to better detection methods (compared to no comparable increase in animal pathogens), but rather seems to be a direct result of crop cultivation and landscape management practices (Meena *et al.*, 2016). These are mainly characterized by a close genetic diversity, large monocultures with low or no crop rotation. Due to this continuous cultivation of fields, and the development of new crop hybrid species, it is possible that unknown or even host-specific plant pathogens such as *Verticillium longisporum* occur (Depotter *et al.*, 2016; Singh *et al.*, 2010).

Another challenge is, that sulfur (S) deficiencies in the soil are now more common than ever. In many areas of the world sulfur deficiency of the soils has been observed and sulfur fertilization is needed to optimize crop yield (Tisdale *et al.*, 1986). Since the beginning of the 1980s higher air quality standards have lowered sulfur emissions and reduced environmentally available sulfur (Dämmgen and Grünhage, 1998; Schnug and Haneklaus, 1994; Schnug and Pissarek, 1982). The influence of sulfurous air pollution on plants is a paradox: on one hand, consistently high levels of sulfur dioxide and hydrogen sulfide (H<sub>2</sub>S) can have a negative effect on plant growth, leading to severe, visible damage in the worst case scenario (Godzik and Krupa, 1982; De Kok *et al.*, 1991). On the other hand, sulfur-containing air pollution can even be very beneficial to the plant and serve as a sulfur source, especially if the growing site is deficient in sulfur (Ernst, 1990; De Kok, 1990). Increased crop yields draw a greater amount of sulfur out of the soil (Schnug, 1991). Greater use of relatively sulfur-free nitrogen and phosphorus fertilizers have reduced sulfur replacement (Syers *et al.*, 1987; Ceccotti *et al.*, 1998; Salvagiotti *et al.*, 2009). The awareness of sulfur deficiency is increasing, mainly due to the fact that many areas of the world, which were previously sufficiently supplied with sulfur, now also indicate a lack of sulfur in the soil (Ahmad *et al.*, 2005; Mansoori, 2012).

## Introduction

Regardless of all these challenges, fact is, that crop production is threatened by various plant pathogens and finding solutions is more important than ever.

### **1.2 Sulfur in nature and the meaning of sulfur fertilization to strengthen the plant against pathogenic infestation**

#### **1.2.1 Biogeochemical cycle of sulfur in nature**

Sulfur is an essential nutrient (Woodard, 1922) and inorganic phytoalexin (Williams and Cooper, 2003) for plants. It is the fourth major plant nutrient after nitrogen (N), phosphorus (P) and potassium (K) (Namvar and Khandan, 2015). The plants need sulfur for the synthesis of amino acids, to build up primary and secondary metabolites and it plays a key role in many enzyme activated systems (Namvar and Khandan, 2015). It is found in cell walls (Popper *et al.*, 2011) and membrane sulfolipids (Benning, 1998). Sulfur exists in many different chemical forms in nature (atmospheric, elemental and organic sulfur), but plants taken up sulfur as a primary source only through their root systems in the inorganic sulfate ( $\text{SO}_4^{2-}$ ) form (Eriksen *et al.*, 1998). The distinguished amount of sulfate take up by the root system is reduced to sulfide ( $\text{S}^{2-}$ ). The reduction is performed by the chloroplasts of the shoots, and subsequently the sulfide is incorporated into cysteine, which is the precursor or sulfur donor for the synthesis of other sulfur-containing compounds (Hell, 1997; Saito, 2004). The reduction of sulfate to sulfide is an assimilative process, which needs energy. The organic sulfur, depends on plants and animal residues, can be degraded by a variety of microorganisms. They regenerated it to inorganic sulfate to close the sulfur cycle (Takahashi *et al.*, 2011). But not only between microorganisms and plants exists a sulfur cycle, also in the atmosphere circulates sulfur. Globally the sulfur in soil, water and atmosphere, is supplied in form of minerals and volatiles to the sulfur cycle, and metabolized by living organisms in assimilated or dissimilated metabolic pathways (Leustek *et al.*, 2000; Norici *et al.*, 2005; Saito, 2004).

#### **1.2.2 Transport and metabolism of sulfur: from root to shoot**

As already mentioned, inorganic sulfur is the main source of sulfur for plants. However, plants are also able to use reduced sulfur from the atmosphere, such as sulfur dioxide or hydrogen sulfide ( $\text{H}_2\text{S}$ ) (Leustek *et al.*, 2000). Sulfate is taken up and distributed by means of sulfate transporter (SULTR), which are located in cells of the root (**Fig. 1.2**). For the different tasks and claims the plant has different sulfate transporters (Buchner *et al.*, 2004). In *Arabidopsis* 14 genes have been found responsible for the expression of sulfate transporters. Based on sequence similarity and function within the sulfate



## Introduction

transport, they are divided into five groups (Smith *et al.*, 1995). By investigating *Arabidopsis* mutants, two high-affinity sulfate transporters, that belong to group one (SULTR1;1 and SULTR1;2) have been identified responsible for the uptake of sulfate from soil into the root cells. They also show this performance exceedingly under sulfur deficient conditions (Yoshimoto *et al.*, 2007; Barberon *et al.*, 2008). These two transporters are mainly expressed in root hairs, in root epidermis and in cortical cells (Shibagaki *et al.*, 2002; Yoshimoto *et al.*, 2002). Unlike group one high-affinity transporters, the low-affinity transporters belonging to group two are responsible for the translocation of sulfate within the plant. These sulfate transporters are located in the parenchyma of the xylem and in phloem cells of the roots and leaves (Takahashi *et al.*, 2000). In the inside of plant membranes dominates a negative gradient potential. The influx of sulfate must be performed against this negative potential with help of plasma membrane-bound transport proteins. The primary system, that plants use to mediate sulfate influx, are proton/sulfate cotransporter (Lass and Ullrich-Eberius, 1984; Smith *et al.*, 1995). This system uses a proton gradient as a driving force, which runs along the cell membranes. When it comes to sulfur-limited conditions, the kinetic phase with a low  $K_M$  value becomes active (Clarkson *et al.*, 1983). Just as important as the influx of sulfate is the efflux of sulfate into plant organs. The sulfate can probably be released by a passive mechanism. This may be based on the outside-positive gradient of the membrane potentials (Leustek and Saito, 1999). **Figure 1.2** shows a simplified schema about sulfur assimilation in the different cell compartments. Prior to reduction of sulfate, it is activated by adenylation to adenosine 5'-phosphosulfate (**APS**), catalyzed by ATP sulfurylase (**ATPS**) (Logan *et al.*, 1996). The reduction from APS to sulfite ( $\text{SO}_3^{2-}$ ) is catalyzed by the key enzyme APS reductase (**APR**), sulfite are then further reduced by the sulfite reductase (**SiR**) to sulfide, taking place in plant plastids. Subsequent sulfide is incorporated into O-acetylserine (**OAS**) to generate cysteine (Bonner *et al.*, 2005; Rennenberg, 1983). O-acetylserine is formed from serine and acetyl coenzyme A, this reaction being carried out by serine acetyltransferase (**SAT**). The synthesis of cysteine is catalyzed by OAS (thiol) lyase (**OASTL**) (Leustek *et al.*, 2000), where OASTL forms a multi-enzyme complex with SAT (Hell *et al.*, 2002). Adenosine 5'-phosphosulfate can also be phosphorylated to 3'-phosphoadenosine 5'-phosphosulfate (**PAPS**), whereby the enzyme APS kinase (**APK**) is involved. Cysteine, which is synthesized in plastids, mitochondria and cytosol (Leustek and Saito, 1999) can be directly incorporated into, for example, glutathione (Meister, 1988).

## Introduction

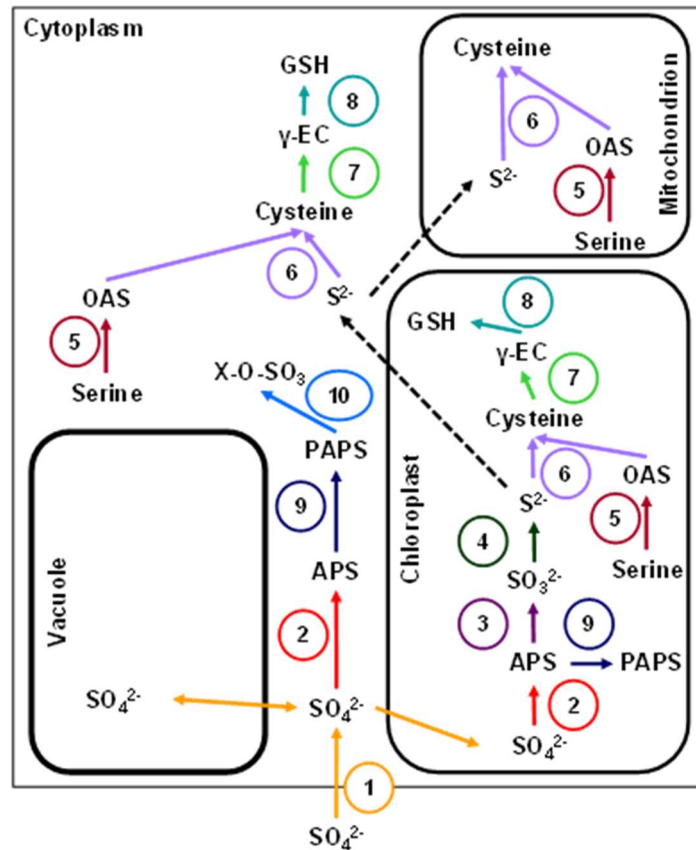


**Figure 1.2: Simplified schema of plant sulfur assimilation.** Shown is the sulfate ( $\text{SO}_4^{2-}$ ) transport from the soil into the root to the shoot, and the distribution in the different compartments (chloroplast, vacuole, cytoplasm, and mitochondrion). The uptake of  $\text{SO}_4^{2-}$  is performed by the  $\text{SO}_4^{2-}$  transporters into the cytoplasm. A part of the  $\text{SO}_4^{2-}$  can be released into the chloroplasts and vacuoles, whereby the  $\text{SO}_4^{2-}$  can be transported back out of the vacuoles. Abbreviations: **APS**: adenosine 5'-phosphosulfate; **PAPS**: 3'-phosphoadenosine 5'-phosphosulfate; **SO<sub>3</sub><sup>2-</sup>**: sulfite; **S<sup>2-</sup>**: sulfide; **OAS**: O-acetylserine; **γ-EC**: γ-glutamylcysteine; **GSH**, glutathione; **X-O-SO<sub>3</sub>**: variety of active sulfur-containing compounds such as glucosionlates; numbers represent enzymes: **1, SULTR**: sulfate transporter; **2, ATPS**: ATP sulfurylase; **3, APR**: APS reductase; **4, SiR**: sulfite reductase; **5, SAT**: serine acetyltransferase; **6, OASTL**: OAS thiollase; **7, γ-ECS**: γ-EC synthetase; **8, GSHS**: glutathione synthetase; **9, APK**: APS kinase; **10, SOT**: sulfotransferase. Adapted from Kopriva (2006).

Glutathione is one of the most abundant low-molecular-weight thiols and the major source of non-protein thiols (Bergmann, 1993), which can perform a variety of functions (Foyer and Noctor, 2001). These tasks include functions in the defense against plant stress, for redox regulation and for the storage and transport of sulfur (Rennenberg and Brunold, 1994; Veljovic-Jovanovic and Foyer, 2000).

## Introduction

### 1.2.3 Sulfur fertilization – long story short of “Sulfur-Induced Resistance” or “Sulfur-Enhanced Resistance”

In the late 1980s, it became apparent that sulfur plays an essential role in crop resistance against pathogens, as the reduction of atmospheric sulfur depositions has led to a widespread nutrient disturbance in European agriculture (Richards, 1990; Booth and Walker, 1992; Kjellquist and Gruvaeus, 1995; Pedersen *et al.*, 1998). In addition, the rate of infection of crop plants with certain pathogens increased and the problem of sulfur deficiency became more and more obvious (Schnug and Ceynowa, 1990; Bloem *et al.*, 2005). In the 1990's, the concept of increased plant resistance or tolerance to fungal pathogens based on sulfur was developed (Schnug *et al.*, 1995). Schnug *et al.* (1995) also has coined the term “Sulfur-Induced Resistance” (**SIR**), which describes the enhancement of natural plant resistance to fungal pathogens by stimulating metabolic processes through targeted sulfur-based and soil-applied fertilizer strategies. As long ago as 1802, William Forsyth (Forsyth, 1810) discovered the fungicidal impact of leaf-applied elemental sulfur ( $S^0$ ). Until the development of organic fungicides, elemental sulfur was used as a major fungicide and known as mankind's oldest fungicide. Further examples of the fungicidal impact of elemental sulfur have been found in *Theobroma cacao* (cacao tree) and *Lycopersicon esculentum* (tomato) in response to the phytopathogenic fungi *Verticillium dahliae*. Both crops accumulated elemental sulfur in the xylem of resistant genotypes to prevent the further spread of the fungi, whereas in susceptible genotypes this phenomenon could not be observed (Cooper *et al.*, 1996; Resende *et al.*, 1996; Williams *et al.*, 2002). However, a clear distinction must be made between leaf-applied elemental sulfur and soil-applied sulfur, which is accompanied by health-beneficial effects. In addition, the term SIR has been renamed to “Sulfur-Enhanced Defense” (**SED**) to avoid possible misunderstandings about resistance in a phytopathological context (Rausch and Wachter, 2005).

### 1.3 The Brassicaceae: a family with many important crop plants

The dicotyledonous angiosperm family Brassicaceae or Cruciferae belongs to the order Brassicales and consists of approximately 338 genera and 3709 plant species (Gómez-Campo, 1980; Warwick *et al.*, 2006). In the Brassicaceae occur many important crop species, for example *Brassica napus*, *B. oleraceae* L. and *B. rapa* L. and one of the most important model species *A. thaliana* L., which was the first plant genome to be sequenced (Arabidopsis Genome Initiative, 2000). The family has major scientific and economic importance and is well represented in DNA sequence data (Hall *et al.*, 2002;

## Introduction

Koch, 2003). Two typical features of the family are the presence of specialized cells (myrosin cells) and the production of sulfur-containing metabolites known as glucosinolates (**GSLs**) (Rössler, 1974; Jørgensen, 1981). Another characteristic feature that can be found in the Brassicaceae are vestured pits in the vessels of the xylem (Judd *et al.*, 2002). Written records from 1500 BCE indicate, that *Brassica* crops were already used and cultivated by humans as crop plants. (Prakash, 1980). Furthermore the archaeological evidence of its importance is dating back to 5000 BCE (Zhang, 1993).

### 1.3.1 The important crop plant *Brassica napus*

*Brassica napus* also called oilseed rape (**OSR**), rapeseed, swede rape (the term "rape" derives from the Latin word for 'turnip', 'rapa' or 'rapum', cognate with the Greek word 'hrapys'; Online Etymology Dictionary, Douglas Harper, 2016; retrieved 26.08.2019) or canola in Canada (Orlovius and Kirgby, 2003) belongs to the family Brassicaceae. The plant is the third economically most important source of vegetable seed oil in the world, after palm and soybean oil (**Fig. 1.3**) (Piazza and Foglia, 2001).

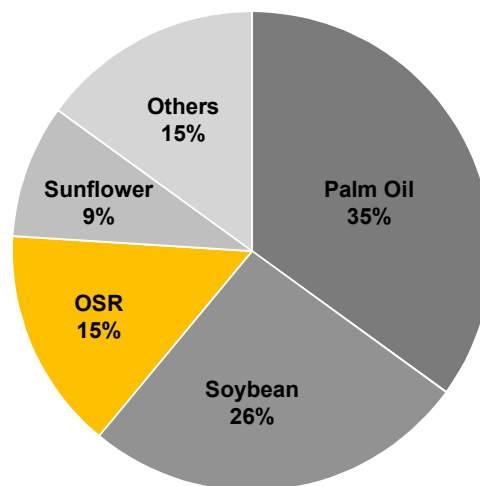


**Figure 1.3: World seed oil production 2013.** Palm oil: 35%; soybean: 26%; oilseed rape (**OSR**): 15%; sunflower: 9%; others: 15%; shown is the market share in percentage; source: oil world database March 2014.

Oilseed rape is as winter or summer (spring) type annual plant available (Song and Osborn, 1962; Snowdon *et al.*, 2007). The winter varieties differ from the summer form regarding to the required vernalisation (winter rest) they need to start the process of flowering. The winter form is the most common rapeseed grown in Europe and China (Carré and Pouzet, 2014). In 1995 was the introduction of the first restored winter OSR hybrid (Paulmann and Frauen, 1997). In the past, various types of OSR have been bred depending on their economic use. For the OSR production in Europe mainly double-low cultivars (double-00; low erucic acid and low GSL content) are grown

## Introduction

(Wittkop *et al.*, 2009) and the first double-low cultivar was released in 1974 (O'Brien, 2008). There is also a small amount of HEAR (high erucic acid content) OSR cultivation in Europe, which is needed for certain industrial end products, prevalent in the oleochemical industry (Piazza and Foglia, 2001; Temple-Heald, 2004). However, double-low cultivars play the most important role for the production of edible oil and for the use as biofuel. This seems to be a good decision, since a high erucic acid content in OSR oil can lead to lesions at the heart muscle, which can cause further cardiovascular complications (Charlton *et al.*, 1975). Different than expected, double-low cultivars show a similar concentration of GSLs in leaves as in high GSL content cultivars (Mithen, 1992).

Depending on the variety and environmental conditions, the plant can grow up to 1.5 m high with pinnatifid and glaucous lower leaves. At the beginning the plants form near-ground leaf rosettes (**Fig. 1.4, A**).

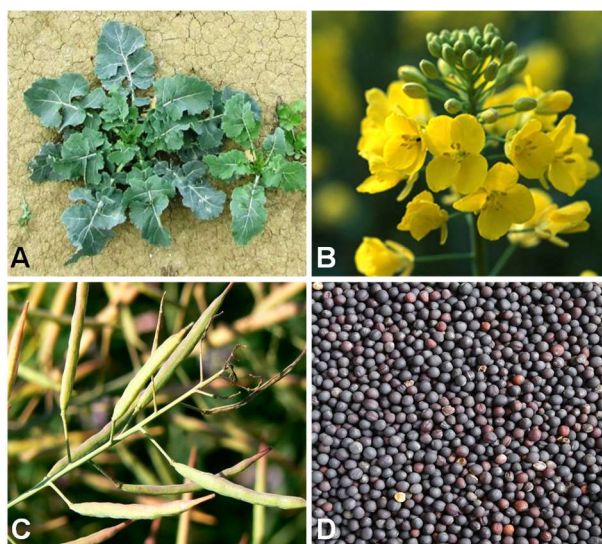


**Figure 1.4: Morphology of *Brassica napus*.** **A:** formation of the typical near-ground leaf rosette; from [luirig.altervista.org](http://luirig.altervista.org), received 26.09.2019; **B:** section of an inflorescence; flower buds and opened flowers in detail; from [agrii.co.uk/journals/agrii\\_articles/pull-it-up-or-leave-it-alone-2/](http://agrii.co.uk/journals/agrii_articles/pull-it-up-or-leave-it-alone-2/), received 26.09.2019; **C:** closed seed pods; formed at the end of maturity stage; from [geograph.org.uk/photo/2545392](http://geograph.org.uk/photo/2545392), received 26.09.2019; **D:** dark brown to black seeds of *B. napus*; from [dsv-seeds.com/oilseed-rape/winter-osr/](http://dsv-seeds.com/oilseed-rape/winter-osr/), received 26.09.2019.

Its stem is well branched and it has two types of roots, a deep tap root and fibrous lateral roots near the surface. Leaves are smooth and dark bluish green with few scattered hairs near the margin. The flowers are yellow with four petals and borne in clusters in the form of elongate racemes (**Fig. 1.4, B**). At the end of the maturity stage the plants form seed pods which are green and elongated (**Fig. 1.4, C**). Seeds have an

## Introduction

almost round shape, small (1.8-2.8 mm in diameter) and coloured in dark brown to black (**Fig. 1.4, D**) (Sattell *et al.*, 1998; Seybold, 2009).

### 1.3.2 Evolutionary history and origin of *B. napus*

For the cultivation of oilseed crops *B. napus*, *B. rapa*, *B. juncea* and *B. carinata* are preferred. The genomic relationships between these *Brassica* species are well understood and can be seen in the “**Triangle of U**” (**Fig. 1.5**) (Nagaharu, 1935). *Brassica rapa* (2n=20; AA genome), *B. nigra* (2n=16; BB genome) and *B. oleracea* (2n=18; CC genome) represent the primary diploid species. *Brassica juncea* (2n=36; AABB genome) and *B. carinata* (2n=34; BBCC genome) are amphidiploids resulting from hybrid combinations of the primary species.

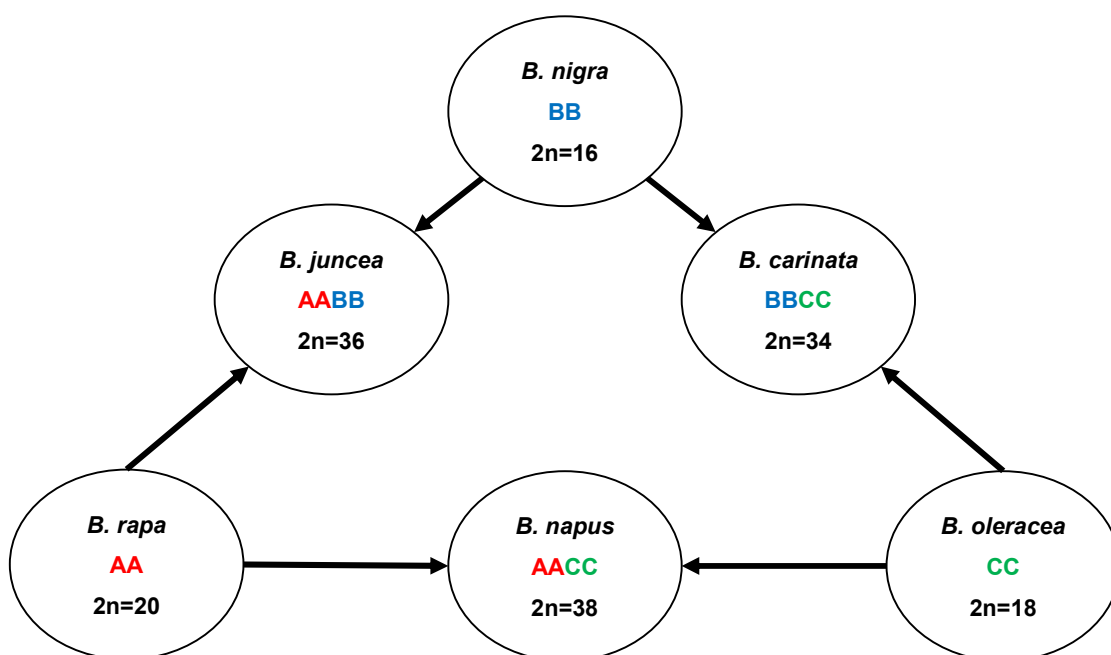


**Figure 1.5: "Triangle of U": *Brassica* species within the triangle of U.** Three diploid species: *B. rapa*, *B. nigra* and *B. oleracea*, which represent the AA, BB and CC genomes; three amphidiploid species: *B. juncea*, *B. napus* and *B. carinata*, which are hybrid combinations of the basic genomes; 2n=diploid chromosome number. Adapted from Koh *et al.* (2017).

*Brassica napus* is also an amphidiploid species (2n=38; AACC genome) derived from a spontaneous hybridization event between *B. rapa* (Asian cabbage or turnip; 2n=20; AA genome) and *B. oleraceae* (Mediterranean cabbage; 2n=18; CC genome) (Nagaharu, 1935). Wild forms of *B. napus* could be found on the coast of Gothland, Sweden, the Netherlands and Britain (Rakow, 2004). The centre of origin for the two diploid parents of *B. napus* is located around eastern Mediterranean or in northern or western Europe (Tsunoda, 1980; Warwick *et al.*, 2009). Regarding *B. napus*, however, the exact period and place of origin is not known but its domestication is believed to have occurred in Europe in the Early Middle Ages (Baranyk and Fábry, 1999).

## Introduction

### 1.4 The plant root as battleground for fungal pathogens

#### 1.4.1 The vascular system of plants

The vascular system of plants is primarily responsible for the transport of water and various nutrients. It consists of two different types of tissue, the xylem and the phloem. The xylem is mainly used for long-distance transport of water, various nutrient salts and a low content of sugars and amino acids. In the xylem sap of OSR are predominant inorganic cations like calcium, potassium, magnesium and manganese (Nakamura *et al.*, 2008). The phloem, which consists of living cells, is responsible for the transport of leaf assimilates. The xylem is assembled from different elements. There are tracheas (xylem vessels or vessel elements), tracheids, sclerenchymatous fibers and xylem parenchyma cells (**Fig. 1.6**). Tracheids are dead at maturity, elongated, tapered cells, which have a primary and secondary cell wall. The tracheas are also dead and their cell walls are partially or completely dissolved in the axial direction. Several trachea cells are connected to each other to form a continuous tube, in contrary to the tracheids. The entirety of the tracheas together with the tracheids forms a continuous tube system, which runs from the root to the shoot along the leaves (Fukuda, 1997; Zhang *et al.*, 2011).

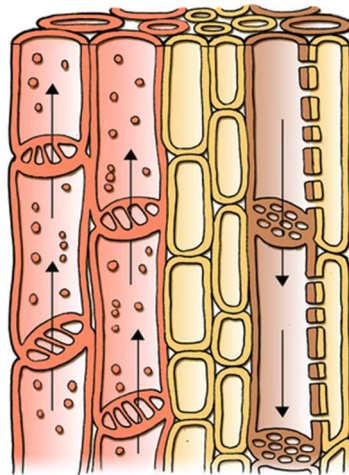


**Figure 1.6: Structure of the xylem of a vascular plant.** The xylem (red) consists of tracheas, and is mainly responsible for the water uptake. The phloem (brown) consists of sieve elements, and is mainly responsible for nutrients transport throughout the plant. The cambium (yellow) lays between the two tissue types, and is responsible for the secondary growth of stems and roots. Adapted from [nigerianscholars.com/tutorials/plant-and-animal-tissues/phloem-tissue/](http://nigerianscholars.com/tutorials/plant-and-animal-tissues/phloem-tissue/), received 23.10.2019.

## Introduction

The root is mainly used for absorption of water and inorganic nutrients and for the anchoring of the plant in the soil. It can also take over other functions, often it serves as a storage organ for reserve materials. The endoderm serves as a natural protective barrier and defends the plants from a variety of pathogens. In addition, the radial cell walls are lined with a suberin-like substance, which acts like an impregnation (Schreiber *et al.*, 1999). This layer of the endodermis is also called the “Casparian strip”. The pericycle, also known as pericambium, plays a role in the secondary thickening and in the formation of the lateral roots. Plant diseases are caused by a huge variety of fungi, bacteria, nematodes, viruses, physiological disturbance and air and water pollution (Treshow and Anderson, 1989; Purcell and Hopkins, 1996; Dordas, 2008; Martinelli *et al.*, 2015). One of the main pathogenic groups are filamentous fungi and they cause in crop plants more economic disadvantages than any other pathogenic microorganisms (Birren *et al.*, 2002). These pathogens can enter their hosts in different ways, e.g. *Botrytis cinerea* is an air borne fungal pathogen (Groves and Drayton, 1939), main cause of grey mould disease in more than 200 plant species worldwide (Williamson *et al.*, 2007). A more likely infection strategy is to colonize the root system first, more precisely the xylem, before the pathogen enters the leaves. These are **soil borne vascular fungi**, e.g. *Fusarium* ssp. or *Verticillium* ssp., which induce serious symptoms in the aerial part of the plant (Babadoost *et al.*, 2004; Eynck *et al.*, 2009). However, the knowledge on fungal root pathogens is limited and the interactions between plant roots and the enormous variety of their surrounding microorganisms are still poorly characterized (Kidd *et al.*, 2011; Millet *et al.*, 2010; Okubara and Paulitz, 2005). A further classification of plant pathogens takes place with help of the infection strategy based on the origin of their required nutrients. The most common forms of infection behaviour are **biotrophic**, which depends on feeding from the living host cells (Thrower, 1966) and **necrotrophic**, which depends on killing the host cells and consuming the remaining dead tissue (Williamson *et al.*, 2007). Generally the infection behaviour of soil borne vascular fungi are a combination of biotrophic and necrotrophic lifestyle and is known as **hemibiotrophic** (Bailey *et al.*, 1992; Perfect *et al.*, 1999).

### 1.4.2 The xylem as a niche for vascular wilt pathogens

The xylem is a tissue type of the vascular system (1.4.1). Based on the nutrient content, it is a very poor habitat for pathogens. However, this can be an important reason, why only a limited number of plant pathogens are able to exploit this environment (Yadeta and Thomma, 2013). This makes the xylem to a unique ecological niche for vascular wilt pathogens and only four genera are able to colonize this environment. These are *Fusarium*, *Verticillium*, *Ceratocystis* and *Ophiostoma* (Agrios, 2005). These specialized pathogens preferentially infect rather the xylem and not the phloem. Although the



## Introduction

phloem is richer in photosynthetic assimilates, such as various sugars, it consists of living cells with an osmotically high pressure. This considerably impedes the penetration of pathogens, hence the xylem is preferred (Yadeta and Thomma, 2013)

Above all, the challenge of vascular pathogens is that they must overcome the highly structured and rigid xylem walls in order to access the vessels. The situation is similar with the pit membranes, which are also a barrier to the vascular pathogens. In addition, most pathogens are too large to pass through the pit membrane pores (Bomsel and Alfsen, 2003; Choat *et al.*, 2004).

### 1.4.3 The genus *Verticillium* ssp.

*Verticillium* is a relatively small genus of ascomycete fungi that currently includes 10 species (Inderbitzin *et al.*, 2011a), whereby five of them belong to the soil borne, vascular plant pathogens (Karapapa *et al.*, 1997; Barbara and Clewes, 2003; Inderbitzin *et al.*, 2011b). Nees von Esenbeck levied *Verticillium* to its own genus in 1816 (Isaac, 1967). Most of the *Verticillium* species are phytopathogenic fungi and responsible for vascular wilts (disease: *Verticillium* wilt) of plants (Dunker *et al.*, 2008; Klosterman *et al.*, 2009; Spencer, 1997). Through their soil borne habitat, their ability to survive for years with the aid of resting structures, and the intriguingly high numbers of potential host plants, pathogenic *Verticillium* species are a serious threat to agriculture and crop production (Depotter *et al.*, 2016; Klosterman *et al.*, 2009; Lazarovits and Subbarao, 2010; Siebold and von Tiedemann, 2013). The best-known pathogens out of this family are *V. dahliae* and *V. albo-atrum*, whose vascular diseases result in yield and quality losses (Pegg and Brady, 2002). *Verticillium dahliae* and *V. albo-atrum* are haploid species and can infested a broad range of host plants (Inderbitzin *et al.*, 2011a). For example, *V. dahliae* is responsible for yield losses in potato crops (*Solanum tuberosum*) in a range between 10-15% (Rowe and Powelson, 2002), in lettuce (*Lactuca sativa*) the yield losses can reach up to 100% (Subbarao *et al.*, 1997). One unique case occurs in this genus: *Verticillium longisporum*, a relative new amphidiploid hybrid (Karapapa *et al.*, 1997; Inderbitzin *et al.*, 2011b), which is highly adapted to brassicaceous hosts (Depotter *et al.*, 2016).

### 1.4.4 *Verticillium longisporum*: the causal agent of *Verticillium* stem striping

*Verticillium longisporum* is an amphidiploid phytopathogenic vascular fungi and the result of more than one interspecific hybridization events between four haploid ancestors (Karapapa *et al.*, 1997; Inderbitzin *et al.*, 2011b). The fungi like to grow in temperate climate regions of the world (Rygulla *et al.*, 2007b; Siebold and von Tiedemann, 2013). *Verticillium longisporum* is the causal agent of the *Verticillium* stem

## Introduction

striping (before: *Verticillium* wilt; disease was renamed by Depotter *et al.* (2016), because there are not occurring any wilting symptoms; Heale and Karapapa, 1999), a major threat in Europe (Heale, 2000). Its preferred host family are the Brassicaceae, more precisely *Brassica* crops like OSR (Karapapa *et al.*, 1997; Zeise and von Tiedemann, 2002). The disease has been observed the first time in the 1960s in Sweden (Kroeker, 1970) and has become a serious problem since the 1970s (Dixelius *et al.*, 2005). In Germany the disease has significantly increased since the 1980s (Daebeler *et al.*, 1988) and menace the OSR production (Sadowski *et al.*, 1995). As already mentioned, the life cycle is hemibiotrophic as in almost all members of the genus *Verticillium*. In addition, the process of infection is similar to that of *V. dahliae* (Klosterman *et al.*, 2011). The life cycle of *V. longisporum* begins in **autumn**, when the OSR is brought to the fields (**Fig. 1.7**).

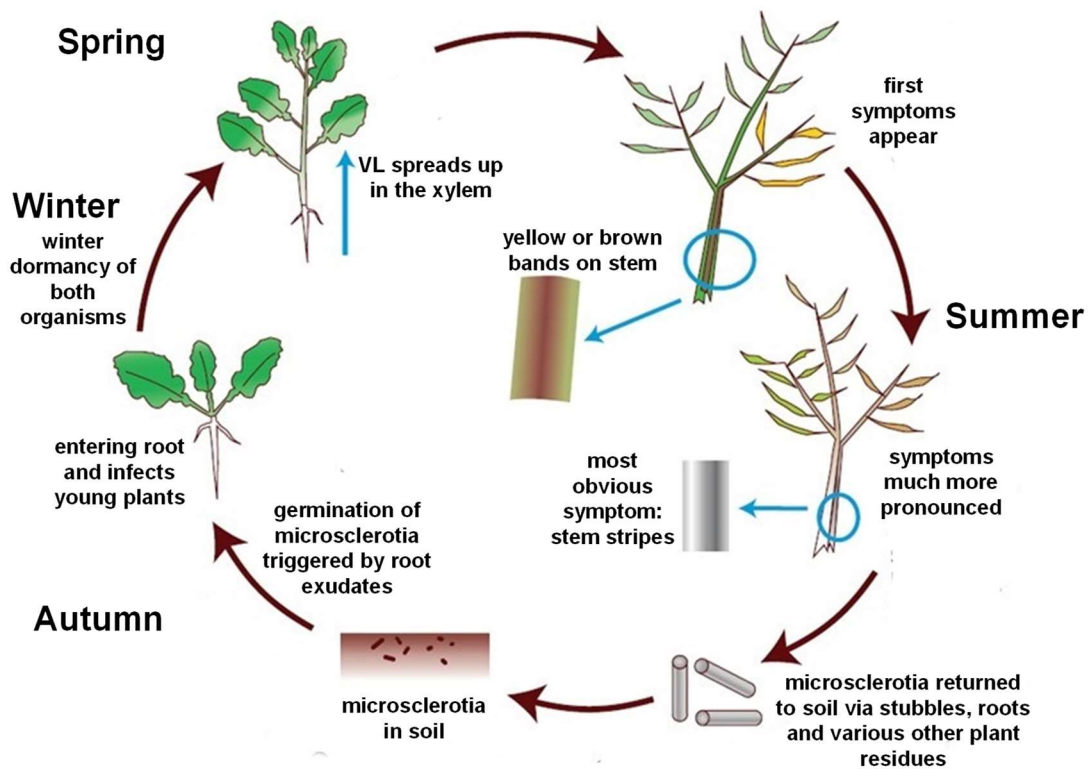


**Figure 1.7: Life cycle of *Verticillium longisporum* (VL) in its preferred host *Brassica napus*.** **Autumn:** microsclerotia of VL are been triggered to grow, because of root exudates of plants; entering root; infects young plants; **winter:** dormancy of both organisms; **spring:** VL colonizes its host systematically; spreads up in xylem; first symptoms appear at the end of spring; **summer:** VL forms microsclerotia; symptoms are more pronounced: chlorotic and necrotic leaves, premature ripening of stems and seed maturity; most obvious symptom: dark unilateral stripes on stems, caused by microsclerotia; plant residues during and after harvesting return to soil and close the cycle. Adapted from [ahdb.org.uk/verticillium-stem-stripe](http://ahdb.org.uk/verticillium-stem-stripe), received 17.09.2019.

## Introduction

By germinating of the OSR seeds root exudates are released, which in turn trigger the germination of the microsclerotia of *V. longisporum* in the soil (Berlanger and Powelson, 2005; Leino, 2006). Microsclerotia are the resting structures of most of *Verticillium* species (Gordee and Porter, 1961). They come from the previous OSR generation by soil tillage, where infested plant residues are buried. Due to the microsclerotia, which are thick-walled and melanized, the fungus can survive more than 10 years in the absence of its host (Schnathorst, 1981). The hyphae from the microsclerotia grows towards the root. *Verticillium longisporum* preferably penetrates through the lateral roots and root hairs (Eynck *et al.*, 2007). In any case, the fungus prefers entry points at the root, where the endodermis is not fully developed yet (Bishop and Cooper, 1983; Pegg and Brady, 2002). Unlike other fungi, that form a so-called appressorium, *V. longisporum* forms a hyphopodium (slight swelling of the hypha apex). This type of swelling is similar to the one that *Magnaporthe oryzae* develops (Marcel *et al.*, 2010). Within the hyphopodium, there is a low pressure sufficient to penetrate the cell wall of the roots, which has already been digested with the help of extracellular enzymes that produce *V. longisporum* (Russel, 1974; Talboys, 1972). There is also the possibility that the fungus may infiltrate into its host plant via feeding lesions caused by nematodes, and grow into the root (Bowers *et al.*, 1996; Back *et al.*, 2002). After the initialization phase, which is completed after successful penetration, *V. longisporum* is in the biotrophic phase of its life cycle. In this, the fungus grows through the cortex in the direction to the central cylinder. When this is reached, the fungus continues to grow in the direction of hypocotyl and colonizes a few vascular vessels (Eynck *et al.*, 2007). Like its host plant, the fungus also takes a break during **winter**, while growth is stagnating in both organisms.

When temperatures rise again in **spring**, the OSR plants start growing again in March (seedtime of summer type OSR is between March/April). Since the temperature minimum is a little higher of *V. longisporum*, the fungus begins its growth time-displaced. The pathogen colonizes its host plant systematically, whereby it first spreads further in the xylem vessels with the help of hyphae and conidia (Eynck *et al.*, 2009). The colonization of the xylem leads to occlusions in the xylem vessels, which can disturb the transport of the xylem sap (Kamble *et al.*, 2013). The conidia are passively disseminated by the help of the xylem sap movement (Buckley *et al.*, 1969; Eynck *et al.*, 2007). When flushed to vessel ends, the conidia germinate and continue to grow into upwardly located vessel elements (Beckman, 1987; Eynck *et al.*, 2007). At the end of spring, the first symptoms of the host plant can appear. The plants show a slight stagnation in their growth, get chlorotic or one-sided yellowed leaves and the roots may turn brownish to blackish (Veronese *et al.*, 2003; Johansson *et al.*, 2006). However,

## Introduction

these symptoms cannot be clearly assigned to *V. longisporum* (Fradin and Thomma, 2006; Häffner and Diederichsen, 2016). Other pathogens like *Leptosphaeria maculans* (disease: stem canker or blackleg) or *Sclerotinia sclerotiorum* (disease: stem rot) show similar patterns of damage (Hall, 1992; Zhou *et al.*, 1999; Saharan and Mehta, 2008; Khangura *et al.*, 2015).

In **summer** *V. longisporum* changes from the biotrophic phase to the necrotrophic phase of its life cycle. The symptoms are now much more pronounced and in addition to chlorotic leaves, there can also occur necrotic leaves. Furthermore, it comes to a premature seed maturity, which is partly responsible for the crop loss. One symptom is the most obvious, named after the disease *Verticillium* stem striping: dark unilateral striping appears on the stems on apparently healthy looking plants at the end of the growing season, which are partly accompanied by stem cracks (Depotter *et al.*, 2016). These stripes are caused by the microsclerotia, which are formed in the stem cortex beneath the epidermis by *V. longisporum* in its necrotrophic phase. The microsclerotia are returned to the soil after harvesting the field via stubbles, roots and various other plant residues (Heale and Karapapa, 1999). The microsclerotia go into a phase of dormancy (Olsson and Nordbring-Hertz, 1985; Wilhelm, 1955). They will not germinate again until the root exudates of their host plants are released into the soil.

### 1.4.5 Evolutionary history and origin: hybridization with fatal consequences

In the evolution hybridization events play a main role and it is to be disposed to accept that over 10% of today existing species are hybrids (Hegarty and Hiscock, 2005). Common examples for plant hybrids are coffee, cotton, oat, wheat and OSR (Osborn *et al.*, 2003). There exists an enormous amount of research and publications of hybridization in plants, especially in crops and model plants (Hejatko *et al.*, 2006; Laurie and Bennett, 1986; Rieseberg and Carney, 1998; Scheffler and Dale, 1994). However, research regarding to fungal hybrids is still in its infancy. Recently it has been possible, through advanced phylogenetic techniques (Schardl and Craven, 2003), to increase the amount of promising results to get a better understanding (Masneuf *et al.*, 1998; Rygulla *et al.*, 2008; Morin *et al.*, 2009).

The history and taxonomic classification of *V. longisporum* is difficult to see due to many renamings and tenuous molecular phylogenetic data in the past (Depotter *et al.*, 2016). Stark (1961) described a strain of *V. dahliae* from horseradish, which produced microsclerotia and also conidia. It has been noticed, that the conidia were 7-9 µm in length. This is almost double the size of the previously known conidia of *V. dahliae* (Karapapa *et al.*, 1997). Due to this morphological variation, the strain was named to *V. dahliae* var. *longisporum*. It took over 37 years according to the first description, until

## Introduction

it was elevated to its own species rank *V. longisporum* (Karapapa *et al.*, 1997). *Verticillium longisporum* is closely related to *V. dahliae* and *V. albo-atrum* (Fahleson *et al.*, 2004). Because of the close relation and misidentifications between *V. longisporum* and *V. dahliae* in the past (Babadoost *et al.*, 2004), molecular phylogenetic investigations are needed to differentiate the disease-causing pathogens (Karapapa *et al.*, 1997; Eynck *et al.*, 2007; Inderbitzin *et al.*, 2011b). **Table 1.1** shows some of the morphological and physiological differences of *V. longisporum* and *V. dahliae*. However, there still may be some confusion with these features, because some *V. longisporum* strains have similarly shaped conidia and/or microsclerotia compare to *V. dahliae* (Inderbitzin *et al.*, 2011a).

**Table 1.1: Morphological and physiological differentiation between *V. longisporum* and *V. dahliae*.**

Parameters	<i>V. longisporum</i>	<i>V. dahliae</i>
<b>Conidia length</b> <sup>1,2,5,7</sup>	long (> 7 µm)	small (< 4 µm) to medium (4-5.5 µm)
<b>Shape of microsclerotia</b> <sup>2,4,7</sup>	elongate	mostly rounded or spherical
<b>Colony surface</b> <sup>4</sup>	black & rough	black & rough or white & fluffy
<b>Sporulation rate in shaking culture</b> <sup>4</sup>	low	high
<b>Culture filtrate fluorescence</b> <sup>2,4</sup>	yes	no
<b>Host range</b> <sup>2,3,6</sup>	mainly restricted to Brassicaceae	broad

<sup>1</sup>Stark (1961); <sup>2</sup>Karapapa *et al.* (1997); <sup>3</sup>Bhat and Subbarao (1999); <sup>4</sup>Zeise and von Tiedemann (2001); <sup>5</sup>Steventon *et al.* (2002); <sup>6</sup>Zeise and von Tiedemann (2002); <sup>7</sup>Inderbitzin *et al.* (2011a)

**Figure 1.8** shows the evolutionary history of *V. longisporum* in a cartoon phylogenetic tree (Inderbitzin *et al.*, 2013). These phylogenetic analysis separates the fungus into three lineages with different ancestors. The four parents include two *V. dahliae* genotypes, *V. dahliae* D2 and *V. dahliae* D3. There are also two unknown species, which are named Species A1 and Species D1. These insights based on molecular phylogenetic investigations using ribosomal internal transcribed spacer (ITS) sequences and intronrich portions of five protein-encoding genes: actin (ACT), elongation factor 1-alpha (EF), glyceraldehyde-3-phosphate dehydrogenase (GPD), mitochondrialoxaloacetate transport proteine (OX) and tryptophan synthase (TS) (Inderbitzin *et al.*, 2011b). All characteristic *V. longisporum* isolates showed, that they contain alleles, each of which originates from Species A1 in combination with Species D1, *V. dahliae* lineage D2 or *V. dahliae* lineage D3 alleles. This eventuate in the following hybrid combinations: A1/D1, A1/D2 and A1/D3. The DNA content of *V.*

## Introduction

*longisporum* is about 1.8 times higher than in *V. dahliae* depending on the particular isolate.

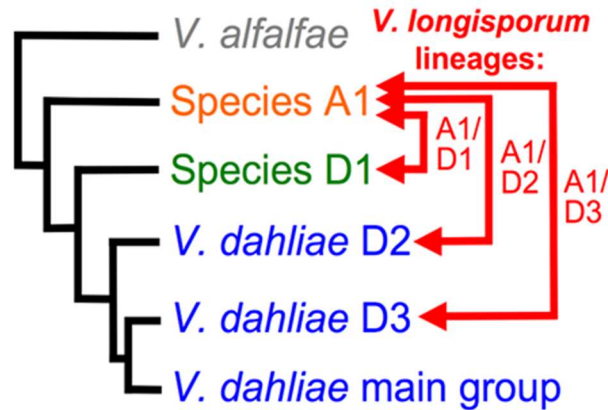


**Figure 1.8: Evolutionary history of *Verticillium longisporum*.** Species A1 (in orange) and D1 (in green) are hitherto undescribed *Verticillium* lineages; *V. dahliae* lineage D2 and *V. dahliae* lineage D3 formed with the unknown parents in three different hybridization events the following *V. longisporum* hybrids: A1/D1, A1/D2 and A1/D3; red arrows indicate the parents of *V. longisporum* hybrid lineages; tree is not to scale. Figure: Evolutionary history illustrated by a cartoon phylogenetic tree based on Inderbitzin *et al.* (2013).

However, it is possible, that there are significant variations between the different isolates (Karapapa *et al.*, 1997; Steventon *et al.*, 2002; Collins *et al.*, 2003). The varieties in the different genome size may be due to the different DNA content of the different ancestors. This reflects the enormous genomic plasticity of fungi (McDonald and Martinez, 1991; Cuomo *et al.*, 2007). It may also be due to the fact that there has been a DNA loss because of hybridization, as the example of the endophyte *Neotyphodium unicanthum* shows (Moon *et al.*, 2004). A particularly interesting observation is, that the pathogenicity and virulence are differ in the three different *V. longisporum* lineages. Tran *et al.* (2013) and Novakazi *et al.* (2015) show in their studies, that *V. longisporum* lineage A1/D1 has the highest pathogenicity for OSR, whereas isolates of the lineage A1/D3 are not pathogenic on OSR. The *V. longisporum* lineage A1/D2 was previously found only in horseradish, which was grown in the USA, Illinois (Eastburn and Chang, 1994). It turned out that this *V. longisporum* lineage is the most pathogenic to this plant (Novakazi *et al.*, 2015).

### 1.5 Plant defense mechanisms – when plants make a counterattack

In general, plants are able to defend themselves against pathogen attack by the apoplastic defense. This includes the inhibition of microbial enzymes, the strengthening of the cell walls, making it difficult for the pathogen to invade nor penetrate further or the poisoning of the pathogen with the help of toxic compounds e.g. phytoalexins (Hückelhoven, 2007). In addition, the reprogramming of the plant metabolism is a characteristic process for plant-pathogen interaction. Because for the activation of defense mechanisms, it is normally necessary for the plant to arrested the growth (König *et al.*, 2014). Mineral nutrients that are involved in metabolism and growth of the plant may show changes in their contents under influence of pathogen-attack. This could be for example sulfur (Weese *et al.*, 2015), calcium (Zhang *et al.*, 2014), potassium (Amtmann *et al.*, 2008) and iron (Aznar *et al.*, 2015). However, it has to be differentiated between defense mechanisms that are present in plants prior the infection and the mechanisms that are induced by pathogen invasions. For example, plants have antibiotics that are subdivided into phytoanticipins and phytoalexins. Phytoanticipins are so-called preformed antibiotics, which are also present in the plant without pathogenic infection, while the phytoalexins are synthesized and accumulated only after exposure of pathogens (Hammerschmidt, 1999; Mansfield, 2000; VanEtten *et al.*, 1994). Data of Pedras (2008) showed that both phytoalexins and phytoanticipins had selective growth-inhibiting activity in fungal pathogen bioassays.

#### 1.5.1 Sulfur-containing defense compounds – SDCs

Section 1.2.2 described the transport and metabolism of sulfate from the plant root to the shoot and the importance of sulfur as an essential macronutrient. Sulfate is assimilated into cysteine, an important amino acid which forms the metabolic crossroad of primary metabolism, protein biosynthesis and sulfur-containing defense compounds (SDCs) formations. In addition to the assimilatory sulfur processes, dissimilatory reactions can also take place. This is, for example, the release of hydrogen sulfide (H<sub>2</sub>S) from cysteine (Léon *et al.*, 2002; Riemenschneider *et al.*, 2005). This release may contribute to the pathogen defense. Sulfur-containing defense compounds, which include GSLs, glutathione, sulfur-rich proteins, phytoalexins, H<sub>2</sub>S, and elemental sulfur (S<sup>0</sup>), are primarily not designed for pathogen-specific defense mechanisms. In some cases, the effectiveness of the pathogen defense of individual SDCs has been demonstrated to be strong, but in others it is still controversial (Rausch and Wachter, 2005). However, SDCs may be beneficial for the gene-to-gene interactions between host and pathogen during induced defense mechanisms.

## Introduction

**Figure 1.9** shows the biosynthesis of SDCs (highlighted in yellow) in a simplified scheme as part of the sulfur metabolism. As already mentioned and for a brief repetition, the product **APS** is reduced by the key enzyme **APR** with glutathione serving as the electron donor. Alternatively, **APS** can be further activated by **APK** to form **PAPS**, which is required for various sulfation reactions including the biosynthesis of GSLs. Sulfite is reduced by the enzyme **SiR** to  $\text{H}_2\text{S}$ , which is incorporated into **OAS** by means of **OASTL**, so that cysteine, the main product of sulfur assimilation, can be formed. Cysteine can be incorporated into sulfur-rich proteins (SRPs) and glutathione. In addition, cysteine serves as a donor of reduced sulfur, which is required for the biosynthesis of GSLs and for the synthesis of phytoalexins. Through the action of desulfhydrases,  $\text{H}_2\text{S}$  may be released from cysteine, while elemental sulfur may be released from glutathione. The activity of sulfite oxidase converts excess sulfite to sulfate, releasing hydrogen peroxide ( $\text{H}_2\text{O}_2$ ), which could potentially act as a defense signal.

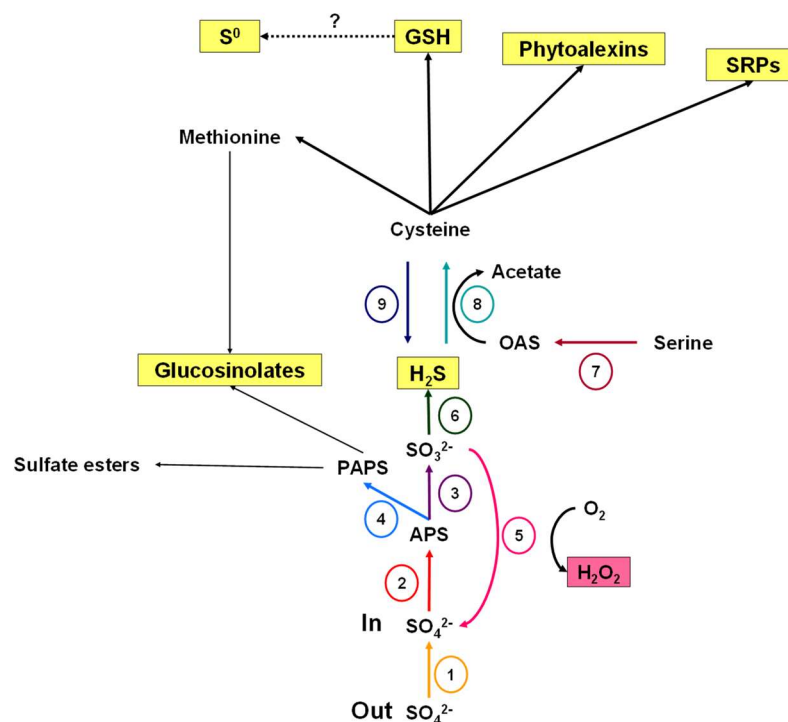


**Figure 1.9: Simplified schema of the biosynthesis of sulfur-containing defense compounds (SDCs) as part of the sulfur assimilation.** SDCs are highlighted in yellow:  $\text{H}_2\text{S}$ , hydrogen sulfide; SRPs, sulfur-rich proteins; phytoalexins; GSH, glutathione;  $\text{S}^0$ , elemental sulfur; glucosinolates; uptake of  $\text{SO}_4^{2-}$  (sulfate) from soil; abbreviations: APS: adenosine 5'-phosphosulfate; PAPS: 3'-phosphoadenosine 5'-phosphosulfate;  $\text{SO}_3^{2-}$ : sulfite; OAS: O-acetylserine;  $\text{H}_2\text{S}_2$ : hydrogen peroxide; numbers represent enzymes: 1, SULTR: sulfate transporter; 2, ATPS: ATP sulfurylase; 3, APR: APS reductase; 4, APK: APS kinase; 5, sulfite oxidase; 6, SiR: sulfite reductase; 7, SAT: serine acetyltransferase; 8, OASTL: O-acetylserine thiollase; 9, desulfhydrases. Adapted from Rausch and Wachter (2005).



## Introduction

Biotic or abiotic stress factors in plants causes an increasing of the synthesis rate of some SDCs or be induced by jasmonic acid (**JA**) and/or other signals (Xiang and Oliver, 1998; Mikkelsen *et al.*, 2003). Marschner (1974) and Bloem *et al.* (2005) showed, that the formation of SDCs is saturated faster with a higher sulfur supply compared to the growth of the plant. Plant growth, depending on plant species and specific growth conditions, shows a typical saturation curve in which the plateau is reached at less than 1 mM sulfate in response to sulfate as the sulfur source (Resurreccion *et al.*, 2001). If the sulfate supply is improved or there is an excess of sulfate, SDCs are increasingly produced despite strict regulation of the cysteine content (Rausch and Wachter, 2005). In the family Brassicaceae the content of cysteine in the tissue is in the range of 20.0 nmol g<sup>-1</sup> FW (fresh weight) (Saito, 2004), for glutathione in the range of 0.1-1.5 μmol g<sup>-1</sup> FW (Mullineaux and Rausch, 2005) and for the total of GSLs in the range of 1.0-10.0 μmol g<sup>-1</sup> FW (Mikkelsen *et al.*, 2003; Petersen *et al.*, 2001). The following three sections describe GSLs, glutathione and H<sub>2</sub>S in more detail.

### **Glucosinolates: the mustard oil bombs**

Glucosinolates are amino acid-derived thioglycosides and nitrogen- and sulfur-containing plant secondary metabolites (Mithen and Campos, 1996). They occur generally in the order Brassicales, intriguingly, they also appear in the family Euphorbiaceae, more precisely in the genus *Drypetes*, which has no affiliation to the other GSL-containing families (Halkier and Gershenzon, 2006). Glucosinolates can be found in almost all plant organs and are located in the inside of the vacuoles (Kelly *et al.*, 1998; Andersson *et al.*, 2009). Glucosinolates and their hydrolysing agent, an endogenous β-thioglucosidase, the myrosinase, are spatially divided within plant cells (Bones and Rossiter, 1996). The myrosinase is stored in idioblasts (myrosin cells) of the cytoplasm (Chen and Andreasson, 2001), which can be found occasionally throughout most plant tissues (Bones and Rossiter, 1996; Halkier and Du, 1997). Lüthy and Matile (1984) described this subcellular model of the GSL-myrosinase system for the first time (“mustard oil bomb”). The GSL molecule is composed of a common glycone moiety and a variable aglycone side chain (Fenwick *et al.*, 1983). There are approximately 130 described GSLs, which share a chemical structure consisting of a β-D-glucopyranose residue linked through a sulfur atom to a (Z)-N-hydroximosulfate ester and a variable side chain (R), whereby this derived from one of eight amino acids (Fahey *et al.*, 2001; Hopkins *et al.*, 2009). Glucosinolates can be classified by reference to the precursor amino acid and the subsequent modification of the side chain (Halkier and Gershenzon, 2006). Glucosinolates of the Brassicaceae are a well described example of SDCs (Agerbirk *et al.*, 2009; Ahuja *et al.*, 2011; Bednarek, 2012; Wittstock and Halkier, 2002). They have been classified into the **aliphatic**, **indolic** and **benzyllic**

## Introduction

GSLs (Agerbirk and Olsen, 2012). The model plant *A. thaliana* synthesizes these three groups of GSLs, methionine-derived aliphatic GSLs (**AGSLs**), tryptophan-derived indolic GSLs (**IGSLs**) and abundant phenylalanine-derived benzylic GSLs (**BGSLs**) (Brown *et al.*, 2003; Petersen *et al.*, 2002). Intact GSLs are nontoxic, but if the plant is subject to tissue injury, such as cutting or chewing, the GSLs come into contact with myrosinases (Wittstock and Halkier, 2002). Typical hydrolysis products of GSLs, such as isothiocyanates and nitriles, have been shown to be toxic or work as inhibitors against several pathogen fungi and bacteria (Chew, 1988), e.g. *Alternaria* ssp. (Milford *et al.*, 1989). Rawlinson *et al.* (1989) and Giamoustaris and Mithen (1995) showed a correlation between the GSL content of leaves on the susceptibility for fungal pathogens. Furthermore several studies demonstrated in *A. thaliana*, that the recognition of pathogen-associated molecular patterns (**PAMPs**; see 1.5.2) stimulates IGSL metabolism (Bednarek *et al.*, 2009; Clay *et al.*, 2009; Sanchez-Vallet *et al.*, 2010). This seems to be a crucial defense response against a broad range of fungal pathogens (Adie *et al.*, 2007; Consonni *et al.*, 2010; Hiruma *et al.*, 2010; Lipka *et al.*, 2005; Maeda *et al.*, 2009; Schlaeppli *et al.*, 2010). The biosynthesis of GSLs is controlled by a complex network of transcription factors, that respond to abiotic and biotic stress of the plant (Celenza *et al.*, 2005; Maruyama-Nakashita *et al.*, 2006; Sønderby *et al.*, 2007). The transcription factors **MYB34**, **MYB51** and **MYB122** in *A. thaliana* are proper regulators of the IGSL biosynthesis (Frigmann and Gigolashvili, 2014; Gigolashvili *et al.*, 2007). They have a huge influence on the expression of genes, **CYP79B2** and **CYP79B3** (Hull *et al.*, 2000), encoding the cytochrome P450 enzymes **CYP79B2** and **CYP79B3**. These enzymes convert in a plenty of tryptophan to indole-3-acetaldoxime (**IAOx**), that can be used for either indole-3-acetic acid (**IAA**) or IGSL biosynthesis (Mikkelsen *et al.*, 2000; Zhao *et al.*, 2002). Iven *et al.* (2012) showed a significantly higher expression of **CYP79B2** and **CYP79B3** in the infection of *Arabidopsis* with *V. longisporum* (isolate VL43). For example, glucobrassicin (GBS) or 3-indolylmethyl GSL is a phytoanticipin and one of the four most common IGSLs, which has been identified in a considerable number of Brassicaceae (McDanell *et al.*, 1988; Windsor *et al.*, 2005). Mithen *et al.* (1986) showed in their experiments with bioassays, the toxicity of the hydrolysis products of GBS that may play a role in the pathogen defence mechanisms of plants.

As already mentioned, **PAPS** plays an important role in the secondary metabolism, as it provides the active sulfate for these reactions (Mugford *et al.*, 2009). The biosynthesis of GSLs is closely linked to the primary sulfur metabolism of plants (Underhill *et al.*, 1973). **Figure 1.10** shows the function of PAPS, which acts as a sulfate donor for GSLs, formed with the enzymatic activity of sulfotransferases (SOTs). The sulfate group of

## Introduction

PAPS is transferred to a free hydroxyl group of a suitable acceptor molecule (Kopriva, 2006). That the PAPS is important for GSL synthesis has been found by Mugford *et al.* (2009).

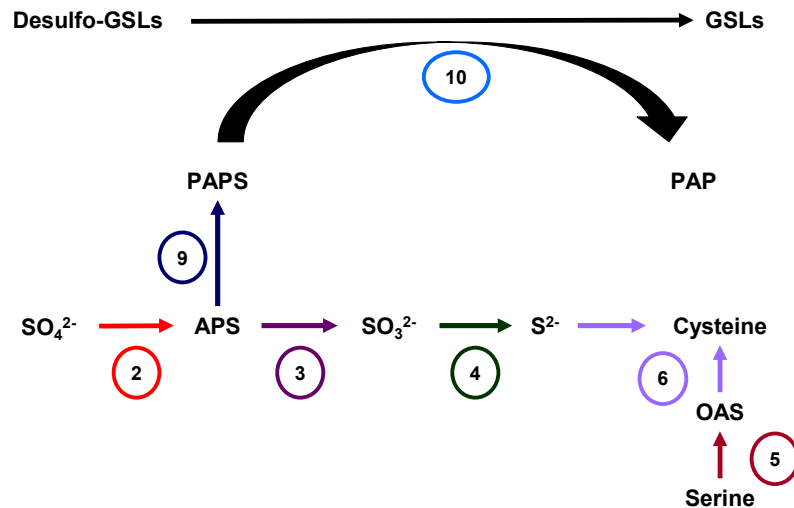


**Figure 1.10: Simplified schema of the last step in the GSL biosynthesis.** Abbreviations:  $\text{SO}_4^{2-}$ : sulfate; APS: adenosine 5'-phosphosulfate; PAPS: 3'-phosphoadenosine 5'-phosphosulfate; PAP: 3'-phosphoadenosine 5'-phosphate;  $\text{SO}_3^{2-}$ : sulfite;  $\text{S}^{2-}$ : sulfide; OAS: O-acetylserine; numbers represent enzymes: 2, ATPS: ATP sulfurylase; 3, APR: adenosine 5'-phosphosulfate reductase; 4, SiR: sulfite reductase; 5, SAT: serine acetyltransferase; 6, OASTL: O-acetylserine thiollase; 9, APK: APS kinase; 10, SOT: sulfotransferase. Adapted from Yatusевич *et al.* (2010).

### **Glutathione: a versatile protector**

Glutathione is widely used by the plant, it serves as a redox buffer (Foyer and Noctor, 2009) and protects the cytosol and other compartments at the cellular level from reactive oxygen species (ROS), which can form in response to biotic and abiotic stress factors (Mullineaux and Rausch, 2005; Ruiz and Blumwald, 2002). In the ascorbate-glutathione cycle (AGC), glutathione plays in a position that is closely related to that of ascorbic acid and the electron flux of NADHP (Potters *et al.*, 2002). Glutathione also plays a crucial role in detoxification mechanisms based on glutathione-S-transferase (GST) (Edwards *et al.*, 2000). Glutathione may play a role in defense against pathogens by determining the redox status of the non-Expressor of Pathogenesis Related Gene 1 (NPR1) protein (Mou *et al.*, 2003). The NPR1 gene is an important transcriptional co-activator which regulates the salicylic acid (SA) dependent plant immune response (Loake and Grant, 2007). NPR1 indirectly appears to transcribe salicylic acid-induced proteins encoding pathogenesis-related proteins (Dong, 2004). After infection with

## Introduction

pathogens, NPR1 is reduced to a monomeric form. It is believed that the altered redox potential of glutathione is responsible for this type of activation of *NPR1*, which is caused by an infection (Mou *et al.*, 2003; Han *et al.*, 2013; Kovacs *et al.*, 2015). *NPR1* genes are required for induction of systemic acquired resistance (**SAR**) by fungi and bacteria (Després *et al.*, 2000; Zhou *et al.*, 2000; Pieterse and Van Loon, 2004; Mukhtar *et al.*, 2009). Systemic acquired resistance belongs to the induced pathogen defense mechanisms of the plant.

### ***Hydrogen sulfide: a foul-smelling affair with benefits***

Previous studies hypothesized the relationship between H<sub>2</sub>S emissions in the plant as response to pathogens in the context of SED (**1.2.3**) (Bloem *et al.*, 2004). Zhang *et al.* (2008) found, that H<sub>2</sub>S is an important cellular signal that plays a key role in protecting plants against copper stress. Furthermore, the importance of the beneficial effects of H<sub>2</sub>S and H<sub>2</sub>S-signaling, which can minimize the effects of, among others, heat stress, drought, osmotic stress, aluminum, cadmium, chromium and boron toxicity has been demonstrated in various studies (Yang *et al.*, 2008; Wang *et al.*, 2010; Zhang *et al.*, 2010; Y. Li *et al.*, 2012; Cheng *et al.*, 2013; Jin *et al.*, 2013; Li *et al.*, 2013). Originally, it was thought that H<sub>2</sub>S is released from cysteine, but recently several specific types of desulhydrases have been found and characterized for their function (Léon *et al.*, 2002; Riemenschneider *et al.*, 2005). However, the individual roles of the found enzymes are not clear yet, but the activity and expression of L-cysteine desulhydrase is induced by the attack of pathogens. This leads to the assumption that H<sub>2</sub>S plays a definite role in the defense mechanisms of plants (Bloem *et al.*, 2004). The extent to which the H<sub>2</sub>S released from the host plant is toxic to the pathogen, depends on the formed amount at the site of invasion and whether the pathogen has the ability to metabolize H<sub>2</sub>S (Bloem *et al.*, 2007).

## Introduction

### 1.5.2 The second line of defense – the pathogen-induced mechanisms

If a pathogen overcomes the apoplastic defense barrier, it will come to the second line of defense of the plants, the induced plant defense. As already mentioned, SDCs can also play a role in the induced pathogen defense or support certain mechanisms. Essentially, there are two steps of induced plant defense mechanisms, one requiring activation of the transmembrane-pattern recognition receptors (**PRRs**), that respond to slow-developing **PAMPs** (Boller, 1995; Zipfel and Felix, 2005).

Since these can also occur in non-pathogenic microorganisms, the alternative term microbe-associated molecular patterns (**MAMPs**) was additionally introduced (Boller and Felix, 2009). Pathogen-associated molecular patterns are highly conserved molecules that are said to be responsible for the essential fitness or survival of microbes (Medzhitov and Janeway, 1997; Nürnberger and Brunner, 2002). The second step of induced plant defense mechanisms, however, acts largely in the cell. This uses the polymorphic nucleotide-binding-leucine-rich repeat receptor (**NB-LRR**) protein products, which are mainly encoded by most resistance (R) genes (Dangl and Jones, 2001). These R genes are named after their distinctive nucleotide binding (**NB**) and leucine rich repeat (**LRR**) domains. Jones and Dangl (2006) show the induced plant immune system as a so-called 'zigzag' model, which runs in four phases, depends on the two steps of the immune pathways, named PAMP-triggered immunity (**PTI**) and effector-triggered immunity (**ETI**). It can be argued that a successful biotrophic pathogen must overcome the PTI in order to colonize its host (Nomura *et al.*, 2005).

**Figure 1.11** shows the process of the different phases. In phase one, PAMPs are recognized by the PRRs. This unspecific detection results in the PTI, which is able to stop further colonization. Relatively well-studied examples of PAMPs are structural molecules, e.g. the bacterial flagellin, peptidoglycan, and lipoolysaccharides, oomycete glucans, and fungal chitin (Ayers *et al.*, 1976; Felix *et al.*, 1993; Dow *et al.*, 2000; Erbs *et al.*, 2008).

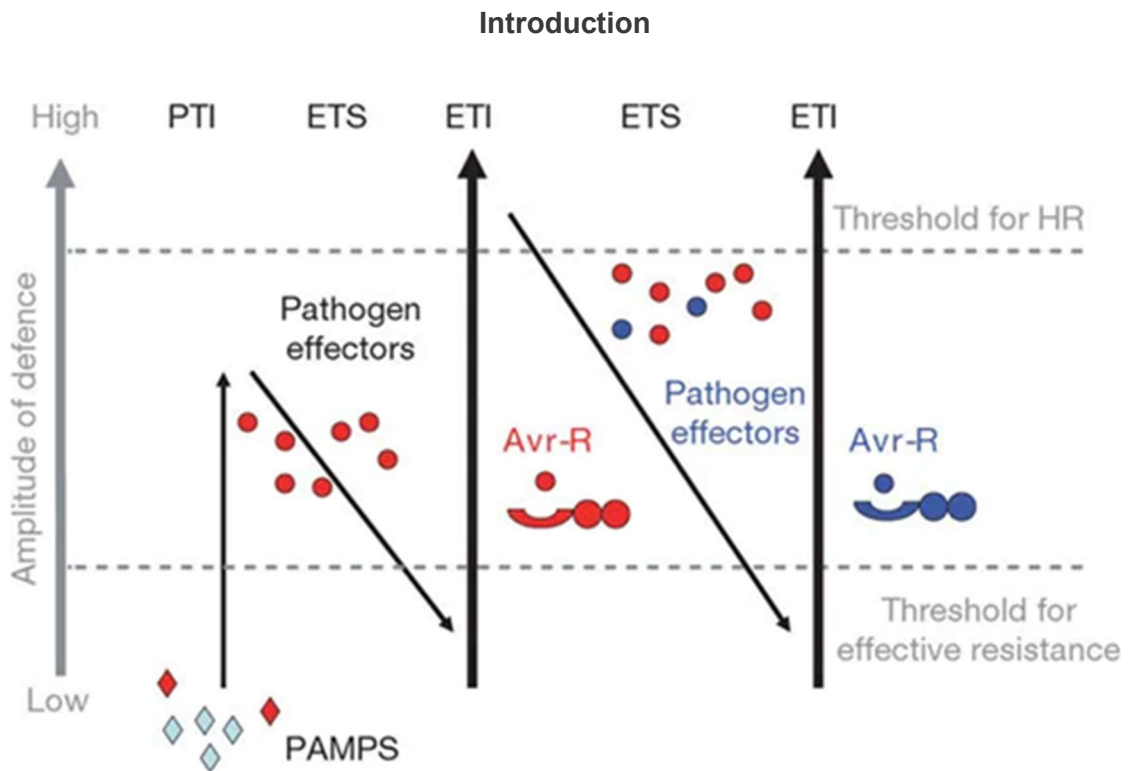


**Figure 1.11: 'Zigzag' immune response model.** Phase one starts with the recognition of pathogen-associated molecular patterns (PAMPs) by transmembrane-pattern recognition receptors (PRRs). This detection results in the PAMP-triggered immunity (PTI). The PTI is able to prevent the further spread of pathogens. However, some pathogens can escape the detection of PTI with the help of pathogen effectors, as shown in phase two. The suppression of the PTI by pathogen effectors is called effector-triggered susceptibility (ETS). But the plant is able to identify the pathogenic effectors with the help of specific disease resistance (R) genes. If it comes to an identification of such an effector by a corresponding nucleotide-binding-leucine-rich repeat receptor (NB-LRR) protein, then phase three, where the effector-triggered immunity (ETI) is initiated, begins. The recognized effectors are called avirulence (Avr) proteins. The ETI is a stronger form of defense response as PTI. Phase four is based on natural selection, which causes the pathogens to turn off or change the already recognized effector. The ETI usually leads to a hypersensitive cell death reaction (HR) at the direct invasion side of the pathogen. Whether it comes to HR or effective resistance depends entirely on which threshold is reached. Figure from Jones and Dangl (2006).

PAMPs are conserved across the genera, while the effectors are specific to their respective species, perhaps even to related species (Jones and Dangl, 2006). Certainly, due to widespread occurrence, several groups of effector proteins may be classified as PAMPs as well. However, there are pathogens that can use certain effectors that in turn disturb the PTI, as shown in phase two. The effectors that enable pathogens to bypass PTI are recognized by specific disease R genes. Most of the R genes encode NB-LRR proteins (more than 125 of these proteins exist in the *Arabidopsis* Col-0 genome). The pathogen effectors lead to an effector-triggered susceptibility (ETS). If there is a recognition of such an effector by a corresponding NB-LRR protein, then the ETI is initiated. These recognized effectors are called avirulence

## Introduction

(Avr) proteins. The ETI is highly specific in contrast to the PTI (based on the gene-for-gene hypothesis by Flor, 1971).

The ETI begins in phase three, when it comes to an identification of such an effector by a corresponding NB-LRR protein. This recognition of the effectors can occur in two ways, either indirectly or through direct NB-LRR detection (Panstruga *et al.*, 2009). The immune responses in ETI occur faster, are more prolonged and significantly more robust compared to PTI (Thilmony *et al.*, 2006; Tsuda and Katagiri, 2010), leading to SAR and usually to a hypersensitive reaction (**HR**) together with a programmed cell death (**PCD**) at the direct invasion side of the pathogen (Heath, 2000; Navarro *et al.*, 2006; Takken *et al.*, 2006). The HR also helps to activate defense in neighboring cells. The SAR, which describes a wide-ranging type of disease resistance, is mediated by the impact of SA (Vlot *et al.*, 2008). Phase four is based on natural selection, which causes the pathogens to turn off or change the already recognized effector. Another possibility is, that the pathogens acquire additional effectors that cause the ETI to be suppressed. However, natural selection also leads to new resistance specificities that can trigger the ETI again. Both in PTI and in ETI, the largest parts of the defense reactions are activated, just the timing makes the difference (Tao *et al.*, 2003).

The production of ROS (**1.5.1**; paragraph **Glutathione**) is one of the earliest responses to infection by pathogens (Lamb and Dixon, 1997). The ROS are major signaling molecules during initiated pathogen defense mechanisms. In addition, they are closely linked to the sulfur metabolism by the Foyer-Halliwel-Asada pathway, in which glutathione is involved namely in the detoxification of ROS (Foyer and Halliwel, 1976). In turn, the association of ROS with the sulfur metabolism combines sulfur metabolism with the recognition of pathogens and the induction of corresponding defense mechanisms. The weak triggering of ROS production occurs at a very early stage of the infection, both in the PTI and in the ETI. But only in the ETI does it come to a second, significantly longer and more extensive activation of the oxidative burst. The previously mentioned HR, which can be induced during the ETI and represents a typical immune response of the plant (Heath, 2000), is promoted by the accumulation of nitric oxide (NO) and SA together with the ROS (Alvarez, 2000; Delledonne *et al.*, 1998). In addition to the phytohormone SA and ROS, cysteine also appears to play a direct or indirect role in establishment and signaling in plant-pathogen interaction and correlated defense mechanisms. Based on their results, Álvarez *et al.* (2012) postulate that cysteine may play a protective role in the PTI. Furthermore, cytosolic cysteine seems to play a significant role in initiating HR during the ETI. Next to ROS, calcium (Ca) also plays a decisive role as a secondary messenger in the immune response (Knight *et al.*, 1991). Studies on pharmacological and genetic perturbation confirmed the pioneering

## Introduction

role for calcium fluxes and the need for downstream oxidative burst in the defense mechanisms of plant (as measured by the growth of plant pathogens) (Blume *et al.*, 2000; Grant *et al.*, 2000; Segonzac *et al.*, 2011). The level of calcium in the cytoplasm is kept low by the secretion of free calcium ions into the apoplast and various subcellular stores. When pathogen recognition occurs, calcium is reversibly released within 1 min and absorbed into the cytoplasm via calcium channels or pumps (Dodd *et al.*, 2010). In addition, ROS-calcium interaction may play an important role in SAR (Dubiella *et al.*, 2013; Gilroy *et al.*, 2014).

In case of infection with vascular wilt pathogens, recognition may be mediated by either extracellular or intracellular receptors. In both cases, this leads to a defense reaction within the xylem vessels. In order to prevent the pathogen from spreading further in the xylem vessels, the plant takes extensive physical defense reactions. In combination with chemical defense mechanisms, not only the spread can be prevented, it is also possible to kill the pathogen. A widespread defense mechanism against vascular pathogens is the tylosis formation (**Fig. 1.12**) in the xylem vessels (Grimault *et al.*, 1994). Tyloses are bubble-like outgrowths of parenchymatous xylem vessel cells, which protrude into the tracheas through pits to block the spreading of the invading vascular pathogens (Meyer and Côté, 1968). Point of time and intensity of tylosis formation can vary widely, based on the compatibility of the host-pathogen interaction. Thus, tyloses forms in resistant plants much faster and more extensively than in susceptible plants (Fradin and Thomma, 2006; Eynck *et al.*, 2007). Another major type of vascular occlusions are gels (also referred as gums in earlier publications) (Rioux *et al.*, 1998), which, like tyloses, derive from paratracheal parenchyma. Gels are amorphous substances secreted by parenchyma cells into the vessel lumen (Harling and Taylor, 1985). During the formation of occlusions, ultrastructural changes in parenchyma cells and cell walls can be observed (Barnett *et al.*, 1993), as well as the accumulation of phenol compounds (Schmitt and Liese, 1993) and crystals (Ranjani and Krishnamurthy, 1988) in the cytoplasm.



## Introduction

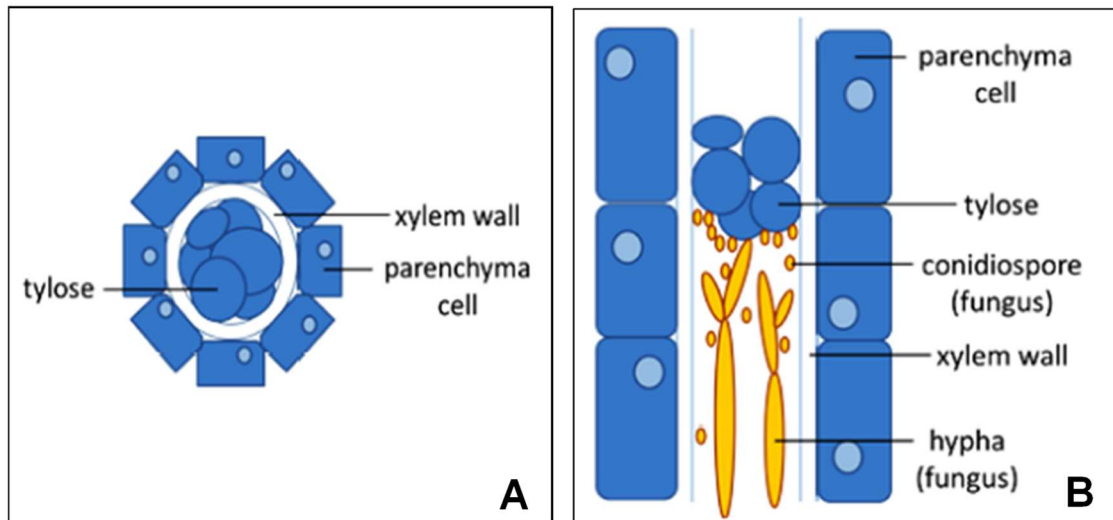


**Figure 1.12: Tylosis formation in the xylem vessels of plants as a pathogen defense mechanism.** **A:** schematic drawing of a cross-section of a resistant plant, which is infected with a vascular pathogen fungi; **B:** schematic drawing of a longitudinal-section of the same infection situation: the tylosis formation is able to stop the spreading of the invading fungi; figure adapted from Yadeta and Thomma (2013).

### 1.6 Through time and defense – does timing matter?

It is no coincidence that farmers sow their seeds on fields at certain seasons and point of time of the day. Fertilization is also not subject to the random principle in some cases, but arises from a certain amount of knowledge and experience value. But what lies behind it? Does time play a role in the defense mechanisms of plants?

#### 1.6.1 Tick-tock: circadian clocks and diurnal rhythms of plants

Every day, plants must defend themselves against pathogens. There is much evidence that the circadian clock plays an important role in regulating the innate immunity of plants (Nürnberg and Brunner, 2002; Roden and Ingle, 2009). This is the internal timekeeping machine, which is essential for the development and growth of the plant (McClung, 2008). The term “circadian” was coined by Franz Halberg in 1959 from the Latin words “circa”=about and “dies”=day (Halberg, 1963). The circadian clock generates rhythms that represent an approx. 24 h period. (Dunlap *et al.*, 2004). A feature of the circadian rhythms is that they can be generated endogenously (McClung, 2000), and sustain themselves as long as they are under constant environmental conditions (light, temperature). These environmental cues are referred to as “Zeitgeber” (Johnson, 1992). Another characteristic feature of circadian rhythms is the so-called temperature compensation. This means that the period remains relatively constant over a range of ambient temperatures (Sawyer *et al.*, 1997; Majercak *et al.*, 1999). The

## Introduction

rhythms are formed by oscillatory changes in transcription and transcriptional regulation. They are generated directly or indirectly by a central oscillator (Doherty and Kay, 2010; McClung, 2011a). In higher plants the central oscillator consists of transcriptional feedback loops and post-translational regulation (Harmer, 2009). The circadian clock is best described in *A. thaliana*, and it appears to be conserved across species (Song *et al.*, 2010). **Figure 1.13** shows a simplified scheme of the central oscillator in *Arabidopsis*. The daily time-keeping is controlled by three interlocking transcription-translation feedback loops (**TTFs**). These are the core loop, the morning loop, and the evening loop. The core loop consists of *TIMING OF CAB 1* (**TOC1**) (Strayer *et al.*, 2000), *CIRCADIAN CLOCK ASSOCIATED 1* (**CCA1**) (Wang and Tobin, 1998) and *LATE ELONGATED HYPOCOTYL* (**LHY**) (Schaffer *et al.*, 1998). **CCA1** and **LHY** are transcription factors while **TOC1** belongs to the transcription regulators (Harmer, 2009; Nakamichi, 2011). In the morning, sunlight activates the expression of **CCA1** and **LHY**, which suppress the transcription of **TOC1**. At the same time **CCA1** and **LHY** activate clock-regulated morning genes, whereas the clock-regulated evening genes may be suppressed. Throughout the day the levels of **CCA1** and **LHY** will decrease, gradually overriding **TOC1**'s suppression and raising the **TOC1** level again. **TOC1** in turn, directly or indirectly induces the expression of **CCA1** and **LHY** and activate clock-regulated evening genes (Nagel and Kay, 2012; Pokhilko *et al.*, 2012).

Relating to a successful pathogenic invasion and consequent disease development, it is necessary that the pathogen, susceptible host and favorable environmental conditions come together at the same time. Conversely, the susceptibility of the host and the virulence of the pathogen may vary with the time of day, as well as the stage of development of the two organisms (Roden and Ingle, 2009). Various publications show that the interaction between plants and their pathogens correlate with light, so there are direct effects of light on both organisms: the plant's defense mechanisms and the virulence of the pathogen (Chandra-Shekara *et al.*, 2006; Griebel and Zeier, 2008; Lu *et al.*, 2017; Oberpichler *et al.*, 2008).

Light has a profound influence on the immunity of plants and often the complete activation of pathogen defense mechanisms is dependent on light (Karpinski *et al.*, 2003; Roberts and Paul, 2006). Genetic studies confirm the earlier hypotheses that plant immunity based on light-dependency is mediated by both photosynthesis and photoreceptor signaling (Roden and Ingle, 2009). Once PAMPs are perceived by the plant, they close their stomata very quickly (Melotto *et al.*, 2006).

## Introduction

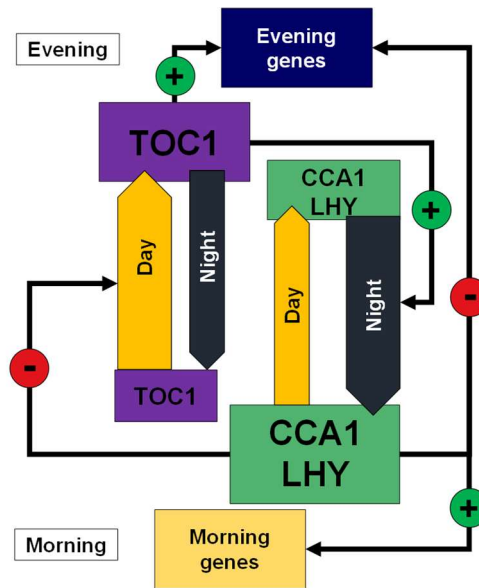


**Figure 1.13: Simplified scheme of the putative role of TOC1, CCA1 and LHY in the central oscillator of *Arabidopsis*.** **Morning:** light induces expression of **CCA1** and **LHY**; **CCA1** and **LHY** suppress the transcription of **TOC1**; simultaneously, **CCA1** and **LHY** activate clock-regulated genes that are expressed early in the day while expression of clock-regulated genes of the evening may be suppressed; during the day the level of **CCA1** and **LHY** decreased, Suppression of **TOC1** also decreased and the level of **TOC1** rises again; **evening:** **TOC1** induces directly or indirectly the expression of **CCA1** and **LHY** and activate clock-regulated evening genes; transcription factors: **CCA1** (CIRCADIAN CLOCK ASSOCIATED 1); **LHY** (LATE ELONGATED HYPOCOTYL); transcriptional regulator: **TOC1** (TIMING OF CAB 1). Adapted from Lüttge (2017).

GRP7 not only participates in stomatal immunity by being part of a peripheral morning loop in the circadian clock (Heintzen *et al.*, 1997), but can also bind to certain PAMP receptor transcripts and upregulate at least one of these transcripts in case of an infection (Nicaise *et al.*, 2013). As discussed earlier, ETI (1.5.2) is a more intrusive defense reaction than PTI and usually leads to PCD in infected tissues of the plant (Spoel and Dong, 2012). The immune receptor *RECOGNITION OF PERONOSPORAPARASITICA 4 (RPP4)* can recognize the effector *Emwa1* in *Hyaloperonospora arabidopsidis* (causal agent of the downy mildew of *A. thaliana*). This process is linked to the core clock component **CCA1**, whose expression in light is highest when the likelihood of *H. arabidopsidis* infection is also highest (McClung, 2011b; Wang *et al.*, 2011). This establishes a direct link between the circadian clock and defense mechanisms (Karapetyan and Dong, 2018). The gene *ISOCHORISMATE SYNTHASE 1 (ICS1)*, which encodes a key enzyme in the biosynthesis of SA (1.5.1), is directed to its expression by the evening-phase clock transcription factor *CCA1 HIKING EXPEDITION (CHE)* (Zheng *et al.*, 2015). Both, gene expression of *ICS1* and the concentration of SA reach the highest peak during the night, possibly in order to be prepared against an infection in the morning. SA not only serves for local defense, but

## Introduction

also plays an important signal function in the aforementioned SAR (1.5.1) (Spoel and Dong, 2012). In contrast to SA, the signal hormone JA (1.5.1), which plays a role especially in the defense mechanisms against necrotrophic pathogens, achieves the highest concentration in the middle of the day (Goodspeed *et al.*, 2012). Another important detail in the light-dependent immunity of plants is the regulation of sulfate assimilation. The key enzyme APR (1.2.2) shows a diurnal rhythm in *Arabidopsis* and maize, which reaches a maximum in the light period (Kocsy *et al.*, 1997; Kopriva *et al.*, 1999). Glutathione synthesis is higher in light than in the dark (Buwalda *et al.*, 1988), but no diurnal change in cysteine and glutathione levels was observed in poplar (Noctor *et al.*, 1997). Other components of sulfur assimilation are also regulated by light, Passera *et al.* (1989) found higher ATPS (1.2.2) activity on irradiated oats, barley and corn. However, the biosynthesis of GSLs does show an ambiguous picture, although they are formed in the course of sulfate assimilation as part of the SDCs (1.5.1), their total content in plants often fluctuate more than the gene expression. Increased levels of GSLs could be observed during the dark period, while the genes involved in it have a low level of expression (Klein *et al.*, 2006). The content of GSLs and the expression of genes involved in the GSL biosynthesis are regulated by a number of factors. In biotic stress defense, these factors can be wounding, jasmonate or pathogen invasion (Mikkelsen *et al.*, 2003; Kuśnierczyk *et al.*, 2007). In *B. oleracea* the GSL and biosynthetic gene levels have been shown to change during a 24 h light-dark cycle, whereby these metabolic fluctuations being primarily influenced by temperature (Rosa *et al.*, 1994; Schuster *et al.*, 2006).

Fact is, plants cannot escape from their pathogens, so mechanisms were developed that help to prevent the invasion of pathogens or to stop or at least mitigate the existing infection. The defense lines are more or less specialized and in parts closely linked to the circadian clock (Wang *et al.*, 2011). Some mechanisms have been identified while others are still unknown. This is mainly because the defense mechanisms are very complex and may also vary depending on the specific host-pathogen interaction system. Therefore, several factors play a role in successful defense against pathogens: environmental conditions, type of infection, access to nutrients, sulfur supply and possibly the right timing. These take affect for both, plant host and pathogen.

## Introduction

### 1.7 Aims of the thesis

Previous inoculation experiments with *V. longisporum* and its preferred host plant *B. napus* and subsequent sufficient and deficient sulfur fertilization demonstrated a correlation between higher amounts of incorporated sulfur and an increase of GSL levels in infected plants. Based on these observations the following hypotheses were postulated: “A specific time point of infection influences the success and/or severity of the infection” and “The fertilization with sufficient sulfur influences the course of the infection and the defense mechanisms of the plants positively.”

A first goal was to modify the existing inoculation system with *V. longisporum* for testing the hypotheses. To examine the influence of sulfur, infected and non-infected plants were fertilized with sufficient and deficient sulfur supply. In addition, experiments with older *B. napus* plants previously fertilized with different amounts of sulfur were performed with the same inoculation system. In order to find differences between the infected and non-infected plants fertilized with different levels of sulfur, analyses were conducted with respect to the elemental content (sulfur, calcium, potassium and iron), GSL and thiol levels (cysteine and glutathione). To quantify a successful infection a detection method via qPCR with primer systems known from the literature was established. Another goal was the histological examination based on literature references of the hypocotyls of infected plants upon the formation of occlusions in the xylem vessels, whereby a possible influence of the different sulfur inputs and the different inoculation time points were investigated. Besides the used staining method with toluidine blue, further staining methods were tried.

## 2. Material and methods

### 2.1 Plant material

For the experiments the winter OSR cultivar Genie from the Deutsche Saatveredelung AG (DSV) (Lippstadt, Germany; breeder: RAPOOL-Ring GmbH, Isernhagen, Germany) was used. Genie is an MSL-hybrid (Male Sterility Lembke) (Frauen and Paulmann, 1999) with a high GSL content in seeds, and a low to medium susceptibility to *Sclerotinia sclerotiorum* (disease: stem rot) ([http://sorten.lh-hessen.de/sb\\_ausgabe\\_raw.php](http://sorten.lh-hessen.de/sb_ausgabe_raw.php), accessed 02.10.2019). In addition, Genie has a valid overall health and an excellent resistant against aggressive stem canker triggering pathogens (*Leptosphaeria maculans*, asexual stage is *Phoma lingam*; *L. biglobosa*) (Sortenkatalog Winterraps 2012 RAPOOL).

#### 2.1.1 Plant seed surface sterilisation

Before the cultivation of the plants could begin, the seeds of OSR cultivar Genie had first to undergo a surface sterilization to remove the disinfectant and any microorganisms (**Table 2.1**). In a 50 ml Falcon tube, the needed amount of seeds were covered with 1.2% (v/v) sodium hypochlorite solution (NaOCl) and mixed for 5 min. The NaOCl was removed with a disposable pipette and the seeds were covered with 95% (v/v) ethanol (EtOH) and mixed for 1 min. The EtOH was removed with a disposable pipette and the seeds were thoroughly washed 1 min with autoclaved desalted water. This washing procedure was repeated three times. Subsequently, the seeds were transferred to a sterile petri dish to be placed on plates with solidified sufficient sulfur supply Blake-Kalff (BK) medium (Blake-Kalff *et al.*, 1998).

**Table 2.1: Solutions and duration of treatment for the surface sterilisation of *Brassica napus* seeds.**

Solutions	1.2% NaOCl solution (v/v)	95% ethanol (v/v)	Autoclaved desalted water
Duration of treatment	5 min	1 min	1 min, 3 times

## Material and methods

### 2.1.2 Blake-Kalff medium

The BK medium was prepared in altogether six 100x concentrated stock solutions (Table 2.2) and stored in the refrigerator (+2°C). Table 2.2 lists the molar concentrations of the individual substances. The micronutrients stock solution consisted of seven substances as described. For sufficient sulfur supply the **1 mM MgSO<sub>4</sub>** (full sulfur supply, optimal growth conditions, **+S**) stock solution was mixed with the three macronutrient stock solutions and with the micronutrients stock solution. For deficient sulfur supply the **0.01 mM MgSO<sub>4</sub>** (severe sulfur limitation, **-S**) stock solution was mixed with the three macronutrient stock solutions and with the micronutrients stock solution. All stock solutions were prepared with desalted water and the pH adjusted to 5.5 with potassium hydroxide (KOH). The same procedure is carried out for the preparation of the plates, in addition, the BK medium is mixed with 8 g L<sup>-1</sup> gelrite and subsequently autoclaved. The preparation of the plates were performed under the clean bench, where the still warm BK medium was filled up into plates. Until use, they were kept in the refrigerator (+2°C), where they were perishable for about six months.

**Table 2.2: Description of the composition of the stock solutions for Blake-Kalff medium.**

Molar concentration	Substance	Manufacturer
<b>I. Stock solutions for sufficient<sup>1</sup> sulfur or deficient<sup>2</sup> sulfur supply</b>		
1 mM	MgSO <sub>4</sub>	Carl Roth, Karlsruhe, Germany
0.01 mM	MgSO <sub>4</sub>	
<b>II. Macronutrient stock solutions (3 separate stock solutions)</b>		
2 mM	Ca(NO <sub>3</sub> ) <sub>2</sub>	Carl Roth, Karlsruhe, Germany
1 mM	NH <sub>4</sub> H <sub>2</sub> PO <sub>4</sub>	
3 mM	KNO <sub>3</sub>	
<b>III. Micronutrients stock solution (1 stock solution)</b>		
50 µM	KCl	Carl Roth, Karlsruhe, Germany
25 µM	H <sub>3</sub> BO <sub>3</sub>	Sigma-Aldrich Chemie GmbH, Munich, Germany
2 µM	MnCl <sub>2</sub>	Merck KGaA, Darmstadt, Germany
2 µM	ZnCl <sub>2</sub>	AppliChem GmbH, Darmstadt, Germany
0.5 µM	CuCl <sub>2</sub>	Carl Roth, Karlsruhe, Germany
0.5 µM	(NH <sub>4</sub> ) <sub>6</sub> MO <sub>7</sub> O <sub>24</sub>	Merck KGaA, Darmstadt, Germany
20 µM	C <sub>10</sub> H <sub>12</sub> FeN <sub>2</sub> NaO <sub>8</sub>	Sigma-Aldrich Chemie GmbH, Munich, Germany

<sup>1</sup> For a sufficient sulfur supply: 1 mM MgSO<sub>4</sub>

<sup>2</sup> For a deficient sulfur supply: 0.01 mM MgSO<sub>4</sub>

## Material and methods

### 2.1.3 Cultivation of *Brassica napus* in climatic chambers

For infection experiments, surfaced sterilised (**Table 2.1**) *B. napus* seeds were placed on BK plates with a sterile spring steel forceps (**2.1.2**; preparation of BK plates). For this, the plates were set upright and with a heated spatula, about a third of the medium was removed in the upper area. Subsequently, 30 seeds were transferred to the resulting surface in two rows. The plates were sealed with parafilm and placed upright in JC climatic chambers equipped with ESC 300 software interface (Johnson Controls; Mannheim, Germany). The seeds needed 7 d under specific settings (12 h light, 22°C, 70% humidity; 12 h night, 20°C, 70% humidity; Photosynthetic Photon Flux Density (PPFD): 480  $\mu\text{mol m}^{-2} \text{s}^{-1}$ ; lamp type CMT 360 LS/W/BH-E40) (Eye Lighting Europe Ltd., Uxbridge, United Kingdom), to germinate, and to be ready for subsequent inoculation experiments.

### 2.2 *Verticillium longisporum* strain

For the infection *V. longisporum* strain VL43 WT (wildtype) was obtained from Prof. Dr. Andreas von Tiedemann (Department of Crop Sciences, Division of Plant Pathology and Crop Protection, Georg-August-University, Göttingen, Germany). The strain was first isolated from OSR in Mecklenburg/Germany in 1990 (Zeise and von Tiedemann, 2001).

#### 2.2.1 *Verticillium longisporum* growth and cultivation

Two media from Difco™ were used for the cultivation of *V. longisporum*, which were prepared as specified by the manufacturer (**Table 2.3**). In order to achieve a uniform mycelium formation, and the highest possible sporulation rate in *V. longisporum*, the fungi was cultivated in two steps. For the first step of cultivation of the fungi, potato dextrose broth (PDB) was set up under sterile conditions in 500 ml glass flasks and autoclaved. 900  $\mu\text{l}$  of glycerol VL43 spore stock solution ( $1 \times 10^6$  spores per ml) were pipetted into the medium, the glass flask was wrapped with aluminum foil and got shaken at 22°C and 120 rpm. After 2 to 3 weeks, in the second step the mycelium was separated under sterile conditions with the aid of gaze (0.2  $\mu\text{m}$ ) and transferred to 500 ml glass flasks with 250 ml of autoclaved Czapek-Dox broth (CDB). The glass flask was wrapped with aluminum foil and got shaken at 22°C and 110 rpm for 2 more weeks.



## Material and methods

**Table 2.3: Media for the cultivation of *V. longisporum* in shaking cultures.**

Media	Weighed portion per litre	Ingredients per litre
Difco™ Potato Dextrose Broth	24 g	Potato starch 4.0 g Dextrose 20.0 g
Difco™ Czapek-Dox Broth	35 g	Saccharose 30.0 g Sodium nitrate 3.0 g Dipotassium phosphate 1.0 g Magnesium sulfate 0.5 g Potassium chloride 0.5 g Ferrous sulfate 0.01 g

### 2.2.2 Preparation of *Verticillium longisporum* spore stock solutions

Shaking cultures of *V. longisporum* were prepared as described in section 2.2.1. Under sterile conditions, the mycelium was separated with the aid of gaze (0.2 µm). The spores were collected in 500 ml glass flasks. In each case, 35 ml of the spore solution were transferred into 50 ml Falcon tubes and centrifuged at 4°C and 1,500 g for 15 min. Subsequently, the supernatant of all Falcon tubes was discarded to 1000 µl, in which the spores were resuspended. The collected spore fractions were combined and the concentration of the spore solution was determined with a Thoma chamber (depth: 0.1 mm; area: 0.0025 mm<sup>2</sup>). Sterilized glycerol was added until the final concentration was  $1 \times 10^6$  spores per ml. The spore stock solution were aliquoted in 2 ml tubes and were stored at -80°C until inoculation experiments.

## 2.3 Various inoculation procedures of *Brassica napus* with *Verticillium longisporum*

### 2.3.1 Inoculation of 16 d old *B. napus* plants (previous fertilization with different sulfur supply) with mycelium-spore mixture of *V. longisporum*

For infection experiments, *B. napus* and *V. longisporum* were cultivated as described in section 2.1.3 and 2.2.1. The required amount of *B. napus* seedlings was taken from the BK plates and transferred to pots filled with autoclaved sand and placed for 9 d in the climatic chambers under specific conditions (2.1.3). Before inoculation with *V. longisporum* the plants were watered with desalted water for the first 3 d and then fertilized with different sulfur supply (+S/-S; 2.1.2) for the remaining 6 d (150 ml each pot). After being pulled out of the sand pots, the roots of the plants were washed with aqua pure before, and placed in glass petri dishes. The glass flasks in which *V. longisporum* has grown, were shaken before removal of the mycelium-spore mixture.

## Material and methods

Into the petri dishes were added 100 ml of the mycelium-spore mixture. The area of the roots was covered with aluminium foil. The control plants were removed in the same manner and the roots were mock-inoculated with 100 ml of autoclaved CDB (**Table 2.3**). The area of the roots was also covered with aluminium foil. The inoculation time was 45 min. Afterwards plants were transferred to pots filled with autoclaved sand (0-2 mm grain size) (Hornbach, Hannover, Germany), and placed in the climatic chambers under specific conditions (**2.1.3**). Care was taken to ensure that the differently treated plants were inoculated with respect to their sulfur supply in various glass petri dishes and subsequently transferred back to the same pot.

### **2.3.2 Inoculation of 16 d old *B. napus* plants (previous fertilization with different sulfur supply) with different dilutions of mycelium-spore mixture of *V. longisporum***

Same procedure as described in section **2.3.1** with following modification concerning to the mycelium-spore mixture: different dilutions of mycelium-spore mixtures for inoculation were tried: **Inoc I**, undiluted mycelium-spore stock solution (50 g mycelium-spore mixture with 50 ml CDB), **Inoc II**, 1:2 dilution (25 g mycelium-spore mixture with 75 ml CDB) and **Inoc III**, 1:10 dilution (10 g mycelium-spore mixture with 90 ml CDB).

### **2.3.3 Inoculation of 7 d old *B. napus* seedlings with mycelium-spore mixture of *V. longisporum***

For infection experiments, *B. napus* and *V. longisporum* were cultivated as described in section **2.1.3** and **2.2.1**. After 7 d the required amount of *B. napus* seedlings was taken from the BK plates and placed with the root in glass petri dishes. Inoculation procedure is the same as described in section **2.3.1**. Afterwards plants were transferred to pots filled with autoclaved sand, or with a 1:1 mixture of sand and soil (Einheitserde) respectively, and placed in the climatic chambers under specific conditions (**2.1.3**). Depend on the chosen substrate, plants in sand were watered for 3 d, plants in sand/soil mixture were watered for 7 d with desalted water.

### **2.3.4 Inoculation of 7 d old *B. napus* seedlings with spore solution of *V. longisporum***

Same procedure as described in section **2.3.3** with following modification: instead of using mycelium-spore mixture for inoculation, a *V. longisporum* spore solution were used with a concentration of  $1 \cdot 10^6$  spores mL<sup>-1</sup> (see **2.2.2**; instead of sterilized glycerol to adjusted the final concentration, there was used CDB). Afterwards plants were transferred to pots filled with autoclaved sand, and placed in the climatic chambers under specific conditions (**2.1.3**).

## 2.4 General experimental design: the definition of different time-points of inoculation (TPIs)

In order to investigate the influence of diurnal rhythm on the infection with *V. longisporum*, four TPIs (**Fig. 2.1**) were defined for the inoculation. The selection of TPIs is based on the work of Weese *et al.* (2015). The **TPI I** (0 h) was 1 h before the onset of light in the climatic chambers. The **TPI II** (4 h) was 3 h after the onset of light. The **TPI III** (12 h) was 1 h before the offset of light, and the **TPI IV** (16 h) was 3 h after the offset of light. The inoculation of the plants was coordinated in time, so that the potted plants were transferred to the climatic chambers regarding to each TPI (I-IV).

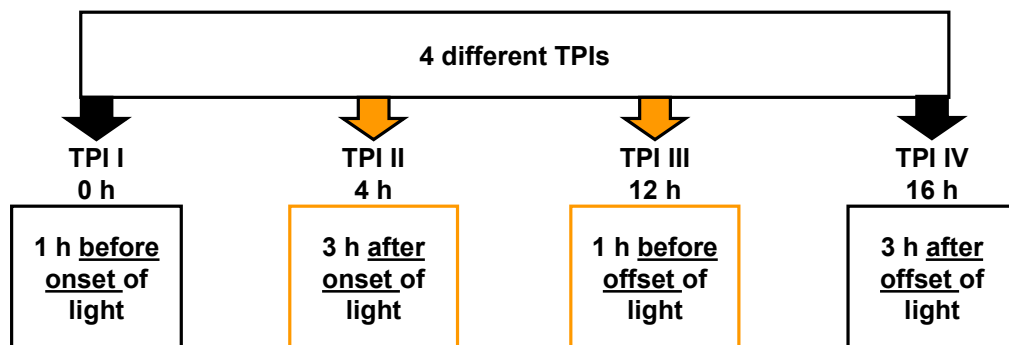


**Figure 2.1: General experimental design: four different TPIs for the inoculation procedure.** TPI I (0 h): 1 h before the onset of light; TPI II (4 h): 3 h after the onset of light; TPI III (12 h): 1 h before the offset of light; TPI IV (16 h): 3 h after the offset of light; inoculation of plants was coordinated in time, so that the potted plants were transferred to the climatic chambers regarding to each TPI.

The following experiments are all based on the same TPIs. The experiments differ with respect to the number and age of plants, type of inoculation, and the substrate, in which the inoculated plants were transferred.

## 2.5 Preliminary inoculation experiments of *Brassica napus* with *Verticillium longisporum* under diurnal rhythmic and with different sulfur supply

Before the experiments under diurnal rhythms and with different sulfur fertilization started, there were a few experiments that focused only on the inoculation with *V. longisporum*. However, it turned out that the used spore stocks were no longer vital and so the infection did not work. These experiments are therefore not shown.

### 2.5.1 Pre-experiment I: inoculation of 7 d old plants with mycelium-spore mixture and subsequent cultivation in sand/soil mixture

For the first pre-experiment 288 seeds of *B. napus* cultivar Genie were grown on BK plates (2.1.3). The inoculation procedure is described in 2.3.3. For each TPI 36 plants were mock-inoculated (control plants) and 36 plants were inoculated with mycelium-spore mixture (VL-infected plants) (Fig. 2.1; 2.2). After inoculation the plants were transferred to pots (8 diameter) filled with a mixture of 1:1 sand and soil.

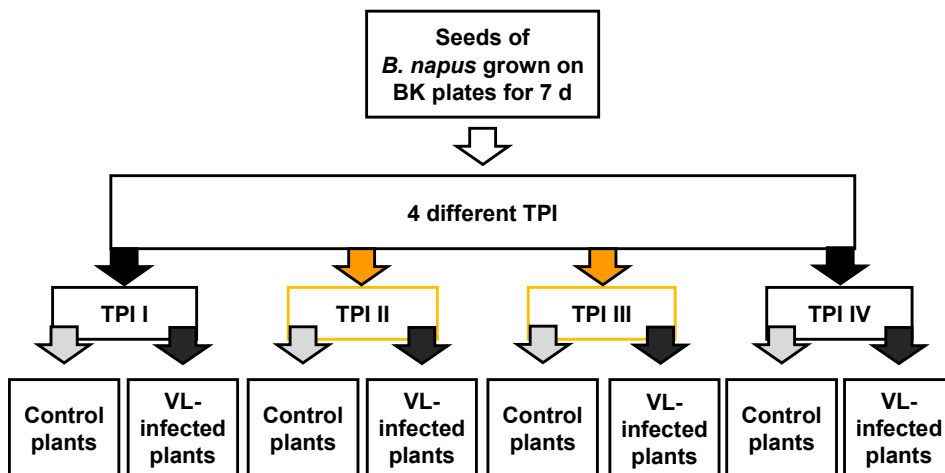


**Figure 2.2: Experimental design with 7 d old seedlings of *B. napus*: different TPIs with *V. longisporum*.** Seeds of *B. napus* cultivar Genie were grown on solidified BK plates containing 1 mM MgSO<sub>4</sub>; inoculation of 7 d old plants was carried out at 4 different TPIs (TPI I-IV); for each TPI **control plants** were mock-inoculated with CDB and **VL-infected plants** were inoculated with mycelium-spore mixture.

Both groups (control and VL-infected plants) were divided into two further groups for each TPI. At the end there were eight control groups and eight VL-infected groups consisted of each 18 plants per trait. The subdivision was necessary to perform sufficient and deficient sulfur supply with BK medium (+S/-S; 2.1.2). During the first 7 days post inoculation (dpi) all groups were watered only with desalted water in order to protect the plants from additional stress. Thereafter, the pots were fertilized in addition to the desalted water with respect to their sulfur supply group with the corresponding

## Material and methods

BK medium (+S/-S; 2.1.2) (Fig. 2.3). Every pot was fertilized with 150 ml of BK medium weekly.

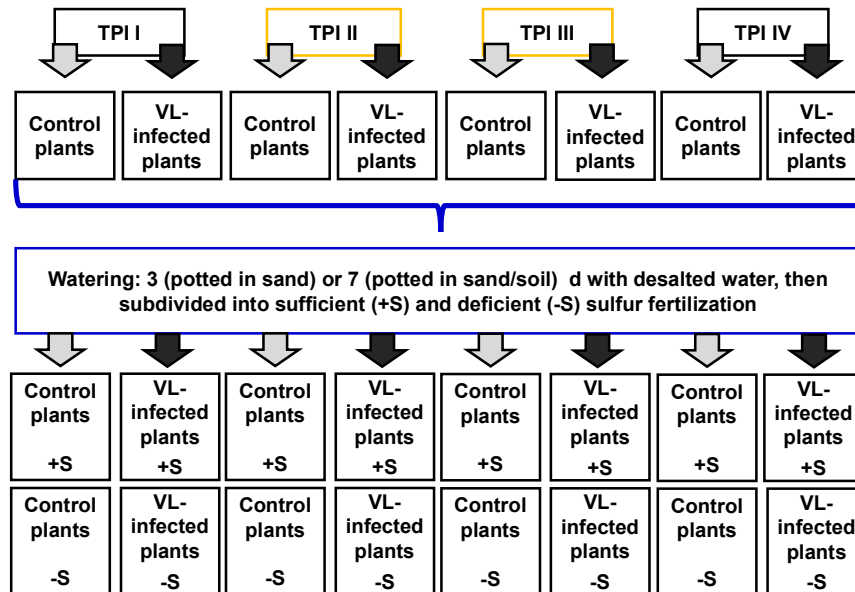


**Figure 2.3: Experimental design with 7 d old seedlings of *B. napus* potted in sand or sand/soil mixture: classification of inoculation groups with respect to the different sulfur fertilization.** After inoculation: two groups each TPI: control and VL-infected plants; after 3 or 7 d of watering (depends on chosen substrate) with desalted water: subdivision of the two groups in two more groups: one group each control and VL-infected plants were fertilized with sufficient (BK-medium with 1 mM MgSO<sub>4</sub>; +S) and the other two groups with deficient (BK medium with 0.01 mM MgSO<sub>4</sub>; -S) sulfur supply (150 ml each pot/weekly).

For **pre-experiment I** Table 2.4 shows the course of fertilization, harvesting at specific dpi, sample size of each group and conducted methods. At 7 dpi six plants and at 14 and 21 dpi three plants from each group were harvested without roots and frozen directly in liquid nitrogen. The frozen samples were grounded to a fine powder in a mortar under liquid nitrogen and subjected to various methods. For histological examination the hypocotyl of one plant per group was harvested at 14 dpi and 21 dpi and initially conserved in formaldehyde-alcohol-acetic acid (FAA).

## Material and methods

**Table 2.4: Pre-experiment I: overview of the course of fertilization, sampling and conducted methods.** Samples of 7 dpi were not fertilized with different sulfur supply.

Fertilization	Harvesting	Sample size of each group	Method
Desalted water as required	7 dpi	6 plants without roots	DNA-extraction qPCR <sup>2</sup> Elemental analysis via ICP-OES <sup>3</sup>
Desalted water as required and corresponding BK medium (+S/-S) <sup>1</sup> : 150 ml each pot weekly	14 dpi	3 plants without roots Histology: hypocotyl of 1 plant	DNA-extraction qPCR <sup>2</sup> Elemental analysis via ICP-OES <sup>3</sup> GSL <sup>4</sup> analysis via HPLC <sup>5</sup> Histology: Toluidine blue staining
	21 dpi	3 plants without roots Histology: hypocotyl of 1 plant	DNA-extraction qPCR <sup>2</sup> Elemental analysis via ICP-OES <sup>3</sup> GSL <sup>4</sup> analysis via HPLC <sup>5</sup> Histology: Toluidine blue staining

<sup>1</sup> +S BK medium with 1 mM MgSO<sub>4</sub>; -S BK medium with 0.01 mM MgSO<sub>4</sub>; start of fertilization after 7 dpi

<sup>2</sup> qPCR: real-time quantitative polymerase chain reaction

<sup>3</sup> ICP-OES: inductively coupled plasma optical emission spectrometry

<sup>4</sup> GSL: glucosinolate

<sup>5</sup> HPLC: high performance liquid chromatography

### 2.5.2 Pre-experiment II: inoculation of 16 d old plants (previous fertilization with different sulfur supply) with mycelium-spore mixture and subsequent cultivation in sand

In addition to the influence of diurnal rhythm and different sulfur supply (+S/-S; 2.1.2) of the course of infection, an attempt was made to examine the influence of different sulfur fertilization on the TPIs. **Figure 2.4** shows the experimental design: 160 seeds of *B. napus* cultivar Genie were grown on BK plates (2.1.3) and transferred to pots (10 diameter) filled with autoclaved sand. Plants were watered for 3 d with desalted water. Subsequently, plants were divided into two groups, one group was fertilized with sufficient and the other with deficient sulfur supply (+S/-S; 2.1.2) for 6 d. The plants were inoculated as described in section 2.3.1 at the known TPIs (**Fig. 2.1**). Each group consisted of 10 plants.

## Material and methods

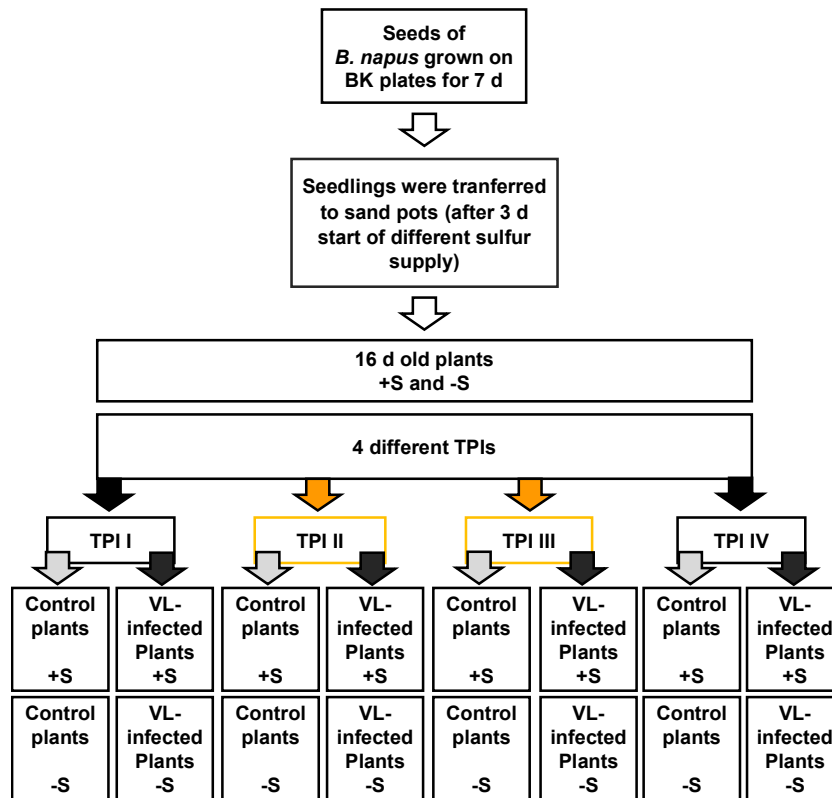


**Figure 2.4: Experimental design with previous fertilized 16 d old plants of *B. napus*: different TPIs of inoculation with *V. longisporum*.** Seeds of *B. napus* cultivar Genie were grown on solidified BK plates containing 1 mM MgSO<sub>4</sub> in climatic chambers; after 7 d: seedlings were transferred in sand pots for 9 more d; desalted water for 3 d; during the next 6 d, 150 ml BK medium each pot (sufficient sulfur supply: 1 mM MgSO<sub>4</sub>; +S; deficient sulfur supply: 0.01 mM MgSO<sub>4</sub>; -S); inoculation of 16 d old plants was carried out at four different TPIs.

Care was taken to ensure that the differently treated plants were inoculated with respect to their sulfur supply in various glass petri dishes and subsequently transferred back to the same pot. During the first 3 dpi all groups were watered only with desalted water. Thereafter, the pots were fertilized in addition to the desalted water with respect to their sulfur supply group with the corresponding BK medium (+S/-S; 2.1.2).

For the **pre-experiment II** Table 2.5 shows the course of fertilization, harvesting at specific dpi, sample size of each group and conducted methods. At 7 dpi four plants without roots and at 15 dpi four plants with separated roots from each group were harvested and frozen directly in liquid nitrogen. The frozen samples were grounded to a fine powder in a mortar under liquid nitrogen and subjected to various methods.

## Material and methods

**Table 2.5: Pre-experiment II: overview of the course of fertilization, sampling and conducted methods.**

Fertilization	Harvesting	Sample size of each group	Method
<b>Desalted water as required and corresponding BK medium (+S/-S)<sup>1</sup>: 150 ml each pot weekly</b>	7 dpi	4 plants without roots	DNA-extraction qPCR <sup>2</sup> Elemental analysis via ICP-OES <sup>3</sup>
	15 dpi	4 plants and separated roots	DNA-extraction qPCR <sup>2</sup> Elemental analysis via ICP-OES <sup>3</sup>

<sup>1</sup> +S BK medium with 1 mM MgSO<sub>4</sub>; -S BK medium with 0.01 mM MgSO<sub>4</sub>; start of fertilization after 3 dpi

<sup>2</sup> qPCR: real-time quantitative polymerase chain reaction

<sup>3</sup> ICP-OES: inductively coupled plasma optical emission spectrometry

### **2.5.3 Pre-experiment IIIa: inoculation of 16 d old plants (previous fertilization with different sulfur supply) with different dilutions of mycelium-spore mixtures and subsequent cultivation in sand**

The aim of this pre-experiment was to try three different dilutions of the mycelium-spore mixtures for inoculation of older plants. The inoculation procedure is described in section 2.3.2. For inoculation **TPI III** was selected (**Fig 2.1**). **Figure 2.5** shows the performance of inoculation: 108 plants were mock-inoculated and 108 plants were inoculated with different mycelium-spore mixture as follows: **Inoc I**: 18 +S- and 18 -S-plants; **Inoc II**: 18 +S- and 18 -S-plants; **Inoc III**: 18 +S- and 18 -S-plants. During the first 3 dpi all groups were watered only with desalted water. Thereafter, the pots were fertilized in addition to the desalted water with respect to their sulfur supply group with the corresponding BK medium (**+S/-S; 2.1.2**). At 1 and 3 dpi six hypocotyls of each group were harvested and frozen directly in liquid nitrogen. At 7 and 14 dpi three hypocotyls of each group were harvested and frozen directly in liquid nitrogen. The frozen samples were grounded to a fine powder in a mortar under liquid nitrogen and subjected to DNA-extraction (**2.7.1**) and subsequent qPCR analysis (**2.7.2**).



## Material and methods

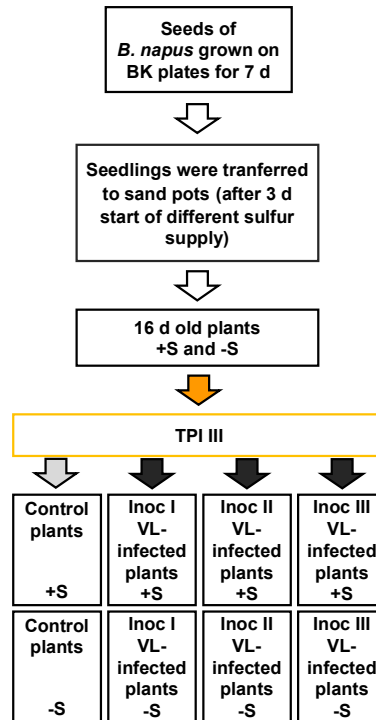


**Figure 2.5: Experimental design with previous fertilized 16 d old plants of *B. napus*: different dilution of mycelium-spore mixtures of *V. longisporum*.** Seeds of *B. napus* cultivar Genie were grown on solidified BK plates containing 1 mM MgSO<sub>4</sub> in climatic chambers; after 7 d: seedlings were transferred in sand pots for 9 more d; desalted water for 3 d; during the next 6 d, 150 ml BK medium each pot (sufficient sulfur supply: 1 mM MgSO<sub>4</sub>; +S; deficient sulfur supply: 0.01 mM MgSO<sub>4</sub>; -S); inoculation of 16 d old plants was carried out at **TPI III**; **Inoc I**: undiluted mycelium-spore stock solution; **Inoc II**: 1:2 dilution; **Inoc III**: 1:10 dilution.

### 2.5.4 Pre-experiment IIIb: inoculation of 16 d old plants (previous fertilization with different sulfur supply) with diluted mycelium-spore mixture and subsequent cultivation in sand

The inoculation procedure is described in section 2.3.2. In the **pre-experiment IIIa**, described in section 2.5.3 the inoculation with different dilutions of mycelium-spore mixtures was investigated, whereby the **1:10 dilution** seemed to be the most promising. For each TPI 20 +S- and 20 -S-plants were mock-inoculated and 20 +S- and 20 -S-plants were inoculated with 1:10 diluted mycelium-spore mixture (see **Fig. 2.4** for the experimental design). The experiment was conducted in the same manner as the **pre-experiment II (2.4.2)**. At 3, 7 and 14 dpi five plants from each group were harvested without roots and frozen directly in liquid nitrogen. The frozen samples were grounded to a fine powder in a mortar under liquid nitrogen and subjected to DNA-extraction (2.7.1) and subsequent qPCR analysis (2.7.2).

### **2.5.5 Pre-experiment IV: inoculation of 7 d old plants with spore solution and subsequent cultivation in sand**

The inoculation procedure was performed as described in section **2.3.4**. The experimental design based on **Figure 2.3**. 432 seeds of *B. napus* cultivar Genie were grown on BK plates (**2.1.3**). For each TPI 54 plants were mock-inoculated and 54 plants were inoculated with a spore solution. After inoculation the plants were transferred to pots (7 diameter) filled with sand. Both groups (control and VL-infected) were divided into two further groups for each TPI. Each group consisted of 27 plants per trait. At 3, 7 and 14 dpi eight plants from each group were harvested without roots and frozen directly in liquid nitrogen. The frozen samples were grounded to a fine powder in a mortar under liquid nitrogen and subjected to DNA-extraction (**2.7.1**) and subsequent qPCR analysis (**2.7.2**).

### **2.6 Main experiment: inoculation of *Brassica napus* with *Verticillium longisporum* under diurnal rhythmic and with different sulfur supply**

#### **2.6.1 Experimental design: different time-points of inoculation of 7 d old plants with mycelium-spore mixture and different sulfur supply**

The procedure of the main experiment is based and described under **2.5.5** (number of plants, division into different sulfur supply groups), using mycelium-spore mixture instead of spores. The inoculation procedure was performed as described in section **2.3.3** with transfer of the inoculated plants to sand pots (7 diameter) (**Fig. 2.3**). The four TPIs shown in **Figure 2.1** were used for the inoculation. This experiment was performed twice in succession.

For the experiment **Table 2.6** shows the course of fertilization, harvesting at specific dpi, sample size of each group and conducted methods. At 3, 7 and 14 dpi eight plants from each group were harvested without roots and frozen directly in liquid nitrogen. The frozen samples were grounded to a fine powder in a mortar under liquid nitrogen and subjected to various methods. For histological examination the hypocotyl of one plant per group was harvested at 14 dpi and 21 dpi and initially conserved in FAA. On each harvest d a photographic documentation of three selected plants per group was made. The procedure of methods listed in **Table 2.6** are described in detail in section **2.7**.

## Material and methods

**Table 2.6: Main experiment: overview of the course of fertilization, sampling and conducted methods.**

Fertilization	Harvesting	Sample size of each group	Method
<b>Desalted water as required</b>	3 dpi	8 plants without root	DNA-extraction qPCR <sup>2</sup>
<b>Desalted water as required and corresponding BK medium (+S/-S)<sup>1</sup>: 150 ml each pot weekly</b>	7 dpi	8 plants without root	DNA-extraction qPCR <sup>2</sup> Elemental analysis via ICP-OES <sup>3</sup> GSL <sup>4</sup> analysis via HPLC <sup>5</sup> Cysteine and glutathione analysis via HPLC <sup>5</sup>
	14 dpi	8 plants without root Histology: hypocotyl of 1 plant	DNA-extraction qPCR <sup>2</sup> Elemental analysis via ICP-OES <sup>3</sup> GSL <sup>4</sup> analysis via HPLC <sup>5</sup> Cysteine and glutathione analysis via HPLC <sup>5</sup> Histology: Toluidine blue staining
	21 dpi	Only Histology: hypocotyl of 1 plant	Histology: Toluidine blue staining

<sup>1</sup> +S BK medium with 1 mM MgSO<sub>4</sub>; -S BK medium with 0.01 mM MgSO<sub>4</sub>; start of fertilization after the first sampling at 3 dpi

<sup>2</sup> qPCR: real-time quantitative polymerase chain reaction

<sup>3</sup> ICP-OES: inductively coupled plasma optical emission spectrometry

<sup>4</sup> GSL: glucosinolate

<sup>5</sup> HPLC: high performance liquid chromatography

### 2.7 Analytical methods

#### 2.7.1 DNA-extraction

The DNeasy Plant Mini Kit (Qiagen, Hilden, Germany) was used for DNA-extraction of *V. longisporum* from *B. napus*. The extraction was carried out as specified by the manufacturer with the following modifications. For each sample approx. 50 mg of grounded and frozen plant material was used. After the incubation step at 65°C the tubes were placed on ice for about 1-2 min to cool down to room temperature. The centrifugation steps to be performed according to the protocol at 20,000 *g* were carried out at 16,100 *g*. In order to remove the residual EtOH from the spin column the tubes were left open for approx. 1-2 min at room temperature (RT) prior elution only once with 50  $\mu$ l Buffer AE. The DNA concentration of the samples was determined photometric at 260 nm with a Microplate-Reader (Synergy Mix, Multi-Mode Microplate Reader) (BioTek Instruments GmbH, Bad Friedrichshall, Germany).

#### 2.7.2 Real-time quantitative PCR

The real-time quantitative polymerase chain reaction (qPCR) was used for the detection and quantification of *V. longisporum* DNA in *B. napus*. The qPCR works with two fluorescent dyes, contained in the used Platinum® SYBR® Green qPCR SuperMix UDG with ROX (Invitrogen™ by Thermo Fisher Scientific GmbH, Dreieich, Germany). The measuring dye (SYBR Green I) is an intercalating dye, that fluoresce when incorporated in a DNA double strand. As a result the fluorescence signal increases as the amplification progresses. The fluorescence of the reference dye (ROX), however, is not dependent on the nucleic acid content and serves to correct differences in the measurement of the individual samples. **Table 2.7** shows the sample preparation for qPCR analysis. For the samples a master mix without template DNA was prepared. 18  $\mu$ l of master mix were placed in the 96-well plates (96-well PCR plates; white; without frame; 0.2 ml) (VWR International GmbH, Darmstadt, Germany), to which 2  $\mu$ l diluted sample DNA (final concentration between 0.5-1 ng  $\mu$ l<sup>-1</sup>), standard DNA of *V. longisporum* or aqua pure (negative controls) were pipetted. For the standard series 1 ng  $\mu$ l<sup>-1</sup>-standard-DNA was prepared from extracted DNA of pure *V. longisporum* VL43 culture (standard series from 1 ng VL-DNA  $\mu$ l<sup>-1</sup> to approx. 1 pg VL-DNA  $\mu$ l<sup>-1</sup>).

## Material and methods

**Table 2.7: Overview of sample preparation for qPCR.** A master mix is used for samples (without template DNA).

Solution	Amount in [ $\mu$ l]
qPCR SuperMix 2x	10
Aqua pure	7.2
Forward Primer <sup>1</sup>	0.4
Reverse Primer <sup>1</sup>	0.4
Template DNA	2

<sup>1</sup> Concentration of primers: 10 pmol  $\mu$ l<sup>-1</sup>

The primers targeting the multicopy ribosomal internal transcribed spacer (ITS) gene region are based on detailed analyses of *Verticillium* ITS sequences (Fahleson *et al.*, 2004; Nazar *et al.*, 1991; Robb *et al.*, 1993). For this study the primer pair OLG70/OLG71 (Table 2.8) from the work of (Eynck *et al.*, 2007) were selected, which were modified for the used qPCR program (Table 2.9). In addition, another for this study modified primer pair (VLTubF2/VLTubR1; Table 2.8) was used for the qPCR specifically targeting the  $\beta$ -tubulin gene from *V. longisporum* isolates (Debode *et al.*, 2011).

**Table 2.8: List of primers used for qPCR.**

Primer	Direction	Gene target	Sequence (5' → 3')	Amplicon size
OLG 70 <sup>1</sup>	Forward	ITS	CGCAGCGAAACGCGATATGTAG	265 bp
OLG 71 <sup>1</sup>	Reverse		CGGGCTTGTAGGGGGTTTAGA	
VLTubF2 <sup>2</sup>	Forward	$\beta$ -tubulin	CGCAAACCCTACCGGGTTATG	145 bp
VLTubR1 <sup>2</sup>	Reverse		GAGATATCCATCGGACTGTTCGTA	

<sup>1</sup> Reference: Eynck *et al.* (2007); modified

<sup>2</sup> Reference: Debode *et al.* (2011); modified

The qPCR analysis was performed with the 7300 Real Time System (Applied Biosystems by Thermo Fisher Scientific, Californian, USA). The software used was Abi 7300 System SDS (Applied Biosystems by Thermo Fisher Scientific, Californian, USA). The used qPCR program consisted of four stages (Table 2.9) starting with a 50°C step for 2 min. This step is necessary, because the used qPCR SuperMix contains uracil-DNA glycosylase (UDG). The incubation step of UDG before PCR cycling destroys any contaminated deoxyuridine (dU)-containing products from previous reactions and eliminates carry-over contamination (Longo *et al.*, 1990). In stage 2 (initial denaturation) UDG is inactivated by the high temperature of 95°C, allowing the amplification of desired target sequences. The melting curve serves to distinguish potential primer dimers and non-specific amplification products.

## Material and methods

**Table 2.9: Overview of the different stages with temperature and time specification of the used qPCR program.**

Stage	Temperature in [°C]	Time in [min:sec]	Cycles
Inactivation of carry-over contamination	50	2:00	1
Initial denaturation	95	2:00	1
Denaturation	95	0:15	40
Annealing and elongation <sup>1</sup>	60	1:00	
Melting curve <sup>2</sup>	60-95	0:01	117

<sup>1</sup> Plate read is performed after elongation

<sup>2</sup> Temperature is increased of 0.3°C each sec ( $\triangleq$  cycle) followed by a plate read

For the evaluation a cycle threshold (Ct) value for the (corrected) fluorescence of the measuring dye is determined. The Ct value indicates after how many PCR cycles the threshold has been reached and is lower, the more DNA of the examined sequence was used. By using the Ct values of the individual samples in the logarithmic straight line equation of a standard series with samples of defined concentration, the concentration of the examined DNA sequence can be calculated. Each sample was measured once.

### 2.7.3 Elemental analysis via ICP-OES

For the elemental measurement the samples were analyzed by inductively coupled plasma optical emission spectrometry (ICP-OES; iCAP 6000 ICP Spectrometer) (Thermo Fisher Scientific GmbH, Dreieich, Germany). For each sample 500 mg of the grounded and frozen plant material was dried at approx. 70°C for approx. 24 h. About 0.038 g of the dried plant material was weighed with a micro scales into scintillation glasses. A scintillation glass without plant material was taken as a sample-blank. The samples were incinerated at 480°C for a minimum of 8 h in a muffle furnace (M104) (Thermo Fisher Scientific GmbH, Dreieich, Germany). After cooling the samples to RT, 1.5 ml of 66% (v/v) nitric acid (HNO<sub>3</sub>) was added. After 10 min and occasional shaking of the samples, 13.5 ml of ultrapure water was added to the samples. The solutions were filtered through filtering paper (Rotilabo®-round filters, type 15A, equivalent blue band, filtration speed of 180 seconds according to DIN 53137) (Carl Roth, Karlsruhe, Germany) and stored in 15 ml Falcon tubes at -20°C before final analysis.

For the measurement with the ICP-OES a method developed for *B. napus* was used. **Table 2.10** shows the composition of the used calibration standard solutions (1 and 2) and of the calibration-blank. The three solutions were prepared in 50 ml Falcon tubes,

## Material and methods

the listed single-element standards, the multi-element standard and the 66% HNO<sub>3</sub> were pipetted together and then made up to 50 ml with ultrapure water. The three calibration standard solutions, the sample-blanks and samples were placed in an autosampler (CETAC™ ASX 520 AutoSampler) (Thermo Fisher Scientific GmbH, Dreieich, Germany) and were measured.

**Table 2.10: Composition of the calibration standard solutions and the blank for the ICP-OES measurement of *B. napus*.**

Element or solution	Manufacturer	Calibration standard solution 1 in [ml]	Calibration standard solution 2 in [ml]	Blank in [ml]
<b>Potassium<sup>1</sup> (K)</b>	CPI International, Amsterdam, Netherlands	0.025	1.000	0.000
<b>Calcium<sup>2</sup> (Ca)</b>		0.450	0.010	0.000
<b>Magnesium<sup>2</sup> (Mg)</b>		0.250	0.005	0.000
<b>Sulfur<sup>1</sup> (S)</b>		0.125	0.005	0.000
<b>Phosphorus<sup>3</sup> (P)</b>		0.200	0.005	0.000
<b>Iron<sup>2</sup> (Fe)</b>		0.000	0.095	0.000
<b>ICP Multi-element standard solution VIII<sup>4</sup></b>	Carl Roth GmbH + Co. KG, Karlsruhe, Germany	0.005	0.500	0.000
<b>66% HNO<sub>3</sub></b>		5.000	5.000	5.000
<b>Ultrapure water</b>		43.945	43.380	45.000
<b>Final volume in [ml]</b>		<b>50.000</b>	<b>50.000</b>	<b>50.000</b>

<sup>1</sup> 10,000 mg<sup>-1</sup> L<sup>-1</sup> in H<sub>2</sub>O

<sup>2</sup> 10,000 mg<sup>-1</sup> L<sup>-1</sup> in 4% HNO<sub>3</sub>

<sup>3</sup> 10,000 mg<sup>-1</sup> L<sup>-1</sup> in 0.05% HNO<sub>3</sub>

<sup>4</sup> Consists of 24 components; 100 mg<sup>-1</sup> L<sup>-1</sup> of each element in 2% HNO<sub>3</sub>

The measuring principle of the ICP-OES is based on the formation of atoms and ions from the sample aerosol, which is initiated into an argon plasma at a temperature between 6,000 to 8,000 Kelvin (K). The ions are induced to emit light by the plasma. The emitted light is decomposed in the spectrometer. The identification of the elements is based on the wavelengths of the emitted light. **Table 2.11** shows the measurable elements of the used method and wavelength for identification.

## Material and methods

**Table 2.11: ICP-OES: measurable elements of the used method.**

Element	Wavelength in [nm]
Calcium (Ca)	315.887
Copper (Cu)	324.754
Iron (Fe)	259.940
Potassium (K)	766.490
Magnesium (Mg)	279.079
Manganese (Mn)	257.610
Phosphorus (P)	177.495
Sulfur (S)	182.034
Selenium (Se)	196.090
Zinc (Zn)	213.856

Each sample was measured three times. The measurement of the samples was started with a sample-blank, after 24 samples a new sample-blank was measured. This type of sample distribution is based on the capacity of the muffle furnace, in which a total of 25 scintillation glasses fit. Therefore, a sample blank comes on 24 samples. For the evaluation of the data, the corresponding mean value of the technical replicates for the measurable elements, the mean value of the corresponding sample-blanks, the exact initial weight and the final volume (0.015 L) are needed for the following formula:

$$\frac{(\text{mean value of sample } [mg L^{-1}] - \text{mean value of sample blank } [mg L^{-1}]) * 0.015 L}{\text{initial weight } [g]} = mg g^{-1}$$

### 2.7.4 Glucosinolate analysis via HPLC

For GSL analysis 500-700 mg of grounded and frozen material was weighed into tubes from each sample. The empty weight of the tubes was previously determined. The samples were freeze-dried (Freeze Dryer Beta 1-16) (Martin Christ Gefriertrocknungsanlagen GmbH, Osterode am Harz, Germany) and weighed again. To the dried plant material was pipetted 1 ml of 80% (v/v) methanol (methanol for HPLC) (Carl Roth, Karlsruhe, Germany). The samples were vortexed and incubated on a shaker (IKA™ VXR Basic Vibrax™ Vortex Shaker) (Fisher Scientific GmbH, Schwerte, Germany) full speed for 40 min at RT. Subsequently, the tubes were centrifuged at 13,000 g for 5 min at RT. The supernatant was transferred to a new tube and the extraction step was repeated. The two supernatants produced per sample were pooled and loaded onto columns (Polypropylene Columns, 1 ml) (Qiagen, Hilden, Germany) containing 2 ml of 5% suspension (in 0.5 M acetic acid, pH 5) of sephadex (DEAE-Sephadex A-25 chloride form) (Sigma-Aldrich Chemie GmbH, Munich,



## Material and methods

Germany). The flow through was discarded and the columns were washed 5 times with 2 ml of aqua pure. Then the columns were washed twice with 2 ml of 0.02 M acetic acid (pH 5). The sephadex acts as an anion exchange column, which binds intact GSLs. To desulfate these intact GSLs, 500  $\mu$ l of a sulfatase solution (50  $\mu$ l of purified sulfatase was mixed with 450  $\mu$ l of 0.02 M acetic acid, pH 5) was loaded onto each column. Desulfation took place over night at RT. For the purification of the sulfatase (Thies 1979) 112 mg sulfatase from *Helix pomatia* (Sigma-Aldrich Chemie GmbH, Munich, Germany) were weighed in a beaker with a micro scales. 4,800  $\mu$ l of aqua pure were pipetted and the beaker was closed with parafilm. The beaker was placed on ice and gently shaken until the sulfatase had dissolved. From the crude sulfatase solution 300  $\mu$ l each were pipetted together with 300  $\mu$ l of 99% EtOH. The tubes were centrifuged at 5,200 g for 20 min at RT. In the meantime, 900  $\mu$ l of 99% EtOH were placed in new reaction tubes. After centrifugation, the supernatant (approx. 600  $\mu$ l) was pipetted to the new tubes with the 99% EtOH. These were centrifuged at 4,500 g for 15 min at RT. The supernatant was discarded. Each pellet was dissolved in 250  $\mu$ l aqua pure (aliquots were frozen at -20°C until use). Thereafter, the sulfatase solution was drained from the column. The desulfated GSLs (ds-GSLs) were eluted three times from the columns with 2 ml of aqua pure. Each sample consisted of three 2 ml tubes. 300  $\mu$ l of aqua pure were pipetted into the first tube and the pellet was dissolved. The solution was then used to dissolve the second pellet and finally the third. The samples were frozen for approx. 1 h at -20°C and then centrifuged at 13,000 g for 10 min at RT.

The analysis of GSLs (Hornbacher *et al.*, 2019) was conducted with a high performance liquid chromatography (HPLC) system (Knauer, Berlin, Germany) with an Ultra AQ C-18 column (150 x 4.6 mm, 5  $\mu$ m particle size) (Restek GmbH, Bad Homburg, Germany). **Table 2.12** shows the time course and percentages of the used gradient consisted of water (Solvent A) and acetonitrile (Solvent B) (Carl Roth, Karlsruhe, Germany) for the 52 min long run. The flow rate was 0.5 ml min<sup>-1</sup> at 45°C with an injection rate of 50  $\mu$ l.

## Material and methods

**Table 2.12: Time course and corresponding percentage of the used gradient for GSL-analysis with the HPLC, consisted of Solvent A and B.** The flow rate for the 52 min run was 0.5 ml min<sup>-1</sup> at 45°C with an injection rate of 50 µl.

Time course in [min]	Solvent A (water) in [%]	Solvent B (Acetonitril) in [%]
0-6	100	0
6-27	100-70	0-30
27-27,1	70-40	30-60
27.1-32	40	60
32-32.1	40-100	60-0
32.1-52	100	0

The detection of GSLs was performed at 229 nm with a diode-array detector (DAD) (Knauer, Berlin, Germany). For the quantification of the measured GSLs the external standard sinigrin (Sigma-Aldrich Chemie GmbH, Munich, Germany) and the relative response factors (**Table 2.13**) were used. Samples of 7 dpi were measured once. From 43.75% of the samples from 14 dpi three methanol-extracts were prepared for measuring and the remaining samples were measured once.

**Table 2.13: Response factors of ds-GSLs at 229 nm found in *B. napus*.** The quantification of the measured GSLs was determined using the external standard sinigrin and the relative response factors.

Trivial name	Relative response factor	Chemical group	Semisystematic name of side chain
<b>Progoitrin</b>	1.09	Aliphatic	2-Hydroxy-3-butenyl
<b>Glucoraphanin</b>	1.07	Aliphatic	4-Methylsulfinylbutyl
<b>Glucoalyssin</b>	1.07	Aliphatic	5-Methylsulfinylpentyl
<b>Gluconapin</b>	1.11	Aliphatic	3-Butenyl
<b>4-Hydroxyglucobrassicin</b>	0.17	Indolic	4-Hydroxyindolyl-3-methyl
<b>Glucobrassicinapin</b>	1.15	Aliphatic	4-Pentenyl
<b>Glucobrassicin</b>	0.29	Indolic	Indolyl-3-methyl
<b>Gluconasturtiin</b>	0.95	Benzylic	2-Phenylethyl
<b>Neoglucobrassicin</b>	0.2	Indolic	1-Methoxyindolyl-3-methyl

## Material and methods

### 2.7.5 Thiol (cysteine and glutathione) analysis via HPLC

For the thiols measurement 50 mg of grounded and frozen plant material were weighed in tubes and mixed with 250  $\mu\text{l}$  of 0.1 M hydrochloric acid (HCl) to prepare an extract. The samples were incubated on ice for 15 min and vortexed regularly. Subsequently, the tubes were centrifuged at 13,000  $g$  for 6 min at 4°C. The supernatants were transferred to new tubes. For the derivatization of the samples the plant extracts were mixed with different solutions (**Table 2.14**): aqua pure, Tris(hydroxymethyl)-aminomethan (Tris, 1 M, pH 8) (AppliChem GmbH, Darmstadt, Germany), dithiothreitol (DTT, 10 mM) (AppliChem GmbH, Darmstadt, Germany) and sodium hydroxide (NaOH, 0.08 M) (Riedel-de Haën AG, Seelze, Germany). NaOH was used for neutralization and pipetted at the end. In addition, 0-controls (negative controls) were prepared without the plant extract and a standard series with plant extract. The final volume of all sample batches were 270  $\mu\text{l}$ .

**Table 2.14: Derivatization of plant samples, controls and standard series for the measurement of cysteine and glutathione with the HPLC.**

Solution	Sample in [ $\mu\text{l}$ ]	Negative Controls in [ $\mu\text{l}$ ]	Standard series in [ $\mu\text{l}$ ]
Plant extract	50	-	10
Aqua pure	180	240	230
1 M Tris <sup>1</sup>	20	20	20
10 mM DTT <sup>2</sup>	10	10	10
0.08 M NaOH <sup>3</sup>	10	-	-
<b>Final volume in [<math>\mu\text{l}</math>]</b>	<b>270</b>	<b>270</b>	<b>270</b>

<sup>1</sup> Tris(hydroxymethyl)-aminomethan, pH 8.0; filtrated and stored at 4°C before use

<sup>2</sup> Dithiothreitol; the solution was prepared freshly before use

<sup>3</sup> Sodium hydroxide; filtrated and stored at 4°C before use; NaOH was used for neutralization, and were pipetted at the end.

The samples pipetted according to **Table 2.14** were mixed and centrifuged shortly. Afterwards, they were incubated for 1 h in dark at RT. It was pipetted to each sample 20  $\mu\text{l}$  of 10 mM monobromobimane (mBBr) (Sigma-Aldrich Chemie GmbH, Munich, Germany) dissolved in acetonitrile. The mBBr derivatized the sulfhydryl-groups. The samples were mixed and centrifuged shortly. The tubes were incubated for 15 min at RT. Subsequently, 710  $\mu\text{l}$  of 5% (v/v) acetic acid were pipetted to each sample. This step stopped the derivatization.

The analysis of thiols (separation, detection, and quantification) was conducted with a high performance liquid chromatography (HPLC) system (Knauer, Berlin, Germany) with a reversed phase column (Nova-Pak C<sub>18</sub>, 4  $\mu\text{m}$ , 3.9 x 150 mm) (Waters, Milford,

## Material and methods

MA, USA). **Table 2.15** shows the time course and percentages of the used gradient consisted of Solvent A (100 mM potassium acetate, pH 5.5) and Solvent B (100% methanol) for the 31 min long run. The flow rate was 0.5 ml min<sup>-1</sup> with an injection rate of 50 µl. The mBBr derivatives were detected photometric by the fluorescence detector ( $\lambda_{\text{ex}}$  380 nm,  $\lambda_{\text{em}}$  480 nm).

**Table 2.15: Time course and corresponding percentage of the used gradient for thiol analysis with the HPLC, consisted of Solvent A and B.** The flow rate for the 31 min run was 0.5 ml min<sup>-1</sup> with an injection rate of 50 µl.

Time course in [min]	Solvent A (100 mM potassium acetate, pH 5.5) in [%]	Solvent B (Methanol) in [%]
0-9	81	19
9-24	0	100
24-31	100	0

The thiols cysteine and glutathione were quantified using genuine standards (L-Cysteine; Sigma-Aldrich Chemie GmbH, Munich, Germany) (Glutathione reduced; Fluka® Analytical, Seelze, Germany). Samples of 7 dpi were measured once. From samples of 14 dpi three HCl-extracts were prepared, which were measured.

### 2.7.6 Histology: Staining of the plant hypocotyl with toluidine blue

The in FAA-preserved (FAA: 70% EtOH, 100% acetic acid, 37% formaldehyde; 18:1:1, v/v/v) hypocotyls for histological examination were first dehydrated in an ascending alcohol series (**Table 2.16**). In the second step the 80% EtOH was mixed with Eosin Y (Eosin yellowish) (Carl Roth GmbH + Co. KG, Karlsruhe, Germany). The dye slightly stains the hypocotyl pieces without affecting the subsequent staining method and thus facilitates the orientation during embedding.

**Table 2.16: Ascending alcohol series for tissue-preserving dehydration of plant material.**

Step	Percentage [%] of EtOH	Duration in [min]
1	70	60
2	80 <sup>1</sup>	120
3	90	120
4	99	120

<sup>1</sup> With Eosin Y; 0.5 g ml<sup>-1</sup>; allowing an easier embedding procedure.

The samples were embedded with Technovit® 7100 (Kulzer GmbH, Hanau, Germany). The embedding-set consists of a glycol methacrylate (GMA) monomer, a Hardener I and a Hardener II. The pre-infiltration, infiltration and polymerisation were carried out

## Material and methods

as specified by the manufacturer with the following modifications. The infiltration step was done for approx. 18 h. The hardening of the samples at the polymerisation step required approx. 24 h in the embedding mouldings (Polyethylene Molding Cup Trays, 6 x 8 x 5 mm hexagon; nine cavities) (Polysciences Europe GmbH, Hirschberg an der Bergstrasse, Germany). Subsequently, the hardened resin blocks were taken out of the moulding cups and dried for a further approx. 48 h at RT before they were cut.

The 25 µm thick cross-sections of the embedded hypocotyls were made with a rotary microtome (R. Jung AG 1960, Heidelberg, Germany) used a d-blade (16 cm steel-blade, d-profile) (Leica Mikrosysteme Vertrieb GmbH, Wetzlar, Germany). The cross sections were threaded with a spring steel forceps and a minucies-needle onto aqua pure-wetted slides. On each slide eight cross sections were placed in two rows. For the cross sections, where possible, the outer resin was removed. The slides were dried at 140°C on a heating plate for histology slides (HB 300) (Gestigkeit Harry GmbH, Düsseldorf, Germany) for approx. 1-2 h.

In order to detect vascular occlusions hypocotyl cross sections were stained with 0.05% (w/v) toluidine blue (Sigma-Aldrich Chemie GmbH, Munich, Germany) (Feder and O'brien 1968) for 10 min at 60°C. The slides were washed with desalted water (until no more stain emerged) and then dried at 100°C for approx. 1 h. The cross sections were mounted with Eukitt® (Sigma-Aldrich Chemie GmbH, Munich, Germany) for permanent conservation. Images of samples were taken with a light microscope in bright field (Microscope: CX31; Camera: U-CMA D3) (Olympus Europa SE & Co. KG, Hamburg, Germany) (Software: NIS Elements, Version 4.50 64-bit) (Nikon GmbH, Düsseldorf, Germany).

Main experiment: from each hypocotyl sample at least two slides with each eight cross sections were prepared. For the evaluation microscopic images of five cross sections were made and the following parameters have been defined: number of total tracheas in the xylem, number of occlusions in the mid area of the xylem (**mXy**) and number of occlusions in the periphery of the xylem (**pXy**). **Figure 2.6, A** shows the distribution of different tissue types in a cross section of a hypocotyl of *B. napus*, starting from the middle with pith (**Pi**), xylem (**Xy**), cambium (**Cam**) and phloem (**Ph**). **Figure 2.6, B** shows the definition of the counting range of occlusions. This area had to be redefined for each microscopic image. From the **Pi** to half of the **Xy** became the **mXy** counting region, the other half the **pXy** counting region. Counting was performed with help of the open source image processing package "Fiji" (Schindelin *et al.*, 2012).

## Material and methods

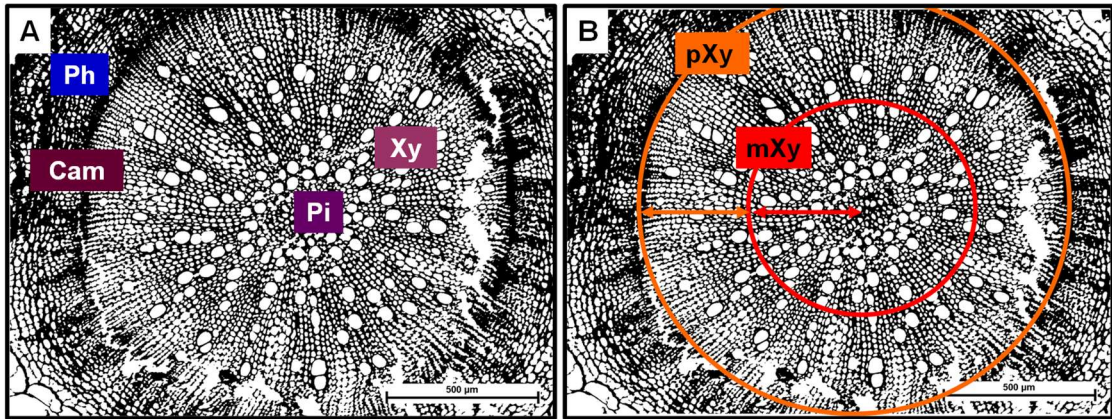


**Figure 2.6: Different tissue types in the cross section of a hypocotyl from *B. napus* and the definition of the counting range of the occlusions.** Image A shows the tissue distribution of a hypocotyl cross section of *B. napus*: **Pi**: Pith; **Xy**: Xylem; **Cam**: Cambium; **Ph**: Phloem; image B shows a simplified representation of the counting ranges of the occlusions for mid area of the xylem (**mXy**; red circle, red arrow) and periphery of the xylem (**pXy**; orange circle, orange arrow). For each cross section, the range from **Pi** to **Cam** was measured. The measured distance was divided in half and defined to **mXy** and **pXy**.

### 2.7.7 Histology: Staining of fungal mycelium with cotton blue

Root dip inoculated roots were stained with 0.5% (w/v) cotton blue (Carl Roth, Karlsruhe, Germany) for 10 min at RT. Roots of mycelium-spore inoculated plants were stained after 24 h and roots of spore inoculated plants after 48 h, washed with aqua pure and directly examined with the light microscope in the bright field. Mock-inoculated roots were prepared the same way. In both cases 7 d old *B. napus* plants were used.

### 2.8 Statistical analysis

Statistical evaluation was performed by Dr. Frank Schaarschmidt (Institut für Zellbiologie und Biophysik, Abteilung Biostatistik; Leibniz Universität Hannover) for the data of the first and second run of the main experiment. Glucosinolate concentrations as well as cysteine and glutathione concentrations were log-transformed before analysis due to finding right skewed distributions and variance increasing with mean. The transformed data were analyzed in general linear models with four factors and all two-way interactions between the four factors. Based on the fitted models, analysis of variance was performed to test the significance of main effects and interactions and Tukey tests for the model based means of factor TPI were performed jointly across all other factor levels and separately for VL-infected and mock-infected groups.

To analyze the histological data of occlusions in the xylem vessels of infected plants, the counted total number of mid occlusions among the total number of trachea per plant was analyzed in a generalized linear model with logit link and assumption of over dispersed binomial data (McCullagh and Nelder, 1989). The model contained main effects for the three factors dpi, TPI and different sulfur supply and their two-way interactions. After model fit, F-tests in analysis of deviance were used to test the significance of these effects.

Data of the elements sulfur, calcium, potassium and iron were analysed without transformation in a model with four factors and their two-way interactions. Based on the fitted Modell ANOVA-tables and multiple comparisons of model based means were performed (R package emmeans).

Log-transformed qPCR data were analysed using a three factorial model with effects dpi (3, 7 and 14) and TPI (I, II, III and IV) crossed, including an interaction term and effect of sulfur supply nested in effect of dpi. Based on the fitted model, analysis of variance tables were computed and multiple comparisons were performed using package emmeans.

Analysis was performed in R 3.6.1 (R Core Team, 2019) using the add-on package emmeans (version 1.4) (Lenth, 2019) for model based comparisons of means.

### **2.9 Necessary additional notes to the used climatic chambers, biological replicates and amount of plant material**

#### **2.9.1 Climatic chambers from Johnson Controls**

Climatic chambers are used for experiments with plants, because it is possible to set the exact conditions (temperature, humidity, course of light/darkness). An experiment can be repeated as many times as needed based on this foundation. Data collected in this way has a stronger and more trustworthy proposition. Two climatic chambers from the company Johnson Controls were used for this work, one for the control plants and the other for the VL-infected plants. During running experiments, light failures, elevated temperatures and humidity occurred several times. Unfortunately, when the main experiment was carried out for the first time, the following disturbances occurred: one day before inoculation there was a light failure during the day. This was remedied within approx. 1 h, but various effects on the plants are possible. In addition, there were temperature and humidity fluctuations due to a malfunction of the brine pump (approx. +10°C and +20% humidity above the default settings). Due to the probable effect of a core drilling on the building foundation, the light turned off again during the running experiment (approx. 1-2 h). When repeating the experiment there were significantly less problems.

#### **2.9.2 Biological replicates and amount of plant material**

As already mentioned, for the present experiments with the specific host-pathogen context, there was a limited space for cultivation. Because of the many different factors needed to investigate the hypotheses of this work, including different TPIs and sulfur fertilization, the plants that belonged to one of the four TPIs with the respective sulfur supply (+S/-S) had to be separated in different traits. Although, the available space was used optimally, many analyses of the sample material were needed in order to substantiate the aims of this work. For the various analytical methods, it was necessary to harvest enough plant material from each group and the sample size should contain the same number of pooled plants for all dpi. For two main experiments, which were prepared for a long time and should consist of two biological replicates, two more climatic chambers were used. After validation with qPCR, whether the infection had worked, it turned out that the infection in the additional climatic chamber was poor to nonexistent. These experiments had to be discarded. Due to the fact that the infection did not work twice in a row in the additional chamber, the performances of the following main experiments was limited again to the original climatic chambers. Due to the small size of the plants at the beginning of the experiment, only one sample consisting of eight plants could be collected per point in time of harvest. Therefore, the analyses



## Material and methods

could be performed only once due to the limited amount of plant material. In some cases, technical replicates were available. With samples of 3 dpi DNA extraction with subsequent qPCR was performed, as the sample material was sufficient for this analysis only. As already mentioned in section **2.9.1**, severe problems in the climatic chambers occurred at the beginning and during the ongoing main experiment, which could largely be remedied on the second run of the experiment. However, the listed problems and the strict limitation of plant material mean lead to a consideration with caution. Because of this, the results of the main experiment, which was carried out twice, are presented separately from each other.

### 3. Results

#### 3.1 Pre-experiment I: inoculation of 7 d old plants with mycelium-spore mixture and subsequent cultivation in sand/soil mixture

The **pre-experiment I** was performed to try the inoculation procedure with mycelium-spore mixture of *V. longisporum* at **different TPIs (2.5.1)**. For verification of a successful infection the content of VL-DNA in the VL-infected plants was first screened by qPCR (**3.1.1**). In addition, cross sections of hypocotyls from **control** and **VL-infected** plants were examined microscopically for the occurrence of occlusions (**3.1.2**). In order to test the influence of the **infection**, the **different TPIs** and **sufficient/deficient sulfur** fertilization on the contents of sulfur, calcium, potassium, iron and GSLs, ICP-OES or HPLC analysis were carried out, respectively (**3.1.3; 3.1.4**).

##### 3.1.1 Detection and verification of the infection with *V. longisporum* in mycelium-spore inoculated *B. napus* plants potted in sand/soil

Following DNA purification (**2.7.1**) from plant material of *B. napus*, DNA of *V. longisporum* (VL-DNA) was quantified by qPCR (**2.7.2**) using **ITS** primers (**Fig. 3.1**). Samples of 7, 14 and 21 dpi were measured and the amount of VL-DNA was calculated in ng g<sup>-1</sup> fresh weight of the plants (FW). Samples of 7 dpi were not fertilized yet, the bars represent two biological replicates. In most control samples probed with ITS primers no signals were detected, or the amplification of VL-DNA was below limit of detection or below limit of quantification, respectively (data not shown).

At 7 dpi in **TPI II/right bar** occurred the highest amount of VL-DNA (15.53 ng g<sup>-1</sup> FW), whereby the other **VL-infected** groups showed an amount of VL-DNA ranged from 0.77 to 8.11 ng g<sup>-1</sup> FW (**Fig. 3.1, A**). The content of VL-DNA decreased in all groups at 14 dpi at all **TPIs (Fig. 3.1, B)**. However, the amount of VL-DNA was highest in **TPI II/-S** (2.3 ng g<sup>-1</sup> FW). **TPI I/+S** and **TPI III/+S** were below limit of detection and then increased again at 21 dpi (**Fig. 3.1, C**). **TPI III/+S** showed the highest content of VL-DNA (1.39 ng g<sup>-1</sup> FW) compared to the other groups. Comparing the remaining **+S**-groups (**TPI I, TPI II** and **TPI IV**) with **-S**-groups, these showed a lower amount of VL-DNA (**+S**-groups: ranged from 0.005 to 0.16 ng g<sup>-1</sup> FW; **-S**-groups: ranged from 0.23 to 0.69 ng g<sup>-1</sup> F

## Results

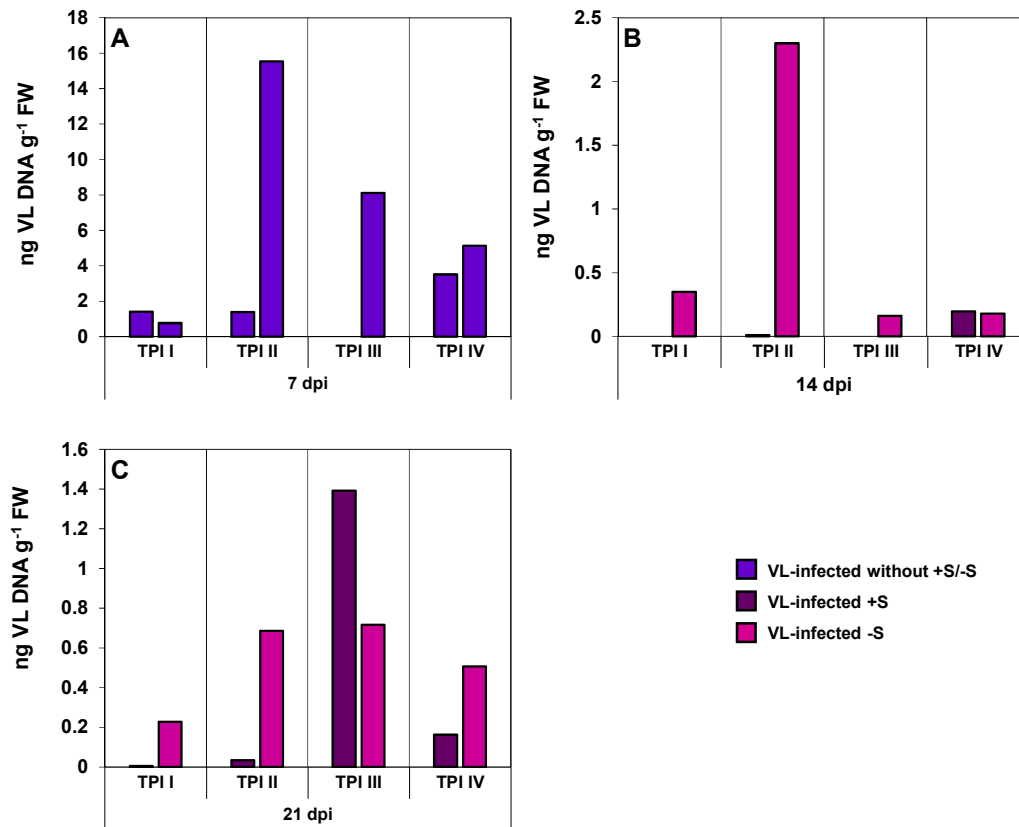


**Figure 3.1: Pre-experiment I: amount of *V. longisporum* VL43-DNA detected by qPCR with ITS primers in *B. napus*.** Status of infection rate in mycelium-spore inoculated plants potted in sand/soil; **A**: at 7 dpi, plants were not fertilized with different sulfur supply; **bluish violet bars** represent two measurements of same treated plants (without roots); **B** and **C**: at 14 dpi and 21 dpi, plants were fertilized with different sulfur supply (1 mM MgSO<sub>4</sub>: +S; 0.01 mM MgSO<sub>4</sub>: -S); **purple bars** represent VL-infected +S, **pink bars** VL-infected -S; data represent the result of one measurement.

### 3.1.2 The occurrence of occlusions in the xylem of mycelium-spore inoculated plants potted in sand/soil

In addition to the verification of *V. longisporum* infection by qPCR, cross sections of mock- and mycelium-spore inoculated hypocotyls were prepared of all TPIs at 14 and 21 dpi. After staining with toluidine blue (2.7.6), occlusions were visible in xylem vessels of *B. napus*. Occlusions could turn pink indicating that they were derived from primary cell wall material (Gerlach, 1977) called vascular gels (VanderMolen *et al.*, 1983) (**Fig. 3.2, A**). Tyloses are formed by invagination of the mid lamella from adjacent parenchymal cells through bordered pits (Agrios, 1997) and are stained in dark blue or dark purple (**Fig. 3.2, B, C**).

## Results

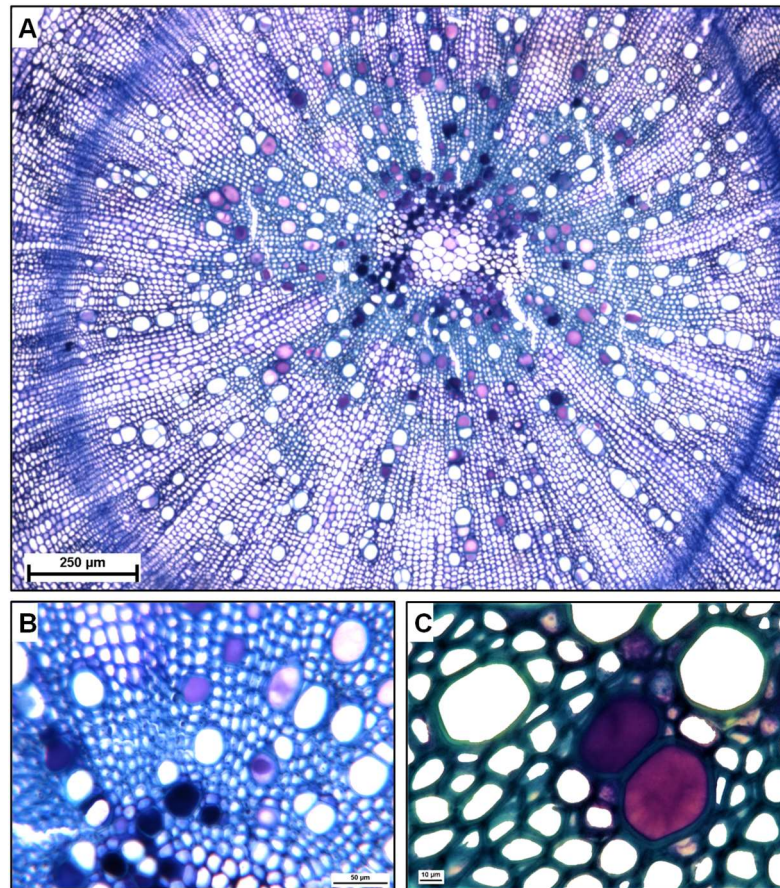


**Figure 3.2: Exemplary representation: occurrence of occlusions in the xylem of *B. napus* after inoculation with *V. longisporum*.** Microscopic pictures of cross sections of hypocotyls from infected *B. napus* plants (cultivar Genie) stained with toluidine blue (21 dpi); **A**: occlusions of xylem vessels particularly in the mid region due to dark blue to pink stained substances (tyloses, vascular gels); scale bar 250 µm; **B** and **C**: representation of individual occlusions; scale bar 50 and 10 µm.

**Figure 3.3** shows microscopic pictures of hypocotyl cross sections stained with toluidine blue (14 dpi). **Mock-inoculated** plants were occlusion-free at all **TPIs** and regardless of different sulfur supply (**Fig. 3.3, A1-A4; C1-C4**). Hypocotyls of **mycelium-spore inoculated** plants showed occlusions in the mid area of the xylem at **TPI III/+S, TPI IV/+S, TPI III/-S** and **TPI IV/-S**, whereby **TPI I/+S** and **TPI II/+S** showed a few occlusions only in the periphery of the xylem (**Fig. 3.3, B3; B4; D3; D4; B1; B2**). However, the severity of occlusions was lower in **-S**-plants compared to the two equivalent **+S**-plants.

## Results

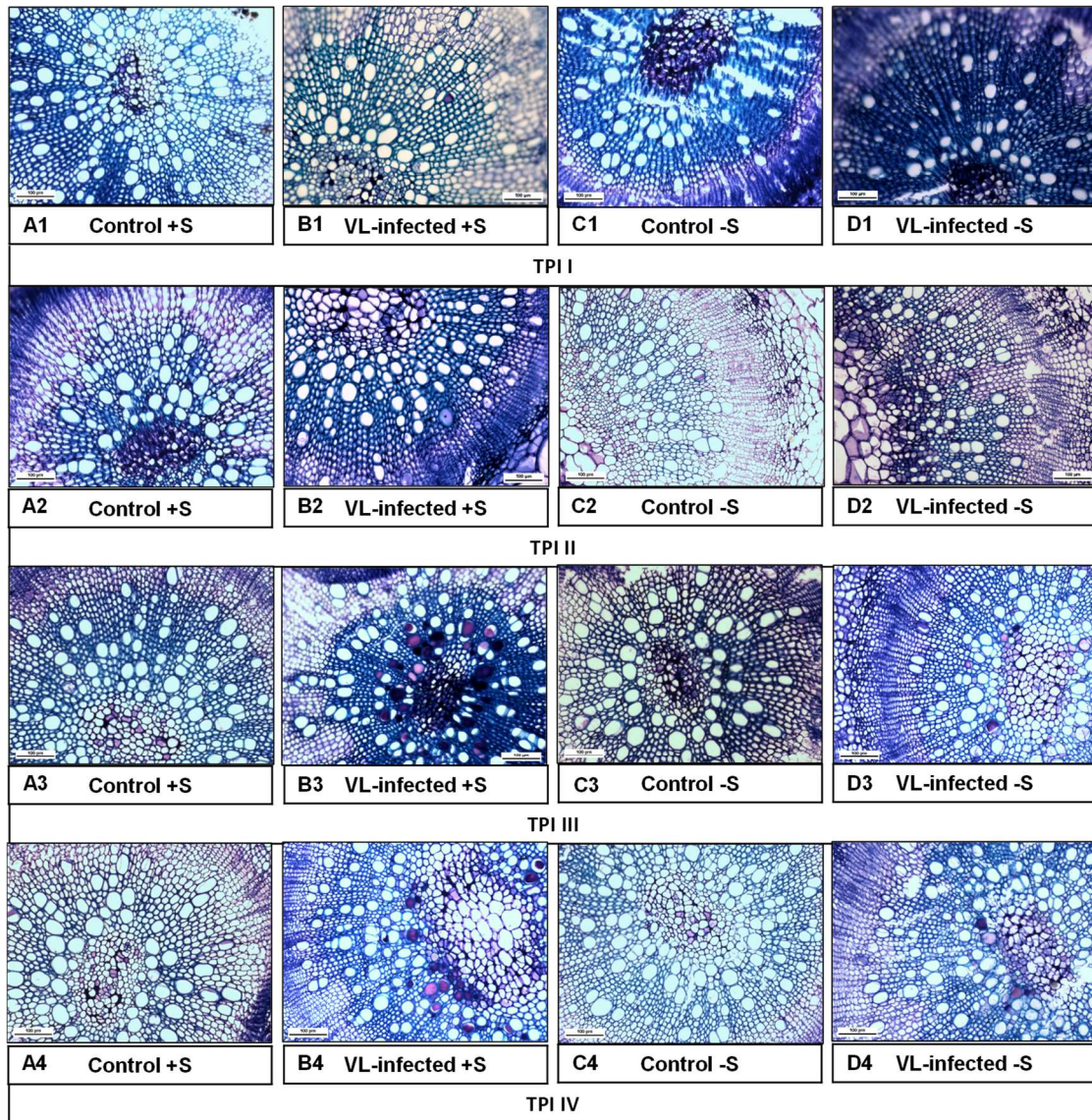


**Figure 3.3: Pre-experiment I: toluidine blue stained cross sections of hypocotyls of mock- and mycelium-spore inoculated plants potted in sand/soil at 14 dpi. A1-A4: control +S-plants; B1-B4: VL-infected +S-plants; C1-C4: control -S-plants; D1-D4: VL-infected -S-plants; control plants were occlusion-free; B3, B4, D3 and D4 show occlusions in the mid area of the xylem; B1 and B2 show occlusions in the periphery of the xylem occasionally; scale bar 100  $\mu$ m.**

## Results

At 21 dpi **control** plants were still occlusion-free (**Fig 3.4, E1-E4 and G1-G4**).

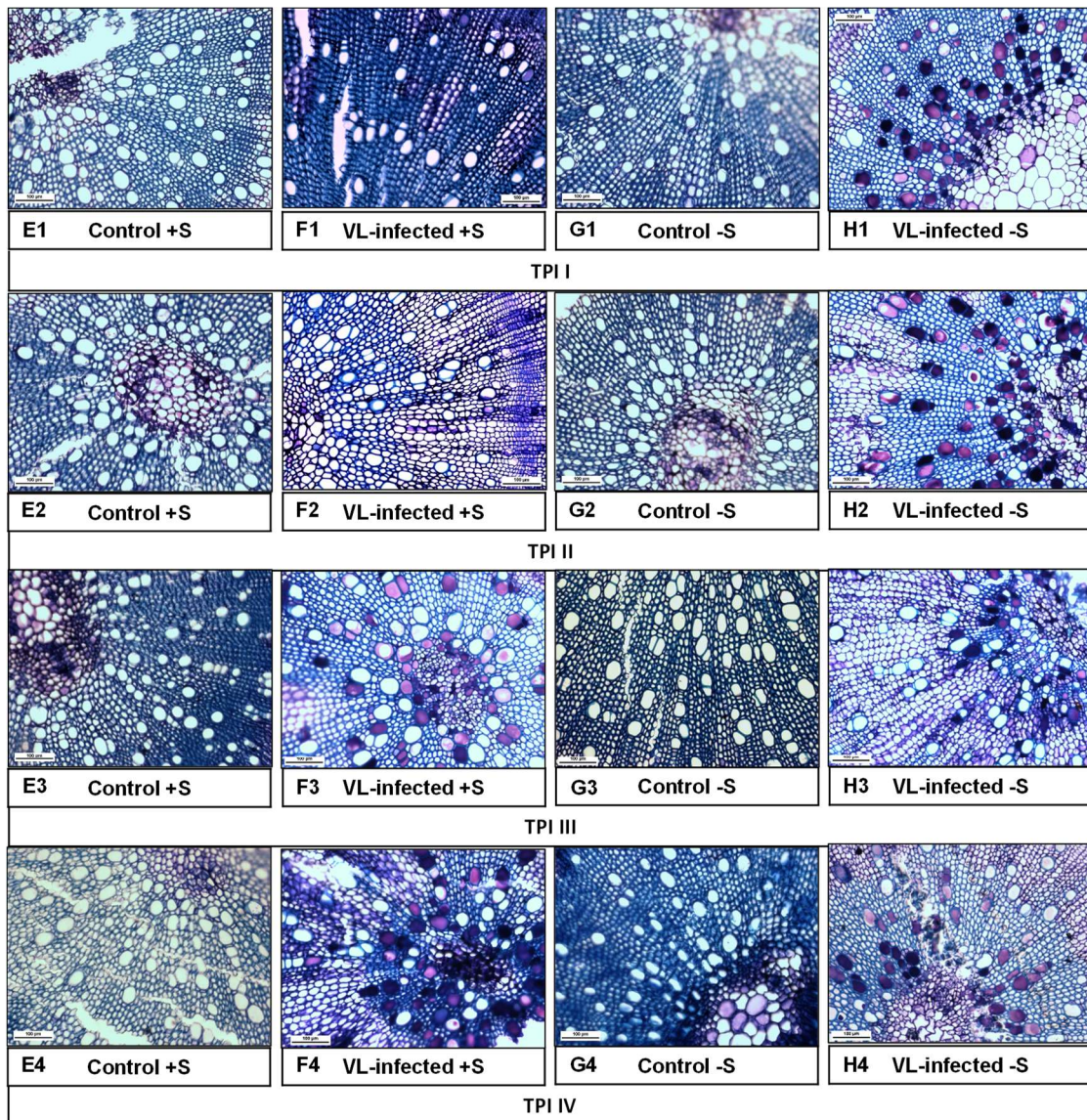


**Figure 3.4: Pre-experiment I: toluidine blue stained cross sections of hypocotyls of mock- and mycelium-spore inoculated plants potted in sand/soil at 21 dpi. E1-E4: control +S-plants; F1-F4: VL-infected +S-plants; G1-G4: control -S-plants; H1-H4: VL-infected -S-plants; control plants were occlusion-free; F3, F4, H1, H2, H3 and H4 show formation of occlusions (tyloses and vascular gels) in the mid area of the xylem; F1 and F2 show occlusions in the periphery of the xylem occasionally; scale bar 100  $\mu$ m.**

Hypocotyls of **VL-infected +S**-plants showed a similar state compared to 14 dpi with the formation of occlusions being even more pronounced for **TPI III/+S** and **TPI IV/+S** (**Fig 3.4, F3; F4**). The **-S**-plants showed a similar formation of occlusions at all **TPIs** (**Fig 3.4, H1-H4**).

## Results

### 3.1.3 Elemental analysis: levels of sulfur, calcium, potassium and iron in mock- and mycelium-spore inoculated plants potted in sand/soil

Since mineral nutrients can show a change in their content during infection with fungal pathogens, levels of **sulfur**, **calcium**, **potassium** and **iron** were examined in **control** and **VL-infected** plants under **sufficient** and **deficient sulfur** supply. Samples were harvested at 7, 14 and 21 dpi and measured with the ICP-OES (2.7.3). Of each sample one extract was made, which was measured thrice. Samples from 7 dpi were not fertilized yet, so that in each respective figure two bars stand for the same treated plants (Fig. 3.5-3.8; **control**: turquoise bars; **VL-infected**: bluish violet bars). One control sample at 7 dpi of TPI II got lost (see asterisk in Fig. 3.5, A; Fig. 3.6, A; Fig 3.7, A; Fig. 3.8, A). The amounts of sulfur, calcium and potassium are shown in mg g<sup>-1</sup> dry weight of the plants (DW) and for iron in µg g<sup>-1</sup> DW.

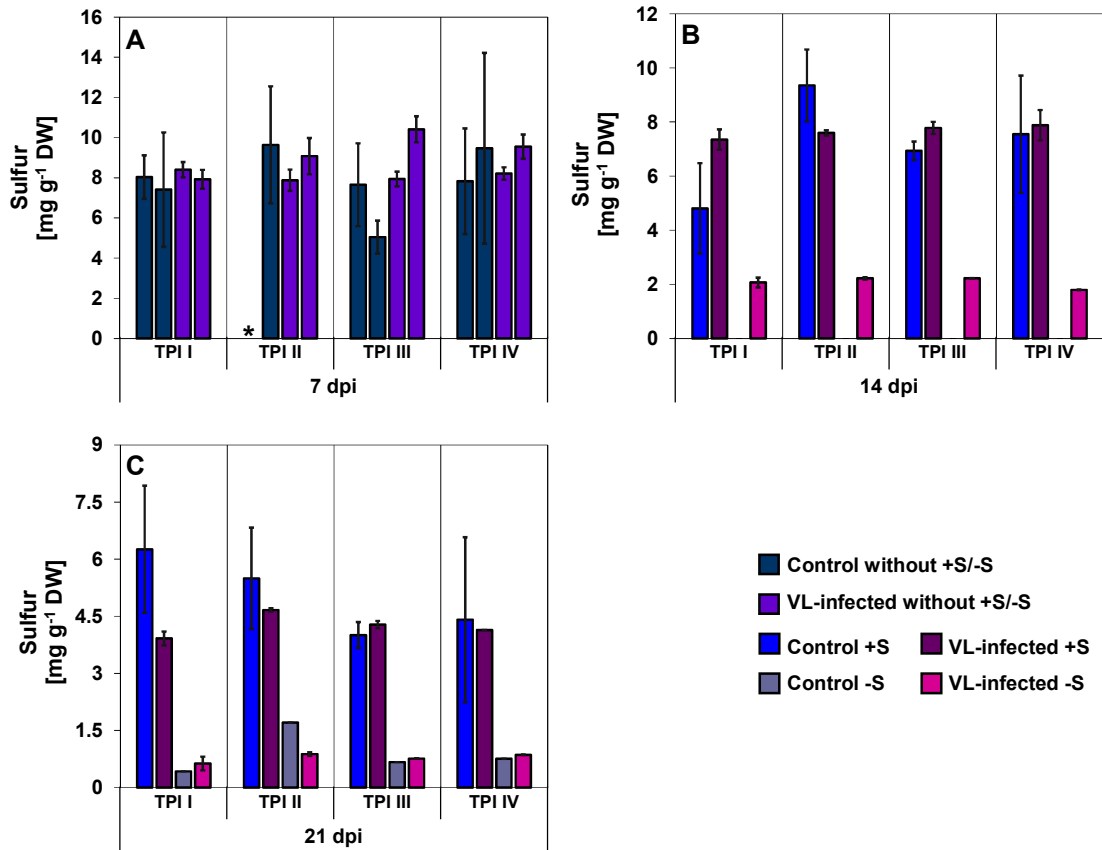


**Figure 3.5: Pre-experiment I: elemental sulfur (S).** Level of S content in mock- and mycelium-spore inoculated plants potted in sand/soil measured by ICP-OES; **A:** samples of 7 dpi without different sulfur supply: **turquoise bars** (left) control plants without +S/-S; **bluish violet bars** (right) VL-infected plants without +S/-S; \*one control sample of TPI II got lost; **B:** samples of 14 dpi with different sulfur supply (+S/-S); **C:** samples of 21 dpi with different sulfur supply (+S/-S); data represent the mean of three dependent technical replicates ± SD.

## Results

At 7 dpi **control** plants showed a **sulfur** content between 5 and 9 mg g<sup>-1</sup> DW, whereby values of **VL-infected** plants were between 8 and 10 mg g<sup>-1</sup> DW (**Fig 3.5, A**). At 14 dpi **control** plants fertilized with **sufficient sulfur** supply had a sulfur content between 5-9 mg g<sup>-1</sup> DW, while the content of **deficient sulfur** supply fertilized **control** plants was not measurable (**Fig. 3.5, B**).

In comparison, **VL-infected +S**-plants values ranged from 7 to 8 mg g<sup>-1</sup> DW and **-S**-plants values were around 2 mg g<sup>-1</sup> DW at all **TPIs**. The sulfur content of **control +S**-plants decreased about 20-30% at 21 dpi and the amount of **VL-infected +S**-plants about 40-50% (**Fig. 3.5, C**). The sulfur content of the **control -S**-plants was measurable again and laid in a range between 0.4-2 mg g<sup>-1</sup> DW, while the content of **VL-infected -S**-plants decreased by a further 55-70%. However, **control** and **VL-infected -S**-groups showed a similar content of sulfur.

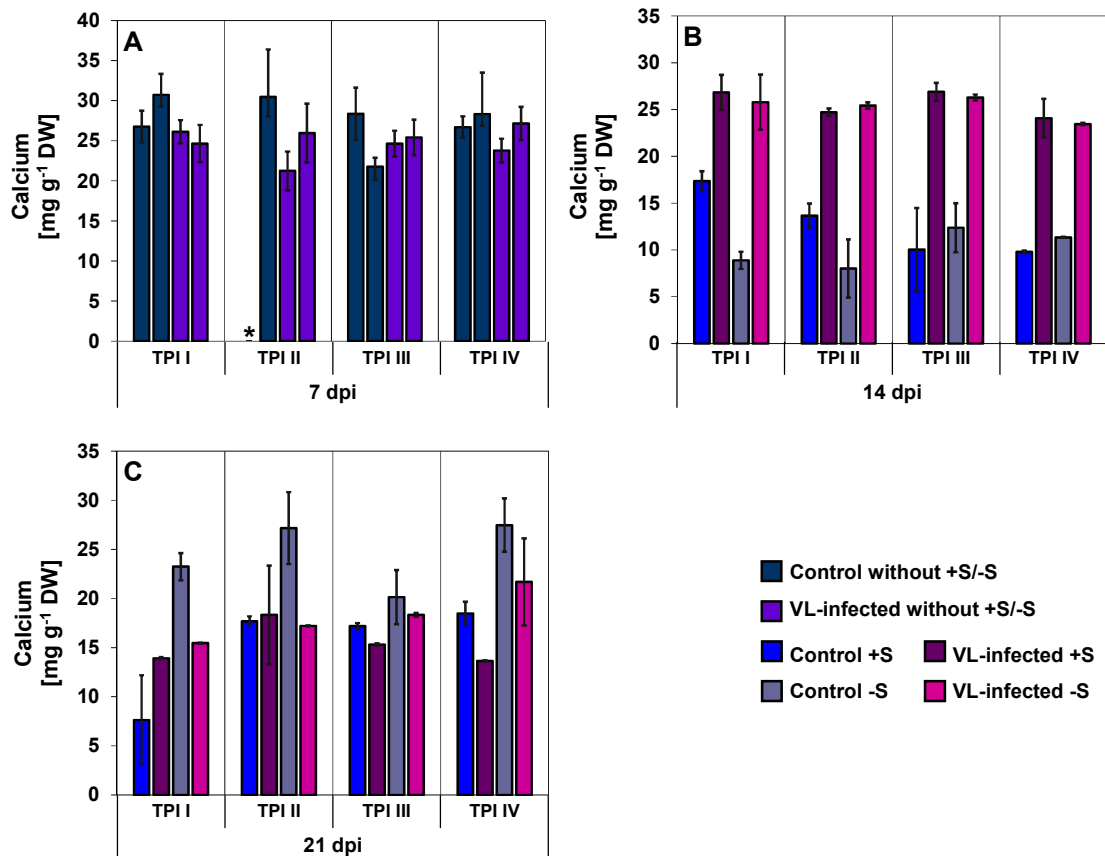


**Figure 3.6: Pre-experiment I: elemental calcium (Ca).** Status of Ca content in mock- and mycelium-spore inoculated plants potted in sand/soil measured by ICP-OES; **A:** samples of 7 dpi without different sulfur supply: **turquoise bars** (left) control plants without +S/-S; **bluish violet bars** (right) VL-infected plants without +S/-S; **\*one** control sample TPI II got lost; **B:** samples of 14 dpi with different sulfur supply (+S/-S); **C:** samples of 21 dpi with different sulfur supply (+S/-S); data represent the mean of three dependent technical replicates  $\pm$  SD.



## Results

The content of **calcium** was also measured by ICP-OES (**Fig 3.6**). At 7 dpi **non-fertilized control** and **VL-infected** groups showed a similar content of calcium ranged from 21 to 31 mg g<sup>-1</sup> DW (**Fig. 3.6, A**). At 14 dpi the distribution of the calcium content changed (**Fig. 3.6, B**). **Control +S**-plants had an amount from 10 to 17 mg g<sup>-1</sup> DW and **control -S**-plants from 8 to 12 mg g<sup>-1</sup> DW.

In comparison, the amount of calcium in **VL-infected +S**-plants laid between 24-27 mg g<sup>-1</sup> DW, whereby the content for **VL-infected -S**-plants was almost in the same range. At 21 dpi the calcium content in **control +S**-plants ranged from 7 to 19 mg g<sup>-1</sup> DW with the highest content at **TPI IV** (**Fig 3.6, C**). In **control -S**-plants the amount increased to 20-27 mg g<sup>-1</sup> DW with the two highest values at **TPI II** and **TPI IV**. In **VL-infected +S**-plants the content of calcium partially decreased about 41%, in case of **VL-infected -S**-plants between 15-35%.

At 7 dpi **VL-infected** plants had higher **potassium** contents than **control** plants (**Fig. 3.7, A**). However, there is also a difference between the two **VL-infected** groups, although they have not been fertilized differently. Thus, **VL-infected/left bar** had potassium levels in a range between 8-19 mg g<sup>-1</sup> DW, while **VL-infected/right bar** showed amounts ranged from 11 to 37 mg g<sup>-1</sup> DW. At 14 dpi the distribution of potassium changed (**Fig 3.7, B**). Overall, **control** plants showed the highest values. An exception is **control +S/TPI I**, in which no potassium could be measured. Within **TPI II** to **TPI III** the amount decreased (**TPI II**: 56.06 mg g<sup>-1</sup> DW; **TPI III**: 32.76 mg g<sup>-1</sup> DW; **TPI IV**: 25.75 mg g<sup>-1</sup> DW). In **control -S**-groups it behaved inversely and the values increased within **TPI I** to **TPI IV** (**TPI I**: 7.59 mg g<sup>-1</sup> DW; **TPI II**: 12.42 mg g<sup>-1</sup> DW; **TPI III**: 30.85 mg g<sup>-1</sup> DW; **TPI IV**: 56.89 mg g<sup>-1</sup> DW). Altogether, the potassium content in **VL-infected** groups decreased, but higher values were observed for **VL-infected -S**-groups (10-31 mg g<sup>-1</sup> DW) compared to **VL-infected +S**-groups (5-13 mg g<sup>-1</sup> DW). At 21 dpi the potassium content decreased in all groups, but it was measurable again in **control +S/TPI I** (33.99 mg g<sup>-1</sup> DW), while **control -S/TPI I** (10.57 mg g<sup>-1</sup> DW ) and **VL-infected -S/TPI IV** (17.4 mg g<sup>-1</sup> DW ) showed a slight increase (**Fig. 3.7, C**).

## Results

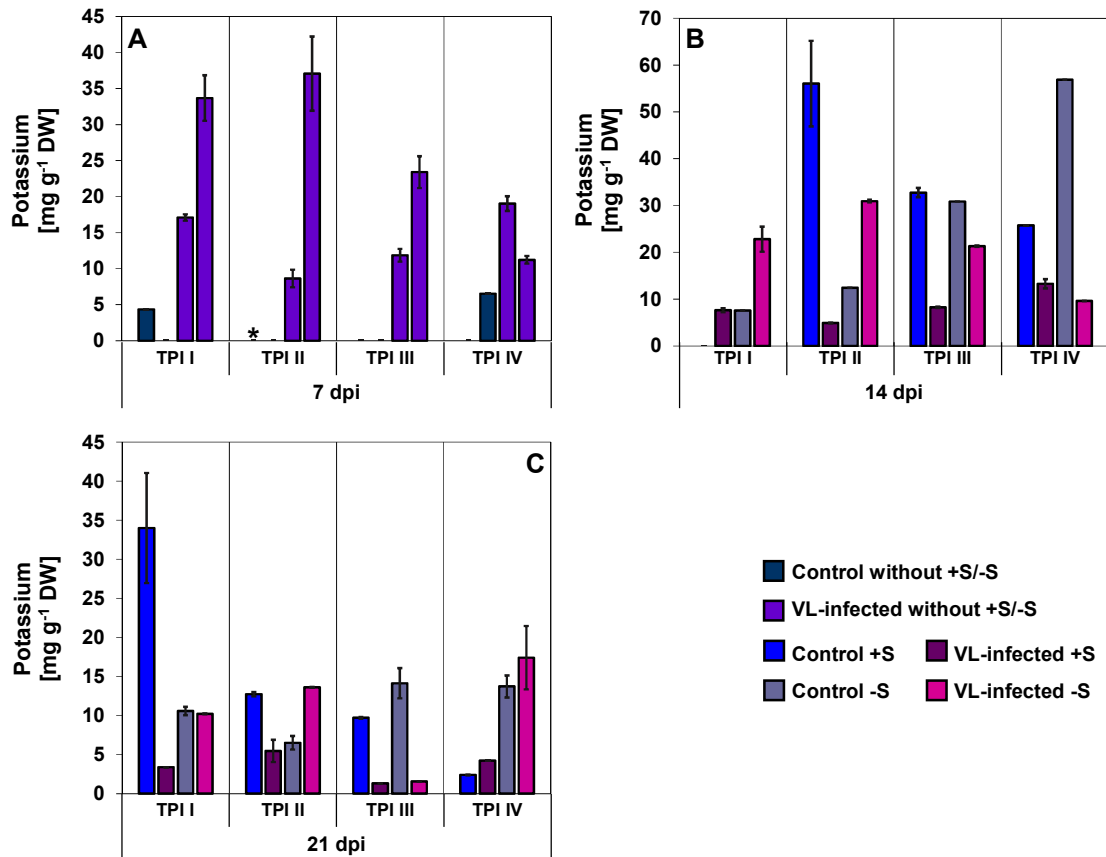


**Figure 3.7: Pre-experiment I: elemental potassium (K).** Status of K content in mock- and mycelium-spore inoculated plants potted in sand/soil measured by ICP-OES; **A:** samples of 7 dpi without different sulfur supply: **turquoise bars** (left) control plants without +S/-S; **bluish violet bars** (right) VL-infected plants without +S/-S; \*one control sample TPI II got lost; **B:** samples of 14 dpi with different sulfur supply (+S/-S); **C:** samples of 21 dpi with different sulfur supply (+S/-S); data represent the mean of three dependent technical replicates  $\pm$  SD.

At 7 dpi **iron** could only be detected in **VL-infected** plants in a range between 107-178  $\mu\text{g g}^{-1}$  DW (**Fig. 3.8, A**). The two **VL-infected** groups, which showed the highest content of VL-DNA also had the highest levels of iron (**Fig. 3.1, A; TPI II/right bar; TPI III/right bar**). At 14 dpi iron was measurable in all groups with the exception of **control +S/TPI I** (**Fig. 3.8, B**). In **VL-infected +S**-groups the content of iron decreased about 6-35%, in **VL-infected -S**-groups it decreased about 25-30%. A very high value around 1400  $\mu\text{g g}^{-1}$  DW showed **control +S/TPI III** and **control -S/TPI IV**. Comparing the different **TPIs** at 21 dpi in **control** groups (48-165  $\mu\text{g g}^{-1}$  DW) occurred higher values of iron than in **VL-infected** groups (37-59  $\mu\text{g g}^{-1}$  DW) (**Fig. 3.8, C**).

## Results

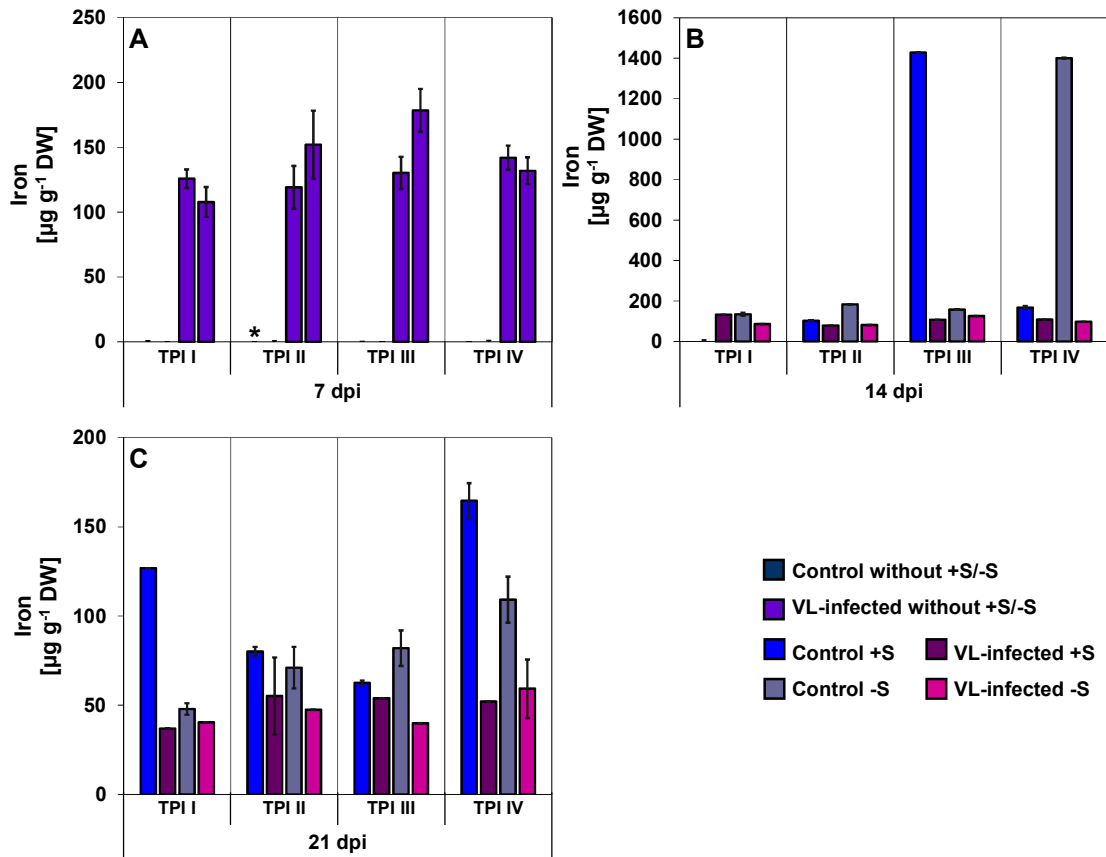


**Figure 3.8: Pre-experiment I: elemental iron (Fe).** Status of Fe content in mock- and mycelium-spore inoculated plants potted in sand/soil measured by ICP-OES; **A:** samples of 7 dpi without different sulfur supply: **turquoise bars** (left) control plants without +S/-S; **bluish violet bars** (right) VL-infected plants without +S/-S; **\*one** control sample TPI II got lost; **B:** samples of 14 dpi with different sulfur supply (+S/-S); **C:** samples of 21 dpi with different sulfur supply (+S/-S); **note:** Fe was calculated as  $\mu\text{g g}^{-1}$  DW; data represent the mean of three dependent technical replicates  $\pm$  SD.

### 3.1.4 The content of indolic, aliphatic and benzylic glucosinolates in mock- and mycelium-spore inoculated plants potted in sand/soil

Glucosinolates belong to the SDCs and it is known, that they play an important role in plant defense mechanisms against fungal pathogens (1.5.1). To further investigate their role in this specific host-pathogen system, samples of 7, 14 and 21 dpi were measured by HPLC (2.7.4). Samples from 7 dpi were not fertilized yet, so that in each respective figure two bars stand for the same treated plants (**Fig. 3.9-3.11; control:** turquoise bars; **VL-infected:** bluish violet bars). One control sample at 7 dpi of **TPI II** got lost (see asterisks in **Fig. 3.9-3.11**). A total of nine GSLs were measured with three belonging to **indolic GSLs (IGSLs):** glucobrassicin, neoglucobrassicin and 4-hydroxyglucobrassicin), five to **aliphatic GSLs (AGSLs):** progointrin, glucoalyssin, glucoraphanin, glucobrassicinapin and gluconapin) and one to **benzylic GLS (BGSL):**

## Results

gluconasturtiin). The amount of GSLs was calculated in  $\text{nmol g}^{-1}$  dry weight (DW). The measurements of samples from 7 dpi indicated higher values in the two **VL-infected** groups compared to the two **control**-groups in **IGSLs**, **AGSLs** and **BGSL** (Fig. 3.9-3.11).

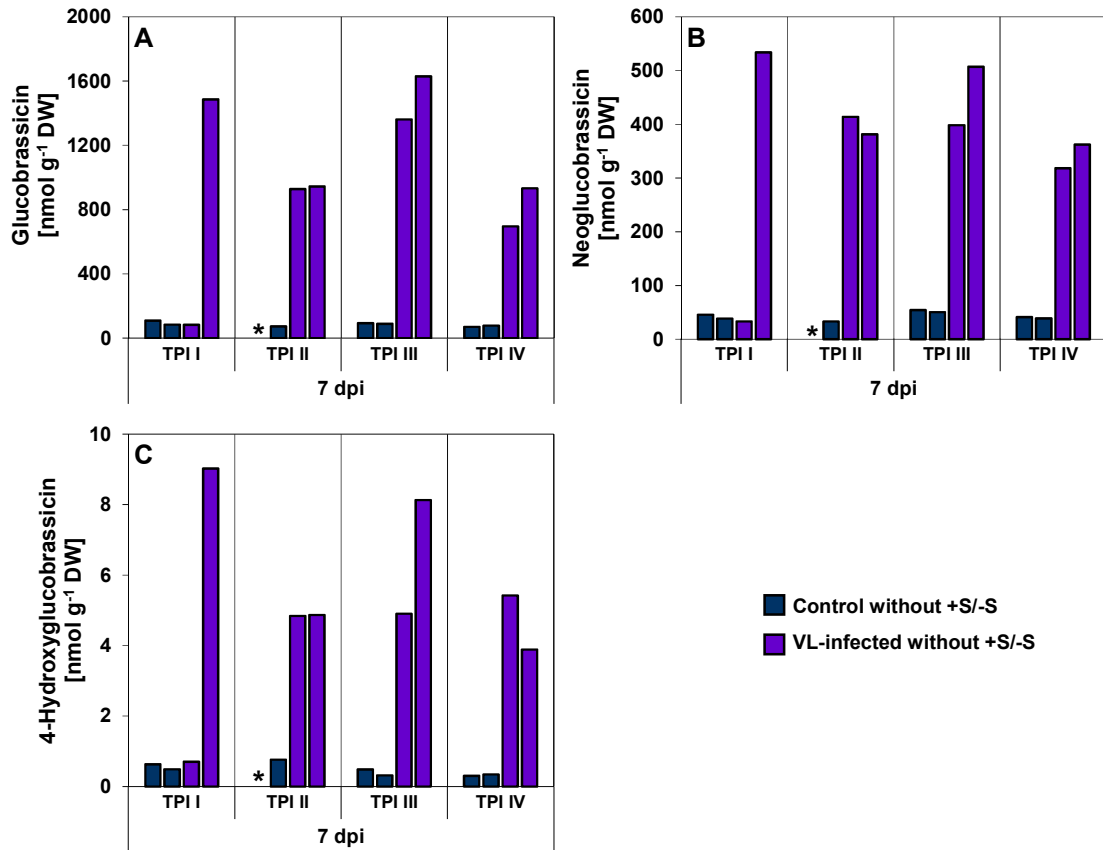


**Figure 3.9: Pre-experiment I: status of IGSL content in mock- and mycelium-spore inoculated plants potted in sand/soil measured by HPLC (7 dpi).** Samples without different sulfur supply: **turquoise bars** (left) control plants without +S/-S; **bluish violet bars** (right) VL-infected plants without +S/-S; **\*one** control sample TPI II got lost; **A**: glucobrassicin; **B**: neoglucobrassicin; **C**: 4-hydroxyglucobrassicin; data represent the result of one measurement.

## Results

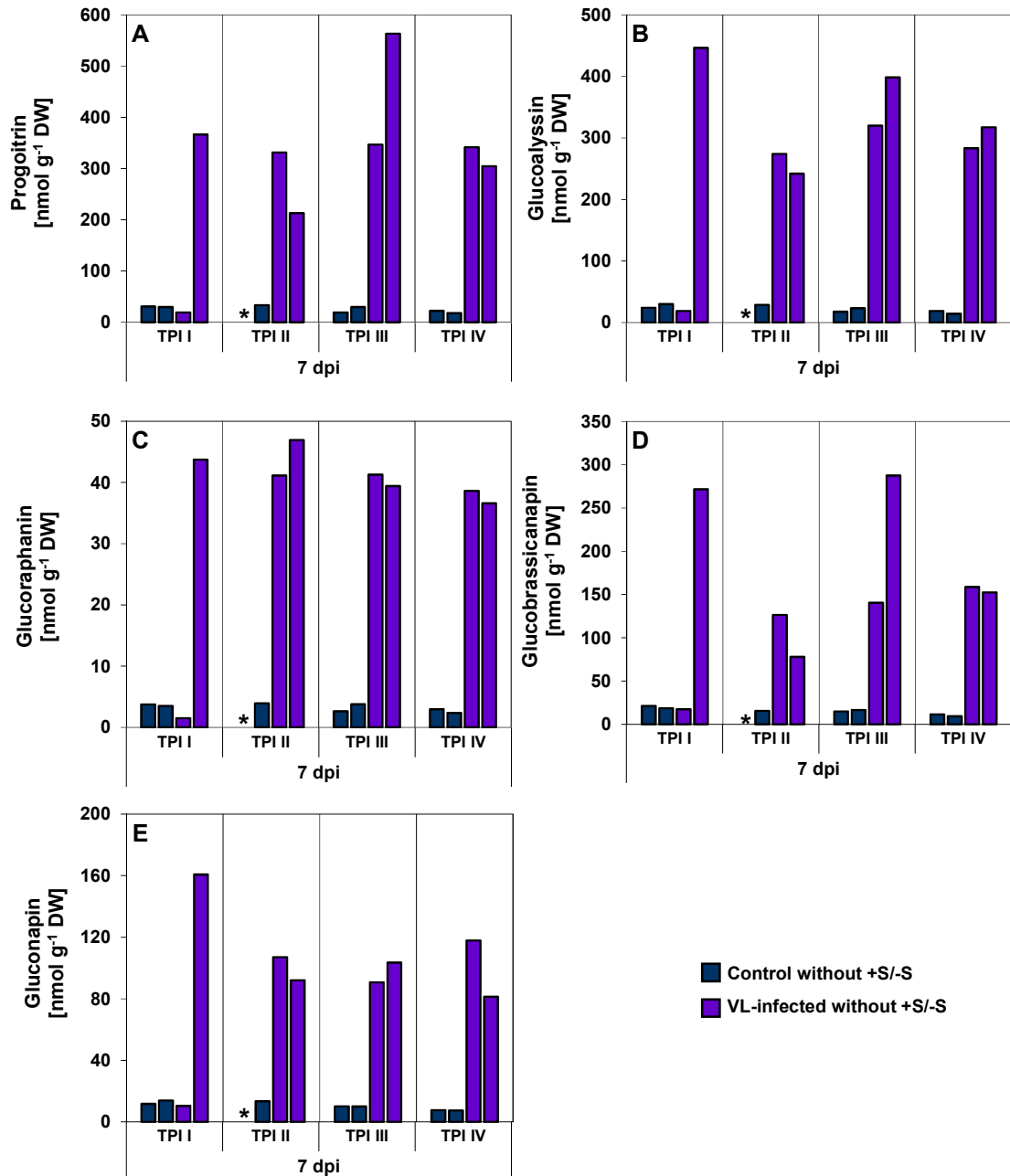


**Figure 3.10: Pre-experiment I: status of AGSL content in mock- and mycelium-spore inoculated plants potted in sand/soil measured by HPLC (7 dpi).** Samples without different sulfur supply: **turquoise bars** (left) control plants without +S/-S; **bluish violet bars** (right) VL-infected plants without +S/-S; \*one control sample TPI II got lost; **A**: progoitrin; **B**: glucoalyssin; **C**: glucoraphanin; **D**: glucobrassicinapin; **E**: gluconapin; data represent the result of one measurement.

An exception can be seen in **VL-infected TPI I/left bar**, these values were in a range of the two corresponding **control** groups. In most cases, both **VL-infected** groups showed a similar value range, but for 4-hydroxyglucobrassicin, progoitrin and glucobrassicinapin each **VL-infected TPI III/right bar** showed an increase of 43% compared to **VL-infected TPI III/left bar** (Fig. 3.9, C; Fig. 3.10, A; Fig. 3.10, D). The

## Results

**VL-infected TPI III/left bar** had the highest amount with 771.24 nmol g<sup>-1</sup> DW of gluconasturtiin (**Fig. 3.11**).

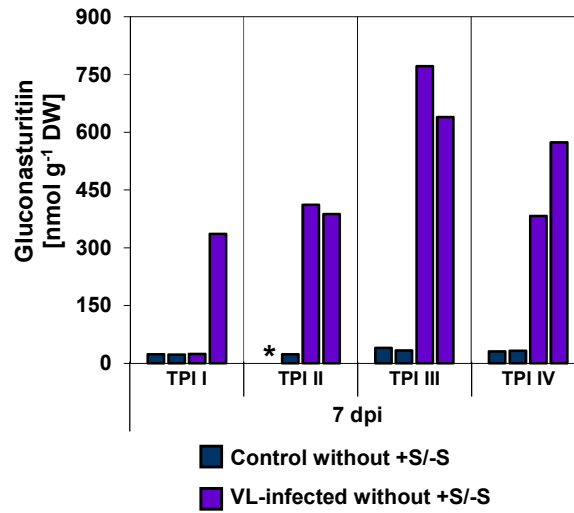


**Figure 3.11: Pre-experiment I: status of the BGLS gluconasturtiin content in mock- and mycelium-spore inoculated plants potted in sand/soil measured by HPLC (7 dpi).** Samples without different sulfur supply: **turquoise bars** (left) control plants without +S/-S; **bluish violet bars** (right) VL-infected plants without +S/-S; \*one control sample TPI II got lost; data represent the result of one measurement.

At 14 dpi the amount of **GSLs** decreased in all groups. In **IGSLs** the **control** and **VL-infected** groups fertilized with **sufficient sulfur** supply were in a similar value range (**Fig. 3.12**). The **VL-infected -S**-groups showed higher levels compared to **control -S**-groups, the amount for 4-hydroxyglucobrassicin was not measurable in most **control -S**-groups (**Fig. 3.12, C**).

## Results

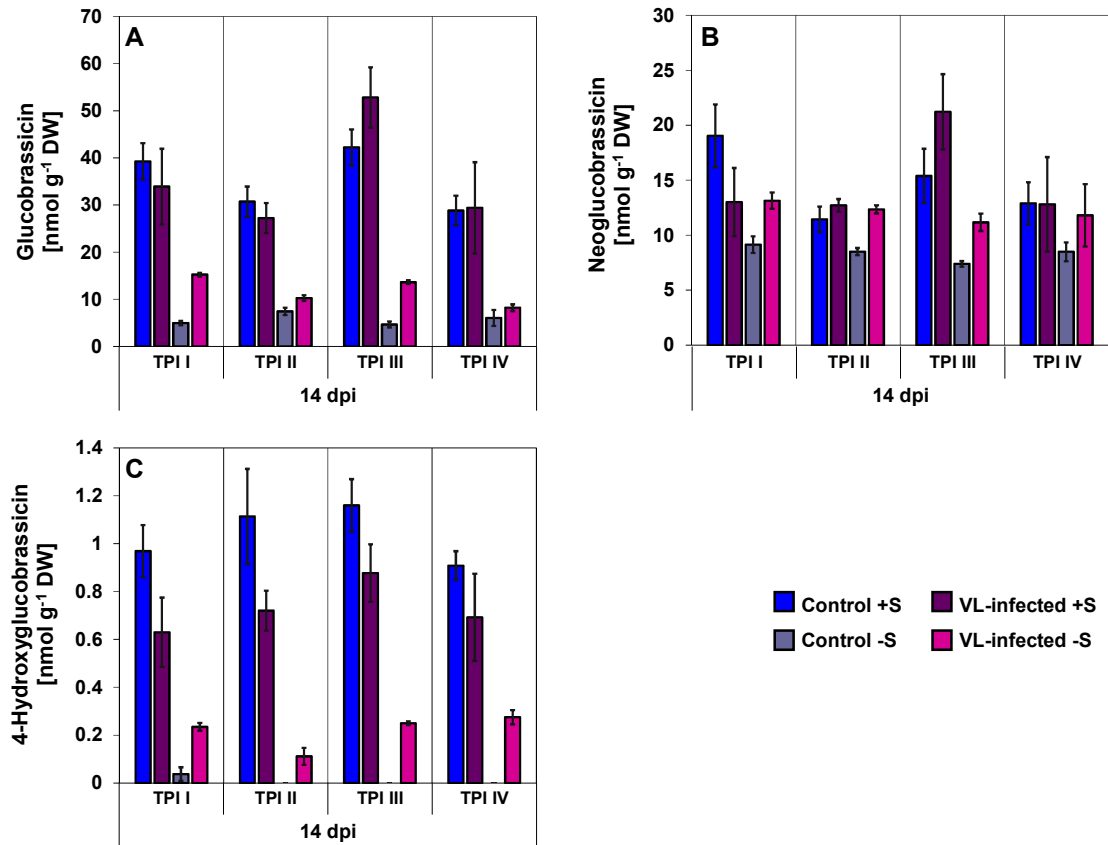


**Figure 3.12: Pre-experiment I: status of IGSL content in mock- and mycelium-spore inoculated plants potted in sand/soil measured by HPLC (14 dpi). A:** glucobrassicin; **B:** neoglucobrassicin; **C:** 4-hydroxyglucobrassicin; data represent the mean of three dependent technical replicates  $\pm$  SD.

In the **AGSLs control +S**-groups showed the highest values, while the **VL-infected +S**-groups showed partly 50% lower values (**Fig. 3.13**). Most **VL-infected -S**-groups decreased even further, while **control -S**-groups were barely measurable.

## Results

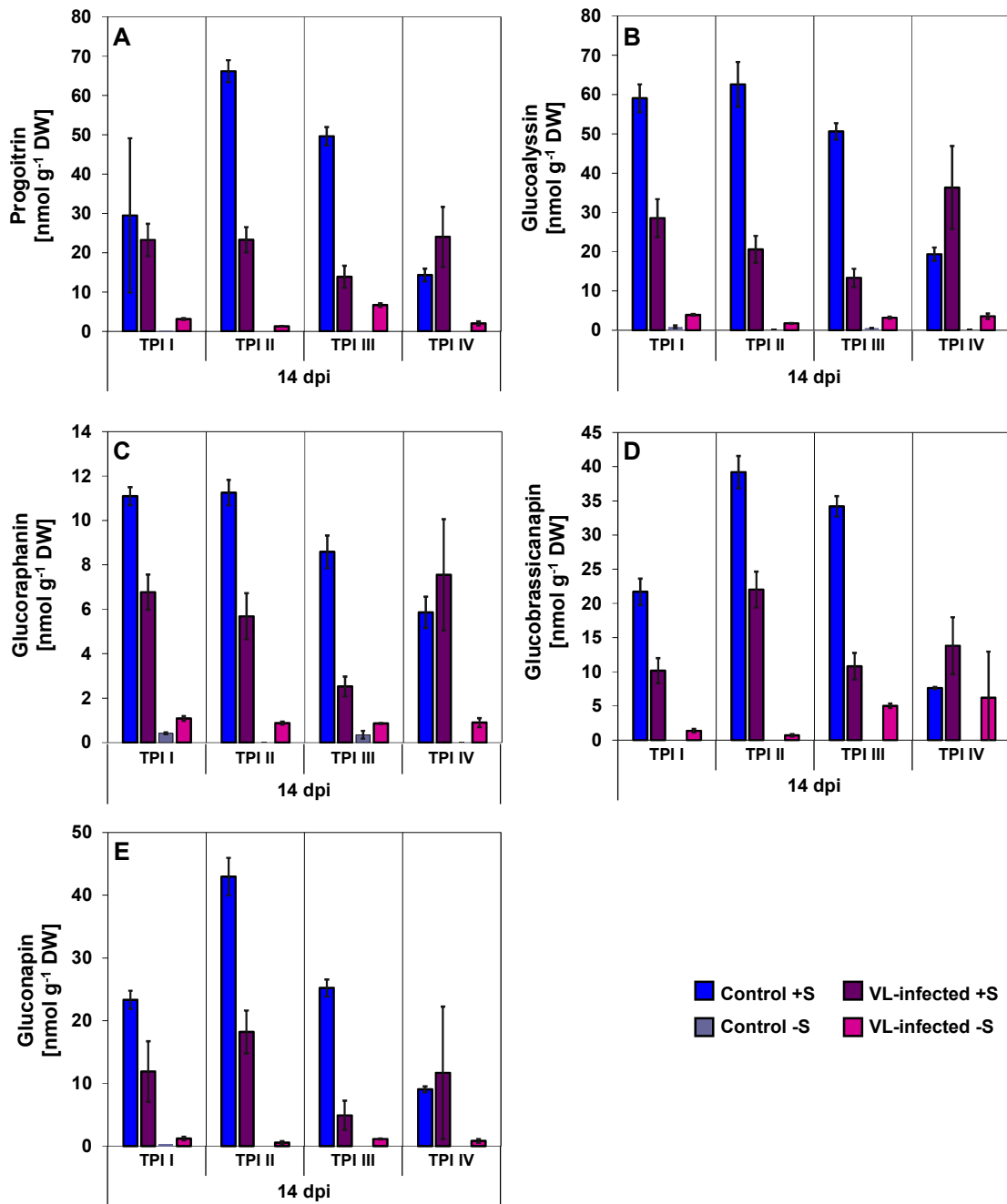


**Figure 3.13: Pre-experiment I: status of AGSL content in mock- and mycelium-spore inoculated plants potted in sand/soil measured by HPLC (14 dpi). A: progoitrin; B: glucoalyssin; C: glucoraphanin; D: glucobrassicinapin; E: gluconapin; data represent the mean of three dependent technical replicates  $\pm$  SD.**

For gluconasturtiin values of **control** and **VL-infected** groups fertilized with **sufficient sulfur** supply ranged at similar levels, but **VL-infected/TPI III** had still the highest value with 25.14 nmol g<sup>-1</sup> DW (**Fig. 3.14**). In addition, higher values were observed in **VL-infected -S**-groups compared to **control -S**-groups.



## Results

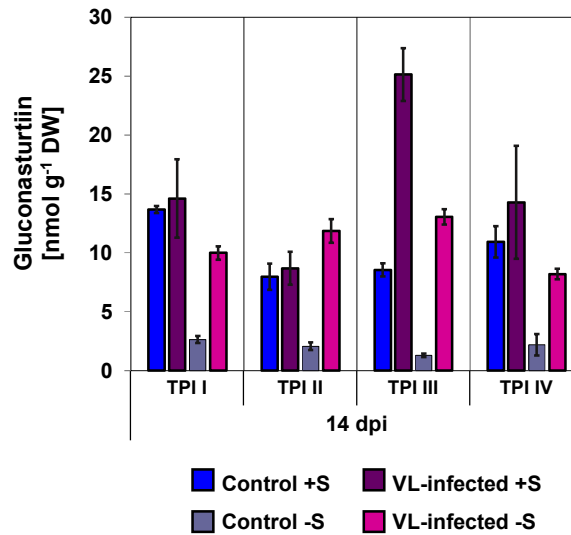


**Figure 3.14: Pre-experiment I: status of the BGS glaucosturtiin content in mock- and mycelium-spore inoculated plants potted in sand/soil measured by HPLC (14 dpi).** Data represent the mean of three dependent technical replicates  $\pm$  SD.

At 21 dpi **control +S**-groups had at most **TPIs** the highest contents of **IGSLs** and **AGSLs**, followed by **VL-infected +S**-groups (**Fig. 3.15**; **Fig. 3.16**). Furthermore, **control -S**-groups showed higher values than **VL-infected -S**-groups. However, values for 4-hydroxyglucobrassicin were not measurable for **VL-infected -S**-groups (**Fig. 3.15, C**). The **AGSLs** could only be measured in parts in **control -S**-groups, whereas they were no longer detectable in the **VL-infected -S**-groups.

## Results

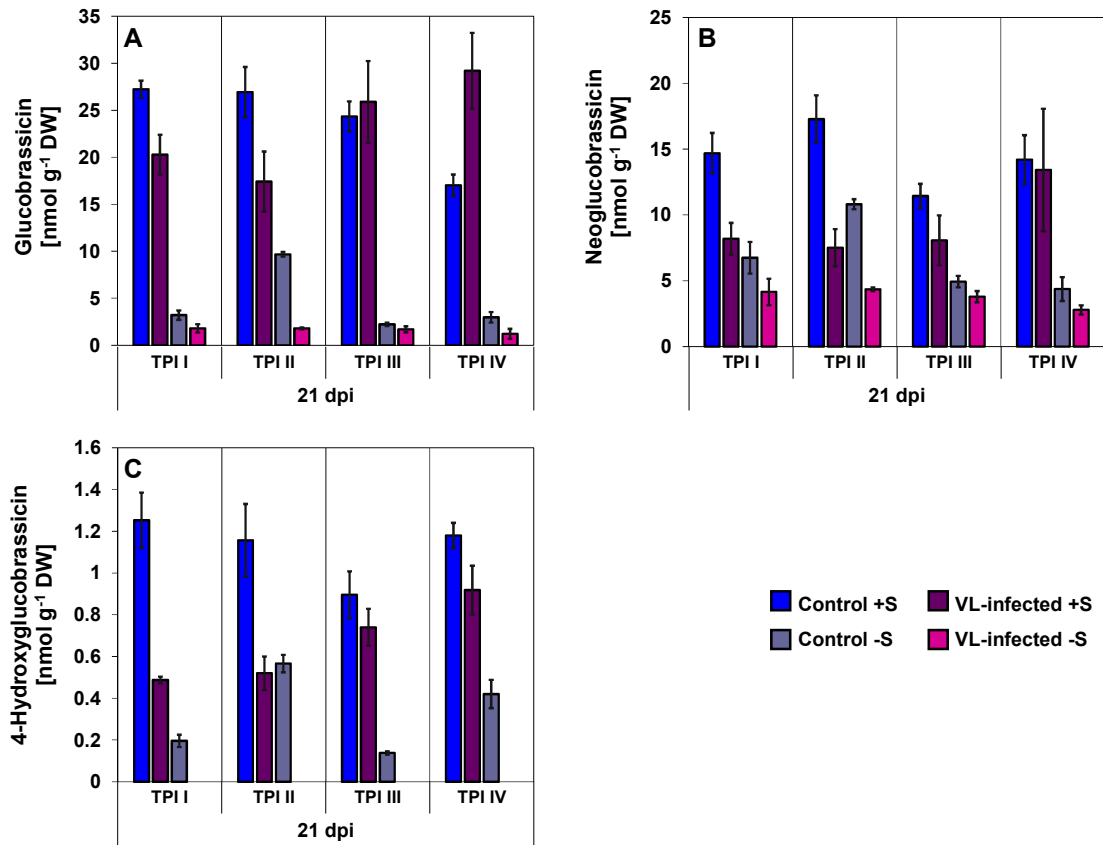


**Figure 3.15: Pre-experiment I: status of IGSL content in mock- and mycelium-spore inoculated plants potted in sand/soil measured by HPLC (21 dpi). A:** glucobrassicin; **B:** neoglucobrassicin; **C:** 4-hydroxyglucobrassicin; data represent the mean of three dependent technical replicates  $\pm$  SD.

## Results

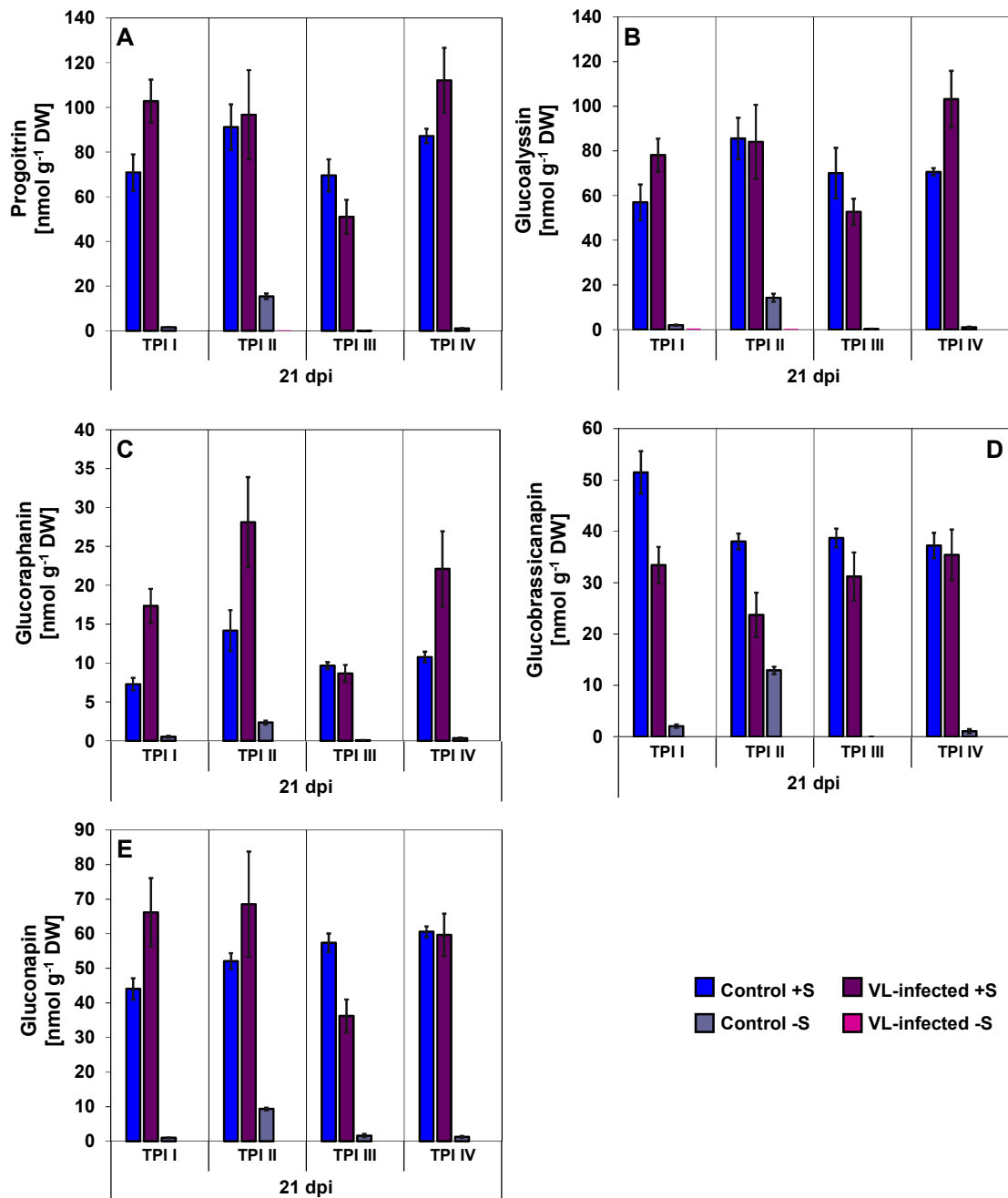


**Figure 3.16: Pre-experiment I: status of AGSL content in mock- and mycelium-spore inoculated plants potted in sand/soil measured by HPLC (21 dpi). A: progoitrin; B: glucoalyssin; C: glucoraphanin; D: glucobrassicinapin; E: gluconapin; data represent the mean of three dependent technical replicates  $\pm$  SD.**

## Results

The amount of gluconasturtiin in **control** and **VL-infected +S**-groups were similar at **TPI I** and **TPI II**, same occurred in **control** and **VL-infected -S**-groups at all **TPIs** (Fig. 3.17). The highest levels were in **VL-infected +S**-groups at **TPI III** and **TPI IV**.

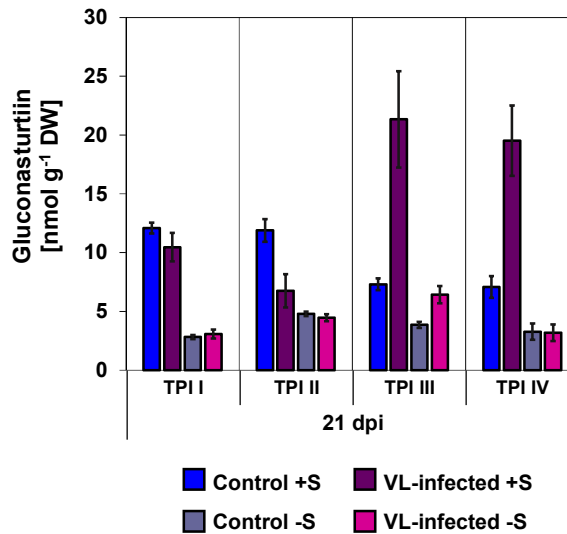


**Figure 3.17: Pre-experiment I: status of the BGSGL gluconasturtiin content in mock- and mycelium-spore inoculated plants potted in sand/soil measured by HPLC (21 dpi).** Data represent the mean of three dependent technical replicates  $\pm$  SD.

### 3.2 Pre-experiment II: inoculation of 16 d old plants (previous fertilization with different sulfur supply) with mycelium-spore mixture and subsequent cultivation in sand

Since the “Einheitserde”, which was used in pre-experiment I for the substrate mixture, may have a potential influence on the analysis due to its ingredients, the plants were only cultivated in autoclaved sand. In addition, the plants should be fertilized with different sulfur supply before inoculation in order to investigate a possible influence on the infection. Therefore already fertilized but older plants (16 d) were used for the **pre-experiment II** (2.5.2). To verify the infection with *V. longisporum* samples were analyzed by qPCR (3.2.1). Levels of elements were measured with ICP-OES, where should be tried out whether roots can also be used for this analysis. (3.2.2).

#### 3.2.1 Detection and verification of the infection with *V. longisporum* in mycelium-spore inoculated *B. napus* plants potted in sand

In order to investigate the fungal spread in the plant, qPCR analysis was performed using **ITS** (Fig. 3.18). Samples of 7 and 15 dpi were measured and the amount of VL-DNA was calculated in  $\text{ng g}^{-1}$  FW. Most control samples analyzed with ITS primers

## Results

were undetected or the detection of VL-DNA was below limit of detection or below limit of quantification, respectively (data not shown).

At 7 dpi the amounts of VL-DNA in **+S**-plants ranged from 7.49 to 39.62 ng g<sup>-1</sup> FW, whereby the amount in **-S**-plants laid in a range between 46.63-73.58 ng g<sup>-1</sup> FW (**Fig 3.18, A**). In **+S**-plants the content of VL-DNA at **TPI I** and **TPI II** was more than half lower than in the corresponding **-S**-plants. At **TPI III** the value of VL-DNA was similar in both **VL-infected** groups. A difference of almost 90% was observed at **TPI IV**.

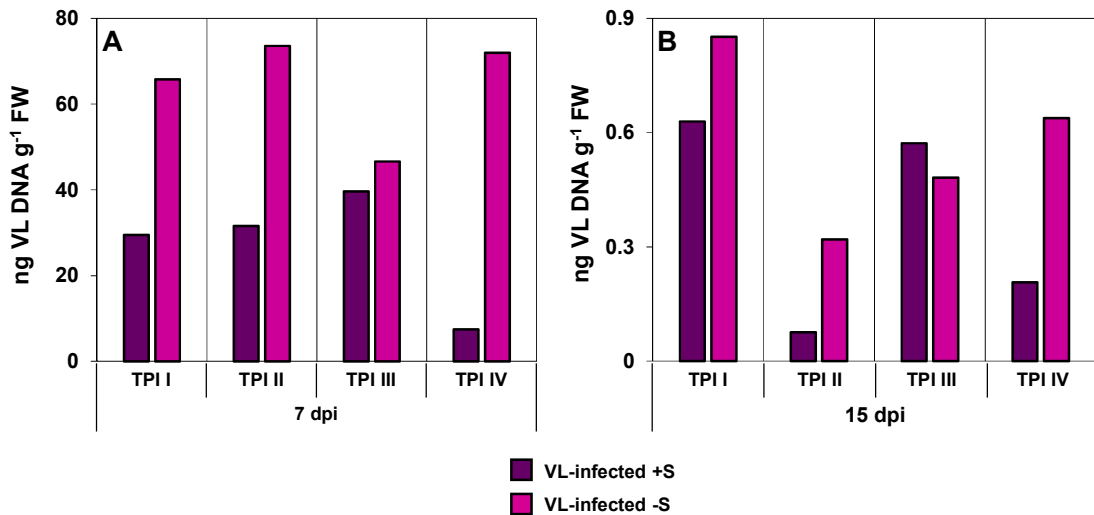


**Figure 3.18: Pre-experiment II: amount of *V. longisporum* VL43-DNA detected by qPCR with ITS primers in *B. napus*.** Status of infection rate in mycelium-spore inoculated plants potted in sand; before inoculation procedure, plants were fertilized with different sulfur supply (1 mM MgSO<sub>4</sub>: +S; 0.01 mM MgSO<sub>4</sub>: -S) **A**: 7 dpi; **B**: 15 dpi; **purple bars** represent VL-infected +S, **pink bars** VL-infected -S; data represent the result of one measurement.

At 15 dpi the amount of VL-DNA decreased in all **VL-infected** groups (**Fig 3.18, B**). At **TPI I**, **TPI II** and **TPI IV VL-infected -S**-groups (0.32-0.85 ng g<sup>-1</sup> FW) showed slightly higher values of VL-DNA compared to the corresponding **+S**-groups (0.08-0.63 ng g<sup>-1</sup> FW), whereby the status in **TPI III** was similar.

### 3.2.2 Elemental analysis: levels of sulfur, calcium, potassium and iron in mock- and mycelium-spore inoculated plants potted in sand

Samples were harvested at 7 and 15 dpi and measured with the ICP-OES. From samples of 15 dpi roots were harvested separately. Depend on root size, there was only enough material of **+S-plants** for the measurement. Of each sample, one extract were made, which were measured thrice.

## Results

At 7 dpi the sulfur content in **control +S**-groups at **TPI I**, **TPI II** and **TPI III** were highest compared to the other groups (**Fig. 3.19, A**). At **TPI II** values in **control** and **VL-infected +S**-plants were similar (about 5 mg g<sup>-1</sup> DW). At **TPI II** the **VL-infected -S**-group (1.57 mg g<sup>-1</sup> DW) showed a slightly higher amount of sulfur compared to the corresponding **control -S**-group (1.19 mg g<sup>-1</sup> DW).

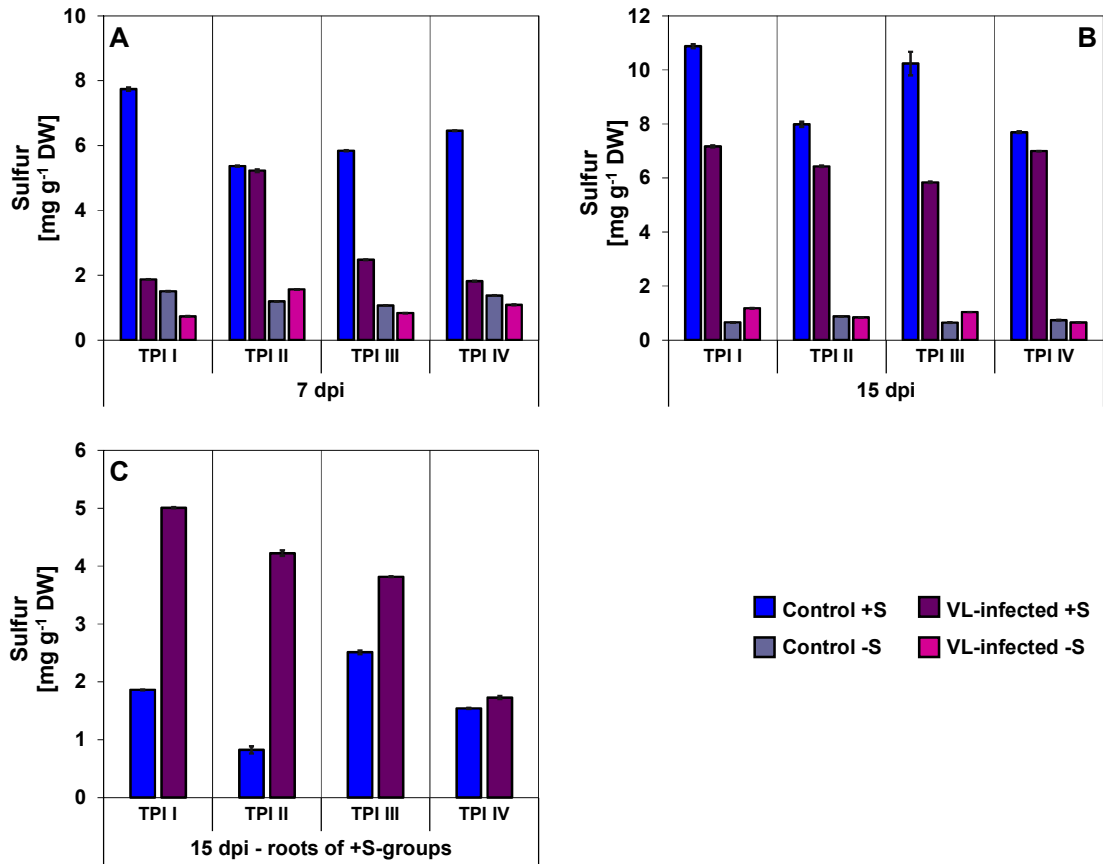


**Figure 3.19: Pre-experiment II: level of elemental S content in mock- and mycelium-spore inoculated plants potted in sand measured by ICP-OES. A: 7 dpi; B: 15 dpi C: 15 dpi, roots of +S-groups; data represent the mean of three dependent technical replicates  $\pm$  SD.**

At 15 dpi the amount of sulfur increased in **control** and **VL-infected** plants, which were fertilized with **sufficient sulfur** supply, whereby the **control** plants showed higher values (7-11 mg g<sup>-1</sup> DW) (**Fig. 3.19, B**). In **control -S**-groups the values decreased about 26-56%. At **TPI I** the amount in **VL-infected -S**-plants increased about 38% and in **TPI III** about 20%. The measurement of the roots of **control** and **VL-infected +S**-plants displayed higher contents of sulfur in **VL-infected** plants at **TPI I-III** (3.82-5 mg g<sup>-1</sup> DW; control: 0.82-2.51 mg g<sup>-1</sup> DW) (**Fig. 3.19, C**). At **TPI IV** both groups had similar values around 1.5 mg g<sup>-1</sup> DW.

The calcium content at 7 dpi were highest in **control -S**-plants at **TPI I** and **TPI II** (around 24 mg g<sup>-1</sup> DW) (**Fig. 3.20, A**). At **TPI III** and **IV** the values for **control +S**- and **-S**-plants were in the same range (17-20 mg g<sup>-1</sup> DW). The amount of calcium was

## Results

slightly higher in **VL-infected -S**-groups (9-16 mg g<sup>-1</sup> DW) at **TPI I**, **TPI II** and **TPI IV** compared to the corresponding **VL-infected +S**-groups (4-13 mg g<sup>-1</sup> DW).

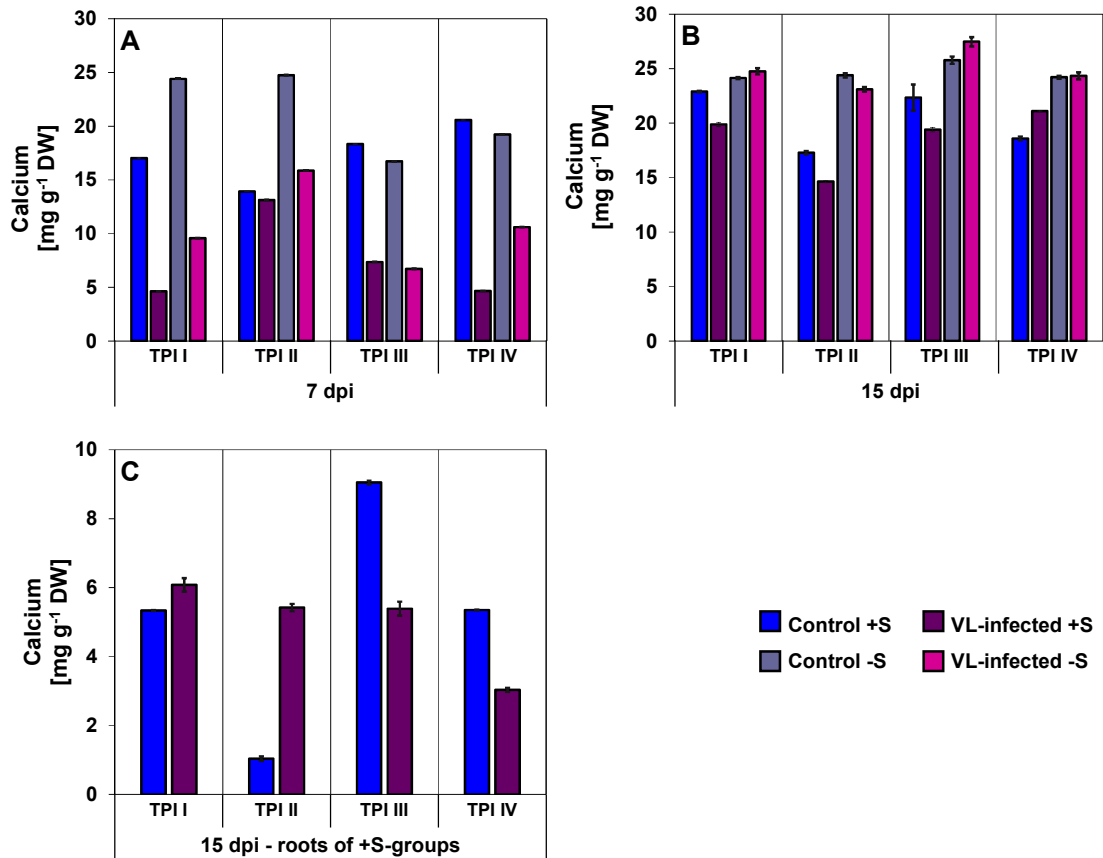


**Figure 3.20: Pre-experiment II: level of elemental Ca content in mock- and mycelium-spore inoculated plants potted in sand measured by ICP-OES. A: 7 dpi; B: 15 dpi C: 15 dpi, roots of +S-groups; data represent the mean of three dependent technical replicates  $\pm$  SD.**

At 15 dpi the content of calcium increased in **control +S**-groups in a range between 18-26% (one exception at **TPI IV**: decreased about 10%) and in **VL-infected +S**-groups between 10-78% (**Fig. 3.20, B**). The **control -S**-groups at **TPI I** and **TPI II** had similar values as on 7 dpi (**Fig. 3.20, A**). At **TPI III** and **IV** the values increased about 21-35%. The **VL-infected +S**-groups displayed an increase of 51-76%.

The content of calcium in roots of **control +S**- and **VL-infected +S**-groups showed the highest value at **TPI III** in the **control** group (9.05 mg g<sup>-1</sup> DW) (**Fig. 3.20, C**). In the corresponding **VL-infected** group a lower value about 40% was observed. At **TPI II** the amount was about 80% higher in the **VL-infected** group (5.42 mg g<sup>-1</sup> DW) compared to the **control** group. The calcium content at **TPI I** was similar in both groups (about 5-6 mg g<sup>-1</sup> DW). At **TPI IV** the value of the **control** group was 40% higher as in the **VL-infected** group.

## Results

The potassium content at 7 dpi was in **control** groups higher as in the corresponding **VL-infected** groups (**Fig. 3.21, A**). The highest values were observed in **control +S**-groups at **TPI I** and **TPI IV** (about 15 mg g<sup>-1</sup> DW). Within the TPIs, **VL-infected -S**-groups (0.68-4.53 mg g<sup>-1</sup> DW) revealed slightly higher values than the **VL-infected +S**-groups (0.44-1.06 mg g<sup>-1</sup> DW). At 15 dpi the content of potassium increased at all TPIs in all **control** and **VL-infected**-groups, with the exception of **control +S**-group and **control -S**-group at **TPI IV** (**Fig. 3.21, B**). An increase about 95-98% was observed in **VL-infected +S**-groups at **TPI III** and **TPI IV** and in **VL-infected -S**-groups at **TPI I** and **TPI III**.

The content of potassium in roots was overall higher in **VL-infected +S**-groups (6.01-13.11 mg g<sup>-1</sup> DW) than in **control** groups (1.57-3.71 mg g<sup>-1</sup> DW) (**Fig. 3.21, C**).

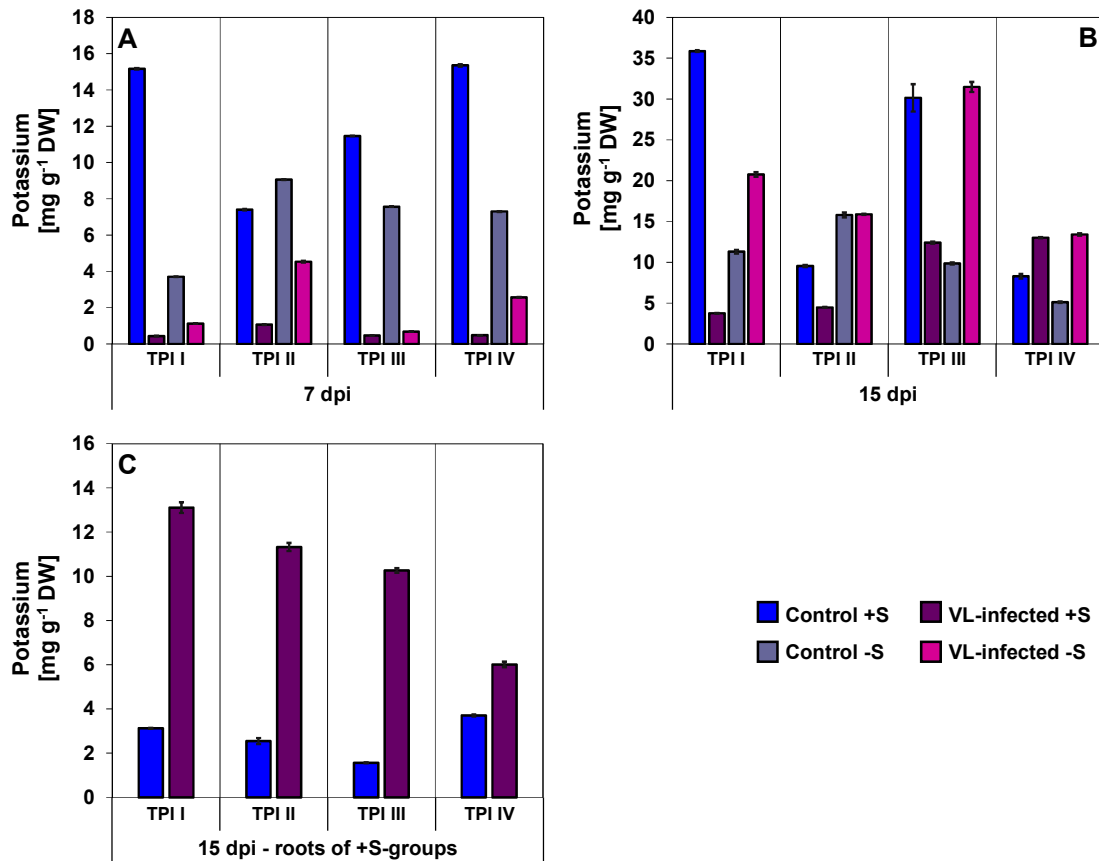


**Figure 3.21: Pre-experiment II: level of elemental K content in mock- and mycelium-spore inoculated plants potted in sand measured by ICP-OES. A: 7 dpi; B: 15 dpi C: 15 dpi, roots of +S-groups; data represent the mean of three dependent technical replicates  $\pm$  SD.**

At 7 dpi the iron content at **TPI I** was the highest in **VL-infected -S**-group (458.27  $\mu$ g g<sup>-1</sup> DW) followed by **control +S**-group (409.09  $\mu$ g g<sup>-1</sup> DW) (**Fig. 3.22, A**). The **VL-infected +S**-group and **control -S**-group showed similar values in a range between 303-330  $\mu$ g g<sup>-1</sup> DW. At **TPI II** the highest content was observed in **VL-infected -S**-group (709.02  $\mu$ g g<sup>-1</sup> DW) and **control -S**-group (671.09  $\mu$ g g<sup>-1</sup> DW). At **TPI III** the **control**



## Results

groups had values between 486-491  $\mu\text{g g}^{-1}$  DW, whereby the **VL-infected** groups laid between 310-379  $\mu\text{g g}^{-1}$  DW. The **VL-infected -S**-group showed at **TPI IV** the highest amount with 503.5  $\mu\text{g g}^{-1}$  DW, while values of the other groups ranged from 361-376  $\mu\text{g g}^{-1}$  DW. The amount of iron decreased at 15 dpi in **VL-infected +S**-group and **control -S**-group at **TPI I** about 61%, in **VL-infected -S**-group at **TPI III** about 51% and in the remaining groups in a range between 77-89% (**Fig. 3.22, B**). The highest content was observed in **VL-infected -S**-group at **TPI III** with 186.25  $\mu\text{g g}^{-1}$  DW.

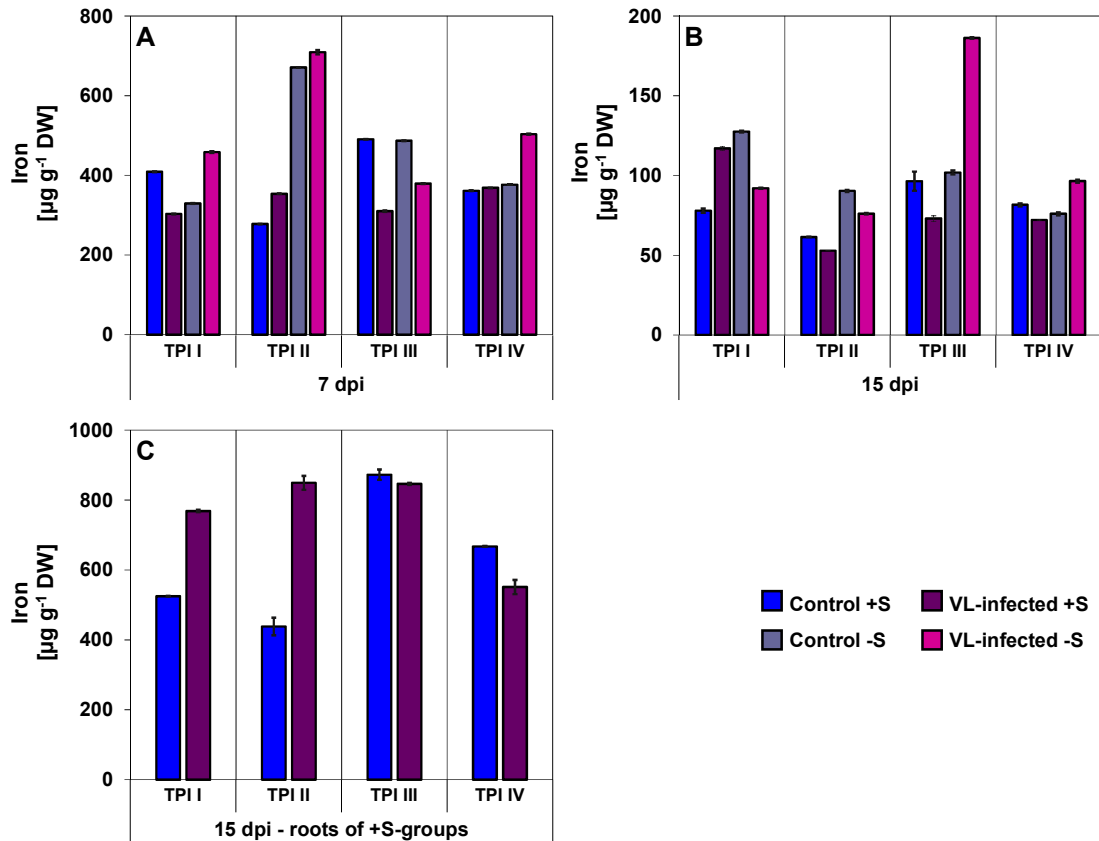


**Figure 3.22: Pre-experiment II: level of elemental Fe content in mock- and mycelium-spore inoculated plants potted in sand measured by ICP-OES. A: 7 dpi; B: 15 dpi C: 15 dpi, roots of +S-groups; note: Fe was calculated as  $\mu\text{g g}^{-1}$  DW; data represent the mean of three dependent technical replicates  $\pm$  SD.**

The values of iron in roots ranged from 438-873  $\mu\text{g g}^{-1}$  DW (**Fig. 3.22, C**). At **TPI I** and **TPI II** **VL-infected +S**-groups showed 32% and 48% higher values, respectively. The amounts of the other two groups were about the same range.

In summary, the **VL-infected -S**-groups, which had the highest levels of VL-DNA at **TPI II** and **TPI IV** (**Fig. 3.18, A**) showed at 7 dpi the highest levels within the four **VL-infected -S**-groups in sulfur, calcium, potassium and iron (**Fig. 3.19, A; Fig. 3.20, A; Fig. 3.21, A; Fig. 3.22, A**).

## Results

### 3.3 Pre-experiment IIIa: inoculation of 16 d old plants (previous fertilization with different sulfur supply) with different dilutions of mycelium-spore mixtures and subsequent cultivation in sand

Because the inoculation with mycelium-spore mixture basically worked at the first two pre-experiments, in **pre-experiment IIIa** different dilutions of the mycelium-spore mixture were tested in order to make the infection system even more controlled (**2.5.3**). Also the inoculation of older pre-fertilized plants seemed to work, therefore they were used again for the inoculation procedure. Since a total of three dilutions were tested (**Inoc I**: undiluted; **Inoc II**: 1:2; **Inoc III**: 1:10), the inoculation was performed at **TPI III**, otherwise there would have been too little space for the differently treated plants.

#### 3.3.1 Detection and verification of the infection with *V. longisporum* in different dilutions of mycelium-spore mixture inoculated *B. napus* plants potted in sand

Fungal biomass was quantified by determination of VL-DNA in infected and non-infected plant extracts of 1, 3, 7 and 14 dpi with qPCR using ITS primers (**Fig. 3.23**) It occurred a contamination problem with VL-DNA at 1 dpi in all **control -S**-groups (between 1.37-2.93 ng g<sup>-1</sup> FW), at 7 dpi in **control +S/Inoc I** (0.07 ng g<sup>-1</sup> FW) and at 14 dpi in **control -S/Inoc I** (0.51 ng g<sup>-1</sup> FW). The contamination could be disregarded, as no further analysis with the plant material should be carried out.

The highest values of VL-DNA were observed at 1 dpi in **VL-infected +S/Inoc III** (1.79 ng g<sup>-1</sup> FW), at 3 dpi in **VL-infected +S/Inoc III** (1.88 ng g<sup>-1</sup> FW) and **VL-infected -S/Inoc III** (1.9 ng g<sup>-1</sup> FW), at 7 dpi in **VL-infected +S/Inoc III** (1.54 ng g<sup>-1</sup> FW) and at 14 dpi in **VL-infected -S/Inoc II** (3.45 ng g<sup>-1</sup> FW). The **VL-infected +S**-plants inoculated with **Inoc I** showed a decrease about 35%, 95% and 20% in the content of VL-DNA over the collection time period, respectively (1-14 dpi: 1.59-0.04 ng g<sup>-1</sup> FW), while **VL-infected -S/Inoc I** showed an increase about 17% from 1 to 3 dpi (0.29-0.35 ng g<sup>-1</sup> FW), followed by a decrease about 80% at 7 dpi (0.07 ng g<sup>-1</sup> FW) and an increase about 84% at 14 dpi (0.43 ng g<sup>-1</sup> FW), respectively. **Sufficiently** fertilized **VL-infected/Inoc II** displayed an increase about 82% (0.22-1.24 ng g<sup>-1</sup> FW) from 1 to 3 dpi, followed by a decrease about 98% at 7 dpi (0.02 ng g<sup>-1</sup> FW) and 50% at 14 dpi (0.01 ng g<sup>-1</sup> FW), respectively. The amount of VL-DNA in **VL-infected -S**-plants decreased from 1 to 3 dpi about 73% (0.73-0.2 ng g<sup>-1</sup> FW) and increased from 3 to 7 dpi about 52% (0.42 ng g<sup>-1</sup> FW) and from 7 to 14 dpi about 88% (3.45 ng g<sup>-1</sup> FW). **VL-infected +S**-plants inoculated with **Inoc III** showed an increase of VL-DNA about 5% from 1 to 3 dpi (1.79-1.88 ng g<sup>-1</sup> FW), followed by a decrease about 18% at 7 dpi (1.54 ng g<sup>-1</sup> FW) and 89% at 14 dpi (0.16 ng g<sup>-1</sup> FW), respectively. The amount of VL-DNA

## Results

increased about 70% in **VL-infected -S/Inoc III** from 1 to 3 dpi (0.57-1.9 ng g<sup>-1</sup> FW), where at 7 dpi the content of VL-DNA was not measurable. However, at 14 dpi *V. longisporum* continued its spread within this group and the value raised again (0.53 ng g<sup>-1</sup> FW).

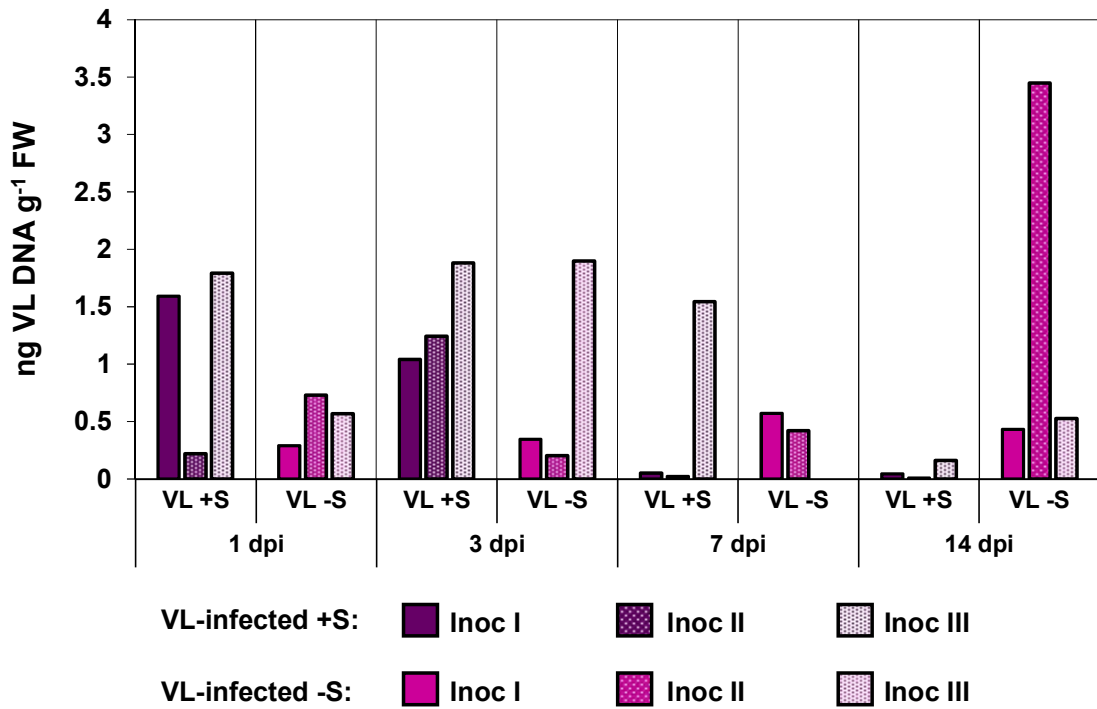


**Figure 3.23: Pre-experiment IIIa: amount of *V. longisporum* VL43-DNA detected by qPCR with ITS primers in *B. napus*.** Status of infection rate in different dilutions of mycelium-spore mixture inoculated plants potted in sand; before inoculation procedure at **TPI III**, plants were fertilized with different sulfur supply (1 mM MgSO<sub>4</sub>: +S; 0.01 mM MgSO<sub>4</sub>: -S); **Inoc I**: undiluted; **Inoc II**: 1:2; **Inoc III**: 1:10; data represent the result of one measurement.

## Results

### 3.4 Pre-experiment IIIb: inoculation of 16 d old plants (previous fertilization with different sulfur supply) with diluted mycelium-spore mixture and subsequent cultivation in sand

Based on the qPCR analysis of **pre-experiment IIIa**, **Inoc III dilution** was selected for **pre-experiment IIIb (2.5.4)**, because it seemed most stable and also worked relatively successfully in **+S-** and **-S-**groups (**3.3.1**).

#### 3.4.1 Detection and verification of the infection with *V. longisporum* in 1:10 dilution of mycelium-spore mixture inoculated *B. napus* plants potted in sand

In plants proliferation of *V. longisporum* was quantified by determining fungal DNA via qPCR using ITS primers (first run: **Fig. 3.24**; second run: **Fig. 3.25**). Samples of 3, 7 and 14 dpi were measured. In most control samples no VL-DNA could be measured, because the detection limit was not reached or the quantification limit, respectively (data not shown). One contamination problem with VL-DNA occurred at 14 dpi (second run) in **control +S/TPI I** (0.13 ng g<sup>-1</sup> FW). This experiment was performed twice.

In the first run of experiment the content of VL-DNA at 3 dpi was highest in **VL-infected +S-** (1.74 ng g<sup>-1</sup> FW) and **-S-**plants (0.8 ng g<sup>-1</sup> FW) at **TPI I**, while the other groups ranged from 0.01-0.02 ng g<sup>-1</sup> FW (**Fig. 3.24, A**). At 7 dpi the amount of VL-DNA increased about 88% at **TPI IV** in **VL-infected +S**, while it decreased in the other groups (**Fig. 3.24, B**). At 14 dpi the values at **TPI I** and **TPI IV** in **VL-infected -S**-groups increased about 20% (0.35 ng g<sup>-1</sup> FW) and 96% (0.28 ng g<sup>-1</sup> FW), respectively (**Fig. 3.24, C**).

## Results

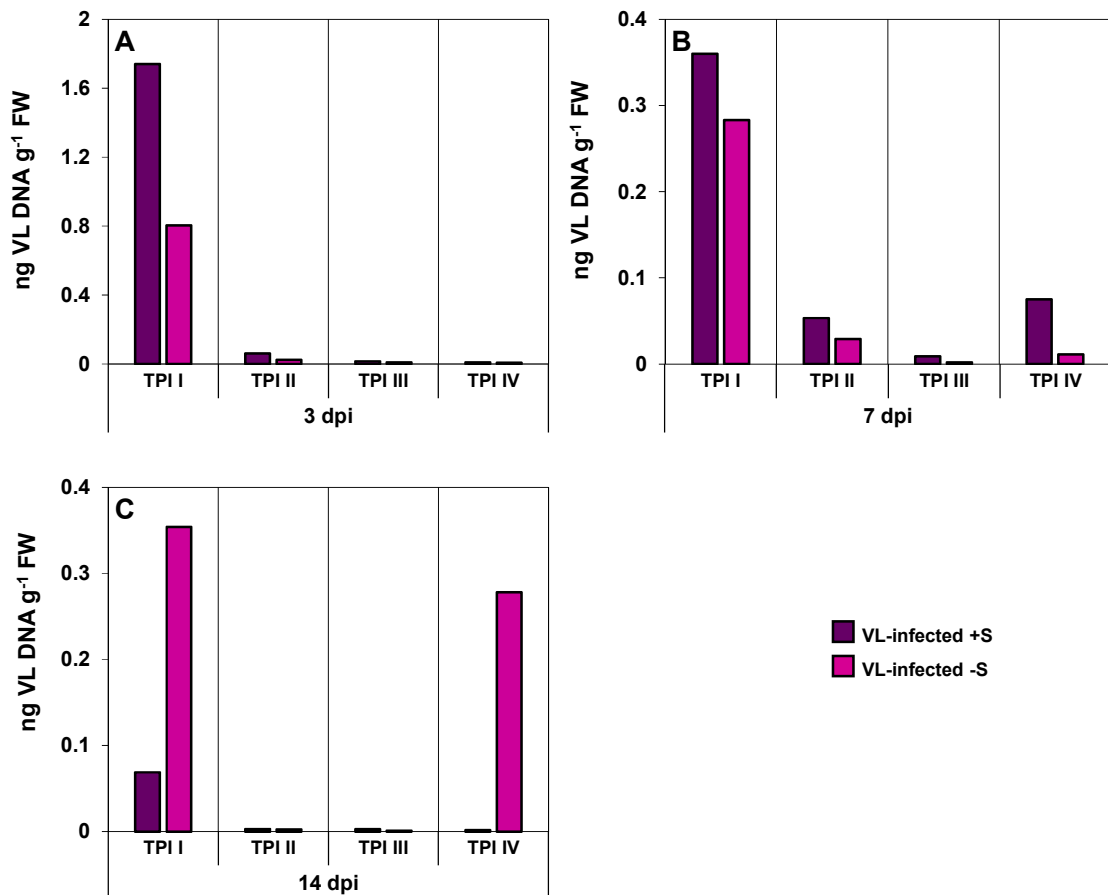


**Figure 3.24: Pre-experiment IIIb, first run: amount of *V. longisporum* VL43-DNA detected by qPCR with ITS primers in *B. napus*.** Status of infection rate in 1:10 diluted mycelium-spore inoculated plants potted in sand; before inoculation procedure, plants were fertilized with different sulfur supply (1 mM MgSO<sub>4</sub>: +S; 0.01 mM MgSO<sub>4</sub>: -S) **A**: 3 dpi; **B**: 7 dpi; **C**: 14 dpi; **purple bars** represent VL-infected +S, **pink bars** VL-infected -S; data represent the result of one measurement.

The second run showed a similar result at 3 dpi with the difference, that the value of at **TPI I** in **VL-infected +S** and **VL-infected -S** was about 42% and 80% higher, respectively (**Fig. 3.25, A**). At 7 dpi the amount of VL-DNA decreased at **TPI I** in both groups (between 43-69%) and at **TPI III** in the **VL-infected +S**-group (about 50%) (**Fig. 3.25, B**). In the other groups occurred an increase between 50-93%, but the values were below 0.5 ng g<sup>-1</sup> FW. At 14 dpi the amount of VL-DNA at **TPI II**, **TPI III** and **TPI IV** was in all groups below 0.01 ng g<sup>-1</sup> FW (**Fig. 3.25, C**). At **TPI I** the **VL-infected +S**-group showed an increase about 5% and the **VL-infected -S**-group a decrease about 75%.

## Results

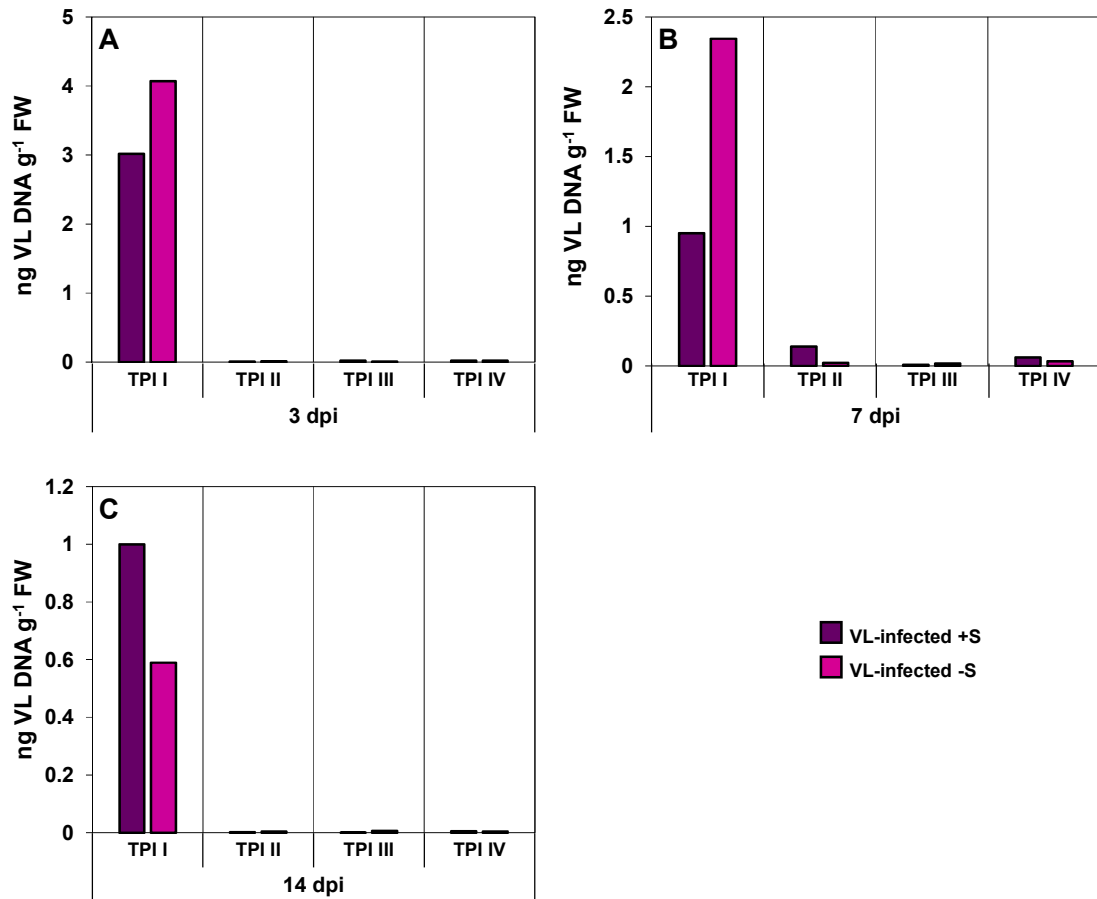


**Figure 3.25: Pre-experiment IIIb, second run: amount of *V. longisporum* VL43-DNA detected by qPCR with ITS primers in *B. napus*. Status of infection rate in 1:10 diluted mycelium-spore inoculated plants potted in sand; before inoculation procedure, plants were fertilized with different sulfur supply (1 mM MgSO<sub>4</sub>: +S; 0.01 mM MgSO<sub>4</sub>: -S) **A**: 3 dpi; **B**: 7 dpi; **C**: 14 dpi; **purple bars** represent VL-infected +S, **pink bars** VL-infected -S; data represent the result of one measurement.**

## Results

### 3.5 Pre-experiment IV: inoculation of 7 d old plants with spore solution and subsequent cultivation in sand

The inoculation procedure in the **pre-experiment IV** was performed with a defined spore solution (2.5.5). Even if the results of the **pre-experiments I-IIIa**, in which the infection with mycelium-spore mixture was successful, looked promising, the “standard inoculation procedure” with spores should be tried at the different TPIs. Since there were problems with the inoculation of older plants that had been fertilized differently with sulfur in advance, 7-days-old plants were used again for this experiment. To determine the levels of VL-DNA in the infected plants,  $\beta$ -tubulin primers were used in the qPCR analysis.

#### 3.5.1 Detection and verification of the infection with *V. longisporum* in spore solution inoculated *B. napus* plants potted in sand

DNA of *V. longisporum* was extracted of samples from 3, 7 and 14 dpi and quantified by qPCR using  $\beta$ -tubulin primers. (Fig. 3.26). Samples of 7 dpi were not fertilized yet, the bars represent two biological replicates. The content of VL-DNA was below detection limit in most control plants (data not shown).

At 3 dpi the amount at **TPI I** and **TPI II** was similar in both **VL-infected** groups (3.61-3.71 ng g<sup>-1</sup> FW; 7.46-7.95 ng g<sup>-1</sup> FW) (Fig. 3.26, A). The value of **TPI III/left bar** was not measurable, while **TPI III/right bar** showed a value about 2.58 ng g<sup>-1</sup> FW. The highest amount of VL-DNA was observed at **TPI IV/left bar** (13.15 ng g<sup>-1</sup> FW), whereby **TPI IV/right bar** showed a 71% lower value.

## Results

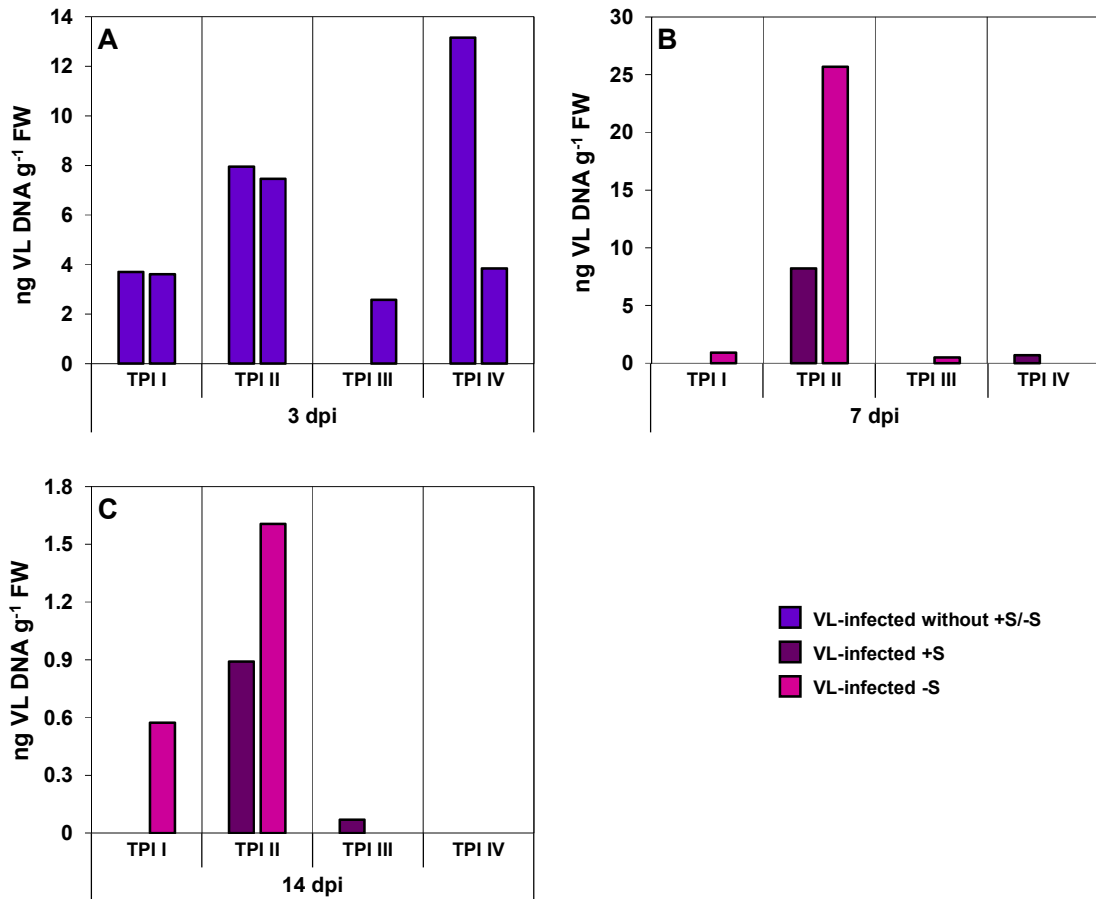


**Figure 3.26: Pre-experiment IV: amount of *V. longisporum* VL43-DNA detected by qPCR with  $\beta$ -tubulin primers in *B. napus*.** Status of infection rate in spore solution inoculated plants potted in sand; **A**: at 3 dpi, plants were not fertilized with different sulfur supply; **bluish violet bars** represent two measurements of the same treated plants (without roots); **B** and **C**: at 7 dpi and 14 dpi, plants were fertilized with different sulfur supply (1 mM MgSO<sub>4</sub>: +S; 0.01 mM MgSO<sub>4</sub>: -S); **purple bars** represent VL-infected +S, **pink bars** VL-infected -S; data represent the result of one measurement.

At 7 dpi values at **TPI I** in **VL-infected +S-**, **TPI III** in **VL-infected +S-** and **TPI IV** in **VL-infected -S-** plants were below limit of detection (**Fig. 3.26, B**). The content of VL-DNA at **TPI II** in **VL-infected +S-** plants was similar compared to the value at 3 dpi, whereby the content in **VL-infected -S-** plants increased about 71% (25.68 ng g<sup>-1</sup> FW). At 14 dpi values of **VL-infected +S-** groups at **TPI I** and **TPI IV** and of **VL-infected -S-** groups at **TPI III** and **TPI IV** were below limit of detection (**Fig. 3.26, C**). The amount in **VL-infected +S-** plants at **TPI III** was measurable again (0.07 ng g<sup>-1</sup> FW), while the amount of VL-DNA at **TPI I** in **VL-infected -S-** plants and at **TPI II** in both **VL-infected** groups decreased. In summary, the **VL-infected -S-** groups revealed the highest values at **TPI I** and **TPI II** compared to the other groups.



## Results

### 3.6 Selection of the experimental design

A number of pre-experiments (**I**, **II**, **IIIa**, **IIIb** and **IV**) based on various designs (**2.5.1 - 2.5.5**) were performed to verify the working hypotheses. It was important to establish an infection system that operates at the four defined **TPIs** and includes the fertilization with sufficient and deficient sulfur supply. In most infection systems with plants and pathogenic fungi, which are carried out under laboratory conditions, spores are used for inoculation. Since this work is mainly about different infection times, an inoculation system had to be particularly effective at **TPIs**, a mixture of mycelium and spores was used for the inoculation procedures. In **pre-experiment I (2.5.1)** 7-days-old plants of *B. napus* were inoculated with mycelium-spore mixture of *V. longisporum*. After inoculation the plants were transferred to pots filled with a 1:1 sand/soil mixture. The reason for choosing the substrate mixture was a better storage of water, in order to obtain an optimal water supply during the course of the experiment. However, the substrate contains an internal sulfur content (200 mg L<sup>-1</sup> fresh mass), and other components (for example long-term fertilizer) that could have influenced the experimental design with respect to the different sulfur supply (results: **3.1.1-3.1.4**). Therefore, in subsequent pre-experiments the cultivation of plants was conducted in autoclaved sand.

Another consideration was related to the influence of already fertilized plants on the inoculation procedure. To study this effect 16-days-old plants, which were previously fertilized with sufficient and deficient sulfur supply, were inoculated with mycelium-spore mixture (**pre-experiment II; 2.5.2**). At 7 dpi plants were harvested without roots for subsequent DNA-extraction (**2.7.1**), qPCR analysis (**2.7.2**) and for elemental analysis via ICP-OES (**2.7.3**). At 15 dpi plants and roots were harvested separately and the aforementioned methods were also performed (roots of +S-plants for ICP-OES analysis) (results: **3.2.1-3.2.3**). In order to make the inoculation system even more controlled, in **pre-experiments IIIa (2.5.3)** different dilutions of the mycelium-spore mixture were tested. As result a well-defined amount should be used for inoculation, as is commonly done for inoculation with spores. In order to make a screening with respect to the dilution, it was inoculated with different dilutions (**Inoc I-III**) only at **TPI III**. This TPI was selected, because a successful infection was assumed. Based on qPCR analysis (**3.3.1-3.3.2**), the **1:10 dilution (Inoc III)** was selected for the **pre-experiment IIIb (2.5.4)**. This experiment was performed twice (with 320 plants each), but the infection only worked in parts for some groups (**3.4.1**). Therefore, the experiments were not further evaluated and discarded. One assumption was, that it was too cold during the inoculation, which was basically in the basement in the immediate vicinity of the climatic chambers. So it could have been, that unforeseen stress factors could have

## Results

had a negative influence on the inoculation procedure. Therefore, the experiment was repeated (also twice with 320 plants each), whereby the procedure of inoculation took place in the climatic chambers themselves. In order to investigate the spread of *V. longisporum* in the plants, qPCR analysis was performed, but an almost similar result emerged, indicating that it was not or not alone due to the cold in the basement (data not shown). Based on studies about clubroot (caused by *Plasmodiophora brassicae*), inoculation of older plants may be limited because of an increased resistance (Horiuchi and Hori, 1980), and younger plants may recover better after inoculation than older plants (Hwang *et al.*, 2011). Also a contamination problem with DNA of *V. longisporum* in control plant material emerged again (3.3.1) due to the used metal spoon (for the weighing of the grounded plant samples; although the spoon was cleaned after each use between control and VL-infected plant material with 70% EtOH, UV light and subsequent autoclaving). Therefore, these two experiments had to be discarded again. The contamination problem has been solved with the help of new metal spoons and a new DNA extraction kit. Although, if it had been interesting to test the infection on plants already treated with different sulfur supply, this type of infection worked only to a limited extent. Furthermore, an inoculation procedure was tried with a defined amount of spores instead of the mycelium-spore mixture (2.5.5). In this experiment, 7-days-old plants were used for inoculation. The infection was successful (3.5.1), but during the staining of roots with cotton blue (2.7.7) it was discovered, that the invasion of *V. longisporum* with mycelium-spore inoculation appeared to act faster than inoculation with spores. **Figure 3.27, A** shows root hairs of a mock-inoculated plant after 24 h. Root hairs show no stained structures inside. **Figure 3.27, B** shows stained structures inside of root hairs (pink arrows) of with mycelium-spore inoculated plants after 24 h. Based on the used staining method, it should be mycelium of *V. longisporum*. **Figure 3.27, C** shows root hairs with spore solution of inoculated plants after 48 h. The inside of root hairs are free of staining structures. Germinating spores can be seen, which penetrate the surface of root hairs (pink arrows).

## Results

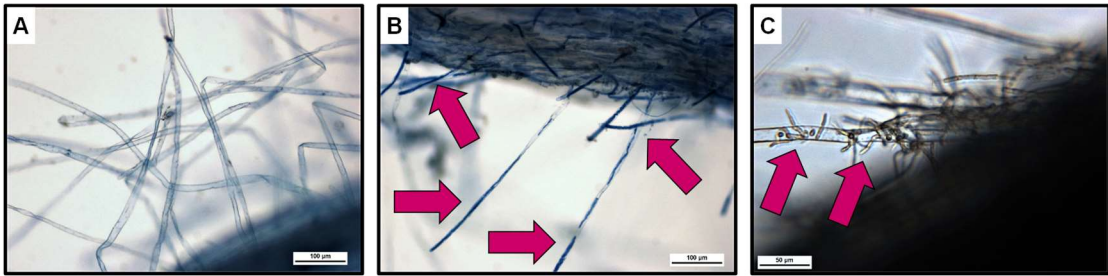


**Figure 3.27: Staining of *B. napus* roots with cotton blue after inoculation with *V. longisporum*.** **A:** mock-inoculated *B. napus* root after 24 h; root hairs were free of stained structures; scale bar 100 µm; **B:** root dip inoculated root with mycelium-spore mixture after 24 h; root hairs showed stained structures (arrows); scale bar 100 µm; **C:** root dip inoculated plant root with spore solution after 48 h; root hairs were free of stained structures inside, germinating spores penetrated the root hair surface (arrows); scale bar 50 µm.

Based on results of pre-experiments (3.1.1-3.5.1) and the observation of different durations of invasion of mycelium-spore mixture and spore solution (Fig. 3.27), it was decided, that plants should be **7-days-old** (without previous fertilization) for inoculation with **mycelium-spore mixture** and further cultivated in **sand**. The following results are based on the main experiment, which has been performed twice (2.6). Due to the mentioned problems with the climatic chambers (2.9.1), the results are shown separately (**first** and **second run**).

## Results

### 3.7 Results of the main experiment: inoculation of *Brassica napus* with *Verticillium longisporum* under diurnal rhythmic and with different sulfur supply

#### 3.7.1 First run: detection and verification of the infection with *V. longisporum* in *B. napus*

In order to investigate the spread of *V. longisporum* in the plant, qPCR analysis was performed with samples of 3, 7 and 14 dpi using ITS and  $\beta$ -tubulin primers. (Fig. 3.28). Samples of 3 dpi were not fertilized yet, the bars therefore show two biological replicates. Figure 3.28 shows only VL-infected samples, because most control samples measured with ITS and  $\beta$ -tubulin primers were undetected, or the detection of VL-DNA were below limit of detection or below limit of quantification, respectively (data not shown).

At 3 dpi values of **VL-infected** groups at **TPI I** (18.65-30.31 ng g<sup>-1</sup> FW) and **TPI IV** (63.54-76.39 ng g<sup>-1</sup> FW) were in a similar range, while same treated groups at **TPI II** and **TPI III** showed differences about 85% and 71%, respectively (Fig 3.28, A). At 7 dpi VL-DNA in **VL-infected +S**-group at **TPI II** increased about 42% (18.69 ng g<sup>-1</sup> FW), while it decreased in all other groups (Fig. 3.28, C). At **TPI I** the amount decreased about 83-87%. The content in **VL-infected -S**-group at **TPI II** decreased about 81%. At **TPI III** a decrease about 58-72% was observed and at **TPI IV** a decrease about 49-74%. The highest values of VL-DNA were revealed in **VL-infected -S**-groups at **TPI III** (63.59 ng g<sup>-1</sup> FW) and **TPI IV** (32.27 ng g<sup>-1</sup> FW). At 14 dpi the amount of VL-DNA in **VL-infected +S**-group at **TPI I** increased about 73% and in **VL-infected -S**-group at **TPI II** about 56% (Fig. 3.28, E). The values of **VL-infected +S**-groups at **TPI II**, **TPI III** and **TPI IV** and **VL-infected -S**-group at **TPI I** laid below 1.0 ng g<sup>-1</sup> FW and 1.5 ng g<sup>-1</sup> FW, respectively. The amount of VL-DNA of the other groups decreased in a range between 83-92%. The highest values of VL-DNA were observed in **VL-infected -S**-groups at **TPI II** (29.06 ng g<sup>-1</sup> FW) and **TPI III** (10.74 ng g<sup>-1</sup> FW). The distribution of VL-DNA detected with  $\beta$ -tubulin primers showed a similar result compare to ITS primers, but for most of samples the amount of VL-DNA was almost twice as much (Fig. 3.28, B, D, F). The decrease of the VL-DNA content is significant from 3 dpi to 14 dpi and from 7 dpi to 14 dpi (p=0.00103; Appendix Table 6.1; Table 6.2).

## Results

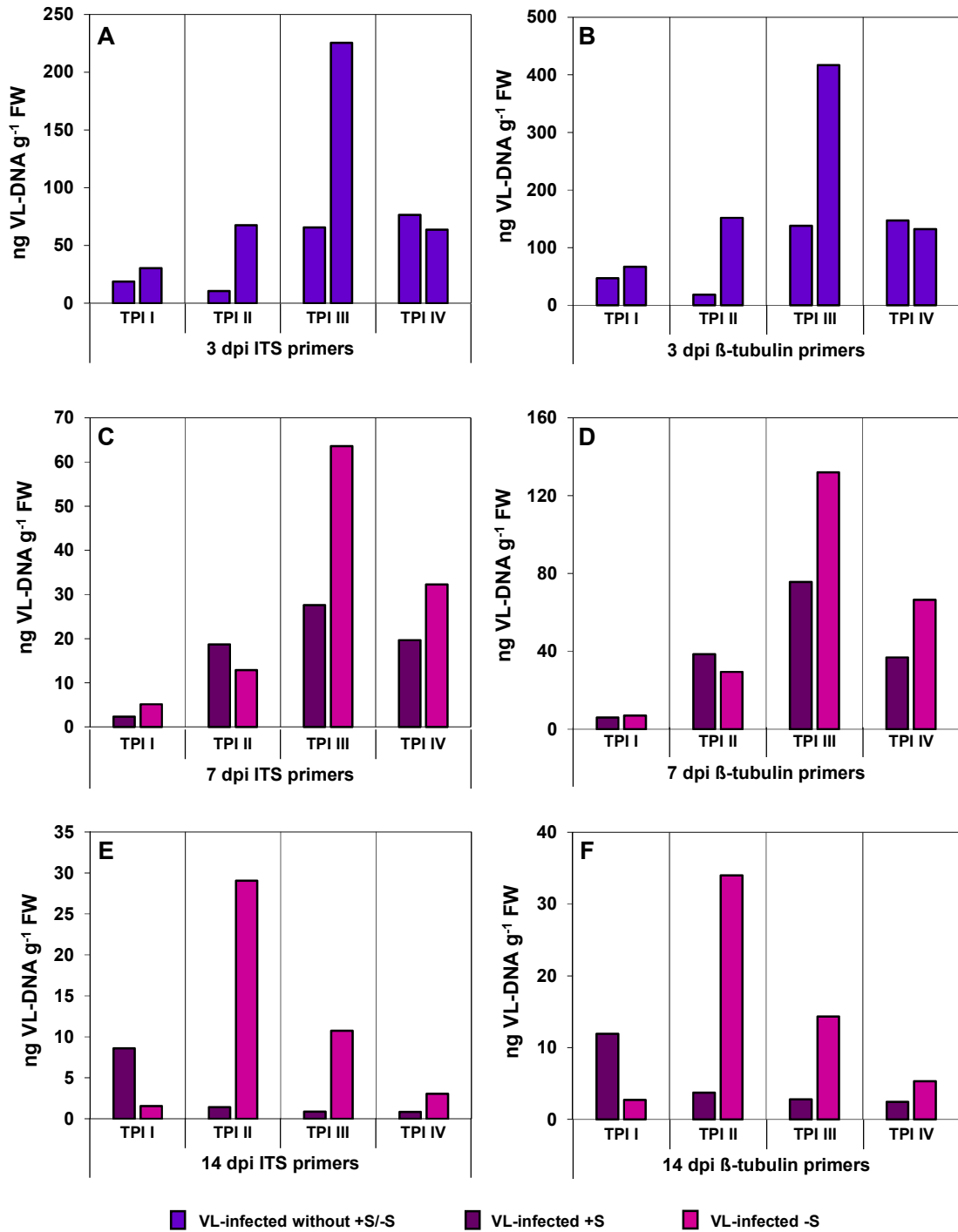


**Figure 3.28: Amount of *V. longisporum* VL43-DNA detected by qPCR with ITS and  $\beta$ -tubulin primers in *B. napus* (first run).** Status of infection rate in mycelium-spore inoculated plants potted in sand; **A and B:** 3 dpi without different sulfur fertilization; **C -F:** 7 dpi and 14 dpi: plants were fertilized with different sulfur supply; **A, C, E:** detection of VL with ITS primers; **B, D, F:** detection of VL with  $\beta$ -tubulin primers; data represent the result of one measurement.

## Results

### 3.7.2 First run: stunting of *B. napus* plants infected with the *V. longisporum* strain VL43 under artificial inoculation

At 3 dpi three plants each group were selected, of which pictures were taken at 3, 7 and 14 dpi. Infection with *V. longisporum* results in stunted growth (“stunting”) and the difference in plant height between infected and non-infected plants appears at 14 dpi (Rygulla *et al.*, 2007a, 2008; Eynck *et al.*, 2009). **Figure 3.29** shows images of three **control** and **VL-infected** plants for each **TPI** under **sufficient sulfur** supply at 14 dpi (images of 7 dpi: **Appendix Fig. 6.1**). Stunting was observed at **TPI II**, **TPI III** and **TPI IV** between **control +S-plants** and **VL-infected +S-plants** (**Fig. 3.29, A2-A4, B2-B4**). At **TPI I** no differences were apparent between the two groups (**Fig. 3.29, A1, B1**). The most pronounced manifestation of stunting was demonstrated by **VL-infected +S-plants** at **TPI III** and **TPI IV**.

## Results

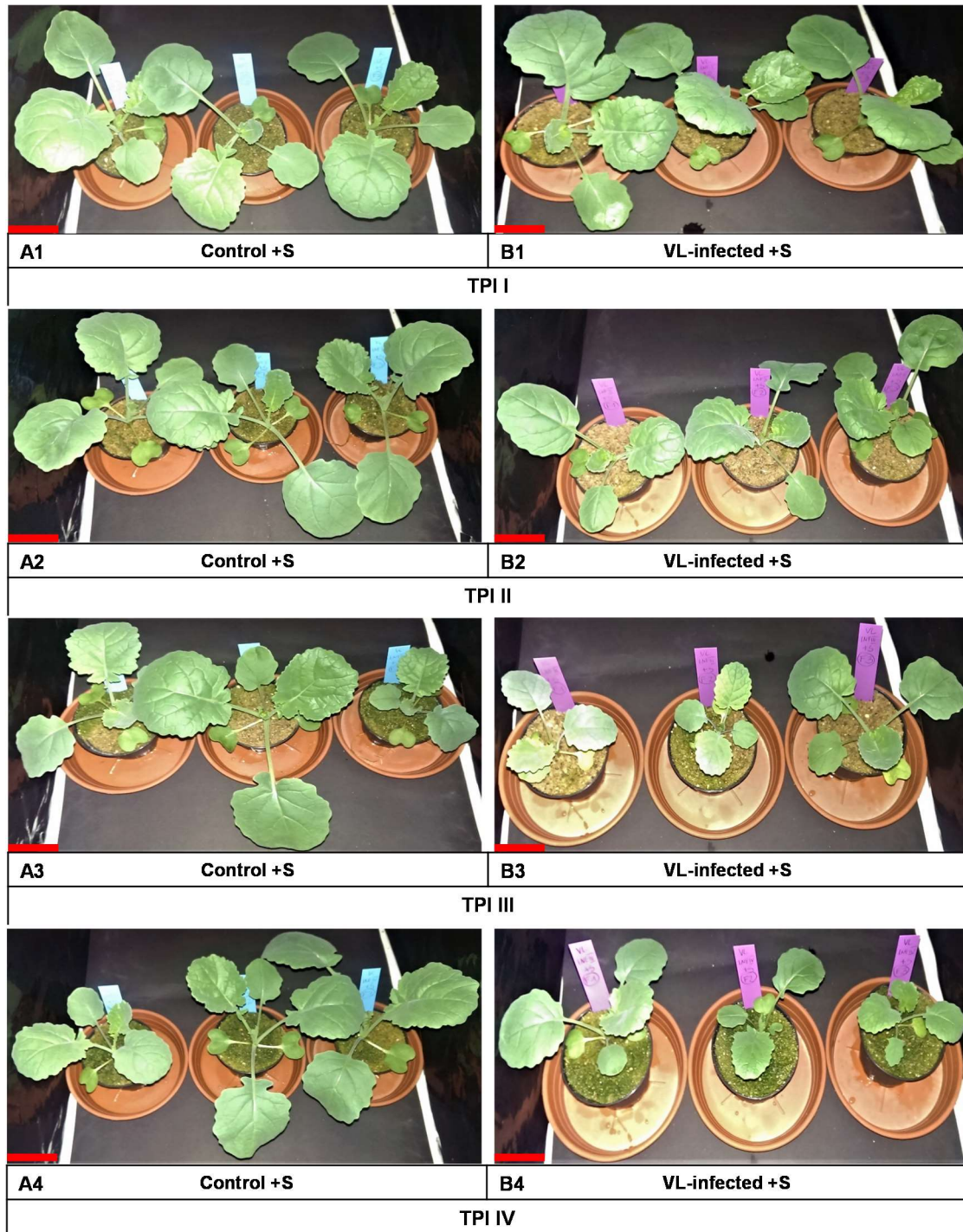


**Figure 3.29: Stunting of *B. napus* plants infected with the *V. longisporum* strain VL43 under artificial inoculation (first run). Plants under sufficient sulfur supply (1 mM MgSO<sub>4</sub>: +S) at 14 dpi; **A1-A4**: control plants; **B1-B4**: VL-infected plants; red scale bar 5 cm.**

Besides, at **TPI III** and **TPI IV** one **control** plant each group showed less growth than the other plants. Since the plants were already selected at 3 dpi for the pictures, possible deficits in the subsequent development could not be predicted.

## Results

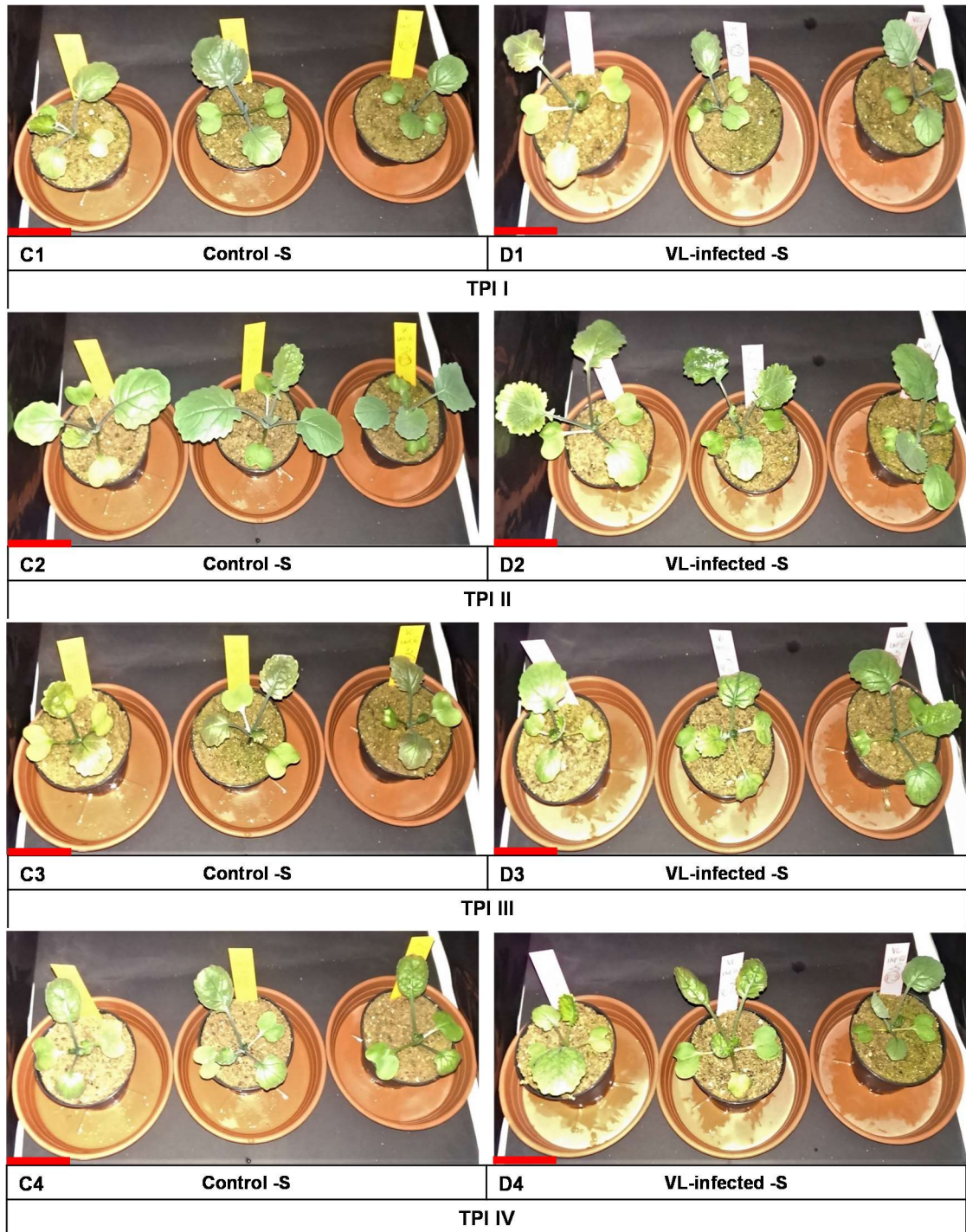


**Figure 3.30: Stunting of *B. napus* plants infected with the *V. longisporum* strain VL43 under artificial inoculation (first run). Plants under deficient sulfur supply (0.01 mM MgSO<sub>4</sub>: -S) at 14 dpi; C1-C4: control plants; D1-D4: VL-infected plants; red scale bar 5 cm.**

Comparing **control** and **VL-infected** plants under **deficient sulfur** supply at 14 dpi, the symptom stunting was not observed (**Fig. 3.30, C1-C4, D1-D4**). Plants were smaller and some of the leaves were partially colored purple and yellow, and bulged inward or outward along the margins. The leaf surface felt leathery and looked shiny. The leaves also had lost their elasticity and were broken easily.



## Results

### 3.7.3 First run: the influence of different TPIs and different sulfur supply on the occurrence of occlusions in the xylem of *B. napus* infected with *V. longisporum* strain VL43

Plants infected with a vascular pathogenic fungi could form occlusions to protect themselves against further invasion (Yadeta and Thomma, 2013). To investigate the influence of **different sulfur fertilization** and **TPIs** on the formation of occlusions, hypocotyls of mock- and mycelium-spore mixture inoculated plants were harvested at 14 and 21 dpi.

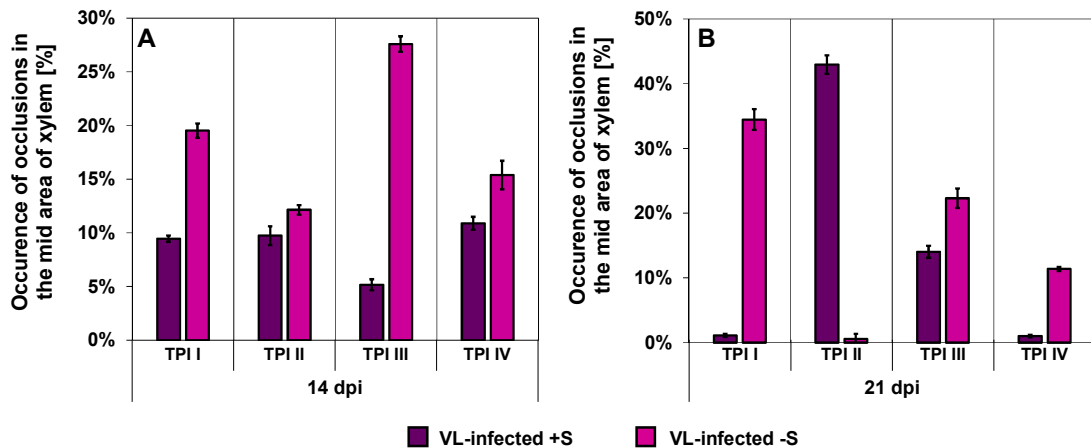


**Figure 3.31: Occurrence of occlusions in the mid area of the xylem of *B. napus* plants infected with *V. longisporum* strain VL43 (first run). A: 14 dpi; B: 21 dpi; data represent the mean of five dependent technical replicates  $\pm$  SD.**

Cross sections were stained with toluidine blue. Tracheas and occlusions were counted from each of five cross sections, the xylem divided into peripheral and mid region (2.7.6). Both, the formation of tylosis and of vascular gels were counted together. The percentage of occlusions that formed in the mid area of the xylem showed in **Figure 3.31**. Control plants occasionally showed occlusions in the peripheral area and were therefore not listed in the statistics or microscopic pictures (**Appendix Fig. 6.2**).

Figure 3.32 shows a selection of microscopic images of **VL-infected** plants at 14 (**Fig. 3.32, A1-A4, B1-B4**) and 21 dpi (**Fig. 3.32, C1-C4, D1-D4**) to visualize the occurrence of occlusions. At 14 dpi the highest value about 28% of occlusions occurred at **TPI III** in **VL-infected -S-plant** (**Fig. 3.31, A; Fig. 3.32, B3**). Compared with qPCR data of 3 and 7 dpi the highest amount of VL-DNA arose in the same group (**Fig. 3.28, A, B**). The remaining **VL-infected -S-plant** showed a higher appearance of occlusions (12-20%) than the **VL-infected +S-plant** (5-11%).

## Results

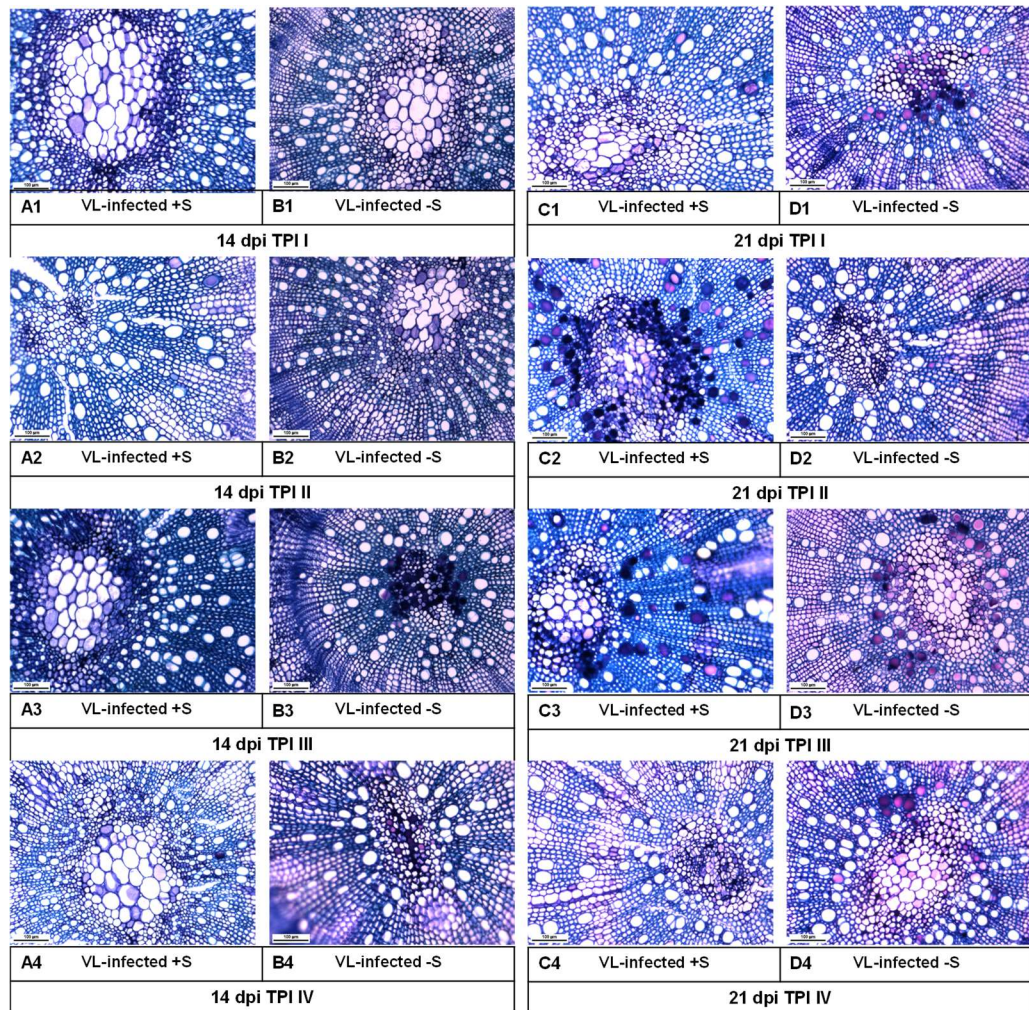


**Figure 3.32: Occurrence of occlusions in xylem: toluidine blue stained cross sections of hypocotyls of mycelium-spore inoculated plants (first run). 14 dpi: A1-A4: VL-infected +S at TPI I-IV; B1-B4: VL-infected -S at TPI I-IV; 21 dpi: C1-C4: VL-infected +S at TPI I-IV; D1-D4: VL-infected -S at TPI I-IV; scale bar 100  $\mu$ m.**

At 21 dpi the highest level of occlusions was observed in **VL-infected +S**-plant at **TPI II** (43%) and in **VL-infected-plant -S**-plant at **TPI I** (34%) (**Fig. 3.31, B**). In **VL-infected +S**-plant at **TPI III**, the occurrence increased about 9%, whereas it decreased in the other plants about 4-11%. Statistical analysis comparing occlusions with the effects of differential sulfur supply, dpi and TPIs revealed no significant differences.

## Results

### 3.7.4 First run: levels of sulfur, calcium, potassium and iron at different TPIs in mock- and mycelium-spore inoculated plants under different sulfur supply

The content of sulfur, calcium, potassium and iron was measured in **control** and **VL-infected** samples of 7 and 14 dpi with ICP-OES. At 7 dpi the highest values between 8.09-9.4 mg g<sup>-1</sup> DW of sulfur were observed in **control +S-groups** together with the **VL-infected +S-group** at **TPI IV** (8.96 mg g<sup>-1</sup> DW) (**Fig. 3.33, A**). The other **VL-infected +S-groups** ranged about 5.46-5.64 mg g<sup>-1</sup> DW. The **control -S-groups** showed values between 1.23-3.27 mg g<sup>-1</sup> DW, whereby the highest content occurred at **TPI III**. The **VL-infected -S-groups** showed, with the exception of **TPI III**, higher sulfur levels compared to the corresponding **control -S-groups**.

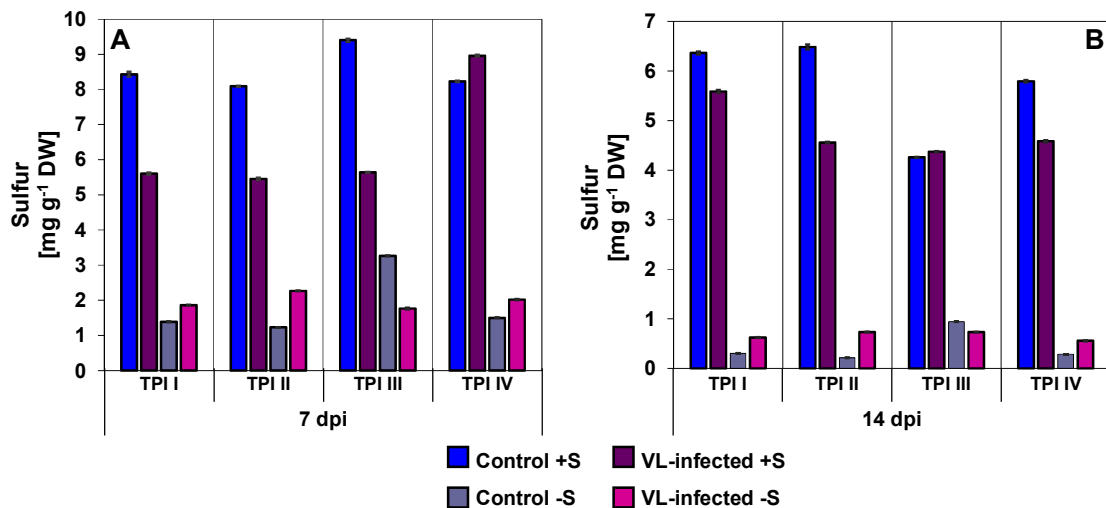


**Figure 3.33: Elemental analysis: level of S content in mock- and mycelium-spore inoculated plants measured by ICP-OES (first run). A: 7 dpi; B: 14 dpi; data represent the mean of three dependent technical replicates  $\pm$  SD.**

At 14 dpi the amount of sulfur decreased in **control +S-groups** about 24-70%, in **VL-infected +S-groups** about 1-49%, in **control -S-groups** about 71-83% and in **VL-infected -S-groups** about 59-72% (**Fig. 3.33, B**). Overall, the **control +S-groups** showed the highest values (4.26-6.49 mg g<sup>-1</sup> DW), where the value of the **VL-infected +S-group** at **TPI III** was almost the same. The comparison between **control-** and **VL-infected -S-groups** showed a similar pattern as on 7 dpi. The content in the plants showed significant differences between sufficient and deficient sulfur supply ( $p=0.00012$ ; **Appendix Table 6.3**).

The highest calcium content at 7 dpi occurred in **control +S-groups** with 21.31-22.89 mg g<sup>-1</sup> DW, followed by **control -S-groups** with values between 19.73-21.22 mg g<sup>-1</sup> DW (**Fig. 3.34, A**). The **VL-infected +S-groups** ranged from 13.19-19.14 mg g<sup>-1</sup> DW and

## Results

the **VL-infected -S**-group from 15.22-21.33 mg g<sup>-1</sup> DW. The highest value in the **VL-infected**-groups showed the **deficient** sulfur supply group at **TPI I**.

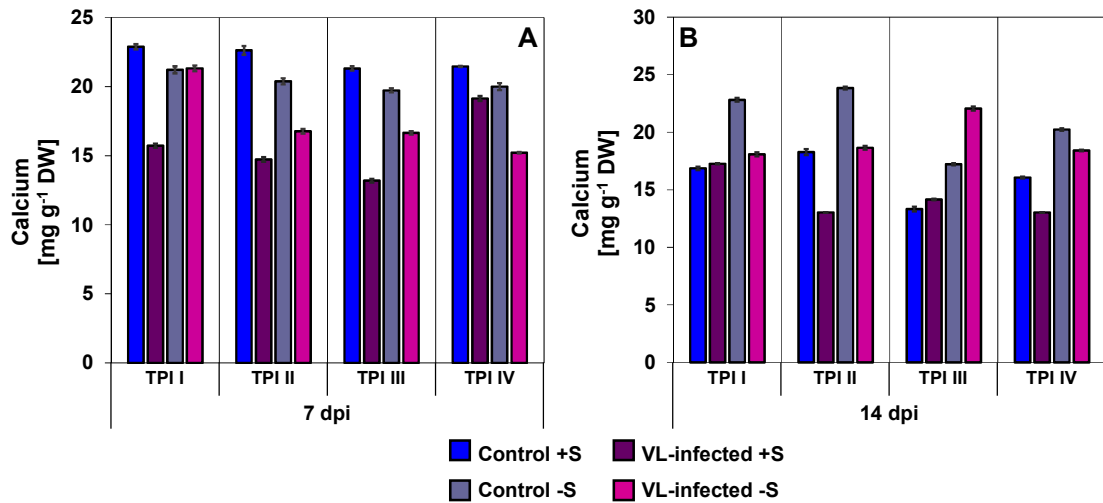


**Figure 3.34: Elemental analysis: level of Ca content in mock- and mycelium-spore inoculated plants measured by ICP-OES (first run). A: 7 dpi; B: 14 dpi; data represent the mean of three dependent technical replicates  $\pm$  SD.**

At 14 dpi the highest values about 20-24 mg g<sup>-1</sup> DW of calcium) were measured in **control -S**-groups at **TPI I**, **TPI II** and **TPI IV** and in **VL-infected -S**-group at **TPI III** (**Fig. 3.34, B**. The content in all **control +S**-groups decreased about 19-38%, in **VL-infected +S**-groups at **TPI II** and **TPI IV** about 11-32%, while at **TPI I** and **TPI III** the content increased about 9 and 7%, respectively. Comparing the control- and VL-infected plants, the differences in the calcium content were significant ( $p=0.00113$ ; **Appendix Table 6.4**).

At 7 dpi the highest potassium levels were observed in **control +S**-plants in a range between 52-63.33 mg g<sup>-1</sup> DW, followed by **control -S**-groups with values between 31.39-48.56 mg g<sup>-1</sup> DW (**Fig. 3.35, A**). **VL-infected** groups showed similar contents at **TPI I** (29.2 and 29.18 mg g<sup>-1</sup> DW) and **TPI II** (19.84 and 18.8 mg g<sup>-1</sup> DW), whereby at **TPI III** and **TPI IV**, the values of **VL-infected +S**-groups were slightly higher. Overall, the amount of potassium decreased about 8-75% at 14 dpi (**Fig. 3.35, B**). The highest values over 21 mg g<sup>-1</sup> DW were measured in both **control** groups at **TPI I**, **TPI II** and **TPI IV**, while **VL-infected +S**-groups ranged from 7.32-11.69 mg g<sup>-1</sup> DW and **VL-infected -S**-groups from 15.91-19.94 mg g<sup>-1</sup> DW. The differences regarding to the two dpi, comparison of control- and VL-infected plants and the comparison of different sulfur fertilization in infected- and non-infected plants were significant ( $p=0.00017$ ;  $p=0.00051$ ;  $p=0.0007$ ; **Appendix Table 6.5**).

## Results

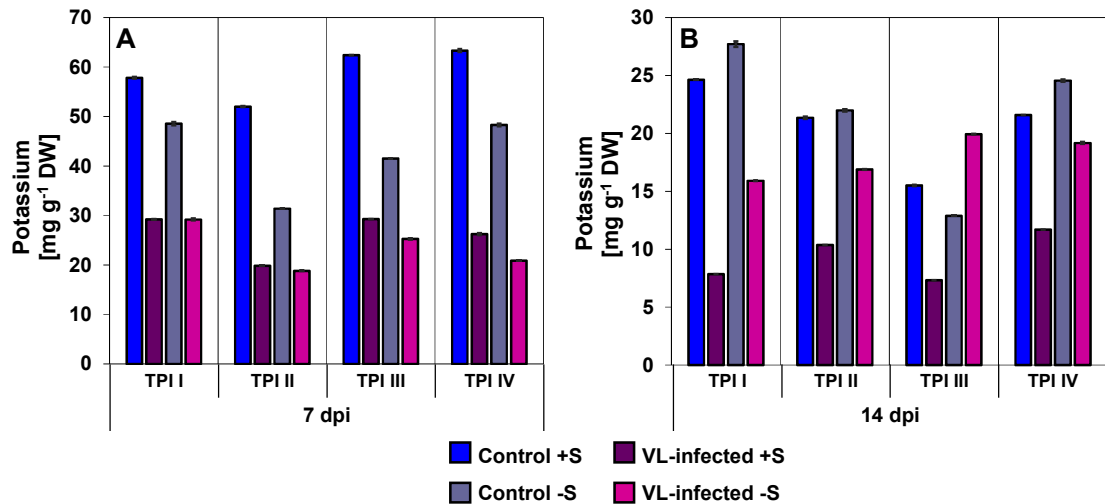


**Figure 3.35: Elemental analysis: level of K content in mock- and mycelium-spore inoculated plants measured by ICP-OES (first run). A: 7 dpi; B: 14 dpi; data represent the mean of three dependent technical replicates  $\pm$  SD.**

At 7 dpi the highest value of iron was measured in **VL-infected -S**-group at **TPI IV** with  $170.63 \mu\text{g g}^{-1}$  DW (**Fig. 3.36, A**). At this time point the remaining groups showed similar values in the range of  $108.58$ - $115.25 \mu\text{g g}^{-1}$  DW. The second highest value was also observed in **VL-infected -S**-group at **TPI III** with  $125.21 \mu\text{g g}^{-1}$  DW, while the remaining groups showed similar values between  $92.44$ - $107.76 \mu\text{g g}^{-1}$  DW again.

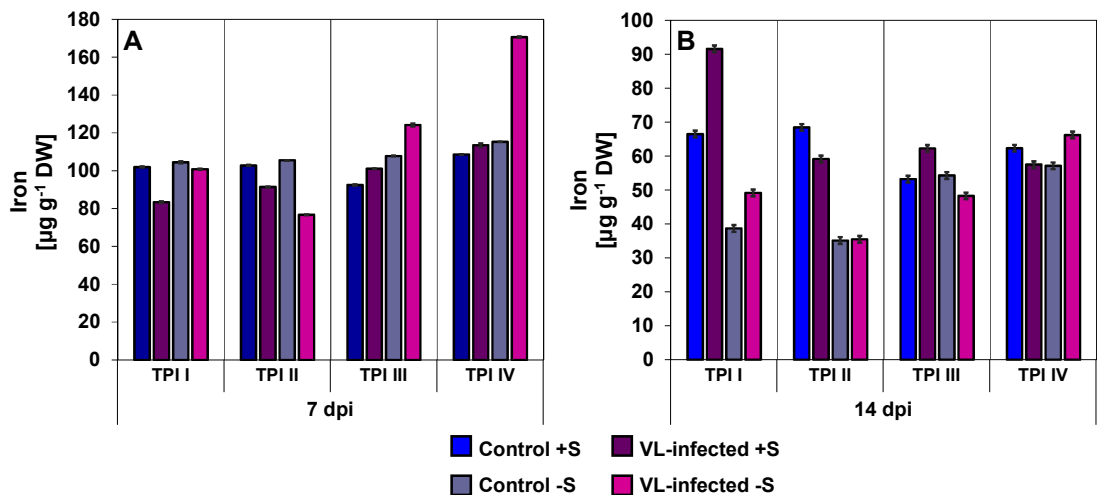


**Figure 3.36: Elemental analysis: level of Fe content in mock- and mycelium-spore inoculated plants measured by ICP-OES (first run). A: 7 dpi; B: 14 dpi; data represent the mean of three dependent technical replicates  $\pm$  SD.**

At **TPI I** and **TPI II** the content of iron was highest in both **control** groups (**+S**:  $101.98$  and  $102.79 \mu\text{g g}^{-1}$  DW; **-S**:  $104.45$  and  $105.55 \mu\text{g g}^{-1}$  DW), closely followed by **VL-infected -S**-group with  $100.86 \mu\text{g g}^{-1}$  DW at **TPI I**. At 14 dpi the highest value with an increase of 9% occurred in **VL-infected +S**-group at **TPI I** (**Fig. 3.36, B**). The amount of iron decreased in all other groups, in **control +S**-groups about 33-43%, in **control -**

## Results

**S**-groups about 50-67%, in the remaining **VL-infected +S**-groups about 35-49% and in **VL-infected -S**-groups about 51-61%. The differences in the content of control- and VL-infected plants were significant ( $p=0.0015$ ; **Appendix Table 6.6**).

### 3.7.5 First run: levels of indolic, aliphatic and benzylic GSLs in mock- and mycelium-spore inoculated plants at different TPIs under different sulfur supply

As already mentioned, GSLs belong to the SDCs and play an important role in the host-pathogen-interaction system. Samples of 7 and 14 dpi were measured with HPLC to identify IGSLs, AGSLs and the BGSGL gluconasturtiin. At 7 dpi the values of the IGSL glucobrassicin were highest in the **VL-infected +S**-groups within the **TPIs** (173.06-238.15  $\text{nmol g}^{-1}$  DW) (**Fig. 3.37, A**). The **VL-infected -S**-groups showed higher amounts at **TPI I, TPI II** and **TPI IV** compared to the **control -S**-groups.

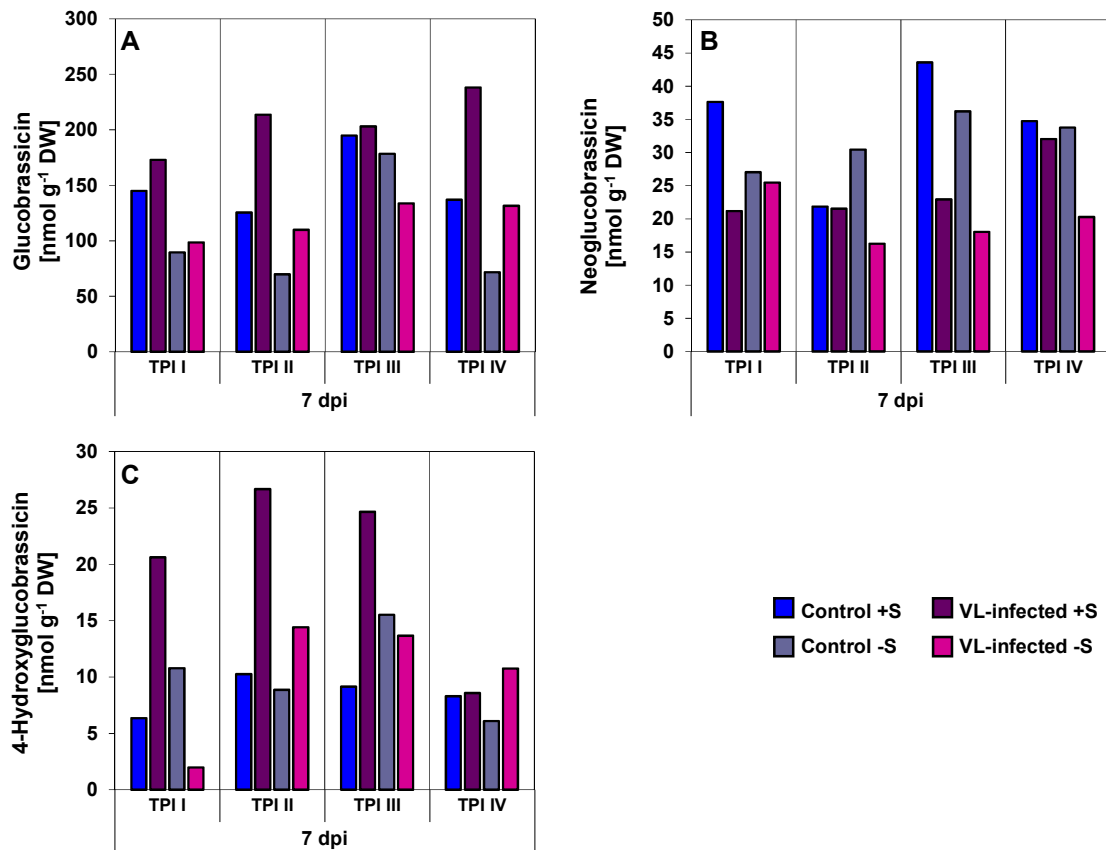


**Figure 3.37: GSL analysis by HPLC: level of IGSL content in mock- and mycelium-spore inoculated plants at 7 dpi (first run). A: glucobrassicin; B: neoglucobrassicin; C: 4-hydroxyglucobrassicin; data represent the result of one measurement; hypothetical SDs based on previous measurements can range between 2-25%.**

## Results

The highest value within the **control +S-**, **-S-** and **VL-infected -S-** groups, respectively occurred at **TPI III** (194.77, 178.41 and 133.67 nmol g<sup>-1</sup> DW) and within the **VL-infected +S-** groups at **TPI IV**. The amount of neoglucobrassicin ranged from 16.26-43.57 nmol g<sup>-1</sup> DW, whereby the lowest value was measured in **VL-infected -S-** group at **TPI II** and the highest in **control +S-** group at **TPI III** (**Fig. 3.37, B**). The content was higher in **control +S-** groups at **TPI I** and **TPI III** compared to the other groups. At **TPI II** the value of **control +S-** group (21.84 nmol g<sup>-1</sup> DW) was similar to the value of **VL-infected +S-** group and at **TPI IV** (34.73 nmol g<sup>-1</sup> DW) similar to the values of **VL-infected +S-** and **control -S-** group. The **VL-infected +S-** groups had the highest levels in 4-hydroxyglucobrassicin at **TPI I-III** (20.62-26.68 nmol g<sup>-1</sup> DW), while the value at **TPI IV** (8.58 nmol g<sup>-1</sup> DW) was similar to the value of **control +S-** group (8.3 nmol g<sup>-1</sup> DW) (**Fig. 3.37, C**). Comparison of the **-S-** groups, the **VL-infected** groups at **TPI II** and **TPI IV** showed higher values (14.41 and 10.76 nmol g<sup>-1</sup> DW).

Overall, the **VL-infected +S-** groups had the highest values in all AGSLs at 7 dpi, whereby the highest value within each AGSL occurred at **TPI III** (**A**: 165.23 nmol g<sup>-1</sup> DW; **B**: 81.34 nmol g<sup>-1</sup> DW; **C**: 12.38 nmol g<sup>-1</sup> DW; **D**: 39.1 nmol g<sup>-1</sup> DW; **E**: 52.75 nmol g<sup>-1</sup> DW) (**Fig. 3.38, A-E**). The same applied to **control +S-** and **-S-** group, which also showed the highest value at **TPI III** within their group. The highest values of AGSLs for the **VL-infected -S-** group were observed at **TPI II** (**Fig. 3.38, A**: 77.83 nmol g<sup>-1</sup> DW; **B**: 41.8 nmol g<sup>-1</sup> DW; **C**: 6.78 nmol g<sup>-1</sup> DW; **D**: 23.85 nmol g<sup>-1</sup> DW; **E**: 24.13 nmol g<sup>-1</sup> DW), however, in progoitrin a similar value was measured at **TPI III** (77.06 nmol g<sup>-1</sup> DW) (**Fig. 3.38, A**).

## Results

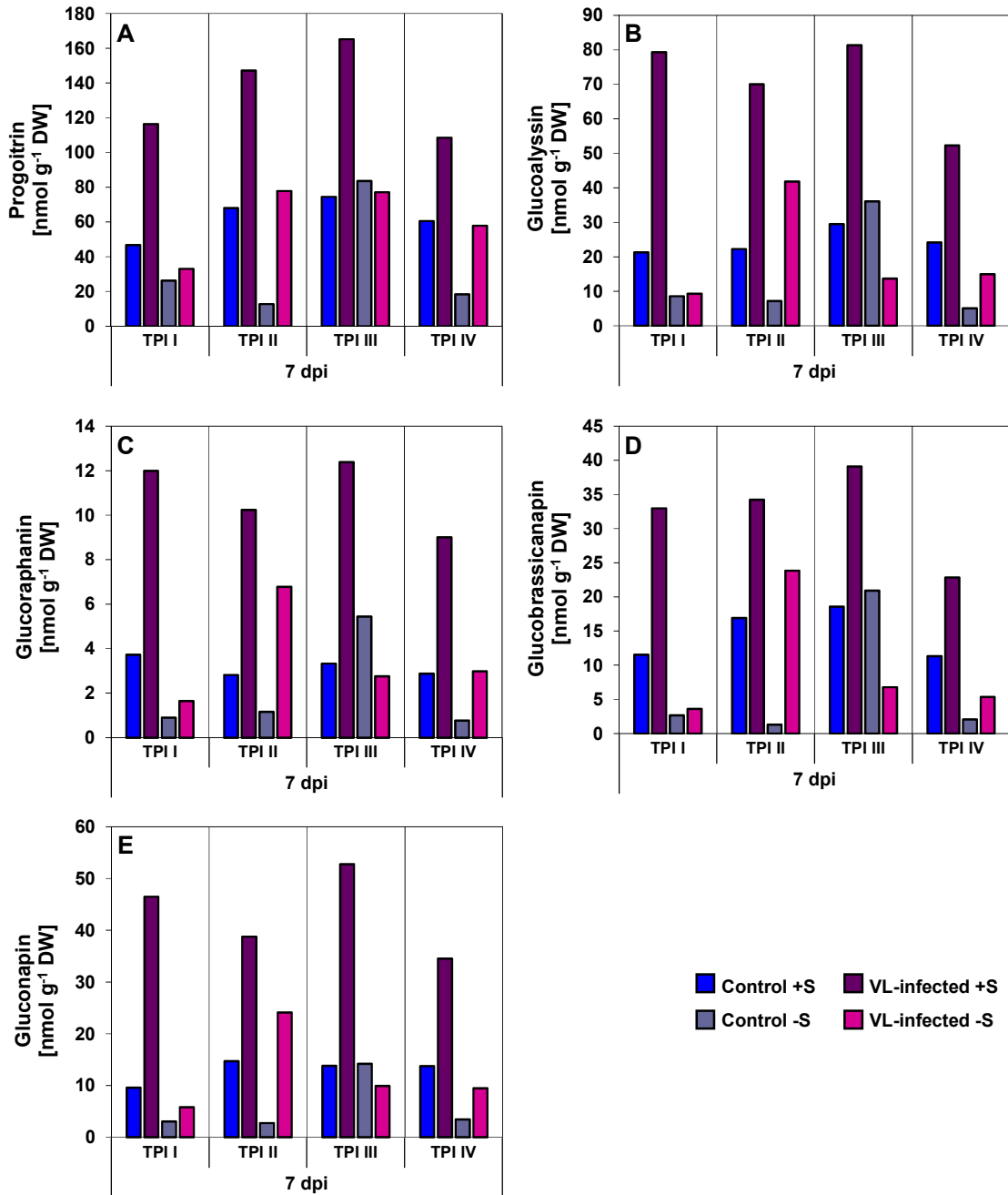


**Figure 3.38: GSL analysis by HPLC: level of AGSL content in mock- and mycelium-spore inoculated plants at 7 dpi (first run).** A: progoitrin; B: glucoalyssin; C: glucoraphanin; D: glucobrassicinapin; E: gluconapin; data represent the result of one measurement; hypothetical SDs based on previous measurements can range between 3-35%.

At 7 dpi the content of gluconasturtiin was highest in **VL-infected +S-** and **-S-** groups, whereby the highest values were observed at **TPI III (+S: 265.78  $\text{nmol g}^{-1} \text{DW}$ ; -S: 246.87  $\text{nmol g}^{-1} \text{DW}$ ) (Fig. 3.49)**. Comparing the **control** groups, the **-S-** groups showed slightly higher values in a range between 56.22-73.67  $\text{nmol g}^{-1} \text{DW}$ .



## Results

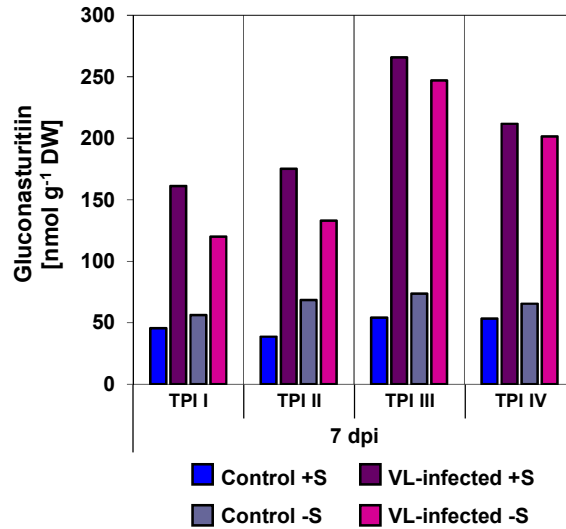


**Figure 3.39: GSL analysis by HPLC: level of the BGS� gluconasturtiin content in mock- and mycelium-spore inoculated plants at 7 dpi (first run).** Data represent the result of one measurement; hypothetical SDs based on previous measurements can range between 1-25%.

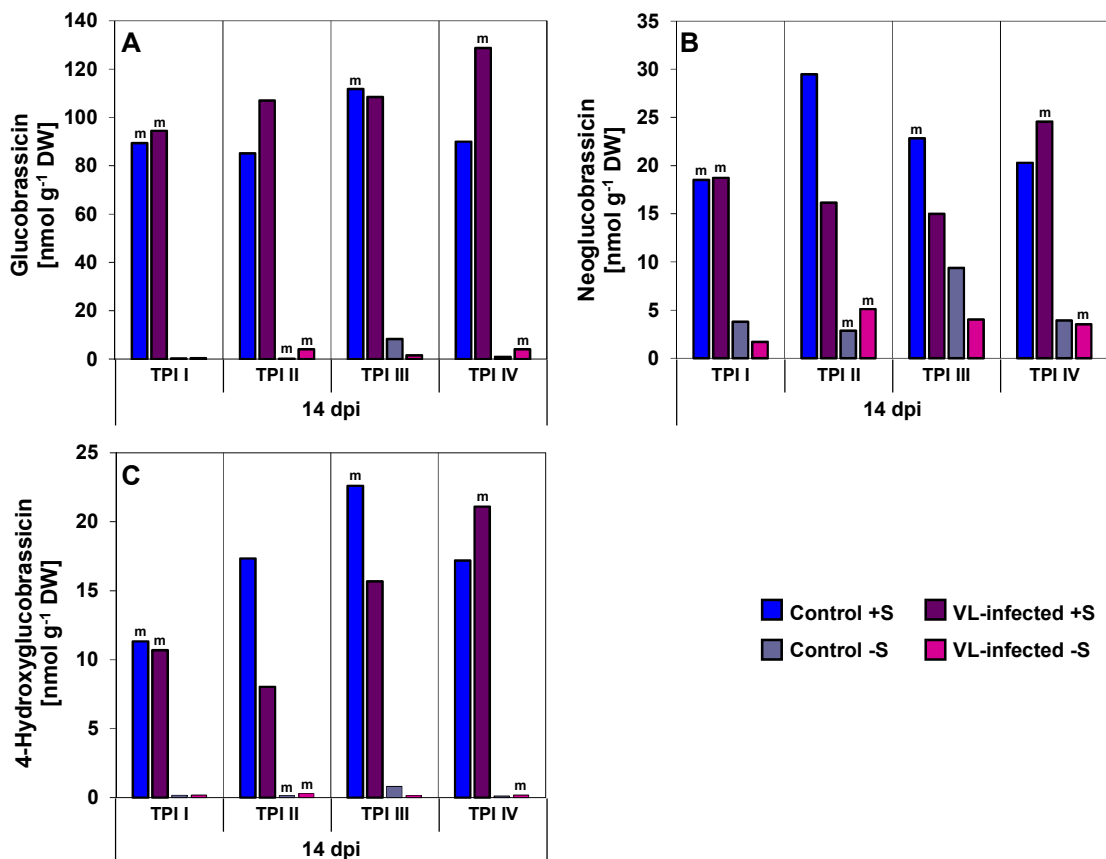


**Figure 3.40: GSL analysis by HPLC: level of IGSL content in mock- and mycelium-spore inoculated plants at 14 dpi (first run).** A: glucobrassicin; B: neoglucobrassicin; C: 4-hydroxyglucobrassicin; data represent the result of one measurement or the mean (m) of three dependent technical replicates (**Appendix Table 6.7**).

## Results

The content of glucobrassicin dropped in **control +S**-groups about 32-43% and in **VL-infected +S**-group about 45-50% at 14 dpi (**Fig. 3.40, A**). In **control -S**- and **VL-infected -S**-groups the decrease was about 95-99%. The highest value was measured in **VL-infected +S**-group at **TPI IV** (128.79 nmol g<sup>-1</sup> DW). Amounts of neoglucobrassicin were also lowered in all groups, with the exception of an increase in **control +S**-group about 26% at **TPI II** (**Fig. 3.40, B**). The highest value within the **VL-infected +S**-groups was measured at **TPI IV** (24.57 nmol g<sup>-1</sup> DW). The content of 4-hydroxyglucobrassicin increased about 41-60% in the **control +S**-groups, where the highest value was measured at **TPI II** (22.61 nmol g<sup>-1</sup> DW) (**Fig. 3.40, C**). In **VL-infected +S**-group at **TPI IV**, the value raised about 59%, while the values at **TPI I-III** decreased about 48-87%. In **control -S**- and **VL-infected -S**-groups the amount dropped about 90-99% and was barely measurable. Altogether, the **control** and **VL-infected** groups fertilized with **sufficient sulfur** had higher values of IGSLs at 14 dpi. Within **VL-infected +S**-groups the highest values were observed at **TPI IV**, while within **VL-infected -S**-groups the highest values occurred at **TPI II**.

The content of progoitrin increased in the **control +S**-groups at **TPI I, III** and **IV** about 28-48%, while the value at **TPI II** dropped about 8% (**Fig. 3.41, A**). In **VL-infected +S**-groups the amount lowered at **TPI I-III** about 30-41%, while the value at **TPI IV** raised about 6%. The highest values compared to the corresponding **control +S**-groups were observed at **TPI II** (91.98 nmol g<sup>-1</sup> DW) and **TPI IV** (115.09 nmol g<sup>-1</sup> DW). The content in **control -S**- and **VL-infected -S**-groups decreased about 91-99% and values ranged from 0.39-1.44 nmol g<sup>-1</sup> DW. The distribution in glucoalyssin (**Fig. 3.41, B**), glucobrassicinapin (**Fig. 3.41, D**) and gluconapin (**Fig. 3.41, E**) was similar to progoitrin. In glucoraphanin the values of **control +S**-groups were the highest in a range between 13.59-15.57 nmol g<sup>-1</sup> DW, whereby in the **VL-infected +S**-group a similar amount about 15.71 nmol g<sup>-1</sup> DW was measured at **TPI II** (**Fig. 3.41, C**). Only in this AGSL the content increased in most **control -S**- and **VL-infected -S**-groups about 34-68% and 17-46%, respectively. Within the **VL-infected +S**-groups the highest values in glucobrassicinapin (63.94 nmol g<sup>-1</sup> DW) and gluconapin (48.91 nmol g<sup>-1</sup> DW) were measured at **TPI IV** (**Fig. 3.41, D, E**), while the highest amounts of glucoalyssin (83.87 nmol g<sup>-1</sup> DW) and glucoraphanin (15.71 nmol g<sup>-1</sup> DW) occurred at **TPI II** (**Fig. 3.41, B, C**).

The statistical analysis, in which the total of IGSLs were compared to the effects of the two dpi, the four TPI, the different sulfur supply and the comparison of control/VL-infected to the four TPI, yielded significant differences (p=0.00013; p=0.2; p=0.00005; p=0.00038; p=0.02). The statistical results of the individual and the entire IGSLs can be found in the appendix (**Table 6.8-6.11**).

## Results

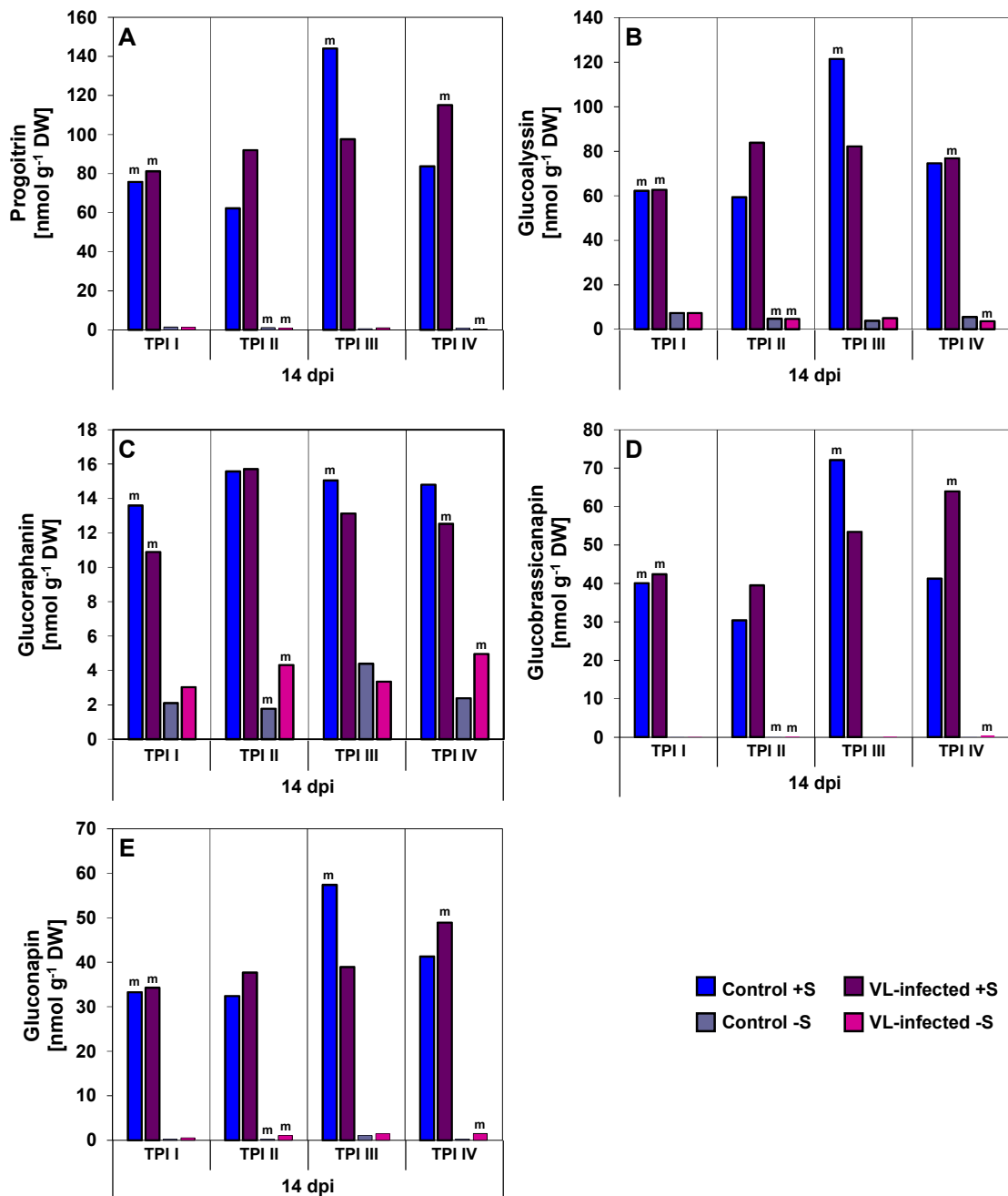


**Figure 3.41: GSL analysis by HPLC: level of AGSL content in mock- and mycelium-spore inoculated plants at 14 dpi (first run). A: progoitrin; B: glucoalyssin; C: glucoraphanin; D: glucobrassicinapin; E: gluconapin; data represent the result of one measurement or the mean (m) of three dependent technical replicates (Appendix Table 6.12).**

The statistical analysis for the entire AGSLs showed significant differences in terms of dpi, TPI and different sulfur fertilization ( $p=0.00155$ ;  $p=0.00415$ ;  $p=0.00006$ ). Furthermore, there was also a significant effect between control and VL-infected groups ( $p=0.00253$ ). This significant difference was also evident when compared to dpi with different sulfur fertilization and to dpi with control and VL-infected groups

## Results

( $p=0.00044$ ;  $p=0.00379$ ). The statistical results of the individual AGSLs and the overall AGSLs can be found in the appendix (**Table 6.13-6.18**).

The content of gluconasturtiin increased in the **control +S**-groups at **TPI I-III** about 7-24%, while the value at **TPI IV** decreased about 10% (**Fig. 3.42**). The highest values occurred at **VL-infected +S**-groups even if they dropped about 49-64%. Overall, the amount in the **-S**-groups lowered about 60-89%, but the **VL-infected** groups showed at **TPI I, TPI II** and **TPI IV** higher values compared to the **control** groups. Contents at **TPI III** were similar (**control**: 29.21 nmol g<sup>-1</sup> DW; **VL-infected**: 27.97 nmol g<sup>-1</sup> DW). The highest value in **VL-infected +S**-group was observed at **TPI IV** (108.5 nmol g<sup>-1</sup> DW) and in **VL-infected -S**-group at **TPI II** (41.63 nmol g<sup>-1</sup> DW). In addition, the lowest amount under 1 ng g<sup>-1</sup> FW of VL-DNA was observed at **TPI IV** in **VL-infected +S**-plants (**Fig. 3.28, C**) with the highest occurrence of occlusions within this group (**Fig. 3.31, A**), while the highest value about 29.06 ng g<sup>-1</sup> FW occurred at **TPI II** in **VL-infected -S**-plants (**Fig. 3.28, C**) with the lowest occurrence of occlusions within this group (**Fig. 3.31, A**).

Gluconasturtiin showed significant differences within the factors dpi, TPI and different levels of sulfur ( $p=0.00447$ ;  $p=0.04342$ ;  $p=0.00011$ ). In addition, there was a significant effect when control and VL-infected groups were compared ( $p=0.00290$ ) and when a comparison of dpi with different sulfur fertilization was included ( $p=0.00245$ ) (**Appendix Table 6.20**).

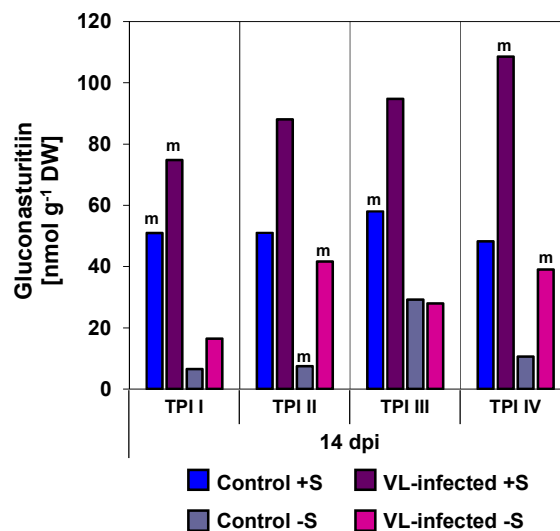


**Figure 3.42: GSL analysis by HPLC: level of the BGS� gluconasturtiin content in mock- and mycelium-spore inoculated plants at 14 dpi (first run).** Data represent the result of one measurement or the mean (m) of three dependent technical replicates (**Appendix Table 6.19**).

## Results

### 3.7.6 First run: levels of cysteine and glutathione in mock- and mycelium-spore inoculated plants at different TPIs under different sulfur supply

Cysteine and glutathione were examined, because both play an important role in plant defense mechanisms. Cysteine can act as a precursor or sulfur donor for the synthesis of sulfur-containing compounds like SDCs (Saito, 2004). In addition, it could play a crucial role in PTI and ETI (Álvarez *et al.*, 2012). Glutathione belongs to the SDCs (Rausch and Wachter, 2005) and is involved in the detoxification of ROS (Mullineaux and Rausch, 2005).

Samples of 7 and 14 dpi were measured with HPLC. At 7 dpi the amount of cysteine were highest in **control** and **VL-infected** groups under **sufficient sulfur** supply (Fig. 3.43, A). In **control** groups the values ranged from 19.46-24.47 nmol g<sup>-1</sup> FW and in **VL-infected** groups from 21.49-25.06 nmol g<sup>-1</sup> FW. The content of **control -S-** and **VL-infected -S-** groups at **TPI I** (**control**: 6.61 nmol g<sup>-1</sup> FW; **VL-infected**: 6.57 nmol g<sup>-1</sup> FW) and **TPI III** (**control**: 16.82 nmol g<sup>-1</sup> FW; **VL-infected**: 15.43 nmol g<sup>-1</sup> FW) were similar. At **TPI II** and **IV** the amount in **VL-infected -S-** groups were about 61 (16.29 nmol g<sup>-1</sup> FW) and 34% (11.99 nmol g<sup>-1</sup> FW) higher, respectively compared to the corresponding **control -S-** groups. The distribution in glutathione is similar to cysteine, where the values ranged from 175.06-718.6 nmol g<sup>-1</sup> FW (Fig. 3.43, B).

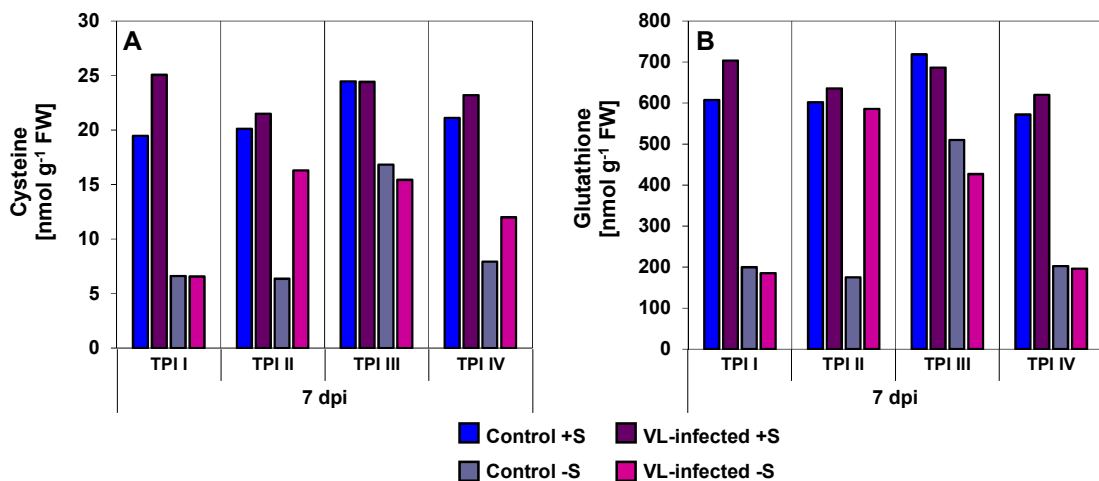
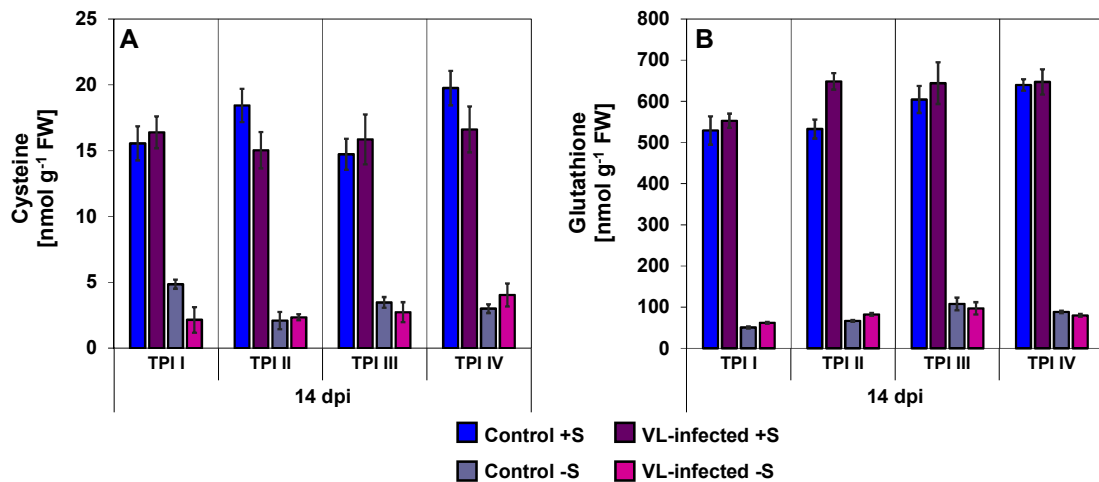


Figure 3.43: Thiol analysis by HPLC: level of cysteine and glutathione content in mock- and mycelium-spore inoculated plants at 7 dpi (first run). A: cysteine; B: glutathione; data represent the result of one measurement.

At 21 dpi the content of cysteine decreased in all groups, but were still the highest in **control +S-** and **VL-infected +S-** groups (Fig. 3.44, A).

## Results



**Figure 3.44: Thiol analysis by HPLC: level of cysteine and glutathione content in mock- and mycelium-spore inoculated plants at 14 dpi (first run).** A: cysteine; B: glutathione; data represent the mean of three dependent technical replicates  $\pm$  SD.

Overall, the values within the **sufficient sulfur** supply groups showed nearly a similar range (**control**: 14.73-19.75 nmol g<sup>-1</sup> FW; **VL-infected**: 15.03-16.61 nmol g<sup>-1</sup> FW). Same occurred for the **deficient sulfur** supply groups (**control**: 2.09-4.86 nmol g<sup>-1</sup> FW; **VL-infected**: 2.15-4.04 nmol g<sup>-1</sup> FW). The content of glutathione slightly increased about 11% in **control +S**-group at **TPI IV** and in **VL-infected +S**-groups at **TPI II** (2%) and **TPI IV** (4%), while in the remaining **control +S**-groups the values lowered about 12-16% and in the **VL-infected +S**-groups about 6 (**TPI III**) and 21% (**TPI I**) (**Fig. 3.44, B**). The amount decreased in the **control -S**-groups about 56-79% and in the **VL-infected -S**-groups about 67-86%. Comparing **control +S**- and **VL-infected +S**-groups within the different **TPIs** the values were higher in **VL-infected** groups.

Cysteine and glutathione showed significant differences in dpi and different sulfur fertilization (cysteine:  $p=0.00322$ ;  $p=0.0005$ ; glutathione:  $p=0.00358$ ;  $p=0.00006$ ). Further significant effects can be seen in the appendix (**Table 6.21, Table 6.22**).

### 3.7.7 Second run: detection and verification of the infection with *V. longisporum* in *B. napus*

As in the first run of the experiment (**3.7.1**) fungal biomass of *V. longisporum* in plants was quantified by qPCR analysis using ITS and  $\beta$ -tubulin primers (**Fig. 3.45**). Samples of 3, 7 and 14 dpi were measured. Samples of 3 dpi were not fertilized yet, the bars therefore show two biological replicates. **Figure 3.45** shows only VL-infected samples. In most control samples no VL-DNA could be detected, because limit of detection or limit of quantification was not reached, respectively (data not shown).

## Results

At 3 dpi content of VL-DNA increased from **TPI I** to **TPI IV**, whereby the cohesive bars represented similar values (**TPI I**: 6.71 and 7.05 ng g<sup>-1</sup> FW; **TPI II**: 13.85 and 10.54 ng g<sup>-1</sup> FW; **TPI III**: 17.22 and 19.54 ng g<sup>-1</sup> FW; **TPI IV**: 27.12 and 27.2 ng g<sup>-1</sup> FW) (**Fig. 3.45, A**). At 7 dpi the amount of VL-DNA was heightened in **VL-infected +S-** and **-S-** group at **TPI I** about 54% and 43%, respectively (**Fig. 3.45, C**). The values at **TPI II-IV** decreased in both **VL-infected** groups. The highest values within **VL-infected +S-** groups occurred at **TPI I** (13.53 ng g<sup>-1</sup> FW), within **VL-infected -S-** groups at **TPI I** (12.37 ng g<sup>-1</sup> FW) and **TPI III** (12.5 ng g<sup>-1</sup> FW). At 14 dpi the content of VL-DNA lowered in both **VL-infected** groups at all **TPIs** (**Fig. 3.45, E**). In **VL-infected +S-** groups the values ranged from 0.29-1.06 ng g<sup>-1</sup> FW, where the highest value was observed at **TPI II**. The amounts in **VL-infected -S-** groups laid between 1.82-5.87 ng g<sup>-1</sup> FW, where the highest values occurred at **TPI II** and **TPI IV** followed by **TPI I**.

The distribution of VL-DNA detected with  $\beta$ -tubulin primers was similar to the result with ITS primers, but for most of samples the content of VL-DNA was almost twice as much (**Fig. 3.45, B, D, F**). Significant effects for TPI depending on dpi and significant effects for sulfur supply depending on dpi were observed (**Appendix Table 6.23; Table 6.24**).

## Results

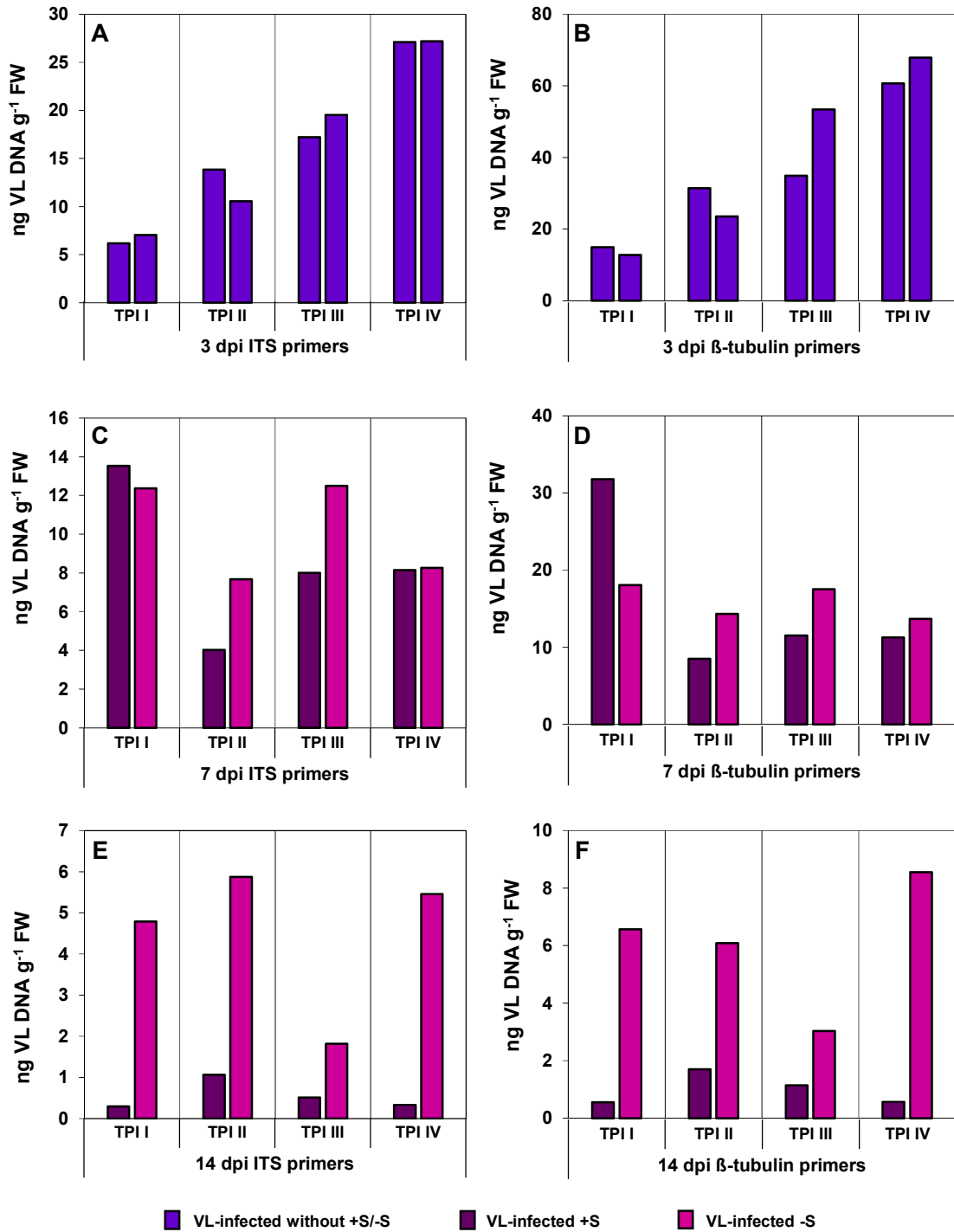


**Figure 3.45: Amount of *V. longisporum* VL43-DNA detected by qPCR with ITS and  $\beta$ -tubulin primers in *B. napus* (second run).** Status of infection rate in mycelium-spore inoculated plants potted in sand; **A and B:** 3 dpi without different sulfur fertilization; **C -F:** 7 dpi and 14 dpi: plants were fertilized with different sulfur supply; **A, C, E:** detection of VL with ITS primers; **B, D, F:** detection of VL with  $\beta$ -tubulin primers; data represent the result of one measurement.



## Results

### 3.7.8 Second run: stunting of *B. napus* plants infected with the *V. longisporum* strain VL43 under artificial inoculation

In order to observe the occurrence of “stunting” in the second run of the experiment as well (first run: **3.7.2**), three plants were selected at 3 dpi from each group, which were documented photographically (images of 7 dpi: **Appendix Fig. 6.3**). Overall, the **VL-infected** plants, which were fertilized with **sufficient sulfur** supply were smaller compared to the corresponding **control** plants at 14 dpi (**Fig. 3.46, A1-A4**: control plants; **B1-B4**: VL-infected plants).

The **control** and **VL-infected** plants, which were fertilized with **deficient sulfur** supply showed altogether a decreased growth and differences were not observed (**Fig. 3.47**). Leaves were partially yellow and purple in color as in the first run of the experiment, with the leaf surface feeling leathery and slightly broken off. In addition, the leaf margin bulged inward or outward on some plants.

## Results

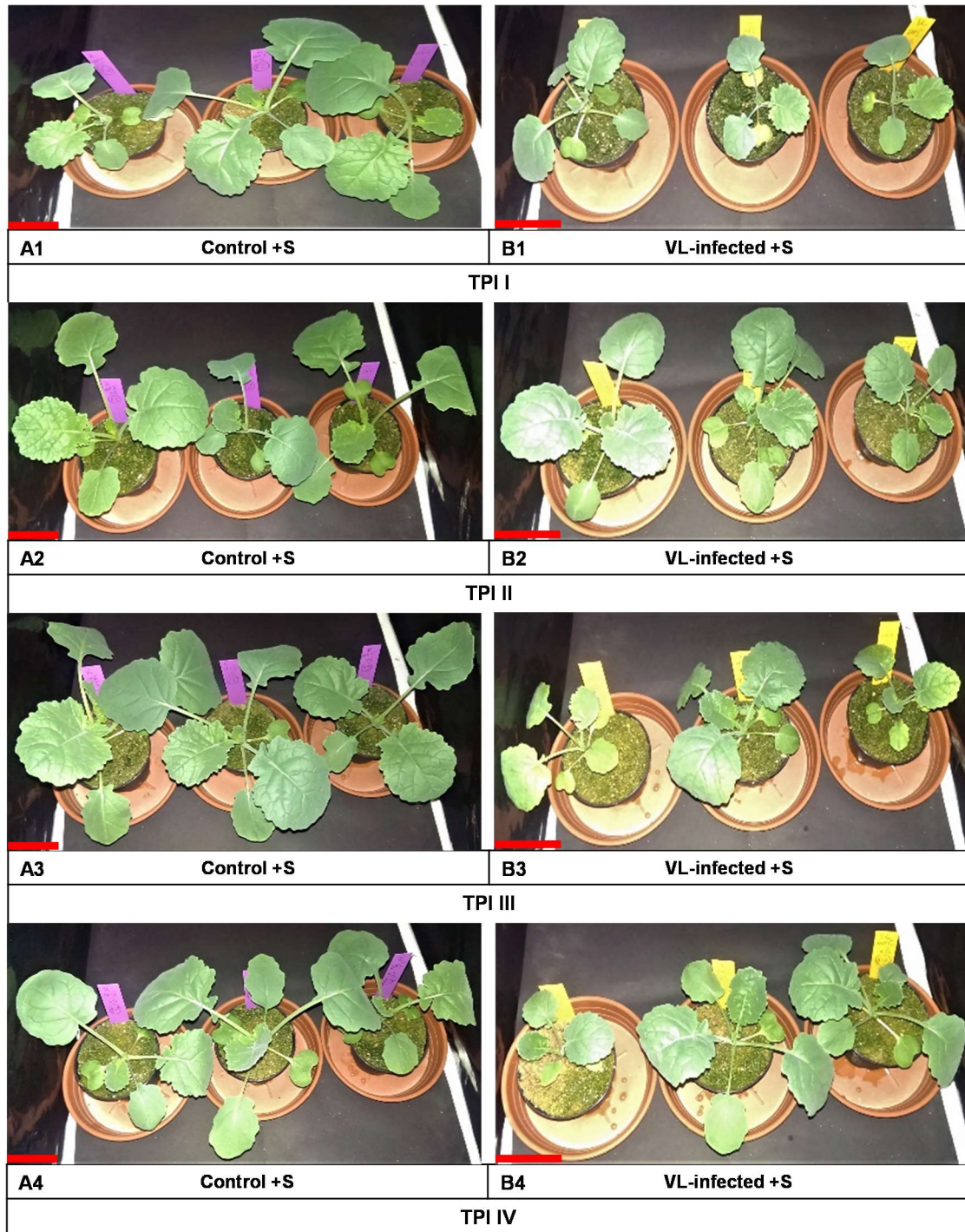


**Figure 3.46: Stunting of *B. napus* plants infected with the *V. longisporum* strain VL43 under artificial inoculation (second run). Plants under sufficient sulfur supply (1 mM MgSO<sub>4</sub>: +S) at 14 dpi; A1-A4: control plants; B1-B4: VL-infected plants; red scale bar 5 cm.**

## Results

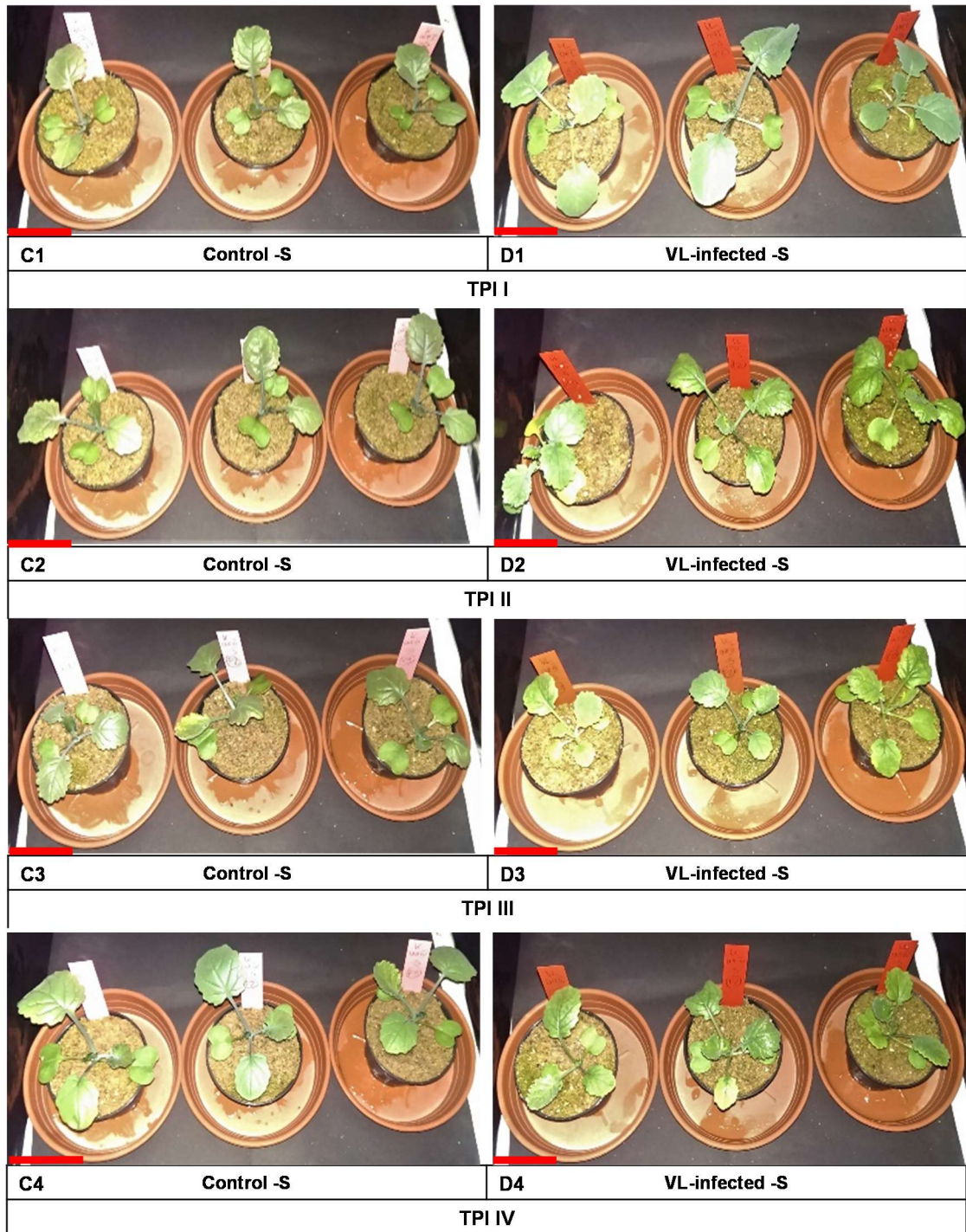


**Figure 3.47: Stunting of *B. napus* plants infected with the *V. longisporum* strain VL43 under artificial inoculation (second run). Plants under deficient sulfur supply (0.01 mM MgSO<sub>4</sub>: -S) at 14 dpi; C1-C4: control plants; D1-D4: VL-infected plants; red scale bar 5 cm.**

## Results

### 3.7.9 Second run: the influence of different TPIs and different sulfur supply on the occurrence of occlusions in the xylem of *B. napus* infected with *V. longisporum* strain VL43

To examine the influence of **different sulfur fertilization** and **TPIs** on the formation of occlusions as in the first run of the experiment (3.7.3), hypocotyls of mock- and mycelium-spore mixture inoculated plants were harvested at 14 and 21 dpi. Cross sections of **control** and **VL-infected** plants were stained with toluidine blue. **Figure 3.49** showed a selection of microscopic pictures of **VL-infected** hypocotyls under **sufficient** and **deficient** sulfur supply from 14 and 21 dpi. Control plants occasionally showed occlusions in the peripheral area and were therefore not listed in the statistics or microscopic pictures (**Appendix Fig. 6.4**). The occurrence of occlusions in the mid area of the xylem were calculated in percentage (**Fig. 3.48**).

At 14 dpi in **VL-infected +S**-plants about 8-35% of occlusions were observed at **TPI I-III** compared to **-S**-plants (4-9%) (**Fig. 3.48, A; Fig. 3.49, A1-A3, B1-B3**). The highest amount occurred in **VL-infected +S**-plants at **TPI I**. At **TPI IV** the content ranged from 3-5% in **VL-infected +S**- and **-S**-plants (**Fig. 3.49, A4, B4**). At 21 dpi the occurrence of occlusions increased in all **VL-infected** plants, whereby the amount decreased from **TPI I** to **TPI IV** (**Fig 3.48, B**). Within the different TPIs **VL-infected +S**-plants showed the highest values (**Fig. 3.49, C1-C4**). At **TPI I** and **TPI II** the content in **VL-infected -S**-plants is about 4% lower compared to the content of **VL-infected +S**-plants (**Fig. 3.49, D1-D2**). At **TPI III** and **TPI IV** the difference is about 10 and 19%, respectively (**Fig. 3.49, D3-D4**).

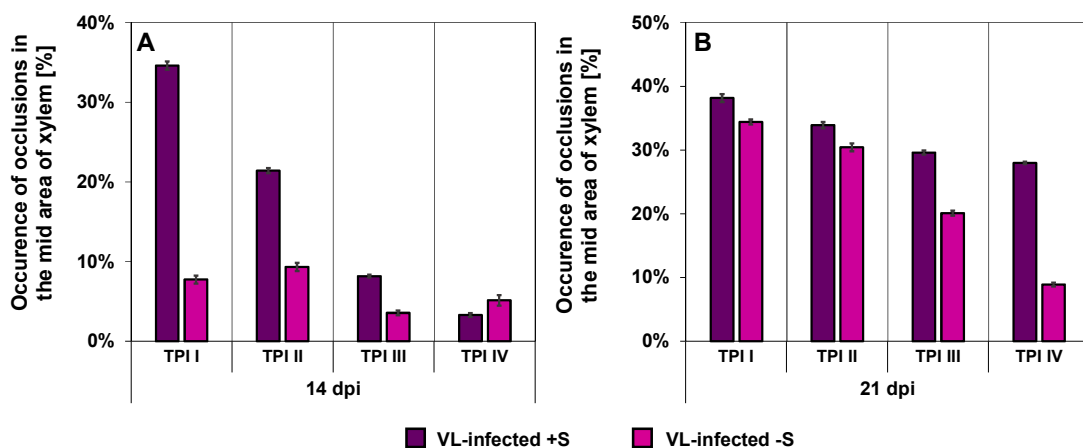


**Figure 3.48: Occurrence of occlusions in the mid area of the xylem of *B. napus* plants infected with *V. longisporum* strain VL43 (second run). A: 14 dpi; B: 21 dpi; data represent the mean of five dependent technical replicates  $\pm$  SD.**

## Results

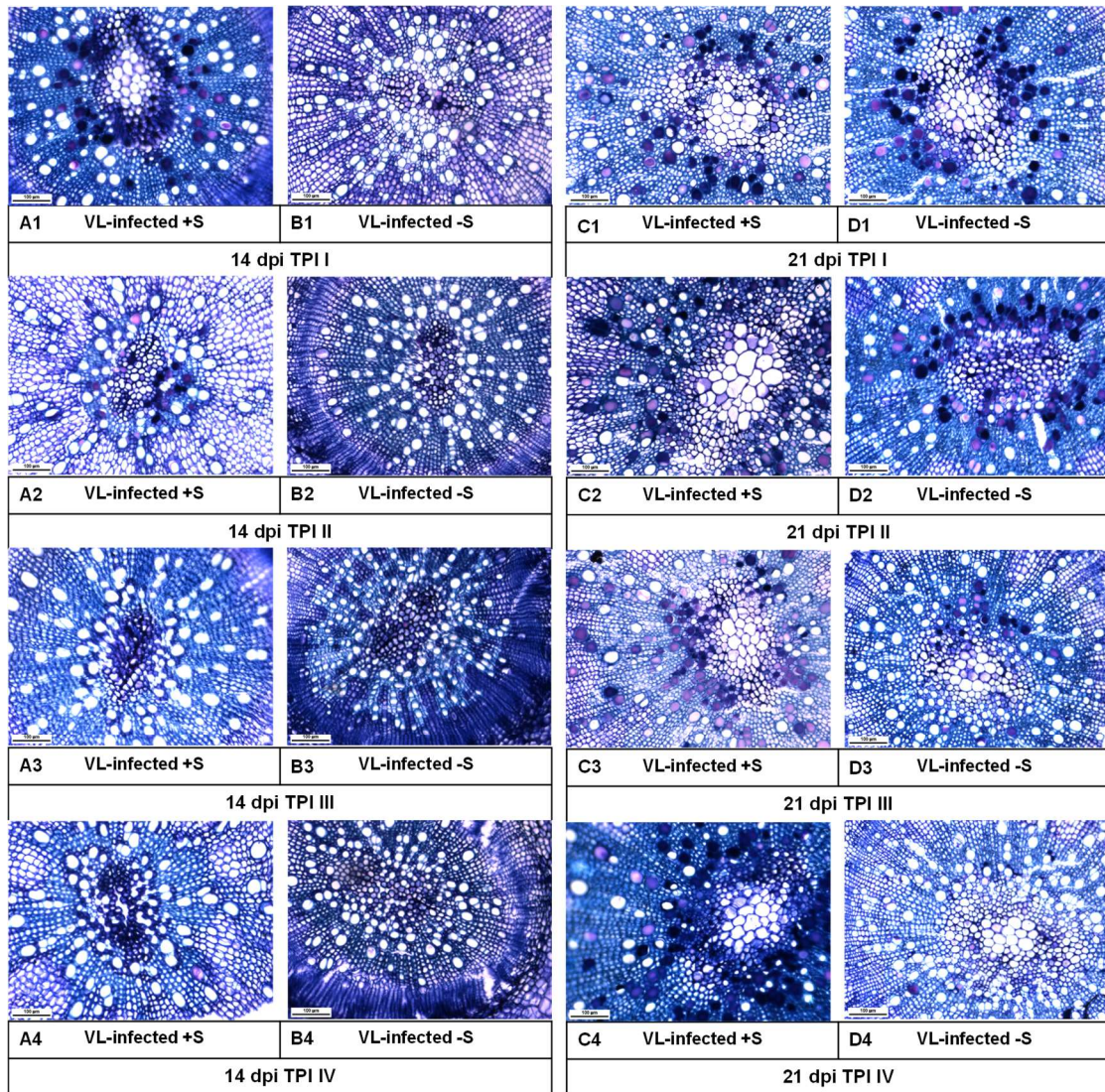


**Figure 3.49: Occurrence of occlusions in xylem: toluidine blue stained cross sections of hypocotyls of mycelium-spore inoculated plants (second run). 14 dpi: A1-A4: VL-infected +S at TPI I-IV; B1-B4: VL-infected -S at TPI I-IV; 21 dpi: C1-C4: VL-infected +S at TPI I-IV; D1-D4: VL-infected -S at TPI I-IV; scale bar 100  $\mu$ m.**

Occurrence of occlusions differ significantly between **TPI I** and **TPI III**, as well as **TPI I** and **TPI IV** ( $p=0.03074$ ; **Appendix Table 6.25**).

## Results

### 3.7.10 Second run: levels of sulfur, calcium, potassium and iron at different TPIs in mock- and mycelium-spore inoculated plants under different sulfur supply

The amounts of sulfur, calcium, potassium and iron were measured in **control** and **VL-infected** samples of 7 and 14 dpi with ICP-OES (first run: 3.7.4). At 7 dpi the highest values between 8.63-10.72 mg g<sup>-1</sup> DW of sulfur were observed in **control +S-groups** together with the **VL-infected +S-group** at **TPI II** (9.52 mg g<sup>-1</sup> DW) and **TPI III** (8.62 mg g<sup>-1</sup> DW) (**Fig. 3.50, A**). At **TPI I-III** the **VL-infected -S-groups** had slightly higher contents compared to the **control -S-groups**, while at **TPI IV** the values of both groups were similar. At 14 dpi contents of sulfur decreased in **+S-groups** about 25-51% and in the **-S-groups** about 45-80% (**Fig. 3.50, B**). At **TPI III** and **TPI IV** **VL-infected +S-groups** showed higher values compared to **control +S-groups**. In the **VL-infected -S-groups** slightly higher amounts were observed at **TPI I** and **TPI II** compared to the corresponding control groups. The difference between 7 and 14 dpi was significant ( $p=0.00133$ ; **Appendix Table 6.26**).

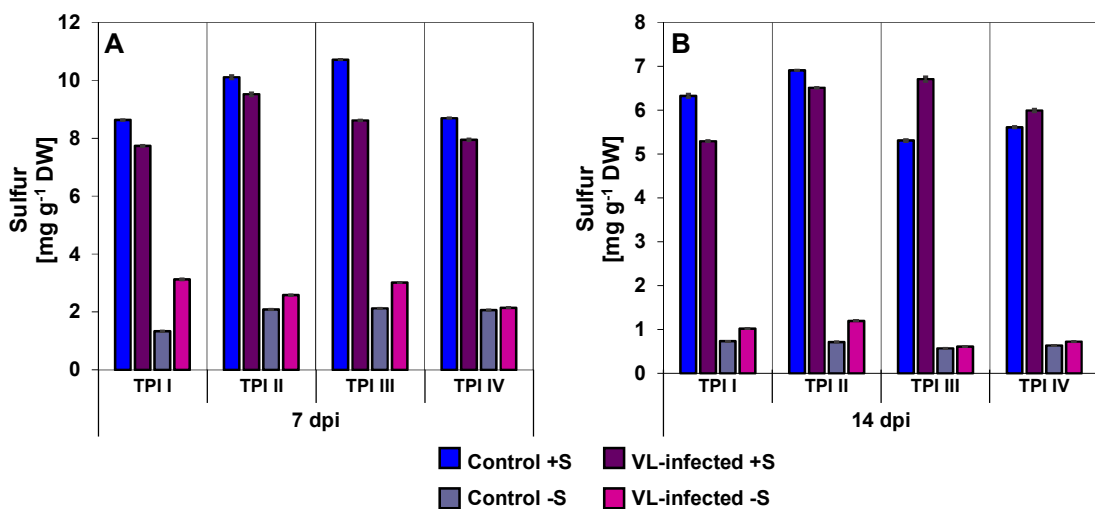


**Figure 3.50: Elemental analysis: level of S content in mock- and mycelium-spore inoculated plants measured by ICP-OES (second run). A: 7 dpi; B: 14 dpi; data represent the mean of three dependent technical replicates  $\pm$  SD.**

At 7 dpi similar amounts of calcium occurred between **control +S-** and **VL-infected-S** groups at **TPI I** (**control**: 17.51 mg g<sup>-1</sup> DW; **VL-infected**: 17.99 mg g<sup>-1</sup> DW) and **TPI II** (**control**: 21.29 mg g<sup>-1</sup> DW; **VL-infected**: 21.74 mg g<sup>-1</sup> DW) (**Fig. 3.51, A**). In **VL-infected +S-group** occurred the highest value at **TPI III** (17.07 mg g<sup>-1</sup> DW) followed by **TPI II** (16.9 mg g<sup>-1</sup> DW). At 14 dpi values in **control +S-groups** decreased about 4-25% at **TPI I-III**, in **VL-infected +S-** and **control -S-groups** about 1-3% at **TPI III** and in **VL-infected -S-group** about 29 and 9%, respectively at **TPI I** and **TPI II** (**Fig. 3.51, B**). The other values increased about 2-28%. The amounts of calcium were similar within the

## Results

**TPIs** in **control +S-** and **VL-infected +S-** groups and ranged from 14.27-17.23 mg g<sup>-1</sup> DW. The highest value occurred in **control -S-** groups at **TPI III** (21.47 mg g<sup>-1</sup> DW) followed by **VL-infected -S-** groups at **TPI II** (19.85 mg g<sup>-1</sup> DW). Differences were not significant (**Appendix Table 6.27**).

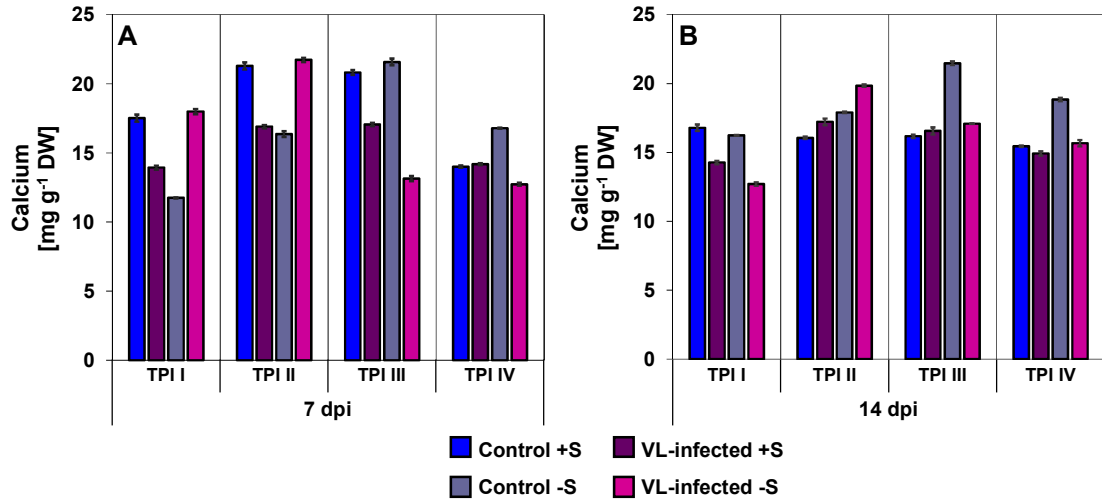


**Figure 3.51: Elemental analysis: level of Ca content in mock- and mycelium-spore inoculated plants measured by ICP-OES (second run). A: 7 dpi; B: 14 dpi; data represent the mean of three dependent technical replicates  $\pm$  SD.**

At 7 dpi the highest content of potassium was observed in **control +S-** groups at **TPI III** with 49.47 mg g<sup>-1</sup> DW and the lowest content in **VL-infected -S-** groups also at **TPI III** with 10.8 mg g<sup>-1</sup> DW (**Fig. 3.52, A**). Within **VL-infected +S-** groups the highest value occurred at **TPI II** (34.01 mg g<sup>-1</sup> DW), within **control -S-** groups at **TPI IV** (43.25 mg g<sup>-1</sup> DW) and within **VL-infected -S-** groups at **TPI II** (40.75 mg g<sup>-1</sup> DW).

## Results

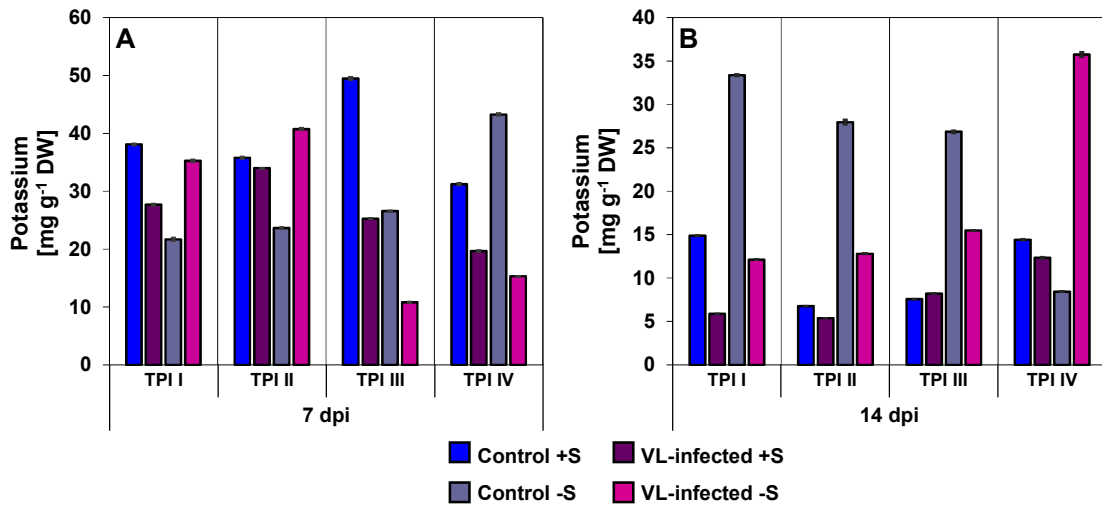


**Figure 3.52: Elemental analysis: level of K content in mock- and mycelium-spore inoculated plants measured by ICP-OES (second run). A: 7 dpi; B: 14 dpi; data represent the mean of three dependent technical replicates  $\pm$  SD.**

At 14 dpi amount of potassium lowered in **control +S**-groups about 54-85%, in **VL-infected +S**-groups about 37-84%, in **control -S**-groups at **TPI IV** about 81% and in **VL-infected -S**-groups at **TPI I** and **TPI II** about 66 and 69%, respectively (**Fig. 3.52, B**). The highest value was observed in **VL-infected -S**-groups at **TPI IV** with 35.74 mg g<sup>-1</sup> DW followed by **control -S**-groups at **TPI I** with 33.36 mg g<sup>-1</sup> DW. At **TPI I-III** the **control -S**-groups showed the highest amounts in a range between 26.86-33.36 mg g<sup>-1</sup> DW. The difference between 7 and 14 dpi was significant ( $p=0.00341$ ; **Appendix Table 6.28**).

At 7 dpi the highest values of iron were observed in **control -S**-groups at **TPI II** with 127.91  $\mu\text{g g}^{-1}$  DW and in **control +S**-groups at **TPI III** with 127.68  $\mu\text{g g}^{-1}$  DW (**Fig. 3.53, A**). The overall lowest content occurred in **control +S**-groups at **TPI IV** with 67.79  $\mu\text{g g}^{-1}$  DW. Within **VL-infected +S**- and **VL-infected -S**-groups the highest amounts displayed at **TPI III** with 83.05  $\mu\text{g g}^{-1}$  DW and 96.23  $\mu\text{g g}^{-1}$  DW, respectively. At 14 dpi the contents of iron decreased in all groups (**Fig. 3.53, B**). The highest values were observed in **VL-infected -S**-groups at **TPI III** with 85.39  $\mu\text{g g}^{-1}$  DW, followed by **VL-infected +S**-groups at **TPI II** (72.47  $\mu\text{g g}^{-1}$  DW) and **TPI III** (72.32  $\mu\text{g g}^{-1}$  DW) and **control +S**-groups at **TPI III** with 70.68  $\mu\text{g g}^{-1}$  DW. Comparing 7 and 14 dpi with control- and VL-infected plants, the differences were significant ( $p=0.00575$ ; **Appendix Table 6.29**).



## Results

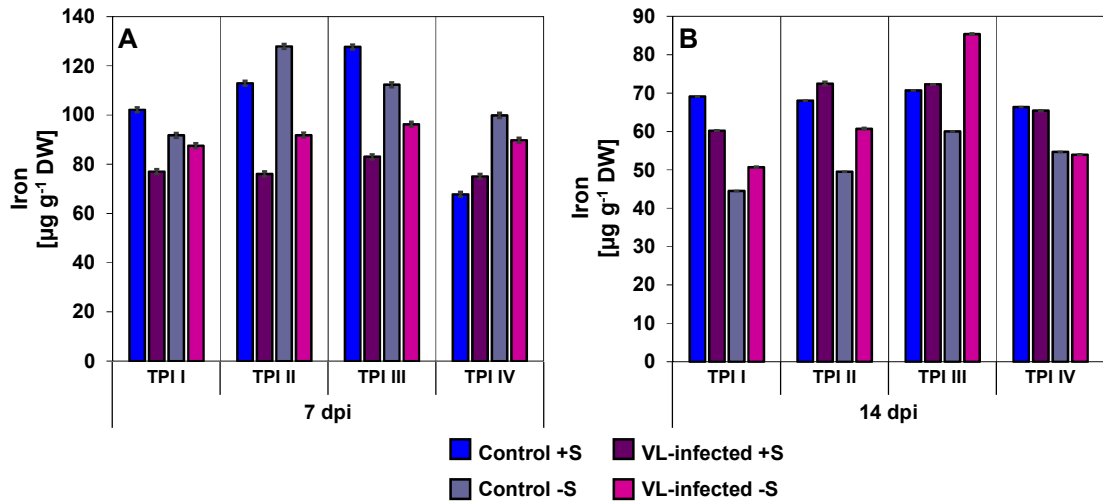


**Figure 3.53: Elemental analysis: level of Fe content in mock- and mycelium-spore inoculated plants measured by ICP-OES (second run). A: 7 dpi; B: 14 dpi; data represent the mean of three dependent technical replicates  $\pm$  SD.**

### 3.7.11 Second run: levels of indolic, aliphatic and benzylic GSLs in mock- and mycelium-spore inoculated plants at different TPIs under different sulfur supply

Like in the first run of the experiment (3.7.5) the GSLs, which belongs to the SDCs were measured of samples from 7 and 14 dpi with HPLC. At 7 dpi the highest values in glucobrassicin within the different TPIs were observed in **VL-infected +S-** (304.14-456.19 nmol g<sup>-1</sup> DW) and **-S**-groups with one exception in **VL-infected -S**-groups at **TPI IV** and a similar content to the **control +S**-group at **TPI II** (Fig. 3.54, A). The highest amount of neoglucobrassicin occurred within **control +S-** (41.08 nmol g<sup>-1</sup> DW), **VL-infected +S-** (43.18 nmol g<sup>-1</sup> DW) and **control -S**-groups (33.6 nmol g<sup>-1</sup> DW) at **TPI IV** and within **VL-infected -S**-groups at **TPI II** (47.18 nmol g<sup>-1</sup> DW) (Fig. 3.54, B).

## Results

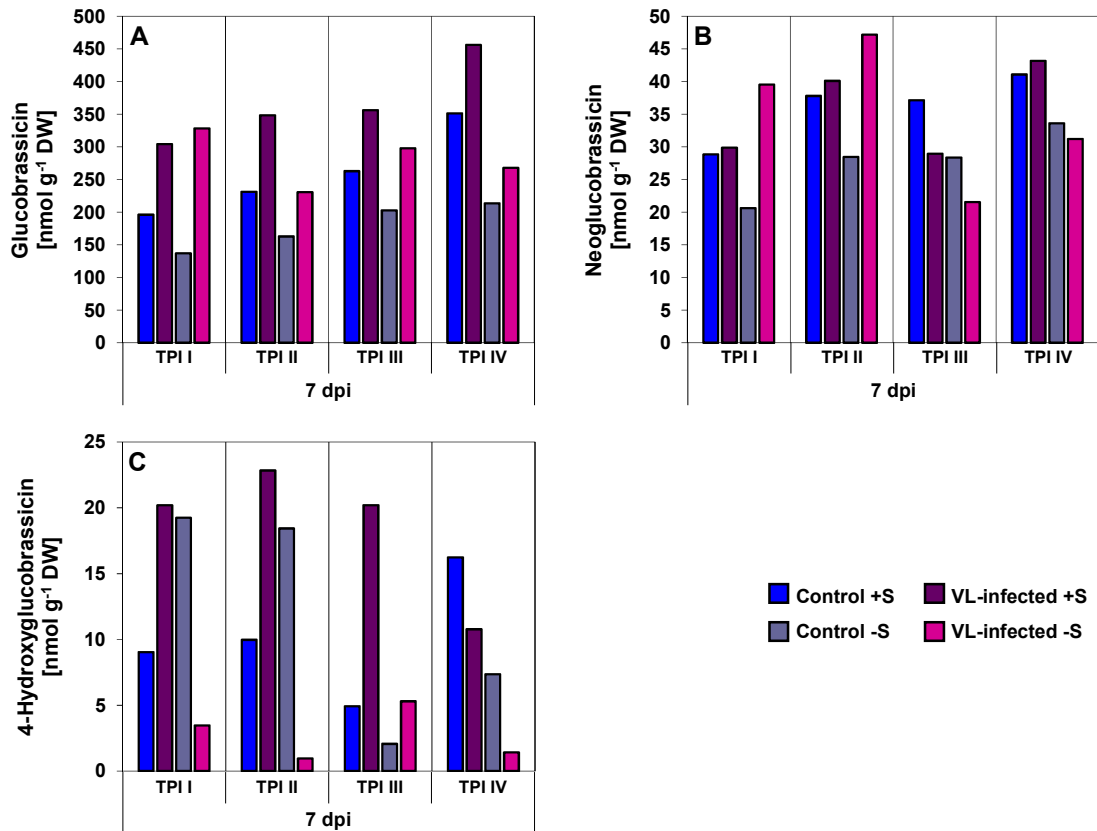


**Figure 3.54: GSL analysis by HPLC: level of IGSL content in mock- and mycelium-spore inoculated plants at 7 dpi (second run).** A: glucobrassicin; B: neoglucobrassicin; C: 4-hydroxyglucobrassicin; data represent the result of one measurement; hypothetical SDs based on previous measurements can range between 2-25%.

In 4-hydroxyglucobrassicin the highest values in a range between 20.19-22.83 nmol g<sup>-1</sup> DW occurred in **VL-infected +S**-groups at **TPI I-III** (Fig. 3.54, C). The **control -S**-groups showed amounts about 19.24 and 18.44 nmol g<sup>-1</sup> DW at **TPI I** and **TPI II**. The highest value in **VL-infected -S**-groups was observed at **TPI III** (5.3 nmol g<sup>-1</sup> DW) and in **control +S**-groups at **TPI IV** (16.24 nmol g<sup>-1</sup> DW).

## Results

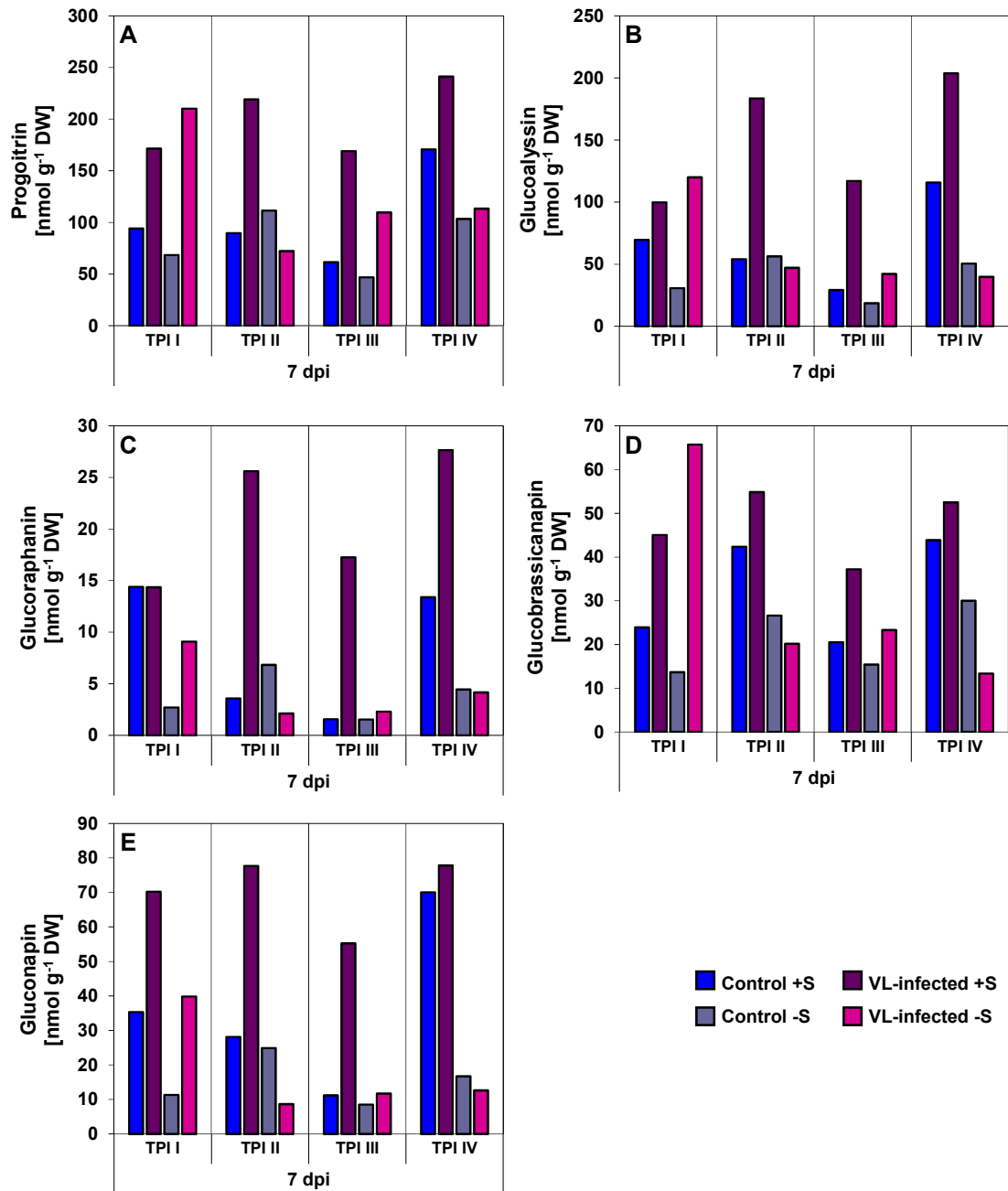


**Figure 3.55: GSL analysis by HPLC: level of AGSL content in mock- and mycelium-spore inoculated plants at 7 dpi (second run).** A: progoitrin; B: glucoalyssin; C: glucoraphanin; D: glucobrassicinapin; E: gluconapin; data represent the result of one measurement; hypothetical SDs based on previous measurements can range between 3-35%.

At 7 dpi the **VL-infected +S**-groups had the highest values at most **TPIs** in AGSLs (**Fig. 3.55**). Four exceptions were observed in progoitrin, glucoalyssin, glucoraphanin and glucobrassicinapin at **TPI I** (**Fig. 3.55, A-D**). Within **VL-infected +S**-groups highest values occurred in progoitrin (241.14 nmol g<sup>-1</sup> DW), glucoalyssin (203.69 nmol g<sup>-1</sup> DW), glucoraphanin (27.65 nmol g<sup>-1</sup> DW) and gluconapin (77.8 nmol g<sup>-1</sup> DW) at **TPI IV** (**Fig. 3.55, A-C, E**). Within **VL-infected -S**-groups the highest amounts of the AGSLs were observed at **TPI I** (progoitrin: 210.08 nmol g<sup>-1</sup> DW; glucoalyssin: 119.98 nmol g<sup>-1</sup>

## Results

DW; glucoraphanin: 9.09 nmol g<sup>-1</sup> DW; glucobrassicinapin: 65.71 nmol g<sup>-1</sup> DW; gluconapin: 39.84 nmol g<sup>-1</sup> DW).

At 7 dpi the amount of the BGS� gluconasturtiin had the highest values in **VL-infected +S-** (190.75-263.75 nmol g<sup>-1</sup> DW) and **VL-infected -S-** groups (171.25-230.38 nmol g<sup>-1</sup> DW), whereby the overall highest values occurred at **TPI IV** (Fig. 3.56). The **control +S-** and **control -S-** groups showed a relatively similar content at **TPI I** (98.71 and 92.05 nmol g<sup>-1</sup> DW). At **TPI II** and **TPI III** the amounts in **control +S-** groups were about 35% lower compared to the corresponding **control -S-** groups, while the value of **control +S-** group was about 18% higher at **TPI IV**.

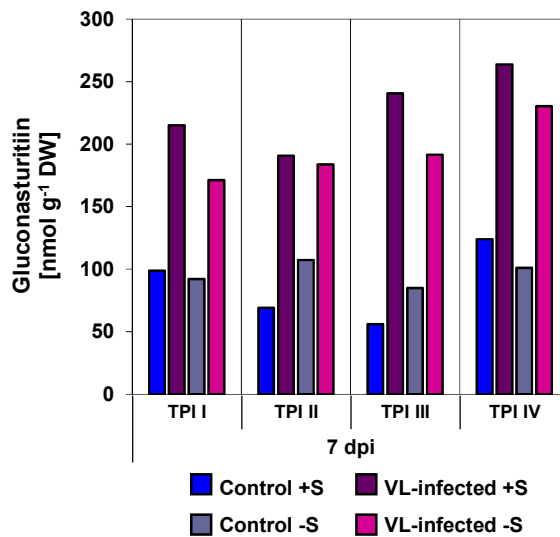


**Figure 3.56: GSL analysis by HPLC: level of the BGS� gluconasturtiin content in mock- and mycelium-spore inoculated plants at 7 dpi (second run).** Data represent the result of one measurement; hypothetical SDs based on previous measurements can range between 1-25%.

At 14 dpi amounts of glucobrassicin decreased in **control +S-** and **VL-infected +S-** groups about 48-70% and in **control -S-** and in **VL-infected -S-** groups about 89-99% (Fig. 3.57, A). Higher contents were observed in **VL-infected +S-** and **-S-** groups compared to their corresponding **control** groups. The overall highest values occurred in **VL-infected +S-** groups at **TPI I** (158.54 nmol g<sup>-1</sup> DW) and **TPI III** (165.79 nmol g<sup>-1</sup> DW). Amounts of neoglucobrassicin lowered in both **sufficient sulfur** supply groups about 28-50% and in both **sufficient sulfur** supply groups about 68-91% (Fig. 3.57, B). The highest values showed **control +S-** (23.32 nmol g<sup>-1</sup> DW) and **VL-infected +S-** group (23.62 nmol g<sup>-1</sup> DW) at **TPI IV**. Comparing **control -S-** and **VL-infected -S-** groups within the different **TPIs** **VL-infected -S-** groups displayed higher contents in a range between 5.83-8.27 nmol g<sup>-1</sup> DW, where the highest value occurred at **TPI IV**. Amounts of 4-hydroxyglucobrassicin raised in **control +S-** groups about 34-67%, where the overall highest value occurred at **TPI IV** (25.93 nmol g<sup>-1</sup> DW) (Fig. 3.57, C). In **VL-**

## Results

**infected +S**-groups contents decreased about 2 and 15% at **TPI I** (19.76 nmol g<sup>-1</sup> DW) and **TPI IV** (9.16 nmol g<sup>-1</sup> DW), respectively, while the decrease was about 71-80% at **TPI II** (6.74 nmol g<sup>-1</sup> DW) and **TPI III** (4 nmol g<sup>-1</sup> DW). The values in **control -S**- and **VL-infected -S**-groups lowered about 78-98% and were below 0.5 nmol g<sup>-1</sup> DW at all **TPIs**. The differences between 7 and 14 dpi were significant ( $p=0.00002$ ) and the effect of different sulfur supply ( $p=0.00005$ ; **Appendix Table 6.31-6.34**).

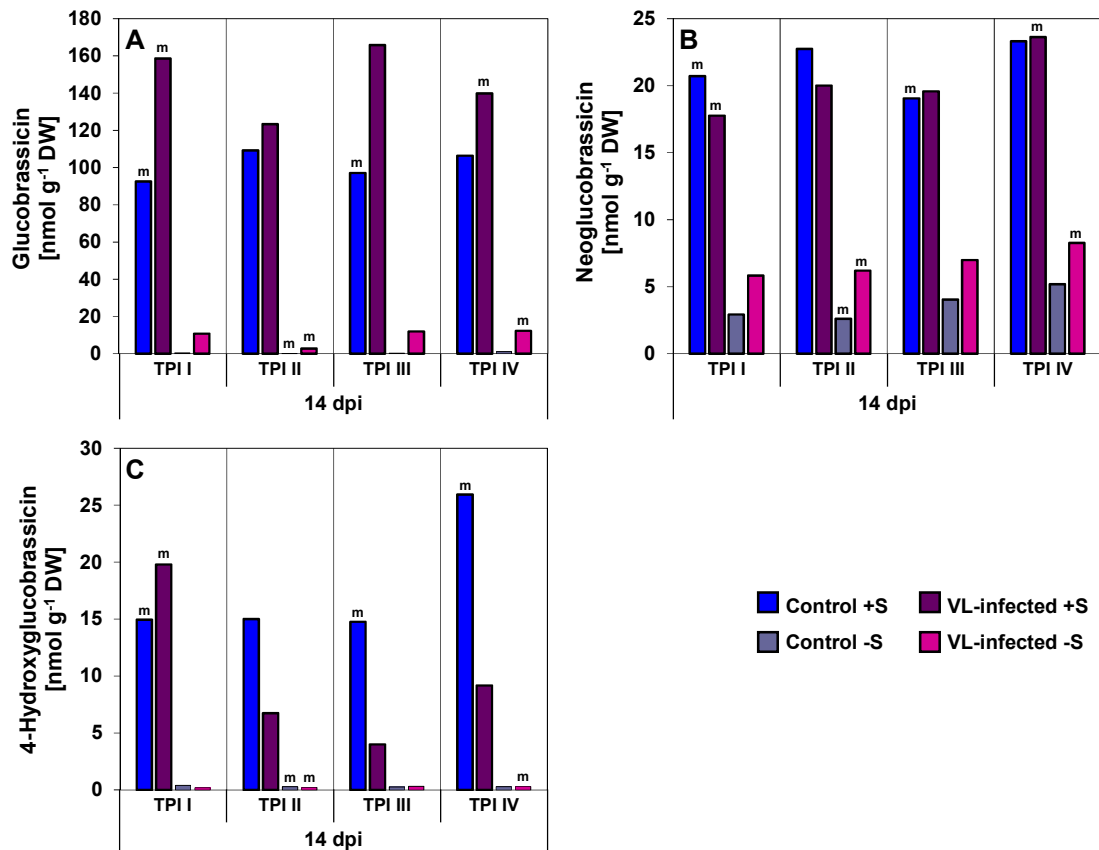


**Figure 3.57: GSL analysis by HPLC: level of IGSL content in mock- and mycelium-spore inoculated plants at 14 dpi (second run). A:** glucobrassicin; **B:** neoglucobrassicin; **C:** 4-hydroxyglucobrassicin; data represent the result of one measurement or the mean (m) of three dependent technical replicates (**Appendix Table 6.30**).

At 14 dpi contents in the AGSL progointrin increased in **control +S**-groups at **TPI II** about 6% (95.27 nmol g<sup>-1</sup> DW) and at **TPI III** about 42% (105.96 nmol g<sup>-1</sup> DW), while a decrease about 38-44% was observed at **TPI I** and **TPI IV** (**Fig. 3.58, A**). In **VL-infected +S**-groups the values lowered about 36-55% and the overall highest contents occurred at **TPI III** (108.96 nmol g<sup>-1</sup> DW) and **TPI IV** (107.59 nmol g<sup>-1</sup> DW). The amounts of progointrin decreased in **control -S**- and **VL-infected -S**-groups about 99% and were below 1.4 nmol g<sup>-1</sup> DW. The values of glucoalyssin heightened in **control +S**-groups about 36 and 68% in **TPI II** (84.88 nmol g<sup>-1</sup> DW) and **TPI III** (91.62 nmol g<sup>-1</sup> DW), respectively, but had still the highest value at **TPI IV** (108.33 nmol g<sup>-1</sup> DW) (**Fig. 3.58, B**). The amounts decreased in **VL-infected +S**-groups about 32-62% at **TPI II-IV**, at

## Results

**TPI I** about 4%, where the highest value (95.48 nmol g<sup>-1</sup> DW) was observed within this group.

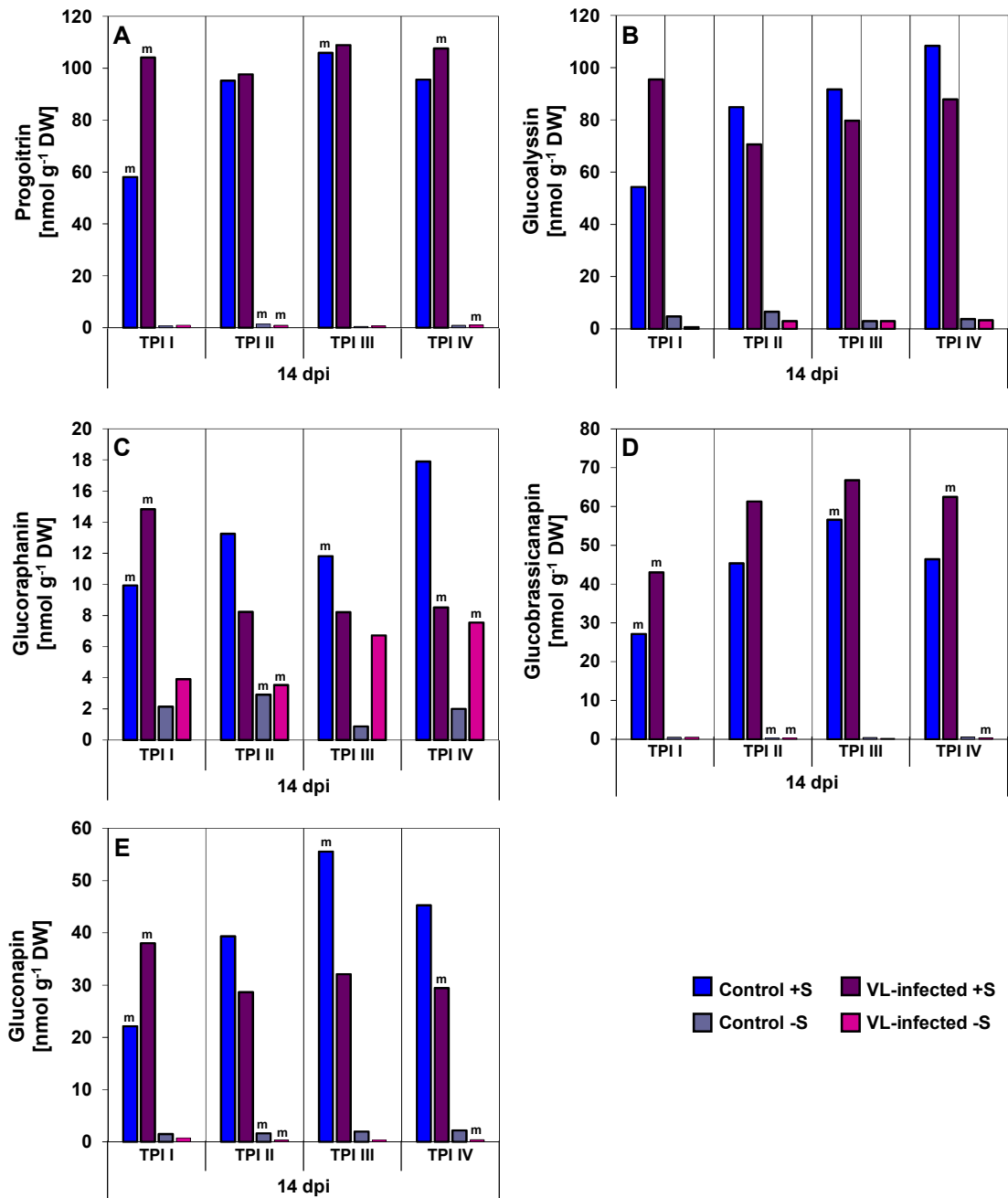


**Figure 3.58: GSL analysis by HPLC: level of AGSL content in mock- and mycelium-spore inoculated plants at 14 dpi (second run).** A: progoitrin; B: glucoalysinn; C: glucoraphanin; D: glucobrassicinapin; E: gluconapin; data represent the result of one measurement or the mean (m) of three dependent technical replicates (Appendix Table 6.35).

A decrease about 84-99% occurred in **control -S-** and **VL-infected -S-** groups. The contents in glucoraphanin increased in **control +S-** groups about 75-87% at **TPI II-IV** and decreased about 31% at **TPI I** (Fig. 3.60, C). The overall highest value was observed at **TPI IV** with 17.89 nmol g<sup>-1</sup> DW. In **VL-infected +S-** groups the amounts lowered about 52-69% at **TPI II-IV** and ranged from 8.21-8.52 nmol g<sup>-1</sup> DW. At **TPI I** the

## Results

amount increased about 3% and showed within the **VL-infected +S**-groups and within **TPI I** the highest value (14.83 nmol g<sup>-1</sup> DW). Contents decreased in **control -S**-groups about 20-57% at all **TPIs** and in **VL-infected -S**-groups about 57% at **TPI I**. At **TPI II-IV** the values in **VL-infected -S**-groups increased about 40-66% and the values were overall higher compared to the **control -S**-groups. Values of glucobrassicinapin raised in **control +S**- groups about 75-87% at all **TPIs** and in **VL-infected +S**-groups about 11-44% at **TPI II-IV** (**Fig. 3.58, D**). The highest amounts within the **TPIs** displayed in **VL-infected +S**-groups, where the overall highest value was observed at **TPI III** (66.76 nmol g<sup>-1</sup> DW). The contents in **control -S**- and **VL-infected -S**-groups decreased about 96-99% and values were below 0.5 nmol g<sup>-1</sup> DW. The contents of gluconapin increased in **control +S**-groups about 29% in **TPI II** and about 80% in **TPI III** (**Fig. 3.58, E**). The overall highest values were observed in this group at **TPI III** (55.56 nmol g<sup>-1</sup> DW) and **TPI IV** (45.3 nmol g<sup>-1</sup> DW). Within **TPI I** **VL-infected +S**-group had a 42% higher value compared to the **control +S**-group. At **TPI II-IV** the contents in **VL-infected +S**-groups were lower compared to the corresponding **control** groups. In **control -S**- and **VL-infected -S**-groups the values decreased about 77-98%, while the contents in **control -S**-groups ranged from 1.47-2.17 nmol g<sup>-1</sup> DW and in **VL-infected -S**-groups from 0.34-0.77 nmol g<sup>-1</sup> DW. Overall, the AGSLs showed a significant effect in terms of dpi on the average over the other factors ( $p=0.00035$ ) and significant differences between control and VL-infected plants ( $p=0.01806$ ; **Appendix Table 6.36-6.41**).

Levels of the BGSL gluconasturtiin lowered in both **sufficient sulfur** supply and both **deficient sulfur** supply groups at 14 dpi (**Fig. 3.59**).

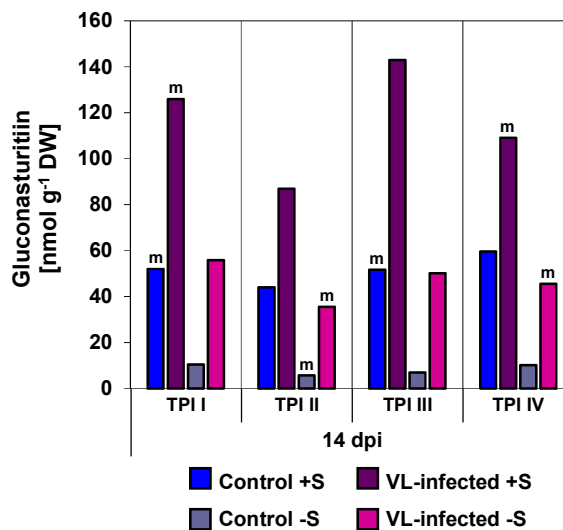


**Figure 3.59: GSL analysis by HPLC: level of the BGSL gluconasturtiin content in mock- and mycelium-spore inoculated plants at 14 dpi (second run).** Data represent the result of one measurement or the mean (m) of three dependent technical replicates (**Appendix Table 6.42**).

## Results

Still, the overall highest values were observed in **VL-infected +S**-groups (**TPI I**: 125.92 nmol g<sup>-1</sup> DW; **TPI II**: 86.9 nmol g<sup>-1</sup> DW; **TPI III**: 142.95; **TPI IV**: 109.09 nmol g<sup>-1</sup> DW). The contents within the **TPIs** in **control +S**- and **VL-infected -S**-groups were nearly similar, while contents in **control -S**-groups were overall the lowest. As for the IGSLs and AGSLs, gluconasturtiin also showed significant differences in terms of various effects (**Appendix Table 6.43**). The differences in the levels of gluconasturtiin in control and VL-infected plants were significant ( $p=0.00334$ ).

### 3.7.12 Second run: levels of cysteine and glutathione in mock- and mycelium-spore inoculated plants at different TPIs under different sulfur supply

Cysteine and glutathione were analysed as in the first run of the experiment (**3.7.6**). Samples from 7 and 14 dpi were measured with HPLC. At 7 dpi values of cysteine in **control +S**-groups ranged from 18.57-28.51 nmol g<sup>-1</sup> FW, in **VL-infected +S**-groups from 24.66-30.26 nmol g<sup>-1</sup> FW, in **control -S**-groups from 8.62-13.8 nmol g<sup>-1</sup> FW and in **VL-infected -S**-groups from 6.57-16.29 nmol g<sup>-1</sup> FW (**Fig. 3.60, A**). Overall, the highest amounts were observed in **VL-infected +S**-groups, whereby the contents were similar to the **control +S**-groups at **TPI I** and **TPI IV**. The **control -S**-groups showed a higher content at **TPI I** compared to the **VL-infected -S**-group, this distribution was vice versa at **TPI II**. At **TPI III** and **TPI IV** in **control -S**- and **VL-infected -S**-groups occurred similar values.

In **control +S**-groups the amount of glutathione ranged from 519.29-646.72 nmol g<sup>-1</sup> FW, while the overall highest value was observed at **TPI II** (**Fig. 3.60, B**).

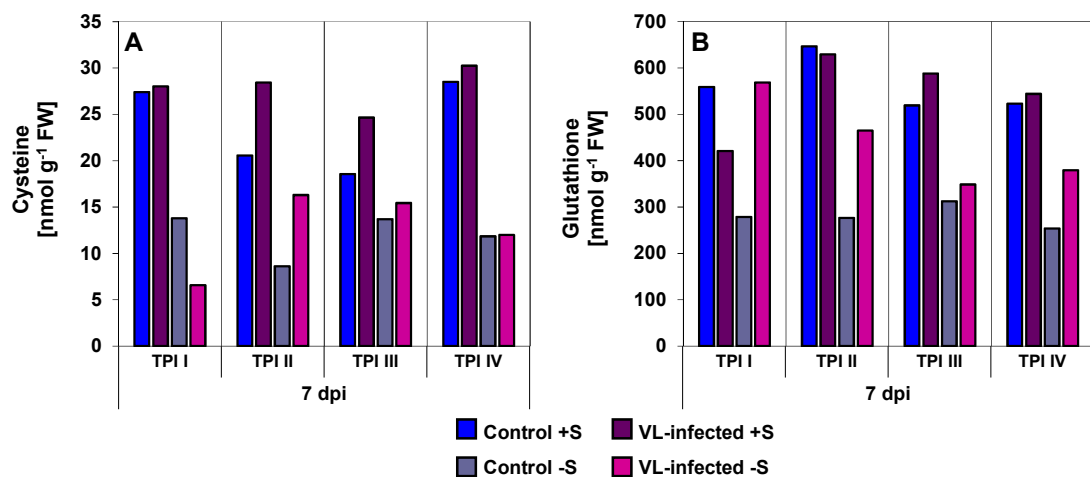


**Figure 3.60: Thiol analysis by HPLC: level of cysteine and glutathione content in mock- and mycelium-spore inoculated plants at 7 dpi (second run). A: cysteine; B: glutathione; data represent the result of one measurement.**



## Results

Within the **VL-infected +S**-groups the highest amount also occurred at **TPI II** (629.21 nmol g<sup>-1</sup> FW). Within **TPI III** the highest value was observed in **VL-infected +S**-group (588.02 nmol g<sup>-1</sup> FW). Contents of glutathione were higher in **VL-infected -S**-groups compared to the **control -S**-groups, whereby the amounts were similar at **TPI III**. Within **VL-infected -S**-groups, the highest value occurred at **TPI I** (568.68 nmol g<sup>-1</sup> FW) and were similar to the value of the **control +S**-group.

At 14 dpi amounts of cysteine raised in **control +S**-groups about 7 and 21% at **TPI II** and **TPI III**, respectively, while the contents lowered about 29-35% at **TPI I** and **TPI IV** (**Fig. 3.61, A**). In **VL-infected +S**-groups the values decreased about 12-38% and the highest values occurred within this group at **TPI II** (21.42 nmol g<sup>-1</sup> FW) and **TPI III** (21.72 nmol g<sup>-1</sup> FW). Within the **TPIs VL-infected -S**-groups showed higher amounts at **TPI I**, **TPI III** and **TPI IV** compared to the corresponding **control -S**-groups, while at **TPI II** values in both groups were similar.

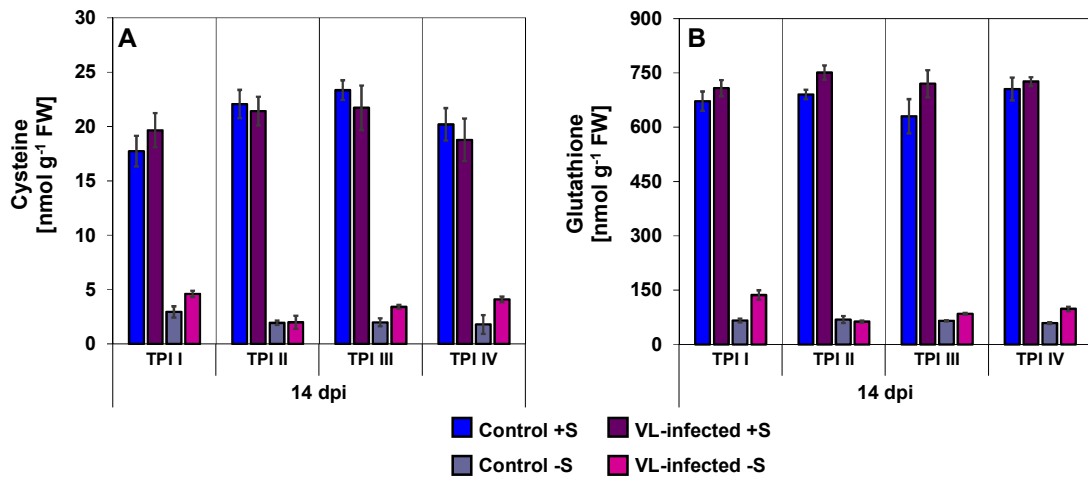


**Figure 3.61: Thiol analysis by HPLC: level of cysteine and glutathione content in mock- and mycelium-spore inoculated plants at 14 dpi (second run). A: cysteine; B: glutathione; data represent the mean of three dependent technical replicates  $\pm$  SD.**

Contents of glutathione increased in **control +S**- and **VL-infected +S**-groups about 6-41% (**Fig. 3.61, B**). Overall, slightly higher values were observed in **VL-infected +S**-groups with the highest amount at **TPI II** (750.78 nmol g<sup>-1</sup> FW). Contents in **control -S**- and **VL-infected -S**-groups decreased about 74-87% and ranged in **control -S**-groups from 58.99-68.52 nmol g<sup>-1</sup> FW and in **VL-infected -S**-groups from 62.99-136.38 nmol g<sup>-1</sup> FW. Within the **TPIs VL-infected -S**-groups showed slightly higher values compared to the corresponding **control -S**-groups at **TPI I**, **TPI III** and **TPI IV**, while the content was similar at **TPI II**. Cysteine and glutathione showed some significant differences in terms of various effects (**Appendix Table 6.44; Table 6.45**), only glutathione showed a significant difference in comparison of control and VL-infected plants ( $p=0.00230$ ).

## 4. Discussion

This thesis focused on the question whether the susceptibility of *B. napus* to an infection with *V. longisporum* differs during the day. In addition, the influence of posterior sufficient and deficient sulfur fertilization on the course of the infection was also investigated (Fig. 4.1). In order to examine the interaction between host and pathogen in the context of the research question, the plants were inoculated at different time points (TPIs) with a mycelium-spore mixture of *V. longisporum* and subsequently fertilized with different sulfur supply (+S/-S). With plant material collected at 7 and 14 dpi, various analyses were carried out to investigate possible differences between the infection groups and their associated control groups.

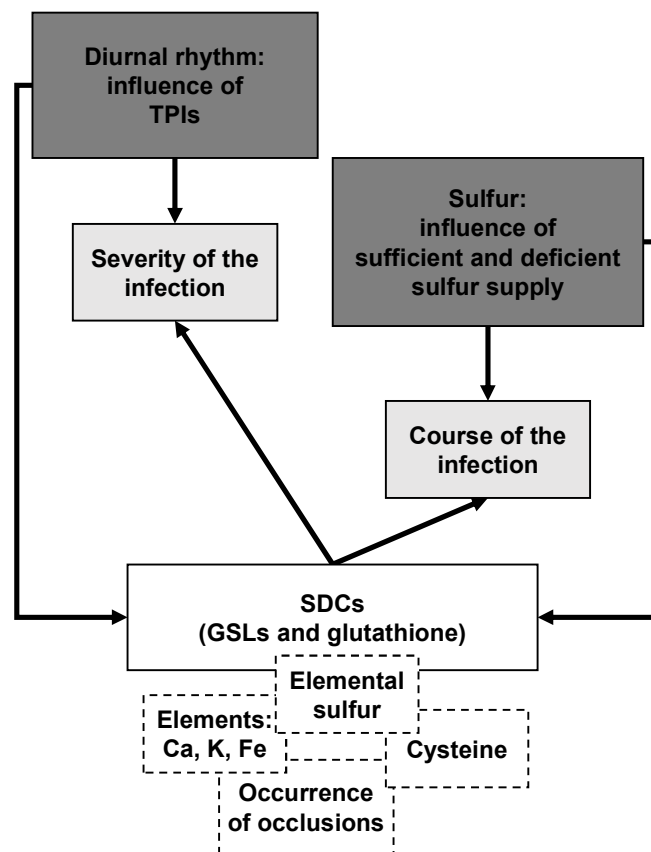


**Figure 4.1: Schematic overview of the aims of this thesis: inoculation of *B. napus* with *V. longisporum* under diurnal rhythmic and posterior sufficient and deficient sulfur supply of inoculated plants.** Main factors of interest are the influence of different TPIs on the severity of the infection and the different sulfur supplies on the course of the infection. In addition, it should be clarified whether the two factors have an influence on the formation of SDCs (GSLs and glutathione) and, furthermore, on the contents of elemental sulfur, nutrient elements (calcium, potassium, iron), cysteine and the occurrence of occlusions in the xylem of infected plants.

## Discussion

A special interest here is on the role of GSLs in pathogen defense mechanisms, as previous studies evaluated their positive effects against the infection with *V. longisporum* (Depotter *et al.*, 2016; Iven *et al.*, 2012; Rygulla *et al.*, 2007a; Witzel *et al.*, 2013, 2015). Another sulfur-containing compound, that has been analysed, was glutathione. The GSLs and glutathione belong to the SDCs, therefore, the content of elemental sulfur in plants has been recorded as well. In addition to elemental sulfur, levels of calcium, potassium and iron were measured, because they contribute in pathogen defense mechanisms. Since cysteine plays a role as precursor or donor of reduced sulfur for the synthesis of sulfur-containing compounds (e.g. glutathione), the content was also examined.

Beyond the importance of various nutrient elements and plant metabolites, it is known that in *B. napus* the formation of blockages in the xylem is induced to protect against the spread of *V. longisporum*, whereby resistant plants are characterized by a significantly stronger appearance of occlusions (Eynck *et al.*, 2009; Kamble *et al.*, 2013). Based on these observations, histological sections of hypocotyls were prepared in order to establish a possible correlation between the occurrence and severity of occlusions within TPIs and different sulfur fertilization conditions. In the main experiment young *B. napus* plants were inoculated directly from BK-plates supplemented with sufficient sulfur supply. Therefore, at the time of inoculation, regardless of mock-inoculation or inoculation with mycelium-spore mixture, the plants should have the same overall sulfur supply status. In order to verify the success of the infection, a qPCR analysis was carried out at 3 dpi, afterwards the fertilization began with sufficient and deficient sulfur supply. Hence, it seems to be useful to include the infection status, from which the different fertilization began, in comparison with the results of the elemental and metabolite analysis from 7 and 14 dpi. However, the two runs of the main experiment proceeded differently with respect to the qPCR results, which means that the VL-infected groups are differentially infected, resulting in varying responses of host plants. The results are discussed together, but always with the reference to which run they belong (first or second run).

### 4.1 Thick as thieves - the many faces of sulfur in fungal pathogen defense mechanisms

Sulfur deficiencies in the soil are a serious threat in agriculture and sulfur fertilization is needed to grow healthy plants and increase crop yield (Tisdale *et al.*, 1986). Besides, sulfur-containing compounds of plants are involved in pathogen defense mechanisms and take place in the plant resistance (Rausch and Wachter, 2005). Thus, sulfur hold a very complex part in plants, for example sufficient sulfur supply is necessary for normal plant development (Blake-Kalff *et al.*, 1998). Limitation of available sulfur in *B. napus* causes chlorosis, leaf deformations and anthocyanin enrichment (Schnug and Haneklaus, 2005). Several studies reported that sulfur plays a key role in the defense against vascular pathogenic fungi (Williams *et al.*, 2002; Bloem *et al.*, 2005; Rausch and Wachter, 2005; Kruse *et al.*, 2007; Weese *et al.*, 2015). A study by Weese *et al.* (2015) demonstrated that *B. napus* plants infected with *V. longisporum* incorporated more sulfur than the corresponding control plants regardless to different sulfur fertilization. In the conducted experiments of this work this observation could be made in in some cases in VL-infected -S-plants, where in both runs of the main experiment slightly more sulfur was measured than in the corresponding control plants. In case of VL-infected +S-plants, the content of sulfur is similar or at some TPIs lower, respectively, compared to the associated control plants. A significantly higher incorporation of sulfur in VL-infected +S-plants could only be observed in pre-experiment II, comparing root samples of sufficient sulfur supplied plants (**Fig. 3.19**).

Concerning the VL-infected plants of the first run, the prospective +S-groups showed the highest infection at TPI IV, the future -S-groups at TPI III. When the levels of measured elemental sulfur are included into account, the highest amount also appears at TPI IV in VL-infected +S-groups and at TPI II in VL-infected -S-groups. In the second run the infection was the strongest at TPI IV in both groups at 3 dpi. The TPIs, at which the highest sulfur levels were measured, show no unambiguous assignment to the contents of VL-DNA. Overall both runs showed no apparent correlation between the highest rate of infection at a specific TPI and the highest levels of incorporated sulfur by the plants at a specific TPI.

Although it could not been shown that the infection with *V. longisporum* results in increased incorporation of sulfur into the plants, but the involvement of the sulfur-containing compounds can still be demonstrated in the further discussion. At least the statement can be made that the expected effects on *B. napus* plants induced by different sulfur fertilization have occurred and the differences are significant in both runs (**Appendix Table 6.3; Table 6.26**).

## Discussion

However, the infection rates of both runs suggest that *B. napus* is more susceptible to an infection with *V. longisporum* at TPI III and TPI IV, whereby the TPI III takes place in the light (1 h before the offset of light), while the TPI IV is in the dark (3 h after the offset of light). This observation agrees in parts with the results of Bhardwaj *et al.* (2011) and Ingle *et al.* (2015), in which *A. thaliana* presented higher a resistance and/or defense responses to *Pseudomonas syringae* and *Botrytis cinerea*, respectively, when inoculated during the day than at night.

### 4.1.1 An important supporting role - glucosinolates as sulfur-containing defense compounds

There are several major classes of secondary metabolites suggested to be involved in the defense mechanisms against *V. longisporum*. In *A. thaliana* predominantly indole and indole-sulfur compounds (Iven *et al.*, 2012), GSLs (Zhou *et al.*, 2006) and phenylpropanoids (König *et al.*, 2014) were identified to play a crucial role in this specific infection system. Although GSLs and phenylpropanoids are synthesized via different biosynthetic pathways and have unique functions, a study by Hemm *et al.* (2003) with the *ref2* *A. thaliana* mutant (reduced epidermal fluorescence; Ruegger and Chapple, 2001) showed that there is a crosstalk between the two pathways. König *et al.* (2014) found that soluble phenylpropanoids accumulate in leaf tissue of *A. thaliana* instead of tryptophan-derived metabolites in response to an infection with *V. longisporum*. Moreover, the phenylpropanoid synthesis seems also to be important for the defense in *B. napus* against *V. longisporum*. This was demonstrated in a study by Eynck *et al.* (2009), in which a resistant *B. napus* line (SEM 05-500256) was found to produce more phenolic compounds when infected with *V. longisporum* compared to the susceptible commercial cultivar "Falcon". In addition, the concentrations of phenolpraponoids correlated with *V. longisporum* resistance in *B. napus* (Obermeier *et al.*, 2013). *Verticillium longisporum* has the ability to synthesize aromatic amino acids, therefore, cross-pathway control of amino acid biosynthesis is required for the severity of pathogenicity (Timpner *et al.*, 2013). The cross-pathway control allows *V. longisporum* to increase the amino acid biosynthesis in case of starvation (Singh *et al.*, 2010; Timpner *et al.*, 2013). In the first stage of infection with *V. longisporum*, the xylem vessels of *B. napus* are colonized. The xylem sap consists of water, inorganic compounds, organic acids and a small amount of amino acids (Kehr *et al.*, 2005). In a study by Singh *et al.* (2010) it was shown, that a reduced activity of *Vlaro2* isogenes, which encodes for the amino acid biosynthesis enzyme chorismate synthase, resulted in a reduced pathogenicity of *V. longisporum*. This enzyme catalysis the last step of the biosynthetic pathway, forming chorismate, which is essential for the synthesis of tryptophan, phenylalanine and tyrosine. Therefore, the study indicated a first evidence,

## Discussion

that the *B. napus* xylem sap does not provide a sufficient amount of aromatic amino acids for *V. longisporum* growth.

It appears that increased production of secondary plant metabolites in response to infection with *V. longisporum* lowers the amino acid concentration in the xylem sap. Therefore, the fungus needs a functional cross-pathway control to ensure its amino acid supply through the xylem sap. In leaf material of infected *A. thaliana* plants with *V. longisporum* little evidence of IGSLs and other phytoalexins (e.g. camalexin) were found, which is in contrast to the reaction in the roots, where the induction of indolic compounds was very strong during the attempted penetration of the fungi (Iven *et al.*, 2012). This difference is not unexpected, since *V. longisporum* displays an invasive growth in the plant roots, whereas the growth in xylem is not accompanied by the attempt of the fungi to colonize living tissue. Therefore, pathogen defense mechanisms, which have already been extensively described for *A. thaliana*, but e.g. for the pathogens *Pseudomonas syringae* pv. *tomato* and *Pythium sylvaticum*, cannot be used for comparison since the defense reactions are likely to be completely different (Tan *et al.*, 2004).

In particular, this study aims to investigate the possible involvement of GSLs during the infection of *B. napus* with *V. longisporum* and also attempts to find a dependency on plants infected in the morning and in the evening, respectively. The role of the available sulfur comes into play again, because it is involved in the formation of the GSLs, that belong to the SDCs (Rausch and Wachter, 2005). The GSLs are derived from amino acids and incorporated at least two sulfur atoms, whereof one originated from glutathione (Geu-Flores *et al.*, 2011). In particular the IGSLs, which are tryptophan-derived, should be significantly involved in the defense of fungal pathogens (Bednarek *et al.*, 2009). However, when plants from the family of Brassicaceae were exposed to excess sulfur supply, the storage for GSLs showed a limited capacity (Van der Kooij *et al.*, 1997; Westerman *et al.* 2001). Furthermore, GSLs are believed to accumulate less under low-sulfur conditions, as plants need the available sulfur for protein biosynthesis and other important functions rather than investing it in defense mechanisms against pathogens (Falk *et al.*, 2007).

In addition to IGSLs, AGSLs and the BGSL gluconasturtiin were measured in control and VL-infected plants. In both runs of the experiment the content of IGSLs under sufficient sulfur supply is overall higher at 7 and 14 dpi in comparison to the deficient supply plants, whereby the difference being more pronounced at 14 dpi. In control +S- and -S-groups (first run) the highest levels of IGSLs, AGSLs and BGSL were measured at TPI III. The control +S- and -S-groups of the second run had their highest amounts

## Discussion

of IGSLs at TPI IV. The same TPI applied for AGSLs and for the BGSL, but only for the control +S-groups, where control -S-groups showed overall higher values at TPI II. Plants were taken from BK-plates before the inoculation procedure, slightly injuring the roots. This facilitates the penetration of *V. longisporum*, but can also lead to increased levels of certain secondary metabolites, depending on the degree of injury of the roots (Endara and Coley, 2011). Thus, plants that receive sufficient sulfur supply may respond to mock-inoculation in the evening similar to increased susceptibility to certain pathogens. Plants that suffer from sulfur deficiency after inoculation, therefore, could react very differently to the TPIs. The VL-infected +S-groups of both runs, which were most infected at TPI IV (3 dpi), show the highest values of IGSLs at the same TPI at 7 dpi. The contents of AGSLs and the BGSL are highest at TPI IV as well, but in case of the first run not until 14 dpi and in the second run only at 7 dpi. Also, when the highest infection was observed in both runs at TPI IV, the infection in the first run was significantly more severe, which may lead to a different response in the course of the infection. The VL-infected -S groups showed the highest infection with *V. longisporum* at TPI III (first run) and TPI IV (second run) at 3 dpi. In the first run the levels of IGSLs, AGSLs and the BGSL are highest at the same TPIs as the infection. However, this picture does not stand out in the second run. Even if these results have to be considered with extreme caution due to the limited data availability, there are significant differences in the first run between the control and VL-infected groups with respect to the total content of AGSLs, independent of the sulfur fertilization (**Appendix Table 6.8, 6.13 and 6.20**). At the second run, this difference is considerably less noticeable, which may be due to the lower overall infection rate (**Appendix Table 6.31, 6.36 and 6.43**). The most interesting result show both runs with respect to the BGSL gluconasturtiin, which is mainly root- and hypocotyl-specific in *B. napus* and has a phenylalanine-derived side chain (Clossais-Besnard and Larher, 1991; Halkier and Gershenzon, 2006). Gluconasturtiin showed significantly higher values in the VL-infected +S- and -S-groups compared to the associated control groups at all TPIs. Karapapa and Baig (1997) found an increased synthesis of gluconasturtiin in the roots of *B. napus* against a non-pathogenic *V. dahliae* strain. This appeared to be a major factor in the active resistance response, which meant that the non-pathogenic fungus could not colonize the plant. A pathogenic strain of *V. longisporum* was either to be able to suppress the synthesis of gluconasturtiin in the roots, or failed to trigger its synthesis by preventing detection. This signifies an adaptation of *V. longisporum* to *B. napus* as its host, because it shows a less sensitive reaction to this kind of host-specific defence compared to the non-pathogenic *V. dahliae* strain (Eynck *et al.*, 2007). In this study the plant roots were not included in the measurements, however, the larger differences to

## Discussion

the control groups leading to the suggestion, that the invasion of *V. longisporum* causes an increased rate of gluconasturtiin. It is possible that the *B. napus* varieties used for the investigations in the study by Karapapa and Baig (1997) were more susceptible to *V. longisporum* infection. The variety “Genie”, which was used in this work has good overall health and may be able to resist the spread of the fungus under the optimal environmental conditions. In addition, gluconasturtiin is a phytoanticipin and Mithen *et al.* (1986) showed in their experiments with bioassays, the toxicity of the hydrolysis products of GBS, that may play a role in the pathogen defence mechanisms of plants. Therefore, the BGSL seems to be an important player in addition to the IGSLs in case of this host-pathogen construct. But the AGSLs seem to take an important part in the response to infection with *V. longisporum* as well. In both runs the highest values could be observed in the VL-infected +S-groups at 7 dpi. Njoroge *et al.* (2011) found in their study that broccoli infected with *V. longisporum* had higher concentrations of AGSLs in the roots than in the shoots, whereas in cauliflower the opposite was observed. This result may be related to the resistance of broccoli against *V. longisporum*.

Although the dataset is very small and there are only two repetitions of the main experiment, which differed in term of the infection severity, it is still possible to speculate that the IGSLs, AGSLs and particularly the BGSL play a major role in the defense mechanisms against *V. longisporum*, when host plants have a sufficient amount of sulfur available. This would also be accompanied by the observation that the infection in the VL-infected +S-plants is overall less severe than in the VL-infected -S-plants at 14 dpi. In addition, the infection rates in the VL-infected +S plants decreased evidently from 3 to 14 dpi. The extent to which the soluble phenylpropanoids are involved can only be assumed, since they were not measured. To investigate the role of gluconasturtiin measurements of roots, hypocotyls, stems and leaves of infected and non-infected *B. napus* plants could be performed. This would determine whether the accumulation of the BGSL in certain parts of the plant is higher compared to control plants. Furthermore, in vitro experiments with gluconasturtiin could be conducted to test for a direct effect on *V. longisporum*.



## Discussion

### 4.1.2 Onlookers or main actors? - The role of cysteine and glutathione

Levels of cysteine and glutathione are suggested as a marker for the increased activity of primary sulfur metabolism after pathogen infection (Kruse *et al.*, 2007). Cysteine acts as a mediator between the reduction of the assimilatory sulfate and the provision of reduced sulfur, which is destined for cell metabolism (Bonner *et al.*, 2005). It would be expected that levels of cysteine would decrease following infection using sulfur-containing compounds. These observations could indeed be made between the two harvest time points in both runs (decrease between 12-38%), however, there were no major differences in cysteine levels between the two VL-infected groups and their associated control groups. There was only one difference to see whether the plants were supplied with sufficient or deficient sulfur supply, with a clear effect observed at 14 dpi. It would be interesting to know what the levels of cysteine were before or immediately after infection with *V. longisporum* since a study by Kruse *et al.* (2012) showed increased levels of cysteine in *A. thaliana* infected with *Alternaria brassicicola* until 7 dpi. Glutathione functioned as the primary sulfur donor in the biosynthesis of GSLs (Geu-Flores *et al.*, 2011). In addition, it is an important stress indicator and serves as a redox buffer in plants (Foyer and Noctor, 2009). When it comes to biotic or abiotic stress factors, ROS could be formed as response, whereby glutathione are able to protect the compartments at the cellular level (Ruiz and Blumwald, 2002). In addition, the altered redox potential of glutathione could be responsible for the activation of *NPR1*, which is an important transcriptional co-activator and regulates the plant immunity based on SA (Loake and Grant, 2007). When plants attacked by, for example, pathogenic fungi, the *NPR1* genes can induce SAR (Després *et al.*, 2000). The amounts of glutathione measured in both runs are generally higher in the control and VL-infected groups under sufficient sulfur supply compared to the corresponding -S-groups. This difference became apparent notably at 14 dpi. Furthermore, at 14 dpi a slight increase in glutathione levels in both runs was observed in the control +S- and VL-infected +S-groups. This result is consistent with the study by Bloem *et al.* (2004), which infected *B. napus* plants with *Pyrenopeziza brassicae*. It appears that levels of cysteine and glutathione are not or just slightly affected by an infection with *V. longisporum*. Only the different sulfur supply has an effect on the respective contents. It may be possible to observe the effects only at a very early stage of the infection (Kruse *et al.*, 2012), In a study by Zechmann (2017) the lowest glutathione levels were found in most cell compartments of *A. thaliana* at the end of the dark period. This decrease due to lack of daylight could also be observed in poplars, spruces and the leaves of *A. thaliana* (Huseby *et al.*, 2013; Noctor *et al.*, 1997; Schupp and Rennenberg, 1988). This observation supports the suggestion that glutathione does not play the

## Discussion

major role in the defense mechanisms of *B. napus* against *V. longisporum*, as increased resistance is likely to exist at TPI I and TPI II. Perhaps glutathione does not serve as a sulfur donor for the GSLs at these specific TPIs, while the GSLs could be served itself as the sulfur donor, since they are suggested to be a storage form of sulfur (Falk *et al.*, 2007). Another reason why no effect can be seen, could also be due the time point when the plants were harvested, because several studies demonstrated the involvement of the diurnal rhythm in the synthesis of sulfur-containing compounds and also the uptake of sulfur (Hornbacher *et al.* 2019; Rausch and Wachter, 2005; Zhang *et al.*, 2013).

### **4.2 Highway of plant response - influence of fungal infection on nutrient element content of *B. napus***

The concentration of certain elements in host plants may influence their resistance to vascular pathogens (Datnoff *et al.*, 2007). In this work other elements were measured in addition to sulfur, since a part of the plants was exposed to deficient sulfur supply. This allowed to examine the overall health status, the effects of insufficient sulfur levels and possible infection-interactions. Calcium is a crucial regulator of plant growth and development (Hetherington and Brownlee, 2004). Furthermore it is an important second messenger in plant cells and is involved in biotic defense responses of plants (Zhang *et al.*, 2014). Grant *et al.* (2000) found a change in calcium concentration during the ETI. In addition, ROS-calcium interactions may play an important role in the SAR (Dubiella *et al.*, 2013). An increased calcium level in plant tissue correlates with the resistance of cell walls and thus impedes the penetration of fungal pathogens. Calcium can stimulate the cell wall deposition, resulting in greater amounts of non-cellulosic polysaccharide and lignin precipitate (Eklund and Eliasson, 1990). This observation is demonstrated in a study by Conway *et al.* (1994), where apple trees indicated an increase of cell wall material under CaCl<sub>2</sub> supply. Besides to calcium, potassium also plays an important role in plant growth and metabolism, and it is a particularly important mineral nutrient for plants. It helps plants to survive under certain biotic (Amtmann *et al.*, 2008) and abiotic (Cakmak, 2005) stress conditions. In addition, there is iron, which plants may use to increase local oxidative stress and it accordingly plays a crucial role in the defense against pathogens (Aznar *et al.*, 2015). In the first and second run of the experiment the VL-infected groups showed relatively similar calcium and potassium levels regardless of the sulfur input at 7 dpi. The results of the measured iron showed similar values in all groups in the first run, in the second run the iron values in the VL-infected +S-groups were slightly lower compared to the control +S-groups at 7 dpi. At

## Discussion

14 dpi there are barely any differences between the two runs, when comparing the respective groups together. When considering the highest levels within the VL-infected groups, it is not possible to detect any association as to whether the TPI is related to sulfur and/or the highest *V. longisporum* infection rate. However, the interesting observation can be made that the levels of calcium, potassium and iron are barely dependent on the different sulfur fertilization.

### 4.3 Don't mess with *B. napus*: occlusions as a mechanical barrier against the spread of *V. longisporum*

Infections caused by *Verticillium* species normally lead to wilting (Fradin and Thomma, 2006). This symptom is mainly triggered by partial vessel occlusions in the water-conducting system, the xylem, by formation of vascular gels and tyloses (Benhamou, 1995). These physical barriers may delay the movement or further invasion of the fungus (Gold and Robb, 1995). In addition, the deposits may contain antifungal components, e.g. elemental sulfur (Williams *et al.*, 2002). Wilting induced by *V. dahliae* infection is due to the formation of toxins (Palmer *et al.*, 2005) or "V. *dahliae* necrosis and ethylene-inducing proteins" (VdNEPs) (Wang *et al.*, 2004). In addition, so far no formation of toxins has been detected in *V. longisporum* (Aroud, 2013). Since it is expected that the blockages affect the transport of water and nutrients, wilting, stunting, chlorosis and premature senescence are thought to be typical symptoms of water and nutrient limitation per se (Johansson *et al.*, 2006). In the case of the *B. napus* - *V. longisporum* infection system, no wilting phenomena occur, as various studies have demonstrated (Depotter *et al.*, 2016; Eynck *et al.*, 2007; Floerl *et al.*, 2008; Reusche *et al.*, 2012). Also, in this study no signs of wilting in *B. napus* plants infected with *V. longisporum* were observed.

Anatomical studies investigating non-wilting despite the formation of occlusions suggested pathogen-induced reprogramming of host vascular tissue, which is seen as a compensatory response to maintenance of functionality (Baayen, 1986; Talboys, 1958). The process of cellular dedifferentiation followed by differentiation into cells with a different function is called transdifferentiation (Sugimoto *et al.*, 2011). Reusche *et al.* (2012) showed in their study with *A. thaliana* plants infected with *V. longisporum* that bundle sheath cells are transdifferentiated into trachea elements. In addition, it has been shown that the impaired functionality induced by the occlusions is restored and that the formation of de novo xylem results in increased water storage capacity and makes the plants more tolerant to drought. In addition, another study showed that no evidence of *V. longisporum* could be detected in the de novo formed xylem cells. This

## Discussion

result excludes the original idea that the pathogen induced de novo xylem formation promotes fungal accommodation (Reusche *et al.*, 2014). Phenolic compounds formed via the phenylpropanoid synthesis pathway play an important role in cell wall reinforcement, among others (Tuncel and Nergiz, 1993). In particular, the phenolic polymer lignin is an important structural major component of the secondary vascular tissue in higher plants (Humphreys and Chapple, 2002). It is known to play an important role in mechanical support, solute conductivity and resistance to pathogens (Harakava, 2005). Deposition of lignin, lignin-like polymers and/or other wall-bound phenolic materials indicates mechanical damage, injury or microbial infection (Boudet *et al.*, 1995). In addition to cell wall strengthening and increased cell wall rigidity (Wardrop, 1971), the deposition of lignin is believed to reduce the diffusion of enzymes and toxins released from pathogenic fungi to their host plant. In return the water and the nutrients, which release from the plant should no longer be available to the pathogen and lead to starvation.

In a study by Beckman *et al.* (1972) vacuolar phenolics in a reduced state were observed in phenolic-storing cells in various higher plants. The histochemical studies by Eynck *et al.* (2009) indicated that this is also the case for *B. napus*. It is believed that the stored phenolics can be released into *V. longisporum*-infected tissue. The phenolics could there oxidize and polymerize to polyphenols, thereby additionally regulating the cellular redox status in the plant in response to invasion of the pathogen (Chong *et al.*, 1999). The oxidized phenols are also involved in the formation of lignin, which can seal off the infection at the site of penetration. If this type of defense does not achieve the desired effect and the stress factor continues, the values for auxin and ethylene may increase, resulting in a cascade of secondary metabolism. Auxin promotes lateral growth in paravascular contact cells and leads to the formation of vascular occlusions (Beckman, 2000). These structures also express *B. napus* in response to *V. longisporum* infection. In addition to their role in the formation of vascular occlusions, soluble phenolic acids can directly inhibit microbial growth (de Ascensao and Dubery, 2003). However, it was not possible to extract antifungal phenolic acids from the xylem sap of infected *B. napus* plants, regardless of whether they are resistant or susceptible cultivars (Eynck *et al.*, 2009). Therefore, it is more likely that the vascular occlusions are about mechanical barriers (Keen, 1992) in case of *B. napus* plants infected with *V. longisporum* that are intended to limit fungal growth (Eynck *et al.*, 2009). Besides, cell wall-bound phenolic acids probably contribute to the resistance of *B. napus* to *V. longisporum* (Obermeier *et al.*, 2013). In this work the focus was on the formation of occlusions within the xylem of infected *B. napus* plants. Microscopic examination of the hypocotyls of VL-infected plants showed that the occlusions occurred under sufficient

## Discussion

and deficient sulfur supply at varying degrees. This observation in both runs leads to the assumption that the supply of different sulfur levels has no influence on the ability of the plants to form blockages as a mechanical barrier in the xylem. It is supposed that resistant *B. napus* plants are more likely to form occlusions in response to *V. longisporum* infection than susceptible plants. A study by Eynck *et al.* (2009) found that the resistant *B. napus* SEM 05-500 256 featured a higher number of occluded xylem vessels than the susceptible cultivar "Falcon". In addition to considering whether sulfur plays a role in the occurrence of occlusions, a possible relationship should be drawn at the TPIs with *V. longisporum*. The first run of the experiment shows no evidence in this regard and the formation of blockages seems to be unrelated to infection severity, sulfur supply or TPI, moreover, no significant differences were observed. At 14 dpi even more blocked vessels can be seen in VL-infected -S- plants. However, the second run shows a slight tendency, where the VL-infected +S-plants show a higher percentage of plugging at TPI I and TPI II (14 dpi) than the remaining VL-infected plants. At 21 dpi the clogging in the xylem increase in all groups, however, the plants under sufficient sulfur supply had slightly higher rates (**Appendix Table 6.25**). Comparing the severity of the infection with the appearance of the clogged xylem vessels, it is not possible to suggest any conclusions. However, this is not unexpected, as occlusions appear to be just a mechanical barrier preventing further growth into the vessel, whereby the fungus does not die and it is still possible to detect the VL-DNA in the plant. In order to be able to make a cautious statement based on the amount of VL-DNA, where the fungus is located in the plant, the plants would have to be differentiated in, e.g. roots, hypocotyls, stems and leaves, before being analysed.

### **4.4 Time to kill - importance of diurnal rhythmic in the defense against *V. longisporum***

Recent studies have shown that the circadian clock plays a crucial role in the defense of plants against pathogens and pests. Therefore, the disturbance of certain clock genes in plants leads to a reduced resistance to bacteria, oomycetes and/or fungal pathogens (Lu *et al.*, 2017). For example, a circadian dysrhythmia caused by misexpression of *LUX* (evening-phased core clock gene *LUX ARRHYTHMO*) or *CCA1* impairs the resistance of plants against insect (Goodspeed *et al.*, 2012). Temporary control defense mechanisms by the circadian clock reveals itself in the rhythmic changes in defense-related molecules, reflecting the role of the circadian clock in the anticipation of probable attacks by pathogens. Numerous studies have shown that defense signaling molecules, such as SA, JA and ROS oscillate with various peaks

## Discussion

during the day, while pathogens are absent (Goodspeed *et al.*, 2012; Lai *et al.*, 2012; Zheng *et al.*, 2015; Zhou *et al.*, 2015). However, when pathogens are present, the defense responses of plants are initiated, which include an increase in levels of SA and other defense compounds, followed by a reprogramming of defense-related genes. The levels of SA can fluctuate daily in non-infected plants (Goodspeed *et al.*, 2012; Zheng *et al.*, 2015), while in the response to pathogens a timely accumulation of SA can be observed with a high frequency in the local infected region (Hamdoun *et al.*, 2013). Genes that are able to trigger this acute SA accumulation play an important role in plant defense (Lu *et al.*, 2016). However, these clock genes have not yet been identified and it is largely unknown how the circadian clock controls acute defense reactions in the presence of pathogens (Zhang *et al.*, 2019).

Plants that grow under light/dark cycles, which correspond to the endogenous cycling of their internal circadian clock, have a growth and reproduction advantage over plants that are exposed to light/dark cycles that do not match their internal oscillator (Dodd *et al.*, 2005; Green *et al.*, 2002). A synchronization of the circadian rhythm with the external environment also promotes the biotic stress resistance of the plants (Goodspeed *et al.*, 2013). However, plants encounter pathogens at different times of the day, but studies have suggested that *A. thaliana* is more resistant to some of its pathogens in the morning than at night. This hypothesis could be demonstrated in inoculation experiments, where during the day a stronger defense reaction than during the night was observed (Bhardwaj *et al.*, 2011; Griebel and Zeier, 2008). This thesis shows a similar result regarding the susceptibility of *B. napus* to *V. longisporum*. The infection rates appear to be overall higher in the plants inoculated in the evening. Plants have evolved various mechanisms, some of them must be pre-formed and others are induced towards the invasion of pathogens. A form of induced defense is activated by plants when they recognize PAMPs. The PTI can be highly effective against non-adapted pathogens and provides a basic level of defense against even some adapted pathogens (Zipfel, 2008). Another type of induced defense is triggered by R-proteins, which recognize specific secreted pathogen effectors and then activate the ETI. The ETI is faster and more effective than PTI and often leads to hypersensitive cell death at the site of infection (Jones and Dangl, 2006). Salicylic acid has been implicated in signal transduction in PTI and ETI (Tsuda *et al.*, 2008). The innate immunity of plants is partly under the control of the circadian clock based on circadian regulation of defense gene expression (Sauerbrunn and Schlaich, 2004). A study by Bhardwaj *et al.* (2011) demonstrated in *A. thaliana* under free running conditions that there are temporal oscillations in susceptibility to infection with *Pseudomonas syringae*, which are disturbed by overexpression of *CCA1*. Misexpression of several clock genes,

## Discussion

including *CCA1*, impairs resistance to the bacterial pathogen *P. syringae* and/or to the oomycete virus *Hyaloperonospora arabidopsidis* (Shin *et al.*, 2012). Although the *lhy* mutants have a similarly shortened circadian period as the *cca1* mutants, it could not be shown that LHY plays a defensive role against *H. arabidopsidis* (Wang *et al.*, 2011). The question arises whether CCA1 is a dual function protein, affecting both the circadian clock and other non-clock related mechanisms (Oliverio *et al.*, 2007). Overall, it has been shown that genes involved in defense are circadian controlled by CCA1. Thus, plants are able to estimate infection in the morning when, for example, pathogenic fungi spread their spores (Wang *et al.*, 2011) and termed as timed defense. The timed defense includes that plants incorporate external and internal time cues to anticipate likely attacks from invading pathogens at different times of the day, whereby immediate defense reactions are available for rapid use against a variety of pathogens at a particular time of day (Lu *et al.*, 2017). But not only the induced immune responses are circadian regulated, a study by Kerwin *et al.* (2011) showed that genes involved in the biosynthesis of GSLs are also subject to circadian regulation. In addition, there is a connection between the nutrient status and the daily rhythm of plants (Haydon *et al.*, 2015). Furthermore, key genes of the major pathways of primary metabolism, carbon, nitrate, and sulfur assimilation show distinct diurnal and/or circadian rhythmicity (Pilgrim *et al.*, 1993; Kopriva *et al.*, 1999; Zeeman *et al.*, 2006). The formation of SDCs appears to be under a complex control, involving not only a variety of endogenous and exogenous signals, but also regulation at various transcriptional to post-translational levels (Rausch and Wachter, 2005). A number of key genes involved in various metabolic pathways, including sulfur metabolism, have been described as circadian regulated in *A. thaliana* (Harmer, 2009). A study by Rosa *et al.* (1994) showed diurnal fluctuations in the GSL content of field-grown *B. oleraceae* plants, which could be confirmed under controlled conditions (Rosa, 1997). Huseby *et al.* (2013) demonstrated in their study that *Arabidopsis* has a higher accumulation of GSLs during the day than during the night. This is in contrast to the results with *B. oleraceae*, where a significant decrease in GSL levels during the day was observed (Rosa, 1997; Rosa *et al.*, 1994). However, the GSL levels are consistent with the variations in sulfur uptake, APR activity, sulfate reduction rate, and the GSL biosynthesis rate measured in the same plants. The difference compared with *B. oleracea* may be due to the different stages of development of the investigated plants or species-specific variations that may be related to the distinct nature of the main herbivores associated with these species. Diurnal rhythms were described for a variety of secondary compounds involved in interactions between plants and herbivores. Some plants show higher leaf accumulation in the light, while other plants, which are mainly attacked by nocturnal

## Discussion

insects, have higher accumulation rates at night (De Moraes *et al.*, 2001; Kim *et al.*, 2011). The diurnal regulation is often associated with light regulation. In sulfur metabolism APR activity and mRNA levels decreased sharply when plants were grown in continuous darkness and increased rapidly when illuminated again (Kopriva *et al.*, 1999). Huseby *et al.* (2013) showed in their study that other components of the signaling pathway are also light-regulated. With the exception of *ATPS4* and *APK4*, genes encoding the two enzymes required for PAPS biosynthesis (ATPS and APK) were down-regulated, when plants were incubated under prolonged darkness. In plant roots *ATPS4* is the major isoform of ATPS, whereas *APK4* is a minor plastidic form of APK, therefore the lack of light regulation is not surprising (Kopriva *et al.*, 2009). By re-illumination of dark adapted *A. thaliana* plants, the *ATPS* and *APK* genes, including *APK4*, but not *ATPS4*, were induced. The regulation of APR is consistent with the aforementioned regulation and demonstrates a well-coordinated response of the entire signaling pathway to changes in lighting conditions (Huseby *et al.*, 2013). A similar coordination was found by Huseby *et al.* (2013) in the regulation of GSL genes. In addition, it has been shown that the expression of genes involved in the biosynthesis of GSLs is well-coordinated, for example, the expression is suppressed by sulfur deficiency (Hirai *et al.*, 2005) or induced in *apk1 apk2* mutants (Mugford *et al.*, 2009). Mechanisms for the regulation of APR and ATPS differ, APR is transcriptionally regulated, while ATPS is down-regulated post-transcriptionally by sulfur limitation-inducible microRNA (miR395) (Kawashima *et al.*, 2011). Therefore, it is not surprising that the light regulation of APR and ATPS turns out differently. Recently, a study was published investigating an interaction between circadian clock and the sulfur status in *B. napus* (Hornbacher *et al.*, 2019). The study by Hornbacher *et al.* (2019) was able to show the diurnal oscillation of genes involved in the transport and reduction of sulfate. The observed period is comparable to that of CCA1. However, the circadian control could not be clearly determined. Another result of the same study demonstrated that GSLs display ultradian oscillations that were altered by the sulfur supply of the plants. Therefore, it was hypothesized that the concentration of individual GSLs is not regulated circadian, but ultradian.

As already mentioned, glutathione has among others an antioxidant role and can protect the plant from ROS and reactive nitrogen species (RNS). These are produced and accumulated in different concentrations in cells and organelles depending on the environmental conditions and their developmental stages (Foyer and Noctor, 2016; Zechmann, 2014). Abiotic and biotic stresses can lead to changes in glutathione levels and redox states that are designed to protect plants from potential adverse effects of these environmental stresses (Kocsy *et al.*, 2013). In addition, the glutathione content



## Discussion

in the various phases of plant growth and development varies considerably as it is part of a regulatory network that affects and controls plant metabolism and includes hormones, ROS, RNS and other antioxidants (Kocsy *et al.*, 2013). Since the total glutathione content and its redox state are very sensitive to environmental conditions, it is not surprising that the glutathione content shows a diurnal rhythm (Schupp and Rennenberg, 1988). This assumption is supported by Zechmann (2017), which clearly revealed that the subcellular glutathione content in leaves of *A. thaliana* in all cell compartments except the vacuoles followed a diurnal rhythm. It was found that the glutathione content increased strongly after a light exposure between two and three hours of the plants, which supports the current hypothesis that the glutathione synthesis is light-dependent regulated. The rate of synthesis of glutathione and the content in plants depends on the availability of its precursors cysteine, glycine and glutamate. While glutamate exhibits a relatively constant level during the diurnal cycle, it is believed that variations in glycine and cysteine levels regulate the glutathione metabolism in plants (Forde and Lea, 2007). Various studies demonstrated that deficiency of glycine due to lack of photorespiration limits the synthesis of glutathione in *A. thaliana* leaves in the dark, whereby the glutathione synthesis could be fully restored by adding glycine and exposure to daylight (Buwalda *et al.*, 1990; Noctor *et al.*, 1997, 1999). An artificial increase of the cysteine led to an accumulation of glutathione, suggesting that cysteine is the most important limiting factor for the synthesis of glutathione in the plant when exposed to daylight (Király *et al.*, 2012; Zechmann *et al.*, 2007). In addition, sulfur uptake and incorporation into thiols (cysteine and glutathione) was significantly reduced in *A. thaliana* during the night compared to daylight conditions (Huseby *et al.*, 2013). These results suggest that cysteine in addition to glycine, regulates the diurnal levels of glutathione in plants as well. In this regard, cysteine appears to play a key role in the diurnal glutathione metabolism since reversible cysteine modifications of proteins induced by oxidation of cysteine thiols via ROS provide a mechanism for the signaling events that activate downstream stress responses. Because the circadian hormones JA and SA affect the glutathione pools and its redox status, cysteine could establish a link between these clock-regulated hormones and the activation of stress responses by regulating the diurnal glutathione metabolism (Spoel and Loake, 2011; Spoel and van Ooijen, 2014).

To illustrate the major observations from the first and second run of the main experiment, **Figures 4.2** and **4.3** show a summary in connection with the most important findings from various studies. In the first run the content of VL-DNA found in plants was about 54% higher at TPI III/TPI IV than at TPI I/TPI II and in the second run about 60% (based on samples of 3 dpi), which leads to the cautious assumption that

## Discussion

*B. napus* is more susceptible to *V. longisporum* at TPI III and TPI IV. The levels of gluconasturtiin in VL-infected plants compared to the control plants at TPI I/TPI II were between 50-75% higher or between 45-60%, depending on the sulfur supply, at TPI III/TPI IV between 70-78% and between 56-65 % (Fig. 4.2; Fig. 4.3).

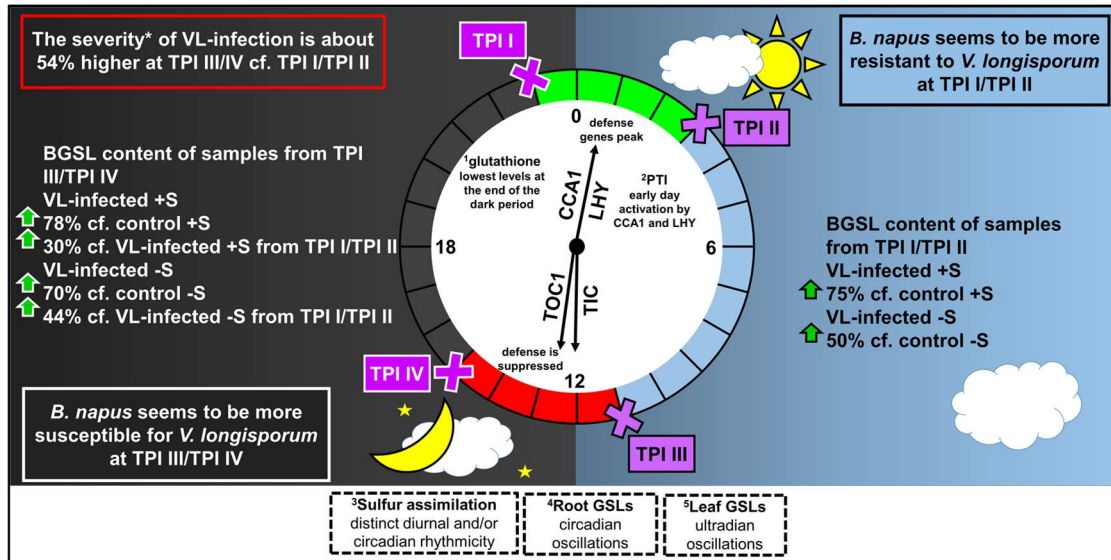


**Figure 4.2: Major observations of the main experiment (first run): increased content of gluconasturtiin in VL-infected plants and a higher susceptibility of *B. napus* at the end of the day against *V. longisporum*.** *B. napus* seems to be more susceptible against *V. longisporum* at TPI III/TPI IV, while the contents of measured VL-DNA were about \*54% higher compared to the contents of TPI I/TPI II; right side: BGS content at 7 dpi of samples from TPI I/TPI II compared with the corresponding control plants; left side: BGS content at 7 dpi of samples from TPI III/TPI IV compared with the corresponding control plants and VL-infected plants from TPI I/TPI II; percentages were estimated from the values of the combined contents of TPI I with TPI II or TPI III and TPI IV, respectively; cf.: comparing; image of circadian clock is adapted from Karapetyan and Dong (2018); <sup>1</sup>Zechmann (2017); <sup>2</sup>Zhang *et al.* (2013); <sup>3</sup>Kopriva *et al.* (1999); <sup>4</sup>Rosa and Rodrigues (1998); <sup>5</sup>Hornbacher *et al.* (2019).

Since the VL-infected plants at TPI III/TPI IV showed even higher levels of gluconasturtiin compared to the other VL-infected plants, it is suspected that this could be due to the stronger infection rate. In addition, **Figure 4.3** shows the comparison of VL-infected plants at TPI I/TPI II compared to the other VL-infected plants with regard to the formation of occlusions in the xylem. The first run did not show a consistent result, probably due to the single plant effect. The formation of the occlusions at TPI I/TPI II is slightly higher than at TPI III/TPI IV. Interestingly, the plants seem to be able to form mechanical barriers in the xylem even if the sulfur deficiency is severe, although not quite as pronounced as with sufficient sulfur supply. Nevertheless, this defense mechanism also appears to be under circadian or diurnal control, at least in parts.

## Discussion

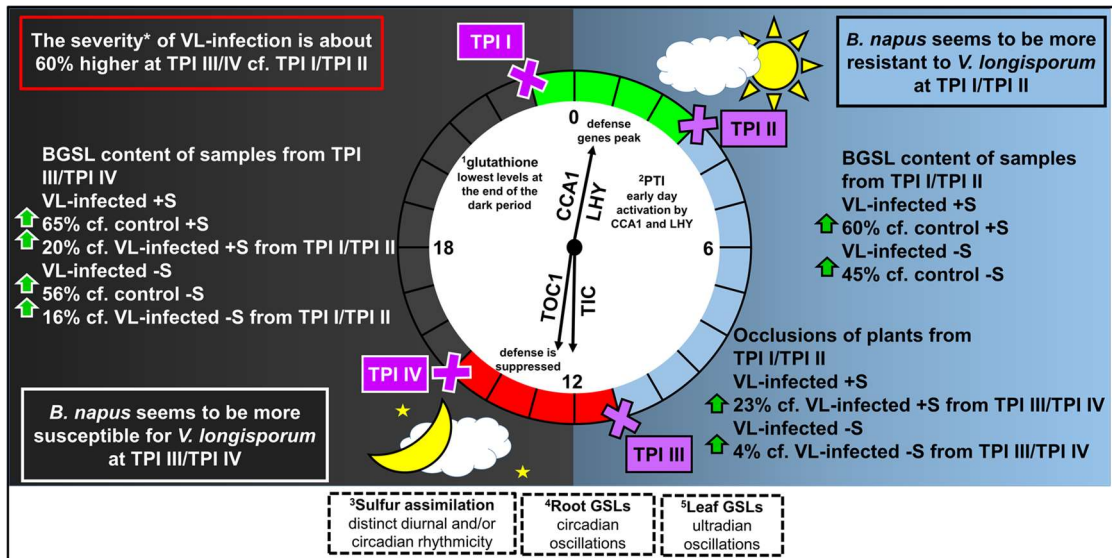


**Figure 4.3: Major observations of the main experiment (second run): occurrence of occlusions in the xylem, increased content of gluconasturtiin in VL-infected plants and a higher susceptibility of *B. napus* against *V. longisporum*. *B. napus* seems to be more susceptible against *V. longisporum* at TPI III/TPI IV, while the contents of measured VL-DNA were about \*60% higher compared to the contents of TPI I/TPI II; right side: BGS content at 7 dpi of samples from TPI I/TPI II compared with the corresponding control plants; occurrence of occlusions at 14 dpi of plants from TPI I/TPI II compared to plants from TPI III/TPI IV; left side: BGS content at 7 dpi of samples from TPI III/TPI IV compared with the corresponding control plants and VL-infected plants from TPI I/TPI II; percentages were estimated from the values of the combined contents of TPI I with TPI II or TPI III and TPI IV, respectively; cf.: comparing; image of circadian clock is adapted from Karapetyan and Dong (2018); <sup>1</sup>Zechmann (2017); <sup>2</sup>Zhang *et al.* (2013); <sup>3</sup>Kopriva *et al.* (1999); <sup>4</sup>Rosa and Rodrigues (1998); <sup>5</sup>Hornbacher *et al.* (2019).**

The circadian and/or diurnal control in plants is complex, regulatory processes are sometimes closely linked, while some seem to be activated at random. Defense mechanisms can be proceeded nonspecific, while others are highly specialized to the particular invader. In addition, a variety of other factors can also have some influence, such as time of day, environmental conditions, general health of the plants and the availability of elemental and mineral nutrients. However, it should be taken into consideration that in this thesis no clock-related genes were examined to establish a direct link between the defense mechanisms of *B. napus* and *V. longisporum*. The observations are based solely on the measurement of various elements and plant metabolites that were carried out in control and VL-infected plants inoculated at different times. Therefore, it can only be suggested with caution that the resistance of *B. napus* plants to *V. longisporum* is higher in the morning than in the evening and accordingly the involved defense mechanisms seem to be regulated in the same manner. Since recent studies about *V. longisporum* interaction have been performed predominantly in *A. thaliana*, although this plant is a non-specific host of the pathogenic

## Discussion

fungi, future investigations should be performed with the preferred host plant *B. napus* due to the possible different defense responses.

### 4.5 Inoculation system with mycelium-spore mixture - creation of ballpark figures?

One challenge was to grow the plants and the fungus that both biological systems were ready for the start of the experiment at the same time. Furthermore, it was difficult to determine the concentration of the mycelium-spore mixture ergo the mixtures had various concentrations in each experiment. This resulted in distinct infection rates of the plants. The critical assumption that the different severity of the infection and the already mentioned problems with the climatic chambers lead to the creation of ballpark figures, is justified. However, this assumption can be invalidated, whereas the severity of the infection was different, the plants showed similar reactions in the investigations, even if the values were partly different. The results do not allow a concrete statement, however, there is evidence to suggest that inoculation at different times causes different responses in the plants, while *B. napus* is more resistant to *V. longisporum* during the day as at night.

### 4.6 Conclusion and outlook

This work is about the effects in *B. napus* infected with *V. longisporum* at different time points and the possible influence of a subsequent fertilization of the plants with sufficient and deficient sulfur supply of the course of the infection. It was necessary to establish an inoculation system that works at these specific TPIs. Since inoculation with spores, which is normally used for inoculation experiments, did not work, a mycelium-spore mixture of *V. longisporum* was used. In preliminary experiments, older *B. napus* plants, which were previously been fertilized with different amounts of sulfur, were inoculated to investigate the possible influence of prior sulfur limitation on the time point of infection. However, these experiments did not work reliably.

#### 4.6.1 What lies beneath? - A critical conclusion

Plants are exposed daily to different abiotic and biotic stress factors. As a result mechanisms have evolved in the plants to protect them against intruders or to make a counterstrike. The pathogenic defense mechanisms are sometimes very complex and build upon each other. Plants have a whole “arsenal of weapons” that they can use against pathogens. For example, they can build up mechanical barriers, produce toxic

## Discussion

metabolites and use their innate immunity. In addition to a sufficient supply of nutrients, the right timing plays a crucial role as well, which decides on success or failure. This work has attempted to show a distinction of different infection times in the *B. napus* - *V. longisporum* system. An additional factor was the fertilization with sufficient and deficient sulfur supply. A number of already mentioned problems and the limitation of the existing plant material do not allow specific statements. Although a large amount of data was produced, these are relatively small for the factors to be investigated, which led to difficulties in the statistical evaluation. Only with regard to the different sulfur supply can the concrete statement be made that it led to significant differences in the plants, which was reflected both in the phenotype and in the measurements. However, even plants in which the infection with *V. longisporum* was successful showed some clear differences to the corresponding control plants. There were differences in the GSL contents, especially in the BGSL gluconasturtiin and in the formation of occlusions in the xylem vessels. A difference in the four TPIs could only be determined in parts. Overall, the work shows interesting results, but they should be viewed with caution. However, the hypotheses, which assumed an influence of the time point on the severity of the infection and an effect of different sulfur supply on the course of the infection, could be demonstrated in parts.

### 4.6.2 Out and look - an outlook

For further investigations in the presented infection system the inoculation system should be refined. One possibility is to grow sufficient amounts of *V. longisporum* shaking culture, aliquot the mycelium-spore mixture and freeze it for future experiments. Regarding to the measurements genes related to the secondary metabolites should be examined. This could also prove a possible involvement of the circadian clock. It would be interesting to subdivide the plants into root, hypocotyl, stems and leaves before the measurements. This would allow statements regarding the location of, for example, VL-DNA, specific GSLs and/or measurable elements. In order to examine the involvement of the different GSLs in the defense mechanisms in more detail, non-infected plants should be harvested at the four TPIs. In the case of, for example gluconasturtiin, this could be used to verify whether there are higher amounts for a certain period of the day. In addition, it would be interesting to test whether a sulfur fertilization at different times of day has an effect on the course of the infection.

The infection system should be performed in different *B. napus* cultivars: a resistant, a susceptible and a variety with an average health. Since cysteine and glutathione may have shown their involvement at very early stages of infection, these measurements

## Discussion

should be taken relative directly after infection (1 and 3 dpi). In order to make the microscopic examination more meaningful, experiments should be carried out in which hypocotyls of at least five plants per harvest time point should be prepared. It would also be important, as already mentioned, that these investigations are performed with the preferred host plant *B. napus*, since this is the vulnerable crop plant. Not only because *A. thaliana* and *B. napus* can respond differently to the infection with *V. longisporum*, but rather the agriculturally important crop *B. napus* needs to be protected.

## 5. References

- Adie, B. A., Pérez-Pérez, J., Pérez-Pérez, M. M., Godoy, M., Sánchez-Serrano, J. J., Schmelz, E. A., & Solano, R. (2007). ABA is an essential signal for plant resistance to pathogens affecting JA biosynthesis and the activation of defenses in *Arabidopsis*. *The Plant Cell*, 19(5), 1665-1681.
- Agerbirk, N., & Olsen, C. E. (2012). Glucosinolate structures in evolution. *Phytochemistry*, 77, 16-45.
- Agerbirk, N., De Vos, M., Kim, J. H., & Jander, G. (2009). Indole glucosinolate breakdown and its biological effects. *Phytochemistry Reviews*, 8(1), 101.
- Agrios, G. N. (2005). Plant diseases caused by fungi. *Plant pathology*, 4.
- Agrios, G. N. (1997). Plant Pathology Academic Press San Diego. *Plant pathology*. 4th ed. Academic Press, San Diego, CA.
- Ahmad, A., Khan, I., Anjum, N. A. M., Diva, I., Abdin, M. Z., & Iqbal, M. (2005). Effect of timing of sulfur fertilizer application on growth and yield of rapeseed. *Journal of plant nutrition*, 28(6), 1049-1059.
- Ahuja, I., Rohloff, J., & Bones, A. M. (2011). Defence mechanisms of Brassicaceae: implications for plant-insect interactions and potential for integrated pest management. In *Sustainable Agriculture Volume 2* (pp. 623-670). Springer, Dordrecht.
- Álvarez, C., Ángeles Bermúdez, M., Romero, L. C., Gotor, C., & García, I. (2012). Cysteine homeostasis plays an essential role in plant immunity. *New Phytologist*, 193(1), 165-177.
- Alvarez, M. E. (2000). Salicylic acid in the machinery of hypersensitive cell death and disease resistance. In *Programmed Cell Death in Higher Plants* (pp. 185-198). Springer, Dordrecht.
- Amtmann, A., Troufflard, S., & Armengaud, P. (2008). The effect of potassium nutrition on pest and disease resistance in plants. *Physiologia plantarum*, 133(4), 682-691.
- Andersson, D., Chakrabarty, R., Bejai, S., Zhang, J., Rask, L., & Meijer, J. (2009). Myrosinases from root and leaves of *Arabidopsis thaliana* have different catalytic properties. *Phytochemistry*, 70(11-12), 1345-1354.
- Arabidopsis* Genome Initiative. (2000). Analysis of the genome sequence of the flowering plant *Arabidopsis thaliana*. *nature*, 408(6814), 796.
- Aroud, H. I. (2013). Chemical interactions between *Verticillium longisporum* and oilseed rape *Brassica napus* (Doctoral dissertation, Niedersächsische Staats- und Universitätsbibliothek Göttingen).

## References

- Atkinson, M. M., Keppler, L. D., Orlandi, E. W., Baker, C. J., & Mischke, C. F. (1990). Involvement of plasma membrane calcium influx in bacterial induction of the K<sup>+</sup>/H<sup>+</sup> and hypersensitive responses in tobacco. *Plant physiology*, 92(1), 215-221.
- Ayers, A. R., Ebel, J., Finelli, F., Berger, N., & Albersheim, P. (1976). Host-pathogen interactions: IX. Quantitative assays of elicitor activity and characterization of the elicitor present in the extracellular medium of cultures of *Phytophthora megasperma* var. *sojae*. *Plant physiology*, 57(5), 751-759.
- Aznar, A., Chen, N. W., Thomine, S., & Dellagi, A. (2015). Immunity to plant pathogens and iron homeostasis. *Plant Science*, 240, 90-97.
- Baayen, R. P. (1986). Regeneration of vascular tissues in relation to *Fusarium* wilt resistance of carnation. *Netherlands Journal of Plant Pathology*, 92(6), 273-285.
- Babadoost, M., Chen, W., Bratsch, A. D., & Eastman, C. E. (2004). *Verticillium longisporum* and *Fusarium solani*: two new species in the complex of internal discoloration of horseradish roots. *Plant Pathology*, 53(5), 669-676.
- Back, M. A., Haydock, P. P. J., & Jenkinson, P. (2002). Disease complexes involving plant parasitic nematodes and soilborne pathogens. *Plant pathology*, 51(6), 683-697.
- Bailey, J. A., O'connell, R. J., Pring, R. J., & Nash, C. (1992). Infection strategies of *Colletotrichum* species. *Infection strategies of Colletotrichum species.*, 88-120.
- Bailey, J. A., Rowell, P. M., & Arnold, G. M. (1980). The temporal relationship between host cell death, phytoalexin accumulation and fungal inhibition during hypersensitive reactions of *Phaseolus vulgaris* to *Colletotrichum lindemuthianum*. *Physiological Plant Pathology*, 17(3), 329-IN15.
- Baker, R. H. A., Sansford, C. E., Jarvis, C. H., Cannon, R. J. C., MacLeod, A., & Walters, K. F. A. (2000). The role of climatic mapping in predicting the potential geographical distribution of non-indigenous pests under current and future climates. *Agriculture, Ecosystems & Environment*, 82(1-3), 57-71.
- Baranyk, P., & Fábry, A. (1999). History of the rapeseed (*Brassica napus* L.) growing and breeding from middle age Europe to Canberra. In *International Rapeseed Congress*.
- Barbara, D. J., & Clewes, E. (2003). Plant pathogenic *Verticillium* species: how many of them are there?. *Molecular Plant Pathology*, 4(4), 297-305.
- Barberon, M., Berthomieu, P., Clairotte, M., Shibagaki, N., Davidian, J. C., & Gosti, F. (2008). Unequal functional redundancy between the two *Arabidopsis thaliana* high-affinity sulphate transporters SULTR1; 1 and SULTR1; 2. *New Phytologist*, 180(3), 608-619.
- Barnett, J. R., Cooper, P., & Bonner, L. J. (1993). The protective layer as an extension of the apoplast. *IAWA Journal*, 14(2), 163-171.



## References

- Beckman, C. H. (1987). The nature of wilt diseases of plants. APS press.
- Beckman, C. H. (2000). Phenolic-storing cells: keys to programmed cell death and periderm formation in wilt disease resistance and in general defence responses in plants?. *Physiological and Molecular Plant Pathology*, 57(3), 101-110.
- Beckman, C. H. (1964). Host responses to vascular infection. *Annual Review of Phytopathology*, 2(1), 231-252.
- Bednarek, P. (2012). Sulfur-containing secondary metabolites from *Arabidopsis thaliana* and other Brassicaceae with function in plant immunity. *ChemBioChem*, 13(13), 1846-1859.
- Bednarek, P., Piślewska-Bednarek, M., Svatoš, A., Schneider, B., Doubský, J., Mansurova, M., ... & Molina, A. (2009). A glucosinolate metabolism pathway in living plant cells mediates broad-spectrum antifungal defense. *Science*, 323(5910), 101-106.
- Benhamou, N. (1995). Immunocytochemistry of plant defense mechanisms induced upon microbial attack. *Microscopy research and technique*, 31(1), 63-78.
- Benning, C. (1998). Biosynthesis and function of the sulfolipid sulfoquinovosyl diacylglycerol. *Annual review of plant biology*, 49(1), 53-75.
- Bent, A. F., & Mackey, D. (2007). Elicitors, effectors, and R genes: the new paradigm and a lifetime supply of questions. *Annu. Rev. Phytopathol.*, 45, 399-436.
- Bergmann, L. (1993). 'Glutathione metabolism in plants'. *Sulfur Nutrition and Assimilation in Higher Plants*, 109–23.
- Berlanger, I., & Powelson, M. L. (2005). *Verticillium* wilt. The plant health instructor. DOI: 10.1094. PHI-I-PHI-I-2000-0801-01.
- Berrocal-Lobo, M., & Molina, A. (2008). *Arabidopsis* defense response against *Fusarium oxysporum*. *Trends in plant science*, 13(3), 145-150.
- Bhardwaj, V., Meier, S., Petersen, L. N., Ingle, R. A., & Roden, L. C. (2011). Defence responses of *Arabidopsis thaliana* to infection by *Pseudomonas syringae* are regulated by the circadian clock. *PLoS one*, 6(10), e26968.
- Bhat, R. G., & Subbarao, K. V. (1999). Host range specificity in *Verticillium dahliae*. *Phytopathology*, 89(12), 1218-1225.
- Birren, B., Fink, G., & Lander, E. (2002). Fungal Genome Initiative: white paper developed by the fungal research community. Cambridge, MA: Whitehead Institute Center for Genome Research.
- Bishop, C. D., & Cooper, R. M. (1983). An ultrastructural study of vascular colonization in three vascular wilt diseases I. Colonization of susceptible cultivars. *Physiological Plant Pathology*, 23(3), 323-343.

## References

- Blake-Kalff, M. M., Harrison, K. R., Hawkesford, M. J., Zhao, F. J., & McGrath, S. P. (1998). Distribution of sulfur within oilseed rape leaves in response to sulfur deficiency during vegetative growth. *Plant physiology*, 118(4), 1337-1344.
- Bloem, E., Haneklaus, S., Salac, I., Wickenhäuser, P., & Schnug, E. (2007). Facts and fiction about sulfur metabolism in relation to plant-pathogen interactions. *Plant Biology*, 9(05), 596-607.
- Bloem, E., Haneklaus, S., & Schnug, E. (2005). Significance of sulfur compounds in the protection of plants against pests and diseases. *Journal of plant nutrition*, 28(5), 763-784.
- Bloem, E., Riemenschneider, A., Volker, J., Papenbrock, J., Schmidt, A., Salac, I., ... & Schnug, E. (2004). Sulphur supply and infection with *Pyrenopeziza brassicae* influence L-cysteine desulphydrase activity in *Brassica napus* L. *Journal of Experimental Botany*, 55(406), 2305-2312.
- Blume, B., Nürnberger, T., Nass, N., & Scheel, D. (2000). Receptor-mediated increase in cytoplasmic free calcium required for activation of pathogen defense in parsley. *The Plant Cell*, 12(8), 1425-1440.
- Boller, T., & Felix, G. (2009). A renaissance of elicitors: perception of microbe-associated molecular patterns and danger signals by pattern-recognition receptors. *Annual review of plant biology*, 60, 379-406.
- Boller, T. (1995). Chemoperception of microbial signals in plant cells. *Annual review of plant biology*, 46(1), 189-214.
- Bomsel, M., & Alfsen, A. (2003). Entry of viruses through the epithelial barrier: pathogenic trickery. *Nature reviews Molecular cell biology*, 4(1), 57.
- Bones, A. M., & Rossiter, J. T. (1996). The myrosinase-glucosinolate system, its organisation and biochemistry. *Physiologia Plantarum*, 97(1), 194-208.
- Bonner, E. R., Cahoon, R. E., Knapke, S. M., & Jez, J. M. (2005). Molecular basis of cysteine biosynthesis in plants structural and functional analysis of o-acetylserine sulfhydrylase from *Arabidopsis thaliana*. *Journal of Biological Chemistry*, 280(46), 38803-38813.
- Booth, E. J., & Walker, K. C. (1992). The effect of site and foliar sulfur on oilseed rape: comparison of sulfur responsive and non-responsive seasons. *Phyton*, 32, 9-13.
- Boudet, A. M., Lapierre, C., & Grima-Pettenati, J. (1995). Tansley review No. 80. Biochemistry and molecular biology of lignification. *New phytologist*, 203-236.
- Bowers, J. H., Nameth, S. T., Riedel, R. M., & Rowe, R. C. (1996). Infection and colonization of potato roots by *Verticillium dahliae* as affected by *Pratylenchus penetrans* and *P. crenatus*. *Phytopathology*, 86(6), 614-621.

## References

- Brown, P. D., Tokuhisa, J. G., Reichelt, M., & Gershenzon, J. (2003). Variation of glucosinolate accumulation among different organs and developmental stages of *Arabidopsis thaliana*. *Phytochemistry*, 62(3), 471-481.
- Buchner, P., Takahashi, H., & Hawkesford, M. J. (2004). Plant sulphate transporters: co-ordination of uptake, intracellular and long-distance transport. *Journal of Experimental Botany*, 55(404), 1765-1773.
- Buckley, P. M., Wyllie, T. D., & DeVay, J. E. (1969). Fine structure of conidia and conidium formation in *Verticillium albo-atrum* and *V. nigrescens*. *Mycologia*, 61(2), 240-250.
- Buwalda, F., Stulen, I., De Kok, L. J., & Kuiper, P. J. C. (1990). Cysteine,  $\gamma$ -glutamyl-cysteine and glutathione contents of spinach leaves as affected by darkness and application of excess sulfur. II. Glutathione accumulation in detached leaves exposed to H<sub>2</sub>S in the absence of light is stimulated by the supply of glycine to the petiole. *Physiologia Plantarum*, 80(2), 196-204.
- Buwalda, F., De Kok, L. J., Stulen, I., & Kuiper, P. J. C. (1988). Cysteine,  $\gamma$ -glutamyl-cysteine and glutathione contents of spinach leaves as affected by darkness and application of excess sulfur. *Physiologia plantarum*, 74(4), 663-668.
- Cakmak, I. (2005). The role of potassium in alleviating detrimental effects of abiotic stresses in plants. *Journal of Plant Nutrition and Soil Science*, 168(4), 521-530.
- Carré, P., & Pouzet, A. (2014). Rapeseed—Tremendous potential for added value generation. *Oilseeds and fats, Crops and Lipids*, 21(1), D102.
- Ceccotti, S. P., Morris, R. J., & Messick, D. L. (1998). A global overview of the sulphur situation: industry's background, market trends, and commercial aspects of sulphur fertilizers. In *Sulphur in agroecosystems* (pp. 175-202). Springer, Dordrecht.
- Celenza, J. L., Quiel, J. A., Smolen, G. A., Merrikh, H., Silvestro, A. R., Normanly, J., & Bender, J. (2005). The *Arabidopsis* ATR1 Myb transcription factor controls indolic glucosinolate homeostasis. *Plant physiology*, 137(1), 253-262.
- Chandra-Shekara, A. C., Gupte, M., Navarre, D., Raina, S., Raina, R., Klessig, D., & Kachroo, P. (2006). Light-dependent hypersensitive response and resistance signaling against Turnip Crinkle Virus in *Arabidopsis*. *The Plant Journal*, 45(3), 320-334.
- Charlton, K. M., Corner, A. H., Davey, K., Kramer, J. K., Mahadevan, S., & Sauer, F. D. (1975). Cardiac lesions in rats fed rapeseed oils. *Canadian Journal of Comparative Medicine*, 39(3), 261.
- Chen, B. Y., Heneen, W. K., & Simonsen, V. (1989). Comparative and genetic studies of isozymes in resynthesized and cultivated *Brassica napus* L., *B. campestris* L. and *B. alboglabra* Bailey. *Theoretical and applied genetics*, 77(5), 673-679.

## References

- Chen, S., & Andreasson, E. (2001). Update on glucosinolate metabolism and transport. *Plant physiology and biochemistry*, 39(9), 743-758.
- Cheng, W., Zhang, L., Jiao, C., Su, M., Yang, T., Zhou, L., ... & Wang, C. (2013). Hydrogen sulfide alleviates hypoxia-induced root tip death in *Pisum sativum*. *Plant physiology and biochemistry*, 70, 278-286.
- Chew, F. S. (1988). Biological Effects of Glucosinolates. *ACS Publications*.
- Chisholm, S. T., Coaker, G., Day, B., & Staskawicz, B. J. (2006). Host-microbe interactions: shaping the evolution of the plant immune response. *Cell*, 124(4), 803-814.
- Choat, B., Ball, M., Luly, J., & Holtum, J. (2003). Pit membrane porosity and water stress-induced cavitation in four co-existing dry rainforest tree species. *Plant Physiology*, 131(1), 41-48.
- Choat, B., Jansen, S., Zwieniecki, M. A., Smets, E., & Holbrook, N. M. (2004). Changes in pit membrane porosity due to deflection and stretching: the role of vestured pits. *Journal of experimental botany*, 55(402), 1569-1575.
- Chong, J., Baltz, R., Fritig, B., & Saindrenan, P. (1999). An early salicylic acid-, pathogen- and elicitor-inducible tobacco glucosyltransferase: role in compartmentalization of phenolics and H<sub>2</sub>O<sub>2</sub> metabolism. *FEBS letters*, 458(2), 204-208.
- Clarkson, D. T., Smith, F. W., & Berg, P. J. V. (1983). Regulation of sulphate transport in a tropical legume, *Macroptilium atropurpureum*, cv. *Siratro*. *Journal of Experimental Botany*, 34(11), 1463-1483.
- Clay, N. K., Adio, A. M., Denoux, C., Jander, G., & Ausubel, F. M. (2009). Glucosinolate metabolites required for an *Arabidopsis* innate immune response. *Science*, 323(5910), 95-101.
- Clossais-Besnard, N., & Larher, F. (1991). Physiological role of glucosinolates in *Brassica napus*. Concentration and distribution pattern of glucosinolates among plant organs during a complete life cycle. *Journal of the Science of Food and Agriculture*, 56(1), 25-38.
- Collins, A., Okoli, C. A. N., Morton, A., Parry, D., Edwards, S. G., & Barbara, D. J. (2003). Isolates of *Verticillium dahliae* pathogenic to crucifers are of at least three distinct molecular types. *Phytopathology*, 93(3), 364-376.
- Consonni, C., Bednarek, P., Humphry, M., Francocci, F., Ferrari, S., Harzen, A., ... & Panstruga, R. (2010). Tryptophan-derived metabolites are required for antifungal defense in the *Arabidopsis mlo2* mutant. *Plant physiology*, 152(3), 1544-1561.
- Conway, W. S., Sams, C. E., & Kelman, A. (1994). Enhancing the natural resistance of plant tissues to postharvest diseases through calcium applications. *HortScience*, 29(7), 751-754.

## References

- Cooper, R. M., Resende, M. L., Flood, J., Rowan, M. G., Beale, M. H., & Potter, U. (1996). Detection and cellular localization of elemental sulphur in disease-resistant genotypes of *Theobroma cacao*. *Nature*, 379(6561), 159.
- Coulthart, M., & Denford, K. E. (1982). Isozyme studies in *Brassica*. I. Electrophoretic techniques for leaf enzymes and comparison of *B. napus*, *B. campestris* and *B. oleracea* using phosphoglucomutase. *Canadian Journal of Plant Science*, 62(3), 621-630.
- Covington, M. F., Maloof, J. N., Straume, M., Kay, S. A., & Harmer, S. L. (2008). Global transcriptome analysis reveals circadian regulation of key pathways in plant growth and development. *Genome biology*, 9(8), R130.
- Craven, K. D., Blankenship, J. D., Leuchtmann, A., Hignight, K., & Schardl, C. L. (2001). Hybrid fungal endophytes symbiotic with the grass *Lolium pratense*. *Sydowia*, 53(1), 44-73.
- Cuomo, C. A., Güldener, U., Xu, J. R., Trail, F., Turgeon, B. G., Di Pietro, A., ... & Adam, G. (2007). The *Fusarium graminearum* genome reveals a link between localized polymorphism and pathogen specialization. *Science*, 317(5843), 1400-1402.
- Daebeler, F., Amelung, D., & Zeise, K. (1988). *Verticillium* wilt in winter rape—Occurrence and importance. *Nachrichtenblatt fuer den Pflanzenschutz in der DDR (German DR)*.
- Dämmgen, U., & Grünhage, L. (1998). Response of a grassland ecosystem to air pollutants. V. A toxicological model for the assessment of dose–response relationships for air pollutants and ecosystems. *Environmental Pollution*, 101(3), 375-380.
- Dangl, J. L., & Jones, J. D. (2001). Plant pathogens and integrated defence responses to infection. *nature*, 411(6839), 826.
- Datnoff, L. E., Elmer, W. H., & Huber, D. M. (2007). Mineral nutrition and plant disease. *American Phytopathological Society (APS Press)*.
- de Ascensao, A. R., & Dubery, I. A. (2003). Soluble and wall-bound phenolics and phenolic polymers in *Musa acuminata* roots exposed to elicitors from *Fusarium oxysporum* f. sp. *cubense*. *Phytochemistry*, 63(6), 679-686.
- Dean, R. A., Talbot, N. J., Ebbole, D. J., Farman, M. L., Mitchell, T. K., Orbach, M. J., ... & Read, N. D. (2005). The genome sequence of the rice blast fungus *Magnaporthe grisea*. *Nature*, 434(7036), 980.
- Debode, J., Van Poucke, K., França, S. C., Maes, M., Höfte, M., & Heungens, K. (2011). Detection of multiple *Verticillium* species in soil using density flotation and real-time polymerase chain reaction. *Plant disease*, 95(12), 1571-1580.
- De Kok, L. J., Rennenberg, H., & Kuiper, P. J. C. (1991). The internal resistance in spinach leaves to atmospheric H<sub>2</sub>S deposition is determined by metabolic processes [H<sub>2</sub>S fixation, H<sub>2</sub>S pollution, sulfur metabolism]. *Plant Physiology and Biochemistry (France)*.

## References

- De Kok, L. J. (1990). Sulfur metabolism in plants exposed to atmospheric sulfur. *higher plants*, 111.
- Delledonne, M., Xia, Y., Dixon, R. A., & Lamb, C. (1998). Nitric oxide functions as a signal in plant disease resistance. *Nature*, 394(6693), 585.
- De Moraes, C. M., Mescher, M. C., & Tumlinson, J. H. (2001). Caterpillar-induced nocturnal plant volatiles repel conspecific females. *Nature*, 410(6828), 577.
- Depotter, J. R., Deketelaere, S., Inderbitzin, P., Tiedemann, A. V., Höfte, M., Subbarao, K. V., ... & Thomma, B. P. (2016). *Verticillium longisporum*, the invisible threat to oilseed rape and other brassicaceous plant hosts. *Molecular plant pathology*, 17(7), 1004-1016.
- Després, C., DeLong, C., Glaze, S., Liu, E., & Fobert, P. R. (2000). The *Arabidopsis* NPR1/NIM1 protein enhances the DNA binding activity of a subgroup of the TGA family of bZIP transcription factors. *The Plant Cell*, 12(2), 279-290.
- Dixelius, C., Happstadius, I., & Berg, G. (2005). *Verticillium* wilt on Brassica oil crops—a Swedish perspective. *J Swed Seed Assoc*, 115, 36-48.
- Dixon, D. P., & Edwards, R. (2010). Glutathione transferases. *The Arabidopsis Book/American Society of Plant Biologists*, 8.
- Dodd, A. N., Kudla, J., & Sanders, D. (2010). The language of calcium signaling. *Annual review of plant biology*, 61, 593-620.
- Dodd, A. N., Salathia, N., Hall, A., Kévei, E., Tóth, R., Nagy, F., ... & Webb, A. A. (2005). Plant circadian clocks increase photosynthesis, growth, survival, and competitive advantage. *Science*, 309(5734), 630-633.
- Doherty, C. J., & Kay, S. A. (2010). Circadian control of global gene expression patterns. *Annual review of genetics*, 44, 419-444.
- Dong, X. (2004). NPR1, all things considered. *Current opinion in plant biology*, 7(5), 547-552.
- Dordas, C. (2008). Role of nutrients in controlling plant diseases in sustainable agriculture. A review. *Agronomy for sustainable development*, 28(1), 33-46.
- Dow, M., Newman, M. A., & Von Roepenack, E. (2000). The induction and modulation of plant defense responses by bacterial lipopolysaccharides. *Annual review of phytopathology*, 38(1), 241-261.
- Downey, R. K., & Rimmer, S. R. (1993). Agronomic improvement in oil seed. *Brassicas Advances in Agronomy*, 50, 1-66.
- Dubiella, U., Seybold, H., Durian, G., Komander, E., Lassig, R., Witte, C. P., ... & Romeis, T. (2013). Calcium-dependent protein kinase/NADPH oxidase activation circuit is required for rapid defense signal propagation. *Proceedings of the National Academy of Sciences*, 110(21), 8744-8749.

## References

- Dunker, S., Keunecke, H., Steinbach, P., & Von Tiedemann, A. (2008). Impact of *Verticillium longisporum* on yield and morphology of winter oilseed rape (*Brassica napus*) in relation to systemic spread in the plant. *Journal of Phytopathology*, 156(11-12), 698-707.
- Dunlap, J. C., Loros, J. J., & DeCoursey, P. J. (2004). *Chronobiology: Biological Timekeeping*. Sinauer Associates, Inc., Sunderland, MA.
- Eastburn, D. M., & Chang, R. J. (1994). *Verticillium dahliae*: a causal agent of root discoloration of horseradish in Illinois. *Plant disease*, 78(5), 496-498.
- Edwards, R., Dixon, D. P., & Walbot, V. (2000). Plant glutathione S-transferases: enzymes with multiple functions in sickness and in health. *Trends in plant science*, 5(5), 193-198.
- Eklund, L., & Eliasson, L. (1990). Effects of calcium ion concentration on cell wall synthesis. *Journal of Experimental Botany* 41(7):863–67.
- Elgersma, D. M. (1973). Tylose formation in elms after inoculation with *Ceratocystis ulmi*, a possible resistance mechanism. *Netherlands Journal of Plant Pathology*, 79(5), 218-220.
- Endara, M. J., & Coley, P. D. (2011). The resource availability hypothesis revisited: a meta-analysis. *Functional Ecology*, 25(2), 389-398.
- Erbs, G., Silipo, A., Aslam, S., De Castro, C., Liparoti, V., Flagiello, A., ... & Newman, M. A. (2008). Peptidoglycan and muropeptides from pathogens *Agrobacterium* and *Xanthomonas* elicit plant innate immunity: structure and activity. *Chemistry & biology*, 15(5), 438-448.
- Eriksen, J., Murphy, M. D., & Schnug, E. (1998). The soil sulphur cycle. In *Sulphur in agroecosystems* (pp. 39-73). Springer, Dordrecht.
- Ernst, W. H. (1990). Ecological aspects of sulfur metabolism. *Sulfur Nutrition and Sulfur Assimilation in Higher Plants*, SPB Academic Publishing, The Hague, 131-144.
- Etterson, J. R., & Shaw, R. G. (2001). Constraint to adaptive evolution in response to global warming. *Science* 294(5540):151–54.
- Eynck, C., Koopmann, B., Karlovsky, P., & von Tiedemann, A. (2009). Internal resistance in winter oilseed rape inhibits systemic spread of the vascular pathogen *Verticillium longisporum*. *Phytopathology*, 99(7), 802-811.
- Eynck, C., Koopmann, B., Grunewaldt-Stoecker, G., Karlovsky, P., & von Tiedemann, A. (2007). Differential interactions of *Verticillium longisporum* and *V. dahliae* with *Brassica napus* detected with molecular and histological techniques. *European Journal of Plant Pathology* 118(3):259–74.
- Fahey, J. W., Zalcmann, A. T., & Talalay, P. (2001). The chemical diversity and distribution of glucosinolates and isothiocyanates among plants. *Phytochemistry*, 56(1), 5-51.

## References

- Fahleson, J., Hu, Q., & Dixelius, C. (2004). Phylogenetic analysis of *Verticillium* species based on nuclear and mitochondrial sequences. *Archives of microbiology*, 181(6), 435-442.
- Falk, K. L., Tokuhisa, J. G., & Gershenzon, J. (2007). The effect of sulfur nutrition on plant glucosinolate content: physiology and molecular mechanisms. *Plant Biology*, 9(05), 573-581.
- Feder, N. E. D., & O'brien, T. P. (1968). Plant microtechnique: some principles and new methods. *American journal of botany*, 55(1), 123-142.
- Felix, G., Duran, J. D., Volko, S., & Boller, T. (1999). Plants have a sensitive perception system for the most conserved domain of bacterial flagellin. *The Plant Journal*, 18(3), 265-276.
- Felix, G., Regenass, M., & Boller, T. (1993). Specific perception of subnanomolar concentrations of chitin fragments by tomato cells: induction of extracellular alkalinization, changes in protein phosphorylation, and establishment of a refractory state. *The Plant Journal*, 4(2), 307-316.
- Fenwick, G. R., Heaney, R. K., Mullin, W. J., & VanEtten, C. H. (1983). Glucosinolates and their breakdown products in food and food plants. *CRC Critical Reviews in Food Science and Nutrition*, 18(2), 123-201.
- Fisher, M. C., Henk, D. A., Briggs, C. J., Brownstein, J. S., Madoff, L. C., McCraw, S. L., & Gurr, S. J. (2012). Emerging fungal threats to animal, plant and ecosystem health. *Nature*, 484(7393), 186.
- Floerl, S., Druebert, C., Majcherczyk, A., Karlovsky, P., Kües, U., & Polle, A. (2008). Defence reactions in the apoplastic proteome of oilseed rape (*Brassica napus* var. *napus*) attenuate *Verticillium longisporum* growth but not disease symptoms. *BMC Plant Biology*, 8(1), 129.
- Flor, H. H. (1971). Current status of the gene-for-gene concept. *Annual review of phytopathology*, 9(1), 275-296.
- Forde, B. G., & Lea, P. J. (2007). Glutamate in plants: metabolism, regulation, and signalling. *Journal of experimental botany*, 58(9), 2339-2358.
- Forsyth, W. (1810). *A Treatise on the Culture and Management of Fruit-Trees*.
- Foster, R. C. (1967). Fine structure of tyloses in three species of the Myrtaceae. *Australian journal of botany*, 15(1), 25-34.
- Foyer, C. H., & Noctor, G. (2016). Stress-triggered redox signalling: what's in pROSpecT?. *Plant, cell & environment*, 39(5), 951-964.



## References

- Foyer, C. H., & Noctor, G. (2009). Redox regulation in photosynthetic organisms: signaling, acclimation, and practical implications. *Antioxidants & redox signaling*, 11(4), 861-905.
- Foyer, C. H., & Noctor, G. (2005). Redox homeostasis and antioxidant signaling: a metabolic interface between stress perception and physiological responses. *The Plant Cell*, 17(7), 1866-1875.
- Foyer, C. H., & Noctor, G. (2001). The molecular biology and metabolism of glutathione. In Significance of glutathione to plant adaptation to the environment (pp. 27-56). *Springer*, Dordrecht.
- Foyer, C. H., & Halliwell, B. (1976). The presence of glutathione and glutathione reductase in chloroplasts: a proposed role in ascorbic acid metabolism. *Planta*, 133(1), 21-25.
- Fradin, E. F., & Thomma, B. P. (2006). Physiology and molecular aspects of *Verticillium* wilt diseases caused by *V. dahliae* and *V. albo-atrum*. *Molecular plant pathology*, 7(2), 71-86.
- Frauen, M., & Paulmann, W. (1999). 'Breeding of hybrid varieties of winter oilseed rape based on the MSL-system'. Pp. 26–29 in *Proceedings of the 10th International Rapeseed Congress*.
- Frerigmann, H., & Gigolashvili, T. (2014). MYB34, MYB51, and MYB122 distinctly regulate indolic glucosinolate biosynthesis in *Arabidopsis thaliana*. *Molecular Plant*, 7(5), 814-828.
- Fry, W. E., & Goodwin, S. B. (1997). Resurgence of the Irish potato famine fungus. *Bioscience*, 47(6), 363-371.
- Fukuda, H. (1997). Programmed cell death during vascular system formation. *Cell death and differentiation*, 4(8), 684.
- Fukushima, A., Kusano, M., Nakamichi, N., Kobayashi, M., Hayashi, N., Sakakibara, H., ... & Saito, K. (2009). Impact of clock-associated *Arabidopsis* pseudo-response regulators in metabolic coordination. *Proceedings of the National Academy of Sciences*, 106(17), 7251-7256.
- Galletti, S., Barillari, J., Iori, R., & Venturi, G. (2006). Glucobrassicin enhancement in woad (*Isatis tinctoria*) leaves by chemical and physical treatments. *Journal of the Science of Food and Agriculture*, 86(12), 1833-1838.
- Garber, R. H. (1966). Penetration and development of *Verticillium albo-atrum* in the cotton plant. *Phytopathology*, 56, 1121-1126.
- Gerlach, D. (1977). Botanische Mikrotechnik Eine Einführung Georg Thieme Verlag, Stuttgart, Germany.

## References

- Geu-Flores, F., Møldrup, M. E., Böttcher, C., Olsen, C. E., Scheel, D., & Halkier, B. A. (2011). Cytosolic  $\gamma$ -glutamyl peptidases process glutathione conjugates in the biosynthesis of glucosinolates and camalexin in *Arabidopsis*. *The Plant Cell*, 23(6), 2456-2469.
- Giamoustaris, A., & Mithen, R. (1995). The effect of modifying the glucosinolate content of leaves of oilseed rape (*Brassica napus* ssp. *oleifera*) on its interaction with specialist and generalist pests. *Annals of Applied Biology*, 126(2), 347-363.
- Gigolashvili, T., Berger, B., Mock, H. P., Müller, C., Weisshaar, B., & Flügge, U. I. (2007). The transcription factor HIG1/MYB51 regulates indolic glucosinolate biosynthesis in *Arabidopsis thaliana*. *The Plant Journal*, 50(5), 886-901.
- Gilroy, S., Suzuki, N., Miller, G., Choi, W. G., Toyota, M., Devireddy, A. R., & Mittler, R. (2014). A tidal wave of signals: calcium and ROS at the forefront of rapid systemic signaling. *Trends in plant science*, 19(10), 623-630.
- Glazebrook, J. (2005). Contrasting mechanisms of defense against biotrophic and necrotrophic pathogens. *Annu. Rev. Phytopathol.*, 43, 205-227.
- Godzik, S., & Krupa, S. V. (1982). Effects of sulphur dioxide on the growth and yield of agricultural and horticultural crops. *Proceedings-Easter School in Agricultural Science, University of Nottingham*.
- Gold, J., & Robb, J. (1995). The role of the coating response in *Craigella tomatoes* infected with *Verticillium dahliae*, races 1 and 2. *Physiological and Molecular Plant Pathology*, 47(3), 141-157.
- Gómez-Gómez, L., & Boller, T. (2000). FLS2: an LRR receptor-like kinase involved in the perception of the bacterial elicitor flagellin in *Arabidopsis*. *Molecular cell*, 5(6), 1003-1011.
- Gonthier, P., Nicolotti, G., Linzer, R., Guglielmo, F., & Garbelotto, M. (2007). Invasion of European pine stands by a North American forest pathogen and its hybridization with a native interfertile taxon. *Molecular Ecology*, 16(7), 1389-1400.
- Goodspeed, D., Chehab, E. W., Covington, M. F., & Braam, J. (2013). Circadian control of jasmonates and salicylates: The clock role in plant defense. *Plant signaling & behavior*, 8(2), e23123.
- Goodspeed, D., Chehab, E. W., Min-Venditti, A., Braam, J., & Covington, M. F. (2012). *Arabidopsis* synchronizes jasmonate-mediated defense with insect circadian behavior. *Proceedings of the National Academy of Sciences*, 109(12), 4674-4677.
- Gordee, R. S., & Porter, C. L. (1961). Structure, germination, and physiology of microsclerotia of *Verticillium albo-atrum*. *Mycologia*, 53(2), 171-182.

## References

- Grant, M., Brown, I., Adams, S., Knight, M., Ainslie, A., & Mansfield, J. (2000). The RPM1 plant disease resistance gene facilitates a rapid and sustained increase in cytosolic calcium that is necessary for the oxidative burst and hypersensitive cell death. *The Plant Journal*, 23(4), 441-450.
- Gray, P. (1995). The Irish Famine (p. 179). London: *Thames and Hudson*.
- Green, R. M., Tingay, S., Wang, Z. Y., & Tobin, E. M. (2002). Circadian rhythms confer a higher level of fitness to *Arabidopsis* plants. *Plant physiology*, 129(2), 576-584.
- Griebel, T., & Zeier, J. (2008). Light regulation and daytime dependency of inducible plant defenses in *Arabidopsis*: phytochrome signaling controls systemic acquired resistance rather than local defense. *Plant physiology*, 147(2), 790-801.
- Grimault, V., G elie, B., Lemattre, M., Prior, P., & Schmit, J. (1994). Comparative histology of resistant and susceptible tomato cultivars infected by *Pseudomonas solanacearum*. *Physiological and molecular plant pathology*, 44(2), 105-123.
- Groves, J. W., & Drayton, F. L. (1939). The perfect stage of *Botrytis cinerea*. *Mycologia*, 31(4), 485-489.
- G nzelmann, H., & Paul, V. H. (1990). Zum Auftreten und zur Bedeutung der *Verticillium*-Welke an Raps in der Bundesrepublik Deutschland in 1989. *Raps*, 8(1), 23-25.
- Gust, A. A., Biswas, R., Lenz, H. D., Rauhut, T., Ranf, S., Kemmerling, B., ... & N rnberger, T. (2007). Bacteria-derived peptidoglycans constitute pathogen-associated molecular patterns triggering innate immunity in *Arabidopsis*. *Journal of Biological Chemistry*, 282(44), 32338-32348.
- H ffner, E., & Diederichsen, E. (2016). Belowground defence strategies against *Verticillium* Pathogens. In *Belowground Defence Strategies in Plants* (pp. 119-150). Springer, Cham.
- Halberg, F. (1963). Circadian (about Twenty-four-hour) *Rhythms in Experimental Medicine* [Abridged].
- Halkier, B. A., & Gershenzon, J. (2006). Biology and biochemistry of glucosinolates. *Annu. Rev. Plant Biol.*, 57, 303-333.
- Halkier, B. A., & Du, L. (1997). The biosynthesis of glucosinolates. *Trends in plant science*, 2(11), 425-431.
- Hall, A. E., Fiebig, A., & Preuss, D. (2002). Beyond the *Arabidopsis* genome: opportunities for comparative genomics. *Plant Physiology*, 129(4), 1439-1447.
- Hall, R. (1992). Epidemiology of blackleg of oilseed rape. *Canadian Journal of Plant Pathology*, 14(1), 46-55.

## References

- Hamdoun, S., Liu, Z., Gill, M., Yao, N., & Lu, H. (2013). Dynamics of defense responses and cell fate change during *Arabidopsis-Pseudomonas syringae* interactions. *PLoS One*, 8(12), e83219.
- Hammerschmidt, R. (1999). Phytoalexins: what have we learned after 60 years?. *Annual review of phytopathology*, 37(1), 285-306.
- Han, Y., Mhamdi, A., Chaouch, S., & Noctor, G. (2013). Regulation of basal and oxidative stress-triggered jasmonic acid-related gene expression by glutathione. *Plant, Cell & Environment*, 36(6), 1135-1146.
- Harakava, R. (2005). Genes encoding enzymes of the lignin biosynthesis pathway in Eucalyptus. *Genetics and Molecular Biology*, 28(3), 601-607.
- Harling, R., & Taylor, G. S. (1985). A light microscope study of resistant and susceptible carnations infected with *Fusarium oxysporum* f. sp. *dianthi*. *Canadian Journal of Botany*, 63(3), 638-646.
- Harmer, S. L. (2009). The circadian system in higher plants. *Annual review of plant biology*, 60, 357-377.
- Hawkesford, M. J. (2007). Sulfur and plant ecology: a central role of sulfate transporters in responses to sulfur availability. In *Sulfur in Plants An Ecological Perspective* (pp. 1-15). Springer, Dordrecht.
- Hawkesford, M. J., & De Kok, L. J. (2006). Managing sulphur metabolism in plants. *Plant, Cell & Environment*, 29(3), 382-395.
- Haydon, M. J., Román, Á., & Arshad, W. (2015). Nutrient homeostasis within the plant circadian network. *Frontiers in plant science*, 6, 299.
- Heale, J. B. (2000). Diversification and speciation in *Verticillium*-an overview. *Advances in Verticillium research and disease management*, 1-14.
- Heale, J. B., & Karapapa, V. K. (1999). The *Verticillium* threat to Canada's major oilseed crop: Canola. *Canadian Journal of Plant Pathology*, 21(1), 1-7.
- Heath, M. C. (2000). Hypersensitive response-related death. In *Programmed cell death in higher plants* (pp. 77-90). Springer, Dordrecht.
- Hegarty, M. J., & Hiscock, S. J. (2005). Hybrid speciation in plants: new insights from molecular studies. *New Phytologist*, 165(2), 411-423.
- Heintzen, C., Nater, M., Apel, K., & Staiger, D. (1997). AtGRP7, a nuclear RNA-binding protein as a component of a circadian-regulated negative feedback loop in *Arabidopsis thaliana*. *Proceedings of the National Academy of Sciences*, 94(16), 8515-8520.
- Hejatko, J., Blilou, I., Brewer, P. B., Friml, J., Scheres, B., & Benkova, E. (2006). In situ hybridization technique for mRNA detection in whole mount *Arabidopsis* samples. *Nature protocols*, 1(4), 1939.

## References

- Hell, R., Jost, R., Berkowitz, O., & Wirtz, M. (2002). Molecular and biochemical analysis of the enzymes of cysteine biosynthesis in the plant *Arabidopsis thaliana*. *Amino acids*, 22(3), 245-257.
- Hell, R. (1997). Molecular physiology of plant sulfur metabolism. *Planta*, 202(2), 138-148.
- Hemm, M. R., Ruegger, M. O., & Chapple, C. (2003). The *Arabidopsis ref2* mutant is defective in the gene encoding CYP83A1 and shows both phenylpropanoid and glucosinolate phenotypes. *The Plant Cell*, 15(1), 179-194.
- Hetherington, A. M., & Brownlee, C. (2004). The generation of Ca<sup>2+</sup> signals in plants. *Annu. Rev. Plant Biol.*, 55, 401-427.
- Hilpert, B., Bohlmann, H., Den Camp, R. O., Przybyla, D., Miersch, O., Buchala, A., & Apel, K. (2001). Isolation and characterization of signal transduction mutants of *Arabidopsis thaliana* that constitutively activate the octadecanoid pathway and form necrotic microlesions. *The Plant Journal*, 26(4), 435-446.
- Hirai, M. Y., Klein, M., Fujikawa, Y., Yano, M., Goodenowe, D. B., Yamazaki, Y., ... & Sakurai, N. (2005). Elucidation of gene-to-gene and metabolite-to-gene networks in *Arabidopsis* by integration of metabolomics and transcriptomics. *Journal of Biological Chemistry*, 280(27), 25590-25595.
- Hiruma, K., Onozawa-Komori, M., Takahashi, F., Asakura, M., Bednarek, P., Okuno, T., ... & Takano, Y. (2010). Entry mode-dependent function of an indole glucosinolate pathway in *Arabidopsis* for nonhost resistance against anthracnose pathogens. *The Plant Cell*, 22(7), 2429-2443.
- Hopkins, R. J., van Dam, N. M., & van Loon, J. J. (2009). Role of glucosinolates in insect-plant relationships and multitrophic interactions. *Annual review of entomology*, 54, 57-83.
- Horiuchi, S., & Hori, M. (1980). A simple greenhouse technique for obtaining high levels of clubroot incidence. *Bulletin of the Chugoku National Agricultural Experiment Station*, E, (17), 33-55.
- Hornbacher, J., Rumlow, A., Pallmann, P., Turcios, A. E., Riemenschneider, A., & Papenbrock, J. (2019). The levels of sulfur-containing metabolites in *Brassica napus* are not influenced by the circadian clock but diurnally. *Journal of Plant Biology*, 62(5), 359-373.
- Hückelhoven, R. (2007). Cell wall-associated mechanisms of disease resistance and susceptibility. *Annu. Rev. Phytopathol.*, 45, 101-127.
- Hull, A. K., Vij, R., & Celenza, J. L. (2000). *Arabidopsis* cytochrome P450s that catalyze the first step of tryptophan-dependent indole-3-acetic acid biosynthesis. *Proceedings of the National Academy of Sciences*, 97(5), 2379-2384.

## References

- Humphreys, J. M., & Chapple, C. (2002). Rewriting the lignin roadmap. *Current opinion in plant biology*, 5(3), 224-229.
- Huseby, S., Koprivova, A., Lee, B. R., Saha, S., Mithen, R., Wold, A. B., ... & Kopriva, S. (2013). Diurnal and light regulation of sulphur assimilation and glucosinolate biosynthesis in *Arabidopsis*. *Journal of experimental botany*, 64(4), 1039-1048.
- Husebye, H., Chadchawan, S., Winge, P., Thangstad, O. P., & Bones, A. M. (2002). Guard cell-and phloem idioblast-specific expression of thioglucoside glucohydrolase 1 (myrosinase) in *Arabidopsis*. *Plant Physiology*, 128(4), 1180-1188.
- Hwang, S. F., Ahmed, H. U., Strelkov, S. E., Gossen, B. D., Turnbull, G. D., Peng, G., & Howard, R. J. (2011). Seedling age and inoculum density affect clubroot severity and seed yield in canola. *Canadian Journal of Plant Science*, 91(1), 183-190.
- Inderbitzin, P., Davis, R. M., Bostock, R. M., & Subbarao, K. V. (2013). Identification and differentiation of *Verticillium* species and *V. longisporum* lineages by simplex and multiplex PCR assays. *PLoS One*, 8(6), e65990.
- Inderbitzin, P., Bostock, R. M., Davis, R. M., Usami, T., Platt, H. W., & Subbarao, K. V. (2011a). Phylogenetics and taxonomy of the fungal vascular wilt pathogen *Verticillium*, with the descriptions of five new species. *PLoS one*, 6(12), e28341.
- Inderbitzin, P., Davis, R. M., Bostock, R. M., & Subbarao, K. V. (2011b). The ascomycete *Verticillium longisporum* is a hybrid and a plant pathogen with an expanded host range. *PLoS one*, 6(3), e18260.
- Ingle, R. A., Stoker, C., Stone, W., Adams, N., Smith, R., Grant, M., ... & Denby, K. J. (2015). Jasmonate signalling drives time-of-day differences in susceptibility of *Arabidopsis* to the fungal pathogen *Botrytis cinerea*. *The Plant Journal*, 84(5), 937-948.
- Ingram, R. (1968). *Verticillium dahliae* var. *longisporum*, a stable diploid. *Transactions of the British Mycological Society*, 51(2), 339-341.
- Isaac, I. (1967). Speciation in *Verticillium*. *Annual Review of Phytopathology*, 5(1), 201-222.
- Iven, T., König, S., Singh, S., Braus-Stromeyer, S. A., Bischoff, M., Tietze, L. F., ... & Dröge-Laser, W. (2012). Transcriptional activation and production of tryptophan-derived secondary metabolites in *Arabidopsis* roots contributes to the defense against the fungal vascular pathogen *Verticillium longisporum*. *Molecular Plant*, 5(6), 1389-1402.
- Jahn, M., Freier, B., Lozan, J. L., Grassl, H., & Hupfer, P. (2001). Changes in the occurrence of plant diseases, pests and beneficials. *Climate of the 21st century. Chances and Risks. Wiss. Auswertungen*, 307-310.
- Jahn, M., Kluge, E., & Enzian, S. (1996). Influence of climate diversity on fungal diseases on field crops-evaluation of long-term monitoring data. *Aspects of Applied Biology (United Kingdom)*.

## References

- Jin, Z., Xue, S., Luo, Y., Tian, B., Fang, H., Li, H., & Pei, Y. (2013). Hydrogen sulfide interacting with abscisic acid in stomatal regulation responses to drought stress in *Arabidopsis*. *Plant Physiology and Biochemistry*, *62*, 41-46.
- Johansson, A., Goud, J. K. C., & Dixelius, C. (2006). Plant host range of *Verticillium longisporum* and microsclerotia density in Swedish soils. *European Journal of Plant Pathology*, *114*(2), 139-149.
- Johansson, A., Staal, J., & Dixelius, C. (2006). Early responses in the *Arabidopsis-Verticillium longisporum* pathosystem are dependent on NDR1, JA-and ET-associated signals via cytosolic NPR1 and RFO1. *Molecular Plant-Microbe Interactions*, *19*(9), 958-969.
- Johnson, C. H. (1992). Phase response curves: what can they tell us about circadian clocks. *Circadian clocks from cell to human*, 209-249.
- Joly, D. L., Langor, D. W., & Hamelin, R. C. (2006). Molecular and morphological evidence for interspecific hybridization between *Cronartium ribicola* and *C. comandrae* on *Pinus flexilis* in southwestern Alberta. *Plant disease*, *90*(12), 1552-1552.
- Jones, J. D., & Dangl, J. L. (2006). The plant immune system. *Nature*, *444*(7117), 323.
- Jost, R., Altschmied, L., Bloem, E., Bogs, J., Gershenzon, J., Hähnel, U., ... & Mendel, R. R. (2005). Expression profiling of metabolic genes in response to methyl jasmonate reveals regulation of genes of primary and secondary sulfur-related pathways in *Arabidopsis thaliana*. *Photosynthesis Research*, *86*(3), 491-508.
- Judd, W. S., Campbell, C. S., Kellogg, E. A., Stevens, P. F., & Donoghue, M. J. (2002). Plant systematics: a phylogenetic approach. Sinauer Assoc. Inc., Sunderland, Mass.
- Juroszek, P., & von Tiedemann, A. (2013). Climate change and potential future risks through wheat diseases: a review. *European Journal of Plant Pathology*, *136*(1), 21-33.
- Kamble, A., Koopmann, B., & von Tiedemann, A. (2013). Induced resistance to *Verticillium longisporum* in *Brassica napus* by  $\beta$ -aminobutyric acid. *Plant Pathology*, *62*(3), 552-561.
- Karapapa, V. K., Bainbridge, B. W., & Heale, J. B. (1997). Morphological and molecular characterization of *Verticillium longisporum* comb. nov., pathogenic to oilseed rape. *Mycological Research*, *101*(11), 1281-1294.
- Karapapa, V. K., & Baig, M. A. (1997). Glucosinolate response in winter oilseed rape *Brassica napus* ssp. *oleifera* to *Verticillium dahliae* (nonpathogenic), *V. longisporum* comb. Nov., (pathogenic). *Advances in Verticillium research and disease management*. St. Paul, Minnesota: APS Press.
- Karapetyan, S., & Dong, X. (2018). Redox and the circadian clock in plant immunity: a balancing act. *Free Radical Biology and Medicine*, *119*, 56-61.

## References

- Karpinski, S., Gabrys, H., Mateo, A., Karpinska, B., & Mullineaux, P. M. (2003). Light perception in plant disease defence signalling. *Current opinion in plant biology*, 6(4), 390-396.
- Kawashima, C. G., Matthewman, C. A., Huang, S., Lee, B. R., Yoshimoto, N., Koprivova, A., ... & Takahashi, H. (2011). Interplay of SLIM1 and miR395 in the regulation of sulfate assimilation in *Arabidopsis*. *The Plant Journal*, 66(5), 863-876.
- Keen, N. T. (1992). The molecular biology of disease resistance. In *10 Years Plant Molecular Biology* (pp. 109-122). Springer, Dordrecht.
- Kehr, J., Buhtz, A., & Giavalisco, P. (2005). Analysis of xylem sap proteins from *Brassica napus*. *BMC Plant Biology*, 5(1), 11.
- Kelly, P. J., Bones, A., & Rossiter, J. T. (1998). Sub-cellular immunolocalization of the glucosinolate sinigrin in seedlings of *Brassica juncea*. *Planta*, 206(3), 370-377.
- Kerwin, R. E., Jimenez-Gomez, J. M., Fulop, D., Harmer, S. L., Maloof, J. N., & Kliebenstein, D. J. (2011). Network quantitative trait loci mapping of circadian clock outputs identifies metabolic pathway-to-clock linkages in *Arabidopsis*. *The Plant Cell*, 23(2), 471-485.
- Khangura, R., Beard, C., & Hills, A. (2015). Managing sclerotinia stem rot in canola. *Department of Agriculture and Food Australian Government* <https://agricwagovau>, (2411).
- Kidd, B. N., Kadoo, N. Y., Dombrecht, B., Tekeoglu, M., Gardiner, D. M., Thatcher, L. F., ... & Kazan, K. (2011). Auxin signaling and transport promote susceptibility to the root-infecting fungal pathogen *Fusarium oxysporum* in *Arabidopsis*. *Molecular plant-microbe interactions*, 24(6), 733-748.
- Kim, S. G., Yon, F., Gaquerel, E., Gulati, J., & Baldwin, I. T. (2011). Tissue specific diurnal rhythms of metabolites and their regulation during herbivore attack in a native tobacco, *Nicotiana attenuata*. *PloS one*, 6(10), e26214.
- Király, L., Künstler, A., Höller, K., Fattinger, M., Juhász, C., Müller, M., ... & Zechmann, B. (2012). Sulfate supply influences compartment specific glutathione metabolism and confers enhanced resistance to Tobacco mosaic virus during a hypersensitive response. *Plant Physiology and Biochemistry*, 59, 44-54.
- Kjellquist, T., & Gruvaeus, I. (1995). Sulphur deficiency in oilseed rape and cereals- Experience from Swedish field trials. *Zeitschrift für Pflanzenernährung und Bodenkunde*, 158(1), 101-103.
- Klein, M., Reichelt, M., Gershenzon, J., & Papenbrock, J. (2006). The three desulfoglucosinolate sulfotransferase proteins in *Arabidopsis* have different substrate specificities and are differentially expressed. *The FEBS journal*, 273(1), 122-136.



## References

- Klosterman, S. J., Subbarao, K. V., Kang, S., Veronese, P., Gold, S. E., Thomma, B. P., ... & Garcia-Pedrajas, M. D. (2011). Comparative genomics yields insights into niche adaptation of plant vascular wilt pathogens. *PLoS pathogens*, 7(7), e1002137.
- Klosterman, S. J., Atallah, Z. K., Vallad, G. E., & Subbarao, K. V. (2009). Diversity, pathogenicity, and management of *Verticillium* species. *Annual review of phytopathology*, 47, 39-62.
- Knight, M. R., Campbell, A. K., Smith, S. M., & Trewavas, A. J. (1991). Transgenic plant aequorin reports the effects of touch and cold-shock and elicitors on cytoplasmic calcium. *Nature*, 352(6335), 524.
- Koch, M. A., & Mummenhoff, K. (2006). Evolution and phylogeny of the Brassicaceae. *Plant Systematics and Evolution*, 259(2/4), 81-83.
- Koch, M. (2003). Molecular phylogenetics, evolution and population biology in the Brassicaceae. *Plant genome: biodiversity and evolution*, 1(Part A), 1-35.
- Koch, M., Al-Shehbaz, I. A., & Mummenhoff, K. (2003). Molecular systematics, evolution, and population biology in the mustard family (Brassicaceae). *Annals of the Missouri Botanical Garden*, 151-171.
- Kocsy, G., Owtrim, G., Brander, K., & Brunold, C. (1997). Effect of chilling on the diurnal rhythm of enzymes involved in protection against oxidative stress in a chilling-tolerant and a chilling-sensitive maize genotype. *Physiologia Plantarum*, 99(2), 249-254.
- Kocsy, G., Tari, I., Vanková, R., Zechmann, B., Gulyás, Z., Poór, P., & Galiba, G. (2013). Redox control of plant growth and development. *Plant Science*, 211, 77-91.
- König, S., Feussner, K., Kaefer, A., Landesfeind, M., Thurow, C., Karlovsky, P., ... & Feussner, I. (2014). Soluble phenylpropanoids are involved in the defense response of *Arabidopsis* against *Verticillium longisporum*. *New Phytologist*, 202(3), 823-837.
- Kopriva, S. (2006). Regulation of sulfate assimilation in *Arabidopsis* and beyond. *Annals of botany*, 97(4), 479-495.
- Kopriva, S., Mugford, S. G., Matthewman, C., & Koprivova, A. (2009). Plant sulfate assimilation genes: redundancy versus specialization. *Plant cell reports*, 28(12), 1769-1780.
- Kopriva, S., Muheim, R., Koprivova, A., Trachsel, N., Catalano, C., Suter, M., & Brunold, C. (1999). Light regulation of assimilatory sulphate reduction in *Arabidopsis thaliana*. *The Plant Journal*, 20(1), 37-44.
- Kovacs, I., Durner, J., & Lindermayr, C. (2015). Crosstalk between nitric oxide and glutathione is required for NONEXPRESSOR OF PATHOGENESIS-RELATED GENES 1 (NPR1)-dependent defense signaling in *Arabidopsis thaliana*. *New Phytologist*, 208(3), 860-872.

## References

- Kroeker, G. (1970). Wilt of Rape and Turnip Rape in Sweden caused by *Verticillium*. *Svensk Frotidning*, 39(1), 10-13.
- Kruse, C., Haas, F. H., Jost, R., Reiser, B., Reichelt, M., Wirtz, M., ... & Hell, R. (2012). Improved sulfur nutrition provides the basis for enhanced production of sulfur-containing defense compounds in *Arabidopsis thaliana* upon inoculation with *Alternaria brassicicola*. *Journal of plant physiology*, 169(7), 740-743.
- Kruse, C., Jost, R., Lipschis, M., Kopp, B., Hartmann, M., & Hell, R. (2007). Sulfur-enhanced defence: effects of sulfur metabolism, nitrogen supply, and pathogen lifestyle. *Plant Biology*, 9(05), 608-619.
- Kuśnierczyk, A., Winge, P., Midelfart, H., Armbruster, W. S., Rossiter, J. T., & Bones, A. M. (2007). Transcriptional responses of *Arabidopsis thaliana* ecotypes with different glucosinolate profiles after attack by polyphagous *Myzus persicae* and oligophagous *Brevicoryne brassicae*. *Journal of Experimental Botany*, 58(10), 2537-2552.
- Lai, A. G., Doherty, C. J., Mueller-Roeber, B., Kay, S. A., Schippers, J. H., & Dijkwel, P. P. (2012). CIRCADIAN CLOCK-ASSOCIATED 1 regulates ROS homeostasis and oxidative stress responses. *Proceedings of the National Academy of Sciences*, 109(42), 17129-17134.
- Lamb, C., & Dixon, R. A. (1997). The oxidative burst in plant disease resistance. *Annual review of plant biology*, 48(1), 251-275.
- Lass, B., & Ullrich-Eberius, C. I. (1984). Evidence for proton/sulfate cotransport and its kinetics in *Lemna gibba* G1. *Planta*, 161(1), 53-60.
- Laurie, D. A., & Bennett, M. D. (1986). Wheat× maize hybridization. *Canadian Journal of Genetics and Cytology*, 28(2), 313-316.
- Lazarovits, G., & Subbarao, K. (2010). Challenges in controlling *Verticillium* wilt by the use of nonchemical methods. In *Recent developments in management of plant diseases* (pp. 247-264). Springer, Dordrecht.
- Lee, R. B. (1982). Selectivity and kinetics of ion uptake by barley plants following nutrient deficiency. *Annals of Botany*, 50(4), 429-449.
- Leino, M. (2006). *Fungal diseases on oilseed rape and turnip rape*. Jordbruksverket.
- Lenth, R. (2019). Emmeans package: Estimated Marginal Means, aka Least-Squares Means. R package version 1.3. 5.1.
- Leustek, T., Martin, M. N., Bick, J. A., & Davies, J. P. (2000). Pathways and regulation of sulfur metabolism revealed through molecular and genetic studies. *Annual review of plant biology*, 51(1), 141-165.
- Leustek, T., & Saito, K. (1999). Sulfate transport and assimilation in plants. *Plant physiology*, 120(3), 637-644.

## References

- Levy, M., Wang, Q., Kaspi, R., Parrella, M. P., & Abel, S. (2005). Arabidopsis IQD1, a novel calmodulin-binding nuclear protein, stimulates glucosinolate accumulation and plant defense. *The Plant Journal*, *43*(1), 79-96.
- Li, Y. W., Gong, Z. H., Mu, Y., Zhang, Y. X., Qiao, Z. J., Zhang, L. P., ... & Pei, Y. X. (2012). An *Arabidopsis* mutant *atcsr-2* exhibits high cadmium stress sensitivity involved in the restriction of H<sub>2</sub>S emission. *Journal of Zhejiang University SCIENCE B*, *13*(12), 1006-1014.
- Li, Z. G., Ding, X. J., & Du, P. F. (2013). Hydrogen sulfide donor sodium hydrosulfide-improved heat tolerance in maize and involvement of proline. *Journal of plant physiology*, *170*(8), 741-747.
- Li, Z. G., Gong, M., Xie, H., Yang, L., & Li, J. (2012). Hydrogen sulfide donor sodium hydrosulfide-induced heat tolerance in tobacco (*Nicotiana tabacum* L) suspension cultured cells and involvement of Ca<sup>2+</sup> and calmodulin. *Plant Science*, *185*, 185-189.
- Lipka, V., Dittgen, J., Bednarek, P., Bhat, R., Wiermer, M., Stein, M., ... & Llorente, F. (2005). Pre- and postinvasion defenses both contribute to nonhost resistance in *Arabidopsis*. *science*, *310*(5751), 1180-1183.
- Liu, Y., Garceau, N. Y., Loros, J. J., & Dunlap, J. C. (1997). Thermally regulated translational control of FRQ mediates aspects of temperature responses in the *Neurospora* circadian clock. *Cell*, *89*(3), 477-486.
- Loake, G., & Grant, M. (2007). Salicylic acid in plant defence—the players and protagonists. *Current opinion in plant biology*, *10*(5), 466-472.
- Logan, H. M., Cathala, N., Grignon, C., & Davidian, J. C. (1996). Cloning of a cDNA encoded by a member of the *Arabidopsis thaliana* ATP sulfurylase multigene family EXPRESSION STUDIES IN YEAST AND IN RELATION TO PLANT SULFUR NUTRITION. *Journal of Biological Chemistry*, *271*(21), 12227-12233.
- Longo, M. C., Berninger, M. S., & Hartley, J. L. (1990). Use of uracil DNA glycosylase to control carry-over contamination in polymerase chain reactions. *Gene*, *93*(1), 125-128.
- Lu, H., McClung, C. R., & Zhang, C. (2017). Tick tock: circadian regulation of plant innate immunity. *Annual review of phytopathology*, *55*, 287-311.
- Lu, H., Greenberg, J. T., & Holuigue, L. (2016). Salicylic acid signaling networks. *Frontiers in plant science*, *7*, 238.
- Lüthy, B., & Matile, P. (1984). The mustard oil bomb: rectified analysis of the subcellular organisation of the myrosinase system. *Biochemie und Physiologie der Pflanzen*, *179*(1-2), 5-12.
- Lüttge, U. (2017). Pflanzen haben eine Uhr. In *Faszination Pflanzen* (pp. 217-228). Springer Spektrum, Berlin, Heidelberg.

## References

- Mace, M. E. (1978). Contributions of tyloses and terpenoid aldehyde phytoalexins to *Verticillium* wilt resistance in cotton. *Physiological Plant Pathology*, 12(1), 1-11.
- Maeda, K., Houjyou, Y., Komatsu, T., Hori, H., Kodaira, T., & Ishikawa, A. (2009). AGB1 and PMR5 contribute to PEN2-mediated preinvasion resistance to *Magnaporthe oryzae* in *Arabidopsis thaliana*. *Molecular plant-microbe interactions*, 22(11), 1331-1340.
- Majercak, J., Sidote, D., Hardin, P. E., & Edery, I. (1999). How a circadian clock adapts to seasonal decreases in temperature and day length. *Neuron*, 24(1), 219-230.
- Mansfield, J. W. (2000). Antimicrobial compounds and resistance. In *Mechanisms of resistance to plant diseases* (pp. 325-370). Springer, Dordrecht.
- Mansoori, I. (2012). Response of canola to nitrogen and sulfur fertilizers. *Int. J. Agric. Crop Sci*, 4(1), 28-33.
- Marcel, S., Sawers, R., Oakeley, E., Angliker, H., & Paszkowski, U. (2010). Tissue-adapted invasion strategies of the rice blast fungus *Magnaporthe oryzae*. *The Plant Cell*, 22(9), 3177-3187.
- Marschner, H. (1974). Mechanisms of regulation of mineral nutrition in higher plants. *Bull R Soc NZ*.
- Martinelli, F., Scalenghe, R., Davino, S., Panno, S., Scuderi, G., Ruisi, P., ... & Davis, C. E. (2015). Advanced methods of plant disease detection. A review. *Agronomy for Sustainable Development*, 35(1), 1-25.
- Maruyama-Nakashita, A., Nakamura, Y., Tohge, T., Saito, K., & Takahashi, H. (2006). *Arabidopsis* SLIM1 is a central transcriptional regulator of plant sulfur response and metabolism. *The Plant Cell*, 18(11), 3235-3251.
- Masneuf, I., Hansen, J., Groth, C., Piskur, J., & Dubourdieu, D. (1998). New hybrids between *Saccharomyces sensu stricto* yeast species found among wine and cider production strains. *Appl. Environ. Microbiol.*, 64(10), 3887-3892.
- May, M. J., Vernoux, T., Sanchez-Fernandez, R., Van Montagu, M., & Inzé, D. (1998). Evidence for posttranscriptional activation of  $\gamma$ -glutamylcysteine synthetase during plant stress responses. *Proceedings of the National Academy of Sciences*, 95(20), 12049-12054.
- McClung, C. R. (2011a). Circadian rhythms: lost in post-translation. *Current Biology*, 21(10), R400-R402.
- McClung, C. R. (2011b). Plant biology: Defence at dawn. *Nature*, 470(7332), 44.
- McClung, C. R. (2008). Comes a time. *Current opinion in plant biology*, 11(5), 514-520.

## References

- McClung, C. R. (2000). Circadian rhythms in plants: a millennial view. *Physiologia Plantarum*, 109(4), 359-371.
- McCullagh, P. and J. Nelder. (1989). Generalized Linear Models Second Edition Chapman & Hall.
- McDanell, R., McLean, A. E. M., Hanley, A. B., Heaney, R. K., & Fenwick, G. R. (1988). Chemical and biological properties of indole glucosinolates (glucobrassicins): a review. *Food and Chemical Toxicology*, 26(1), 59-70.
- McDonald, B. A., & Martinez, J. P. (1991). Chromosome length polymorphisms in a *Septoria tritici* population. *Current Genetics*, 19(4), 265-271.
- McElrone, A. J., Sherald, J. L., & Forseth, I. N. (2003). Interactive effects of water stress and xylem-limited bacterial infection on the water relations of a host vine. *Journal of Experimental Botany*, 54(381), 419-430.
- Medzhitov, R., & Janeway, C. A. (1997). Innate immunity: the virtues of a nonclonal system of recognition. *Cell*, 91(3), 295-298.
- Meena, V. S., Maurya, B. R., Meena, S. K., Meena, R. K., Kumar, A., Verma, J. P., & Singh, N. P. (2016). Can *Bacillus* species enhance nutrient availability in agricultural soils?. In *Bacilli and Agrobiotechnology* (pp. 367-395). Springer, Cham.
- Meister, A. (1988). Glutathione metabolism and its selective modification. *Journal of biological chemistry*, 263(33), 17205-17208.
- Meister, A., & Anderson, M. E. (1983). Glutathione. *Annual review of biochemistry*, 52(1), 711-760.
- Melotto, M., Underwood, W., Koczan, J., Nomura, K., & He, S. Y. (2006). Plant stomata function in innate immunity against bacterial invasion. *Cell*, 126(5), 969-980.
- Meyer, R. W., & Côté, W. A. (1968). Formation of the protective layer and its role in tylosis development. *Wood science and technology*, 2(2), 84-94.
- Michielse, C. B., & Rep, M. (2009). Pathogen profile update: *Fusarium oxysporum*. *Molecular plant pathology*, 10(3), 311-324.
- Mikkelsen, M. D., Petersen, B. L., Glawischnig, E., Jensen, A. B., Andreasson, E., & Halkier, B. A. (2003). Modulation of CYP79 genes and glucosinolate profiles in *Arabidopsis* by defense signaling pathways. *Plant physiology*, 131(1), 298-308.
- Mikkelsen, M. D., Hansen, C. H., Wittstock, U., & Halkier, B. A. (2000). Cytochrome P450 CYP79B2 from *Arabidopsis* catalyzes the conversion of tryptophan to indole-3-acetaldoxime, a precursor of indole glucosinolates and indole-3-acetic acid. *Journal of biological chemistry*, 275(43), 33712-33717.

## References

- Milford, G. F. J., Fieldsend, J. K., Porter, A. J. R., Rawlinson, C. J., Evans, E. J., & Bilsborrow, P. E. (1989). Changes in glucosinolate concentrations during the vegetative growth of single and double-low cultivars of winter oilseed rape. *Aspects of Applied Biology (United Kingdom)*.
- Millet, Y. A., Danna, C. H., Clay, N. K., Songnuan, W., Simon, M. D., Werck-Reichhart, D., & Ausubel, F. M. (2010). Innate immune responses activated in *Arabidopsis* roots by microbe-associated molecular patterns. *The Plant Cell*, 22(3), 973-990.
- Mithen, R., & Campos, H. (1996). Genetic variation of aliphatic glucosinolates in *Arabidopsis thaliana* and prospects for map based gene cloning. In *Proceedings of the 9th International Symposium on Insect-Plant Relationships* (pp. 202-205). Springer, Dordrecht.
- Mithen, R. (1992). Leaf glucosinolate profiles and their relationship to pest and disease resistance in oilseed rape. In *Breeding for Disease Resistance* (pp. 71-83). Springer, Dordrecht.
- Mithen, R. F., Lewis, B. G., & Fenwick, G. R. (1986). In vitro activity of glucosinolates and their products against *Leptosphaeria maculans*. *Transactions of the British Mycological Society*, 87(3), 433-440.
- Mittler, R., Vanderauwera, S., Suzuki, N., Miller, G. A. D., Tognetti, V. B., Vandepoele, K., ... & Van Breusegem, F. (2011). ROS signaling: the new wave?. *Trends in plant science*, 16(6), 300-309.
- Moon, C. D., Craven, K. D., Leuchtman, A., Clement, S. L., & Schardl, C. L. (2004). Prevalence of interspecific hybrids amongst asexual fungal endophytes of grasses. *Molecular Ecology*, 13(6), 1455-1467.
- Morin, L., Van Der Merwe, M., Hartley, D., & Müller, P. (2009). Putative natural hybrid between *Puccinia lagenophorae* and an unknown rust fungus on *Senecio madagascariensis* in KwaZulu-Natal, South Africa. *Mycological research*, 113(6-7), 725-736.
- Mou, Z., Fan, W., & Dong, X. (2003). Inducers of plant systemic acquired resistance regulate NPR1 function through redox changes. *Cell*, 113(7), 935-944.
- Mugford, S. G., Yoshimoto, N., Reichelt, M., Wirtz, M., Hill, L., Mugford, S. T., ... & Gigolashvili, T. (2009). Disruption of adenosine-5'-phosphosulfate kinase in *Arabidopsis* reduces levels of sulfated secondary metabolites. *The Plant Cell*, 21(3), 910-927.
- Mukhtar, M. S., Nishimura, M. T., & Dangl, J. (2009). NPR1 in plant defense: it's not over'til it's turned over. *Cell*, 137(5), 804-806.
- Mullineaux, P. M., & Rausch, T. (2005). Glutathione, photosynthesis and the redox regulation of stress-responsive gene expression. *Photosynthesis research*, 86(3), 459-474.

## References

- Nagaharu, U. (1935). Genome analysis in *Brassica* with special reference to the experimental formation of *B. napus* and peculiar mode of fertilization. *Jpn J Bot*, 7(7), 389-452.
- Nagel, D. H., & Kay, S. A. (2012). Complexity in the wiring and regulation of plant circadian networks. *Current Biology*, 22(16), R648-R657.
- Nakamichi, N. (2011). Molecular mechanisms underlying the *Arabidopsis* circadian clock. *Plant and Cell Physiology*, 52(10), 1709-1718.
- Nakamura, S. I., Akiyama, C., Sasaki, T., Hattori, H., & Chino, M. (2008). Effect of cadmium on the chemical composition of xylem exudate from oilseed rape plants (*Brassica napus* L.). *Soil science and plant nutrition*, 54(1), 118-127.
- Namvar, A., & Khandan, T. (2015). Inoculation of rapeseed under different rates of inorganic nitrogen and sulfur fertilizer: impact on water relations, cell membrane stability, chlorophyll content and yield. *Archives of Agronomy and Soil Science*, 61(8), 1137-1149.
- Navarro, L., Dunoyer, P., Jay, F., Arnold, B., Dharmasiri, N., Estelle, M., ... & Jones, J. D. (2006). A plant miRNA contributes to antibacterial resistance by repressing auxin signaling. *Science*, 312(5772), 436-439.
- Nazar, R. N., Hu, X., Schmidt, J., Culham, D., & Robb, J. (1991). Potential use of PCR-amplified ribosomal intergenic sequences in the detection and differentiation of *Verticillium* wilt pathogens. *Physiological and Molecular Plant Pathology*, 39(1), 1-11.
- Nibbe, M., Hilpert, B., Wasternack, C., Miersch, O., & Apel, K. (2002). Cell death and salicylate- and jasmonate-dependent stress responses in *Arabidopsis* are controlled by single genes. *Planta*, 216(1), 120-128.
- Nicaise, V., Joe, A., Jeong, B. R., Korneli, C., Boutrot, F., Westedt, I., ... & Zipfel, C. (2013). *Pseudomonas* HopU1 modulates plant immune receptor levels by blocking the interaction of their mRNAs with GRP7. *The EMBO journal*, 32(5), 701-712.
- Njoroge, S. M. C., Vallad, G. E., Park, S. Y., Kang, S., Koike, S. T., Bolda, M., ... & Subbarao, K. V. (2011). Phenological and phytochemical changes correlate with differential interactions of *Verticillium dahliae* with broccoli and cauliflower. *Phytopathology*, 101(5), 523-534.
- Noctor, G., Mhamdi, A., Chaouch, S., Han, Y. I., Neukermans, J., Marquez-Garcia, B. E. L. E. N., ... & Foyer, C. H. (2012). Glutathione in plants: an integrated overview. *Plant, cell & environment*, 35(2), 454-484.
- Noctor, G., Veljovic-Jovanovic, S., & Foyer, C. H. (2000). Peroxide processing in photosynthesis: antioxidant coupling and redox signalling. *Philosophical Transactions of the Royal Society of London. Series B: Biological Sciences*, 355(1402), 1465-1475.

## References

- Noctor, G., Arisi, A. C. M., Jouanin, L., & Foyer, C. H. (1999). Photorespiratory glycine enhances glutathione accumulation in both the chloroplastic and cytosolic compartments. *Journal of Experimental Botany*, *50*(336), 1157-1167.
- Noctor, G., & Foyer, C. H. (1998). Ascorbate and glutathione: keeping active oxygen under control. *Annual review of plant biology*, *49*(1), 249-279.
- Noctor, G., Arisi, A. C. M., Jouanin, L., Valadier, M. H., Roux, Y., & Foyer, C. H. (1997). Light-dependent modulation of foliar glutathione synthesis and associated amino acid metabolism in poplar overexpressing  $\gamma$ -glutamylcysteine synthetase. *Planta*, *202*(3), 357-369.
- Nomura, K., Melotto, M., & He, S. Y. (2005). Suppression of host defense in compatible plant–*Pseudomonas syringae* interactions. *Current opinion in plant biology*, *8*(4), 361-368.
- Norici, A., Hell, R., & Giordano, M. (2005). Sulfur and primary production in aquatic environments: an ecological perspective. *Photosynthesis Research*, *86*(3), 409-417.
- Novakazi, F., Inderbitzin, P., Sandoya, G., Hayes, R. J., von Tiedemann, A., & Subbarao, K. V. (2015). The three lineages of the diploid hybrid *Verticillium longisporum* differ in virulence and pathogenicity. *Phytopathology*, *105*(5), 662-673.
- Nürnbergger, T., & Brunner, F. (2002). Innate immunity in plants and animals: emerging parallels between the recognition of general elicitors and pathogen-associated molecular patterns. *Current opinion in plant biology*, *5*(4), 318-324.
- O'Brien, R. D. (2008). *Fats and oils: formulating and processing for applications*. CRC press.
- Obermeier, C., Hossain, M. A., Snowdon, R., Knüfer, J., von Tiedemann, A., & Friedt, W. (2013). Genetic analysis of phenylpropanoid metabolites associated with resistance against *Verticillium longisporum* in *Brassica napus*. *Molecular breeding*, *31*(2), 347-361.
- Oberpichler, I., Rosen, R., Rasouly, A., Vugman, M., Ron, E. Z., & Lamparter, T. (2008). Light affects motility and infectivity of *Agrobacterium tumefaciens*. *Environmental microbiology*, *10*(8), 2020-2029.
- Oerke, E. C. (2006). Crop losses to pests. *The Journal of Agricultural Science*, *144*(1), 31-43.
- Okubara, P. A., & Paulitz, T. C. (2005). Root defense responses to fungal pathogens: a molecular perspective. *Plant and Soil*, *274*(1-2), 215-226.
- Oliverio, K. A., Crepy, M., Martin-Tryon, E. L., Milich, R., Harmer, S. L., Putterill, J., ... & Casal, J. J. (2007). GIGANTEA regulates phytochrome A-mediated photomorphogenesis independently of its role in the circadian clock. *Plant Physiology*, *144*(1), 495-502.
- Olsson, S., & Nordbring-Hertz, B. (1985). Microsclerotial germination of *Verticillium dahliae* as affected by rape rhizosphere. *FEMS Microbiology Ecology*, *1*(5), 293-299.



## References

- Orlovius, K., & Kirgby, E. A. (2003). Fertilizing for high yield and quality oilseed rape. *IPI Bulletin*, (16), 125.
- Osborn, T. C., Pires, J. C., Birchler, J. A., Auger, D. L., Chen, Z. J., Lee, H. S., ... & Martienssen, R. A. (2003). Understanding mechanisms of novel gene expression in polyploids. *Trends in genetics*, 19(3), 141-147.
- Palmer, C. S., Saleeba, J. A., & Lyon, B. R. (2005). Phytotoxicity on cotton ex-plants of an 18.5 kDa protein from culture filtrates of *Verticillium dahliae*. *Physiological and molecular plant pathology*, 67(6), 308-318.
- Panstruga, R., Parker, J. E., & Schulze-Lefert, P. (2009). SnapShot: plant immune response pathways. *Cell*, 136(5), 978-e1.
- Passera, C., Ghisi, R., & Ferretti, M. (1989). Light-activation of ATP-sulphurylase in leaves and chloroplasts of *Zea mays*. *Photosynthetica*, 23(2), 166-172.
- Paulmann, W., & Frauen, M. (1997). The first fully restored F1-hybrids of winter oilseed rape. *GCIRC Bulletin (France)*.
- Pearce, R. B., & Holloway, P. J. (1984). Suberin in the sapwood of oak (*Quercus robur* L.): its composition from a compartmentalization barrier and its occurrence in tyloses in undecayed wood. *Physiological plant pathology*, 24(1), 71-81.
- Pedersen, C. A., Knudsen, L., & Schnug, E. (1998). Sulphur fertilisation. In *Sulphur in agroecosystems* (pp. 115-134). Springer, Dordrecht.
- Pedras, M. S. C. (2008). The chemical ecology of crucifers and their fungal pathogens: Boosting plant defenses and inhibiting pathogen invasion. *The Chemical Record*, 8(2), 109-115.
- Pegg, G. F., & Brady, B. L. (2002). *Verticillium wilts*. CABI.
- Perfect, S. E., Hughes, H. B., O'Connell, R. J., & Green, J. R. (1999). *Colletotrichum*: a model genus for studies on pathology and fungal-plant interactions. *Fungal genetics and Biology*, 27(2-3), 186-198.
- Petersen, B., Chen, S., Hansen, C., Olsen, C., & Halkier, B. (2002). Composition and content of glucosinolates in developing *Arabidopsis thaliana*. *Planta*, 214(4), 562-571.
- Petersen, B. L., Andréasson, E., Bak, S., Agerbirk, N., & Halkier, B. A. (2001). Characterization of transgenic *Arabidopsis thaliana* with metabolically engineered high levels of p-hydroxybenzylglucosinolate. *Planta*, 212(4), 612-618.
- Piazza, G. J., & Foglia, T. A. (2001). Rapeseed oil for oleochemical usage. *European journal of lipid science and technology*, 103(7), 450-454.
- Pieterse, C. M., & Van Loon, L. C. (2004). NPR1: the spider in the web of induced resistance signaling pathways. *Current opinion in plant biology*, 7(4), 456-464.

## References

- Pilgrim, M. L., Caspar, T., Quail, P. H., & McClung, C. R. (1993). Circadian and light-regulated expression of nitrate reductase in *Arabidopsis*. *Plant molecular biology*, 23(2), 349-364.
- Pittendrigh, C. S. (1954). On temperature independence in the clock system controlling emergence time in *Drosophila*. *Proceedings of the National Academy of Sciences of the United States of America*, 40(10), 1018.
- Pokhilko, A., Fernández, A. P., Edwards, K. D., Southern, M. M., Halliday, K. J., & Millar, A. J. (2012). The clock gene circuit in *Arabidopsis* includes a repressilator with additional feedback loops. *Molecular systems biology*, 8(1).
- Popper, Z. A., Michel, G., Hervé, C., Domozych, D. S., Willats, W. G., Tuohy, M. G., ... & Stengel, D. B. (2011). Evolution and diversity of plant cell walls: from algae to flowering plants. *Annual review of plant biology*, 62, 567-590.
- Potters, G., De Gara, L., Asard, H., & Horemans, N. (2002). Ascorbate and glutathione: guardians of the cell cycle, partners in crime?. *Plant Physiology and Biochemistry*, 40(6-8), 537-548.
- Powelson, M. L., & Rowe, R. C. (1993). Biology and management of early dying of potatoes. *Annual review of phytopathology*, 31(1), 111-126.
- Prakash, S. (1980). Cruciferous oilseeds in India. *Cruciferous oilseeds in India.*, 151-163.
- Purcell, A. H., & Hopkins, D. L. (1996). Fastidious xylem-limited bacterial plant pathogens. *Annual review of phytopathology*, 34(1), 131-151.
- Rakow, G. (2004). Species origin and economic importance of *Brassica*. In *Brassica* (pp. 3-11). Springer, Berlin, Heidelberg.
- Ranjani, K., & Krishnamurthy, K. V. (1988). Nature of vestures in the vested pits of some Caesalpinaceae. *IAWA Journal*, 9(1), 31-33.
- Rausch, T., & Wachter, A. (2005). Sulfur metabolism: a versatile platform for launching defence operations. *Trends in plant science*, 10(10), 503-509.
- Rawlinson, C. J., Doughty, K. J., Bock, C. H., Church, V. J., Milford, G. F. J., & Fieldsend, J. K. (1989). Diseases and responses to disease and pest control on single-and double-low cultivars of winter oilseed rape. *Aspects of applied biology*.
- Rennenberg, H. (1983). Role of O-acetylserine in hydrogen sulfide emission from pumpkin leaves in response to sulfate. *Plant Physiology*, 73(3), 560-565.
- Rennenberg, H., & Brunold, C. (1994). Significance of glutathione metabolism in plants under stress. In *Progress in botany* (pp. 142-156). Springer, Berlin, Heidelberg.
- Resende, M. L. V., Flood, J., Ramsden, J. D., Rowan, M. G., Beale, M. H., & Cooper, R. M. (1996). Novel phytoalexins including elemental sulphur in the resistance of cocoa (*Theobroma cocoa* L.) to *Verticillium* wilt (*Verticillium dahliae* Kleb.). *Physiological and molecular plant pathology*, 48(5), 347-359.

## References

- Resurreccion, A. P., Makino, A., Bennett, J., & Mae, T. (2001). Effects of sulfur nutrition on the growth and photosynthesis of rice. *Soil Science and Plant Nutrition*, 47(3), 611-620.
- Reusche, M., Truskina, J., Thole, K., Nagel, L., Rindfleisch, S., Tran, V. T., ... & Lipka, V. (2014). Infections with the vascular pathogens *Verticillium longisporum* and *Verticillium dahliae* induce distinct disease symptoms and differentially affect drought stress tolerance of *Arabidopsis thaliana*. *Environmental and Experimental Botany*, 108, 23-37.
- Reusche, M., Thole, K., Janz, D., Truskina, J., Rindfleisch, S., Drübert, C., ... & Teichmann, T. (2012). Verticillium infection triggers VASCULAR-RELATED NAC DOMAIN7-dependent de novo xylem formation and enhances drought tolerance in *Arabidopsis*. *The Plant Cell*, 24(9), 3823-3837.
- Richards, I. R. (1990). Sulphur as a crop nutrient in the United Kingdom. *Sulphur in Agriculture*, 14, 8-9.
- Riemenschneider, A., Wegele, R., Schmidt, A., & Papenbrock, J. (2005). Isolation and characterization of ad-cysteine desulphydrase protein from *Arabidopsis thaliana*. *The FEBS journal*, 272(5), 1291-1304.
- Rieseberg, L. H., & Carney, S. E. (1998). Plant hybridization. *The New Phytologist*, 140(4), 599-624.
- Rioux, D., Nicole, M., Simard, M., & Ouellette, G. B. (1998). Immunocytochemical evidence that secretion of pectin occurs during gel (gum) and tylosis formation in trees. *Phytopathology*, 88(6), 494-505.
- Rioux, D., & Ouellette, G. B. (1989). Light microscope observations of histological changes induced by *Ophiostoma ulmi* in various nonhost trees and shrubs. *Canadian Journal of Botany*, 67(8), 2335-2351.
- Robb, J., Moukhamedov, R., Hu, X., Platt, H., & Nazar, R. N. (1993). Putative subgroups of *Verticillium albo-atrum* distinguishable by PCR-based assays. *Physiological and Molecular Plant Pathology*, 43(6), 423-436.
- Robb, J., Powell, D. A., & Street, P. F. S. (1989). Vascular coating: a barrier to colonization by the pathogen in *Verticillium* wilt of tomato. *Canadian Journal of Botany*, 67(2), 600-607.
- Roberts, M. R., & Paul, N. D. (2006). Seduced by the dark side: integrating molecular and ecological perspectives on the influence of light on plant defence against pests and pathogens. *New Phytologist*, 170(4), 677-699.
- Rocquelin, G., Sergiel, J. P., Martin, B., Leclerc, J., & Cluzan, R. (1971). The nutritive value of refined rapeseed oils: A review. *Journal of the American Oil Chemists Society*, 48(11), 728-732.

## References

- Roden, L. C., & Ingle, R. A. (2009). Lights, rhythms, infection: the role of light and the circadian clock in determining the outcome of plant–pathogen interactions. *The Plant Cell*, 21(9), 2546-2552.
- Rosa, E. A., & Rodrigues, P. M. (1998). The effect of light and temperature on glucosinolate concentration in the leaves and roots of cabbage seedlings. *Journal of the Science of Food and Agriculture*, 78(2), 208-212.
- Rosa, E. A. (1997). Daily variation in glucosinolate concentrations in the leaves and roots of cabbage seedlings in two constant temperature regimes. *Journal of the Science of Food and Agriculture*, 73(3), 364-368.
- Rosa, E. A., Heaney, R. K., Rego, F. C., & Fenwick, G. R. (1994). The variation of glucosinolate concentration during a single day in young plants of *Brassica oleracea* var *acephala* and *capitata*. *Journal of the Science of Food and Agriculture*, 66(4), 457-463.
- Rössler, W. (1974). Myrosinzellen bei Tovariva. *Phyton (Horn)*, 16, 231-522.
- Rowe, R. C., & Powelson, M. L. (2002). Potato early dying: management challenges in a changing production environment. *Plant Disease*, 86(11), 1184-1193.
- Rowe, R. C., Davis, J. R., Powelson, M. L., & Rouse, D. I. (1987). Potato early dying: causal agents and management strategies. *Plant Disease*, 71(6), 482-489.
- Ruegger, M., & Chapple, C. (2001). Mutations that reduce sinapoylmalate accumulation in *Arabidopsis thaliana* define loci with diverse roles in phenylpropanoid metabolism. *Genetics*, 159(4), 1741-1749.
- Ruiz, J., & Blumwald, E. (2002). Salinity-induced glutathione synthesis in *Brassica napus*. *Planta*, 214(6), 965-969.
- Russel, S. (1974). Cellulolytic activity of *Verticillium albo-atrum*. *Acta microbiologica Polonica. Series B: Microbiologia applicata*, 6(3), 97.
- Rygulla, W., Snowdon, R. J., Friedt, W., Happstadius, I., Cheung, W. Y., & Chen, D. (2008). Identification of quantitative trait loci for resistance against *Verticillium longisporum* in oilseed rape (*Brassica napus*). *Phytopathology*, 98(2), 215-221.
- Rygulla, W., Friedt, W., Seyis, F., Lühs, W., Eynck, C., von Tiedemann, A., & Snowdon, R. J. (2007a). Combination of resistance to *Verticillium longisporum* from zero erucic acid *Brassica oleracea* and oilseed *Brassica rapa* genotypes in resynthesized rapeseed (*Brassica napus*) lines. *Plant breeding*, 126(6), 596-602.
- Rygulla, W., Snowdon, R. J., Eynck, C., Koopmann, B., von Tiedemann, A., Lühs, W., & Friedt, W. (2007b). Broadening the genetic basis of *Verticillium longisporum* resistance in *Brassica napus* by interspecific hybridization. *Phytopathology*, 97(11), 1391-1396.

## References

- Sadowski, C., Zielinski, D., Klepin, J., & Zawislak, K. (1995, July). The health status of winter rape cultivated for many years with monoculture and crop rotation. In *9th International GCIRC Rapeseed Congress* (pp. 4-7).
- Saharan, G. S., & Mehta, N. (2008). *Sclerotinia diseases of crop plants: biology, ecology and disease management*. Springer Science & Business Media.
- Saito, K. (2004). Sulfur assimilatory metabolism. The long and smelling road. *Plant Physiology*, *136*(1), 2443-2450.
- Salvagiotti, F., Castellarín, J. M., Miralles, D. J., & Pedrol, H. M. (2009). Sulfur fertilization improves nitrogen use efficiency in wheat by increasing nitrogen uptake. *Field Crops Research*, *113*(2), 170-177.
- Sanchez-Vallet, A., Ramos, B., Bednarek, P., López, G., Piślewska-Bednarek, M., Schulze-Lefert, P., & Molina, A. (2010). Tryptophan-derived secondary metabolites in *Arabidopsis thaliana* confer non-host resistance to necrotrophic *Plectosphaerella cucumerina* fungi. *The Plant Journal*, *63*(1), 115-127.
- Sanghera, G. S., Wani, S. H., Singh, G., Kashyap, P. L., & Singh, N. B. (2011). Designing crop plants for biotic stresses using transgenic approach. *Vegetos-An International Journal of Plant Research*, *24*(1), 1-25.
- Sattell, R., Dick, R., Ingham, R., Karow, R. S., Kaufman, D., & McGrath, D. M. (1998). Rapeseed (*Brassica campestris/Brassica napus*).
- Sauerbrunn, N., & Schlaich, N. L. (2004). PCC1: a merging point for pathogen defence and circadian signalling in *Arabidopsis*. *Planta*, *218*(4), 552-561.
- Sawyer, L. A., Hennessy, J. M., Peixoto, A. A., Rosato, E., Parkinson, H., Costa, R., & Kyriacou, C. P. (1997). Natural variation in a *Drosophila* clock gene and temperature compensation. *Science*, *278*(5346), 2117-2120.
- Schaffer, R., Ramsay, N., Samach, A., Corden, S., Putterill, J., Carré, I. A., & Coupland, G. (1998). The late elongated hypocotyl mutation of *Arabidopsis* disrupts circadian rhythms and the photoperiodic control of flowering. *Cell*, *93*(7), 1219-1229.
- Schardl, C. L., & Craven, K. D. (2003). Interspecific hybridization in plant-associated fungi and oomycetes: a review. *Molecular Ecology*, *12*(11), 2861-2873.
- Scheffler, J. A., & Dale, P. J. (1994). Opportunities for gene transfer from transgenic oilseed rape (*Brassica napus*) to related species. *Transgenic research*, *3*(5), 263-278.
- Schieber, E. (1975). Present status of coffee rust in South America. *Annual Review of Phytopathology*, *13*(1), 375-382.
- Schindelin, J., Arganda-Carreras, I., Frise, E., Kaynig, V., Longair, M., Pietzsch, T., ... & Tinevez, J. Y. (2012). Fiji: an open-source platform for biological-image analysis. *Nature methods*, *9*(7), 676.

## References

- Schlaeppli, K., Abou-Mansour, E., Buchala, A., & Mauch, F. (2010). Disease resistance of *Arabidopsis* to *Phytophthora brassicae* is established by the sequential action of indole glucosinolates and camalexin. *The Plant Journal*, 62(5), 840-851.
- Schmitt, U., & Liese, W. (1993). Response of xylem parenchyma by suberization in some hardwoods after mechanical injury. *Trees*, 8(1), 23-30.
- Schnathorst, W. C. (1981). Life cycle and epidemiology of *Verticillium*. *Fungal wilt diseases of plants*, 82.
- Schnug, E., & Haneklaus, S. (2005). Sulphur deficiency symptoms in oilseed rape (*Brassica napus* L.)-the aesthetics of starvation. *PHYTON-HORN-*, 45(3), 79.
- Schnug, E., Booth, E., Haneklaus, S., & Walker, K. C. (1995, July). Sulphur supply and stress resistance in oilseed rape. In *Proceedings of the 9th international rapeseed congress, Cambridge* (Vol. 1995, pp. 229-231).
- Schnug, E., & Haneklaus, S. (1994). Sulphur deficiency in *Brassica napus*-biochemistry-symptomatology-morphogenesis. *Landbauforschung Voelkenrode. Sonderheft (Germany). no. 144*.
- Schnug, E. (1991). Sulphur nutritional status of European crops and consequences for agriculture. *Sulphur in agriculture*, 15, 7-12.
- Schnug, E., & Ceynowa, J. (1990, March). Crop protection problems for double low rape associated with decreased disease resistance and increased pest damage. In *Proceedings of the Conference on Crop Protection in Northern Britain, Dundee* (pp. 275-282).
- Schnug, E., & Pissarek, H. P. (1982). Kalium und Schwefel, Minimumfaktoren des schleswig-holsteinischen Rapsanbaus. *Kali-Briefe (Büntehof)*, 16, 77-84.
- Schreiber, L., Hartmann, K., Skrabs, M., & Zeier, J. (1999). Apoplastic barriers in roots: chemical composition of endodermal and hypodermal cell walls. *Journal of Experimental Botany*, 50(337), 1267-1280.
- Schupp, R., & Rennenberg, H. (1988). Diurnal changes in the glutathione content of spruce needles (*Picea abies* L.). *Plant Science*, 57(2), 113-117.
- Schuster, J., Knill, T., Reichelt, M., Gershenzon, J., & Binder, S. (2006). Branched-chain aminotransferase4 is part of the chain elongation pathway in the biosynthesis of methionine-derived glucosinolates in *Arabidopsis*. *The Plant Cell*, 18(10), 2664-2679.
- Segonzac, C., Feike, D., Gimenez-Ibanez, S., Hann, D. R., Zipfel, C., & Rathjen, J. P. (2011). Hierarchy and roles of pathogen-associated molecular pattern-induced responses in *Nicotiana benthamiana*. *Plant physiology*, 156(2), 687-699.

## References

- Seidel, D. & Zeise, K. (1990). Verticillium wilt of oilseed rape. in *5th International Verticillium Symposium, Leningrad, USSR, Abstract*. Vol. 18.
- Seybold, S. (2009). Schmeil-Fitschen: Flora von Deutschland und angrenzender Länder. *Quelle and Meyer, Heidelberg, Wiesbaden*.
- Shibagaki, N., Rose, A., McDermott, J. P., Fujiwara, T., Hayashi, H., Yoneyama, T., & Davies, J. P. (2002). Selenate-resistant mutants of *Arabidopsis thaliana* identify Sultr1; 2, a sulfate transporter required for efficient transport of sulfate into roots. *The Plant Journal*, 29(4), 475-486.
- Shin, J., Heidrich, K., Sanchez-Villarreal, A., Parker, J. E., & Davis, S. J. (2012). TIME FOR COFFEE represses accumulation of the MYC2 transcription factor to provide time-of-day regulation of jasmonate signaling in Arabidopsis. *The Plant Cell*, 24(6), 2470-2482.
- Siebold, M., & von Tiedemann, A. (2013). Effects of experimental warming on fungal disease progress in oilseed rape. *Global change biology*, 19(6), 1736-1747.
- Singh, S., Braus-Stromeier, S. A., Timpner, C., Tran, V. T., Lohaus, G., Reusche, M., ... & Braus, G. H. (2010). Silencing of Vlaro2 for chorismate synthase revealed that the phytopathogen *Verticillium longisporum* induces the cross-pathway control in the xylem. *Applied microbiology and biotechnology*, 85(6), 1961-1976.
- Smith, F. W., Ealing, P. M., Hawkesford, M. J., & Clarkson, D. T. (1995). Plant members of a family of sulfate transporters reveal functional subtypes. *Proceedings of the National Academy of Sciences*, 92(20), 9373-9377.
- Sønderby, I. E., Hansen, B. G., Bjarnholt, N., Ticconi, C., Halkier, B. A., & Kliebenstein, D. J. (2007). A systems biology approach identifies a R2R3 MYB gene subfamily with distinct and overlapping functions in regulation of aliphatic glucosinolates. *PLoS One*, 2(12), e1322.
- Song, Y. H., Ito, S., & Imaizumi, T. (2010). Similarities in the circadian clock and photoperiodism in plants. *Current opinion in plant biology*, 13(5), 594-603.
- Sonntag, N. O. V. (1995). Industrial utilization of long-chain fatty acids and their derivatives. *Brassica Oilseeds. CAB International, Oxon, UK*, 339-352.
- Spencer, G. A. (1997). *Verticillium* wilt, Compendium of lettuce diseases The American Phytopathological Society St. Paul, MN.
- Spoel, S. H., & Loake, G. J. (2011). Redox-based protein modifications: the missing link in plant immune signalling. *Current opinion in plant biology*, 14(4), 358-364.
- Spoel, S. H., & van Ooijen, G. (2014). Circadian redox signaling in plant immunity and abiotic stress. *Antioxidants & redox signaling*, 20(18), 3024-3039.
- Spoel, S. H., & Dong, X. (2012). How do plants achieve immunity? Defence without specialized immune cells. *Nature reviews immunology*, 12(2), 89.

## References

- Staiger, D., & Green, R. (2011). RNA-based regulation in the plant circadian clock. *Trends in plant science*, 16(10), 517-523.
- Stark, C. (1961). Das Auftreten der *Verticillium*-Tracheomykosen in Hamburger Gartenbaukulturen: Ein Beitrag zur Kenntnis ihrer Erreger. *Gartenbauwissenschaft*, 493-528.
- Steventon, L. A., Fahleson, J., Qiong, H. U., & Dixelius, C. (2002). Identification of the causal agent of *Verticillium* wilt of winter oilseed rape in Sweden, *V. longisporum*. *Mycological Research*, 106(5), 570-578.
- Strayer, C., Oyama, T., Schultz, T. F., Raman, R., Somers, D. E., Más, P., ... & Kay, S. A. (2000). Cloning of the *Arabidopsis* clock gene TOC1, an autoregulatory response regulator homolog. *Science*, 289(5480), 768-771.
- Subbarao, K. V., Hubbard, J. C., & Schulbach, K. F. (1997). Comparison of lettuce diseases and yield under subsurface drip and furrow irrigation. *Phytopathology*, 87(8), 877-883.
- Sugimoto, K., Gordon, S. P., & Meyerowitz, E. M. (2011). Regeneration in plants and animals: dedifferentiation, transdifferentiation, or just differentiation?. *Trends in cell biology*, 21(4), 212-218.
- Svensson, C., & Lerenius, C. (1987). An investigation on the effect of *Verticillium* wilt (*Verticillium dahliae* Kleb.) on oilseed rape. *Bulletin SROP*, 10(4), 30-34.
- Syers, J. K., Curtin, D., & Skinner, R. J. (1987). Soil and fertiliser sulphur in UK agriculture. *Proceedings-the Fertiliser Society of London*.
- Takahashi, H., Kopriva, S., Giordano, M., Saito, K., & Hell, R. (2011). Sulfur assimilation in photosynthetic organisms: molecular functions and regulations of transporters and assimilatory enzymes. *Annual review of plant biology*, 62, 157-184.
- Takahashi, H., Watanabe-Takahashi, A., Smith, F. W., Blake-Kalff, M., Hawkesford, M. J., & Saito, K. (2000). The roles of three functional sulphate transporters involved in uptake and translocation of sulphate in *Arabidopsis thaliana*. *The Plant Journal*, 23(2), 171-182.
- Takken, F. L., Albrecht, M., & Tameling, W. I. (2006). Resistance proteins: molecular switches of plant defence. *Current opinion in plant biology*, 9(4), 383-390.
- Talboys, P. W. (1972). Resistance to vascular wilt fungi. *Proceedings of the Royal Society of London. Series B. Biological Sciences*, 181(1064), 319-332.
- Talboys, P. W. (1958). Association of tylosis and hyperplasia of the xylem with vascular invasion of the hop by *Verticillium albo-atrum*. *Transactions of the British Mycological Society*, 41(2), 249-IN8.



## References

- Tan, J., Bednarek, P., Liu, J., Schneider, B., Svatoš, A., & Hahlbrock, K. (2004). Universally occurring phenylpropanoid and species-specific indolic metabolites in infected and uninfected *Arabidopsis thaliana* roots and leaves. *Phytochemistry*, 65(6), 691-699.
- Tao, Y., Xie, Z., Chen, W., Glazebrook, J., Chang, H. S., Han, B., ... & Katagiri, F. (2003). Quantitative nature of *Arabidopsis* responses during compatible and incompatible interactions with the bacterial pathogen *Pseudomonas syringae*. *The Plant Cell*, 15(2), 317-330.
- Tatum, L. A. (1971). The southern corn leaf blight epidemic. *Science*, 171(3976), 1113-1116.
- Team, R. Core. (2019). R: A Language and Environment for Statistical Computing, Version 3.3. 1. Vienna, Austria: R Foundation for Statistical Computing; 2016.
- Temple-Heald, C. (2004). High erucic oil: its production and uses. *Rapeseed and Canola Oil: Productions, Properties and Uses*, Blackwell Publishing, CRC Press, Oxford, 111-129.
- Thies, W. (1979). Detection and utilization of a glucosinolate sulfohydrolase in the edible snail, *Helix pomatia*. *Naturwissenschaften*, 66(7), 364-365.
- Thilmony, R., Underwood, W., & He, S. Y. (2006). Genome-wide transcriptional analysis of the *Arabidopsis thaliana* interaction with the plant pathogen *Pseudomonas syringae* pv. *tomato* DC3000 and the human pathogen *Escherichia coli* O157: H7. *The Plant Journal*, 46(1), 34-53.
- Thrower, L. B. (1966). Terminology for plant parasites. *Journal of Phytopathology*, 56(3), 258-259.
- Timpner, C., Braus-Stromeyer, S. A., Tran, V. T., & Braus, G. H. (2013). The Cpc1 regulator of the cross-pathway control of amino acid biosynthesis is required for pathogenicity of the vascular pathogen *Verticillium longisporum*. *Molecular plant-microbe interactions*, 26(11), 1312-1324.
- Tisdale, S. L., Reneau, R. B., & Platou, J. S. (1986). Atlas of sulfur deficiencies. *Sulfur in agriculture*, (sulfurinagricul), 295-322.
- Tran, S. A. B., Stromeyer, C. T., & Gerhard, H. B. (2013). Molecular diagnosis to discriminate pathogen and apathogen species of the hybrid *Verticillium longisporum* on the oilseed crop *Brassica napus*. *Applied microbiology and biotechnology*, 97(10), 4467.
- Treshow, M., & Anderson, F. K. (1989). *Plant stress from air pollution*. John Wiley and Sons Ltd.
- Truman, W., de Zabala, M. T., & Grant, M. (2006). Type III effectors orchestrate a complex interplay between transcriptional networks to modify basal defence responses during pathogenesis and resistance. *The Plant Journal*, 46(1), 14-33.

## References

- Tsuda, K., & Katagiri, F. (2010). Comparing signaling mechanisms engaged in pattern-triggered and effector-triggered immunity. *Current opinion in plant biology*, 13(4), 459-465.
- Tsuda, K., Sato, M., Glazebrook, J., Cohen, J. D., & Katagiri, F. (2008). Interplay between MAMP-triggered and SA-mediated defense responses. *The Plant Journal*, 53(5), 763-775.
- Tsunoda, S. (1980). Eco-physiology of wild and cultivated forms in *Brassica* and allied genera. *Eco-physiology of wild and cultivated forms in Brassica and allied genera.*, 109-120.
- Tuncel, G., & Nergiz, C. (1993). Antimicrobial effect of some olive phenols in a laboratory medium. *Letters in applied microbiology*, 17(6), 300-302.
- Ullstrup, A. J. (1972). The impacts of the southern corn leaf blight epidemics of 1970-1971. *Annual review of phytopathology*, 10(1), 37-50.
- Underhill, E. W., Wetter, L. R., & Chisholm, M. D. (1973). Biosynthesis of glucosinolates. In *Biochemical Society Symposium* (No. 38, pp. 303-326).
- Van der Kooij, T. A. W., De Kok, L. J., Haneklaus, S., & Schnug, E. (1997). Uptake and metabolism of sulphur dioxide by *Arabidopsis thaliana*. *The New Phytologist*, 135(1), 101-107.
- VanderMolen, G. E., Labavitch, J. M., Strand, L. L., & DeVay, J. E. (1983). Pathogen-induced vascular gels: Ethylene as a host intermediate. *Physiologia Plantarum*, 59(4), 573-580.
- VanEtten, H. D., Mansfield, J. W., Bailey, J. A., & Farmer, E. E. (1994). Two classes of plant antibiotics: phytoalexins versus "phytoanticipins". *The Plant Cell*, 6(9), 1191.
- van Kan, J. A. (2006). Licensed to kill: the lifestyle of a necrotrophic plant pathogen. *Trends in plant science*, 11(5), 247-253.
- Vaughan, J. G. (1977). A multidisciplinary study of the taxonomy and origin of Brassica crops. *BioScience*, 27(1), 35-40.
- Veronese, P., Narasimhan, M. L., Stevenson, R. A., Zhu, J. K., Weller, S. C., Subbarao, K. V., & Bressan, R. A. (2003). Identification of a locus controlling Verticillium disease symptom response in *Arabidopsis thaliana*. *The Plant Journal*, 35(5), 574-587.
- Vlot, A. C., Klessig, D. F., & Park, S. W. (2008). Systemic acquired resistance: the elusive signal (s). *Current opinion in plant biology*, 11(4), 436-442.
- Wang, Z. Y., & Tobin, E. M. (1998). Constitutive expression of the CIRCADIAN CLOCK ASSOCIATED 1 (CCA1) gene disrupts circadian rhythms and suppresses its own expression. *Cell*, 93(7), 1207-1217.

## References

- Wang, J. Y., Cai, Y., Gou, J. Y., Mao, Y. B., Xu, Y. H., Jiang, W. H., & Chen, X. Y. (2004). VdNEP, an elicitor from *Verticillium dahliae*, induces cotton plant wilting. *Appl. Environ. Microbiol.*, 70(8), 4989-4995.
- Wang, B. L., Shi, L., Li, Y. X., & Zhang, W. H. (2010). Boron toxicity is alleviated by hydrogen sulfide in cucumber (*Cucumis sativus* L.) seedlings. *Planta*, 231(6), 1301-1309.
- Wang, W., Barnaby, J. Y., Tada, Y., Li, H., Tör, M., Caldelari, D., ... & Dong, X. (2011). Timing of plant immune responses by a central circadian regulator. *Nature*, 470(7332), 110.
- Wardrop, A. B. (1971). Lignins in the plant kingdom. Occurrence and formation in plants. In KV Sarkanen, CH Ludwig, eds, Lignins. Occurrence, Formation, Structure and Reactions.
- Warwick, S. I., Francis, A., & Gugel, R. K. (2009). Guide to wild germplasm of Brassica and allied crops (tribe Brassiceae, Brassicaceae). *Canada: Agriculture and Agri-Food Canada*, 1-6.
- Weese, A., Pallmann, P., Papenbrock, J., & Riemenschneider, A. (2015). *Brassica napus* L. cultivars show a broad variability in their morphology, physiology and metabolite levels in response to sulfur limitations and to pathogen attack. *Frontiers in plant science*, 6, 9.
- West, J. S., Townsend, J. A., Stevens, M., & Fitt, B. D. (2012). Comparative biology of different plant pathogens to estimate effects of climate change on crop diseases in Europe. *European Journal of Plant Pathology*, 133(1), 315-331.
- Westerman, S., Stulen, I., Suter, M., Brunold, C., & De Kok, L. J. (2001). Atmospheric H<sub>2</sub>S as sulphur source for *Brassica oleracea*: consequences for the activity of the enzymes of the assimilatory sulphate reduction pathway. *Plant Physiology and Biochemistry*, 39(5), 425-432.
- Wilhelm, S. (1955). Longevity of the *Verticillium* wilt fungus in the laboratory and field. *Phytopathology*, 45, 180-181.
- Williams, J. S., & Cooper, R. M. (2003). Elemental sulphur is produced by diverse plant families as a component of defence against fungal and bacterial pathogens. *Physiological and Molecular Plant Pathology*, 63(1), 3-16.
- Williams, J. S., Hall, S. A., Hawkesford, M. J., Beale, M. H., & Cooper, R. M. (2002). Elemental sulfur and thiol accumulation in tomato and defense against a fungal vascular pathogen. *Plant Physiology*, 128(1), 150-159.
- Williamson, B., Tudzynski, B., Tudzynski, P., & van Kan, J. A. (2007). *Botrytis cinerea*: the cause of grey mould disease. *Molecular plant pathology*, 8(5), 561-580.
- Williamson, V. M., & Hussey, R. S. (1996). Nematode pathogenesis and resistance in plants. *The Plant Cell*, 8(10), 1735.

## References

- Wilson, R. A., & Talbot, N. J. (2009). Under pressure: investigating the biology of plant infection by *Magnaporthe oryzae*. *Nature Reviews Microbiology*, 7(3), 185.
- Windsor, A. J., Reichelt, M., Figuth, A., Svatoš, A., Kroymann, J., Kliebenstein, D. J., ... & Mitchell-Olds, T. (2005). Geographic and evolutionary diversification of glucosinolates among near relatives of *Arabidopsis thaliana* (Brassicaceae). *Phytochemistry*, 66(11), 1321-1333.
- Wittkop, B., Snowdon, R. J., & Friedt, W. (2009). Status and perspectives of breeding for enhanced yield and quality of oilseed crops for Europe. *Euphytica*, 170(1-2), 131.
- Wittstock, U., & Halkier, B. A. (2002). Glucosinolate research in the *Arabidopsis* era. *Trends in plant science*, 7(6), 263-270.
- Witzel, K., Hanschen, F. S., Klopsch, R., Ruppel, S., Schreiner, M., & Grosch, R. (2015). *Verticillium longisporum* infection induces organ-specific glucosinolate degradation in *Arabidopsis thaliana*. *Frontiers in plant science*, 6, 508.
- Witzel, K., Hanschen, F. S., Schreiner, M., Krumbein, A., Ruppel, S., & Grosch, R. (2013). *Verticillium* suppression is associated with the glucosinolate composition of *Arabidopsis thaliana* leaves. *PLoS One*, 8(9), e71877.
- Woodard, J. (1922). Sulphur as a factor in soil fertility. *Botanical Gazette*, 73(2), 81-109.
- Xiang, C., & Oliver, D. J. (1998). Glutathione metabolic genes coordinately respond to heavy metals and jasmonic acid in *Arabidopsis*. *The Plant Cell*, 10(9), 1539-1550.
- Yadeta, K., & Thomma, B. (2013). The xylem as battleground for plant hosts and vascular wilt pathogens. *Frontiers in plant science*, 4, 97.
- Yang, G., Wu, L., Jiang, B., Yang, W., Qi, J., Cao, K., ... & Snyder, S. H. (2008). H<sub>2</sub>S as a physiologic vasorelaxant: hypertension in mice with deletion of cystathionine  $\gamma$ -lyase. *Science*, 322(5901), 587-590.
- Yoshimoto, N., Inoue, E., Watanabe-Takahashi, A., Saito, K., & Takahashi, H. (2007). Posttranscriptional regulation of high-affinity sulfate transporters in *Arabidopsis* by sulfur nutrition. *Plant physiology*, 145(2), 378-388.
- Yoshimoto, N., Takahashi, H., Smith, F. W., Yamaya, T., & Saito, K. (2002). Two distinct high-affinity sulfate transporters with different inducibilities mediate uptake of sulfate in *Arabidopsis* roots. *The Plant Journal*, 29(4), 465-473.
- Zechmann, B. (2017). Diurnal changes of subcellular glutathione content in *Arabidopsis thaliana*. *Biologia plantarum*, 61(4), 791-796.
- Zechmann, B. (2014). Compartment-specific importance of glutathione during abiotic and biotic stress. *Frontiers in plant science*, 5, 566.

## References

- Zechmann, B., Zellnig, G., Urbanek-Krajnc, A., & Müller, M. (2007). Artificial elevation of glutathione affects symptom development in ZYMV-infected *Cucurbita pepo* L. plants. *Archives of virology*, *152*(4), 747-762.
- Zeeman, S. C., Smith, S. M., & Smith, A. M. (2006). The diurnal metabolism of leaf starch. *Biochemical Journal*, *401*(1), 13-28.
- Zeise, K., & von Tiedemann, A. (2002). Host specialization among vegetative compatibility groups of *Verticillium dahliae* in relation to *Verticillium longisporum*. *Journal of Phytopathology*, *150*(3), 112-119.
- Zeise, K., & von Tiedemann, A. (2001). Morphological and physiological differentiation among vegetative compatibility groups of *Verticillium dahliae* in relation to *V. longisporum*. *Journal of Phytopathology*, *149*(7-8), 469-475.
- Zhang, C., Gao, M., Seitz, N. C., Angel, W., Hallworth, A., Wiratan, L., ... & Egoshi, R. (2019). LUX ARRHYTHMO mediates crosstalk between the circadian clock and defense in *Arabidopsis*. *Nature communications*, *10*(1), 2543.
- Zhang, C., Xie, Q., Anderson, R. G., Ng, G., Seitz, N. C., Peterson, T., ... & Lu, H. (2013). Crosstalk between the circadian clock and innate immunity in *Arabidopsis*. *PLoS pathogens*, *9*(6), e1003370.
- Zhang, H., Hu, L. Y., Li, P., Hu, K. D., Jiang, C. X., & Luo, J. P. (2010). Hydrogen sulfide alleviated chromium toxicity in wheat. *Biologia Plantarum*, *54*(4), 743-747.
- Zhang, H., Hu, L. Y., Hu, K. D., He, Y. D., Wang, S. H., & Luo, J. P. (2008). Hydrogen sulfide promotes wheat seed germination and alleviates oxidative damage against copper stress. *Journal of Integrative Plant Biology*, *50*(12), 1518-1529.
- Zhang, J., Elo, A., & Helariutta, Y. (2011). *Arabidopsis* as a model for wood formation. *Current Opinion in Biotechnology*, *22*(2), 293-299.
- Zhang, L., Du, L., & Poovaiah, B. W. (2014). Calcium signaling and biotic defense responses in plants. *Plant signaling & behavior*, *9*(11), e973818.
- Zhang, Y. (1993). Overview of rapeseed production and research in China. In *Oil crops: Brassica Subnetwork; proceedings of the Third Workshop, Quality Training, and Chinese Project Reports, held in Shanghai, People's Republic of China, 21-24 Apr. 1990*. IDRC, Ottawa, ON, CA.
- Zhao, Y., Hull, A. K., Gupta, N. R., Goss, K. A., Alonso, J., Ecker, J. R., ... & Celenza, J. L. (2002). Trp-dependent auxin biosynthesis in *Arabidopsis*: involvement of cytochrome P450s CYP79B2 and CYP79B3. *Genes & development*, *16*(23), 3100-3112.
- Zheng, X. Y., Zhou, M., Yoo, H., Pruneda-Paz, J. L., Spivey, N. W., Kay, S. A., & Dong, X. (2015). Spatial and temporal regulation of biosynthesis of the plant immune signal salicylic acid. *Proceedings of the National Academy of Sciences*, *112*(30), 9166-9173.

## References

- Zhou, J. M., Trifa, Y., Silva, H., Pontier, D., Lam, E., Shah, J., & Klessig, D. F. (2000). NPR1 differentially interacts with members of the TGA/OBF family of transcription factors that bind an element of the PR-1 gene required for induction by salicylic acid. *Molecular Plant-Microbe Interactions*, 13(2), 191-202.
- Zhou, L., Hu, Q., Johansson, A., & Dixelius, C. (2006). *Verticillium longisporum* and *V. dahliae*: infection and disease in *Brassica napus*. *Plant Pathology*, 55(1), 137-144.
- Zhou, M., Wang, W., Karapetyan, S., Mwimba, M., Marqués, J., Buchler, N. E., & Dong, X. (2015). Redox rhythm reinforces the circadian clock to gate immune response. *Nature*, 523(7561), 472.
- Zhou, Y., Fitt, B. D., Welham, S. J., Gladders, P., Sansford, C. E., & West, J. S. (1999). Effects of severity and timing of stem canker (*Leptosphaeria maculans*) symptoms on yield of winter oilseed rape (*Brassica napus*) in the UK. *European Journal of Plant Pathology*, 105(7), 715-728.
- Zipfel, C. (2008). Pattern-recognition receptors in plant innate immunity. *Current opinion in immunology*, 20(1), 10-16.
- Zipfel, C., & Felix, G. (2005). Plants and animals: a different taste for microbes?. *Current opinion in plant biology*, 8(4), 353-360.

## 6. Appendix

Supplement data for the first and second run of the main experiment.

Significant codes for the statistical evaluations: extremely significant: '\*\*\*\*' <0.001; very significant: '\*\*\*' <0.01; significant: '\*' <0.05.

### First run: Statistical data of qPCR analysis

**Table 6.1: First run: statistical analysis of VL-DNA (ITS primers) compared with different effects.** Df: degrees of freedom in the source; Sum seq: sum of squares due to the source; Mean seq: mean squares; F value: F ratio of two mean square value; P value: level of marginal significance within a statistical hypothesis test representing the probability of the occurrence of a given event.

Effect	Df	Sum Sq	Mean Sq	F value	P value
dpi	2	5.51	2.75	14.78	0.00103
TPI	3	0.99	0.33	1.77	0.22
dpi:TPI	6	1.39	0.23	1.24	0.36
dpi:+/- sulfur supply	2	0.69	0.34	1.85	0.21

**Table 6.2: First run: statistical analysis of VL-DNA ( $\beta$ -tubulin primers) compared with different effects.** Df: degrees of freedom in the source; Sum seq: sum of squares due to the source; Mean seq: mean squares; F value: F ratio of two mean square value; P value: level of marginal significance within a statistical hypothesis test representing the probability of the occurrence of a given event.

Effect	Df	Sum Sq	Mean Sq	F value	P value
dpi	2	5.91	2.95	21.99	0.00022
TPI	3	1.17	0.39	2.90	0.09
dpi:TPI	6	1.21	0.20	1.51	0.27
dpi:+/- sulfur supply	2	0.26	0.13	0.97	0.41

## Appendix

**First run: images of control and VL-infected plants under sufficient and deficient sulfur supply at 7 dpi**

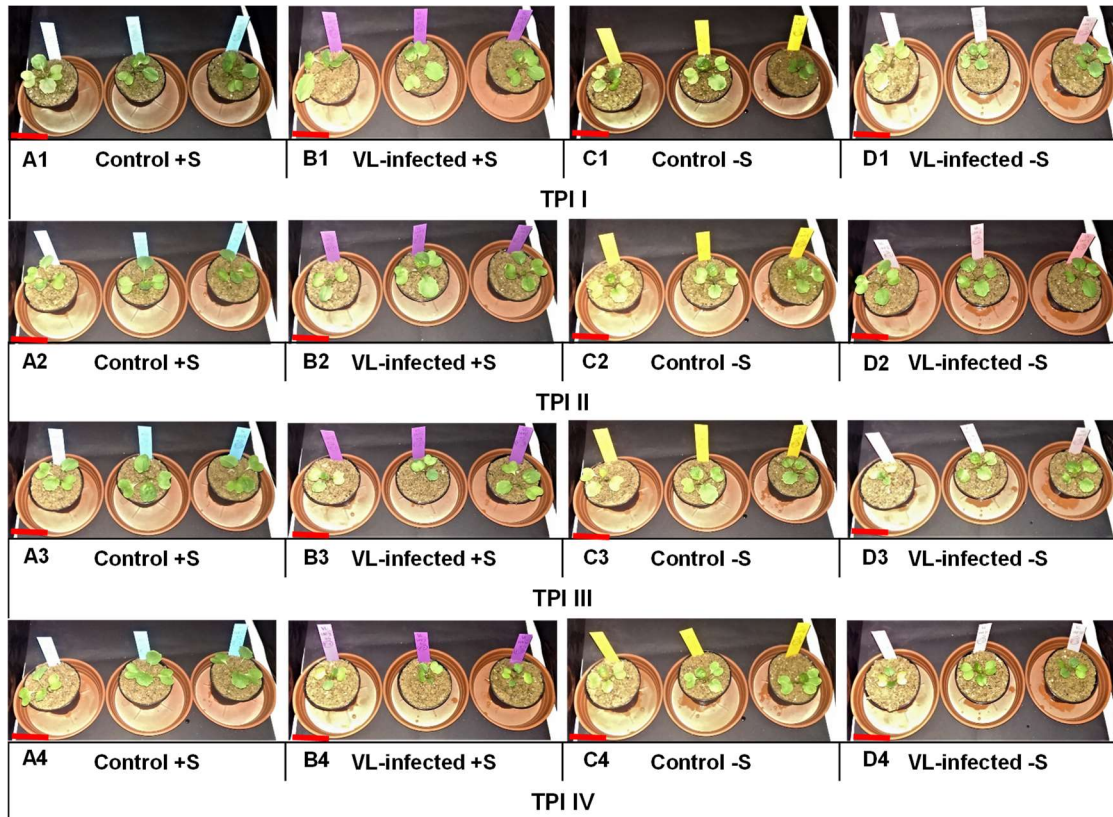


**Figure 6.1: First run: control and VL-infected plants under sufficient and deficient sulfur supply at 7 dpi. A1-A4: control +S at TPI I-IV; B1-B4: VL-infected +S at TPI I-IV; C1-C4: control -S at TPI I-IV; D1-D4: VL-infected -S at TPI I-IV; red scale bar 5 cm.**

### **First run: cross sections of hypocotyls of control plants**

Toluidine blue stained cross sections of hypocotyls of control plants under sufficient and deficient sulfur supply were occlusions-free (**Fig. 6.2**). They occasionally showed occlusions in the peripheral area.



## Appendix

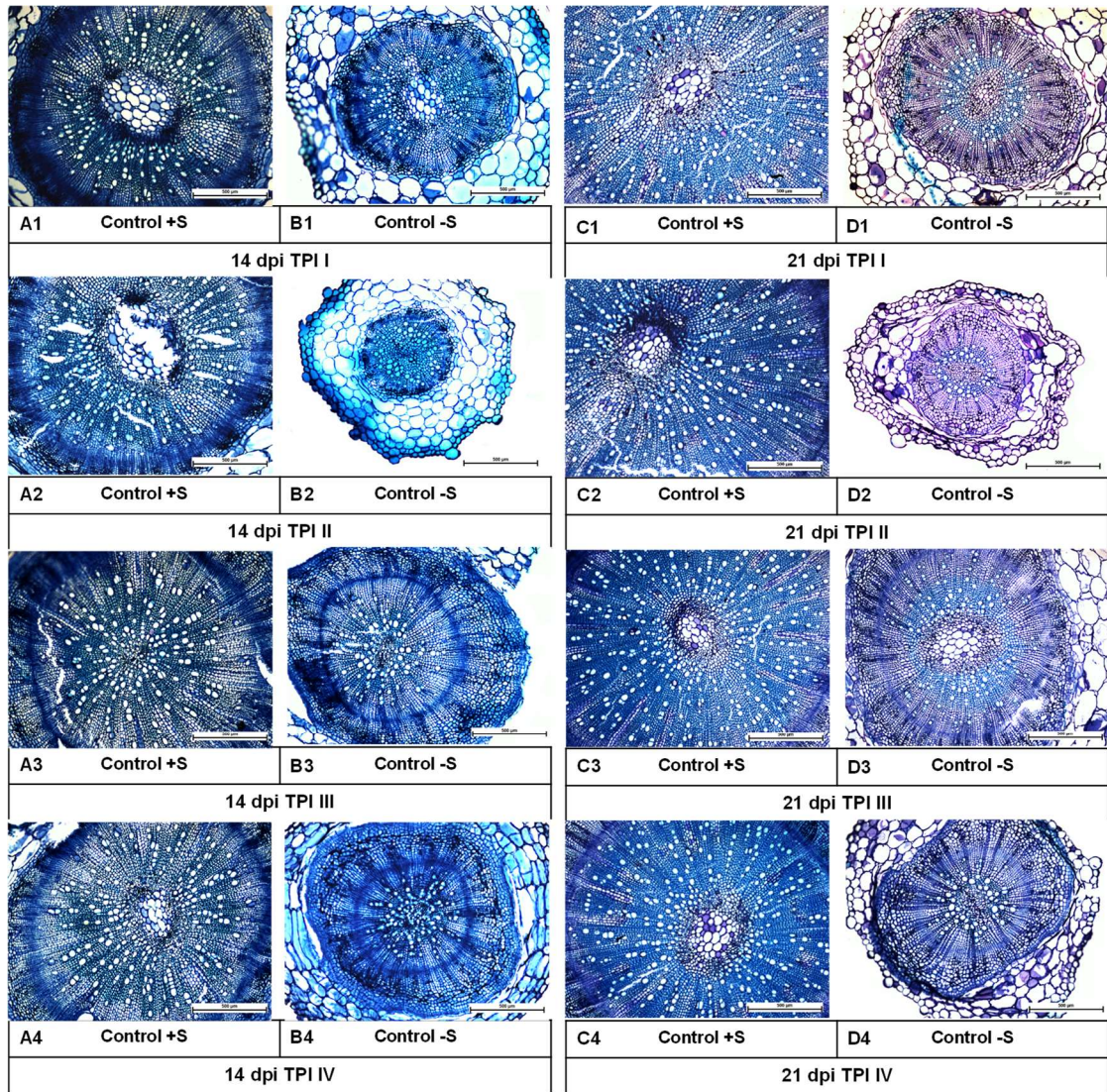


**Figure 6.2: First run: cross sections of hypocotyls of control plants at 14 and 21 dpi.** Cross-sections were stained with toluidine blue; **14 dpi: A1-A4:** control +S at TPI I-IV; **B1-B4:** control -S at TPI I-IV; **21 dpi: C1-C4:** control +S at TPI I-IV; **D1-D4:** control -S at TPI I-IV; scale bar 500  $\mu\text{m}$ .

## Appendix

### First run: statistical data of sulfur, calcium, potassium and iron

**Table 6.3: First run: statistical analysis of sulfur compared with different effects.** Df: degrees of freedom in the source; Sum seq: sum of squares due to the source; Mean seq: mean squares; F value: F ratio of two mean square value; P value: level of marginal significance within a statistical hypothesis test representing the probability of the occurrence of a given event: significant codes.

Effect	Df	Sum Sq	Mean Sq	F value	P value
dpi	1	25.80	25.80	36.13	0.02944
control.VL-infected	1	3.69	3.69	5.16	0.04071
TPI	3	0.53	0.18	0.25	0.86
+/- sulfur supply	1	210.76	210.76	295.18	0.00012
dpi:control.VL-infected	1	0.80	0.80	1.12	0.31
dpi:TPI	3	3.02	1.01	1.41	0.28
dpi:+/- sulfur supply	1	1.48	1.48	2.07	0.17
control.VL-infected:TPI	3	2.03	0.68	0.95	0.45
control.VL-infected:+/- sulfur supply	1	5.89	5.89	8.25	0.01
TPI:+/- sulfur supply	3	2.71	0.90	1.26	0.33

**Table 6.4: First run: statistical analysis of calcium compared with different effects.** Df: degrees of freedom in the source; Sum seq: sum of squares due to the source; Mean seq: mean squares; F value: F ratio of two mean square value; P value: level of marginal significance within a statistical hypothesis test representing the probability of the occurrence of a given event: significant codes.

Effect	Df	Sum Sq	Mean Sq	F value	P value
dpi	1	11.41	11.41	2.44	0.14
control.VL-infected	1	80.71	80.71	17.25	0.00113
TPI	3	22.91	7.637	1.63	0.23
+/- sulfur supply	1	48.83	48.83	10.44	0.00656
dpi:control.VL-infected	1	16.40	16.40	3.51	0.08
dpi:TPI	3	3.71	1.24	0.2641	0.85
dpi:+/- sulfur supply	1	47.66	47.66	10.19	0.00708
control.VL-infected:TPI	3	17.31	5.77	1.23	0.34
control.VL-infected:+/- sulfur supply	1	6.36	6.36	1.36	0.26
TPI:+/- sulfur supply	3	6.08	2.02	0.43	0.73

**Table 6.5: First run: statistical analysis of potassium compared with different effects.** Df: degrees of freedom in the source; Sum seq: sum of squares due to the source; Mean seq: mean squares; F value: F ratio of two mean square value; P value: level of marginal significance within a statistical hypothesis test representing the probability of the occurrence of a given event.

Effect	Df	Sum Sq	Mean Sq	F value	P value
dpi	1	3293.10	3293.10	277.07	0.00017
control.VL-infected	1	2240.20	2240.20	188.49	0.00051
TPI	3	182.90	61.0	5.13	0.01472
+/- sulfur supply	1	43.90	43.90	3.70	0.07676
dpi:control.VL-infected	1	662.1	662.10	55.70	0.01175
dpi:TPI	3	176.0	58.70	4.94	0.01672
dpi:+/- sulfur supply	1	413.0	413.0	34.75	0.03558
control.VL-infected:TPI	3	70.50	23.50	1.98	0.17
control.VL-infected:+/- sulfur supply	1	231.30	231.30	19.46	0.00070
TPI:+/- sulfur supply	3	22.90	7.60	0.64	0.60

## Appendix

**Table 6.6: First run: statistical analysis of iron compared with different effects.** Df: degrees of freedom in the source; Sum seq: sum of squares due to the source; Mean seq: mean squares; F value: F ratio of two mean square value; P value: level of marginal significance within a statistical hypothesis test representing the probability of the occurrence of a given event.

Effect	Df	Sum Sq	Mean Sq	F value	P value
dpi	1	19760.40	19760.40	126.73	0.00150
control.VL-infected	1	100.80	100.80	0.65	0.44
TPI	3	2015.70	671.90	4.31	0.02568
+/- sulfur supply	1	21.70	21.70	0.14	0.72
dpi:control.VL-infected	1	3.80	3.80	0.02	0.88
dpi:TPI	3	973.0	324.30	2.08	0.15
dpi:+/- sulfur supply	1	1904.30	1904.30	12.21	0.00395
control.VL-infected:TPI	3	844.70	281.60	1.81	0.20
control.VL-infected:+/- sulfur supply	1	77.60	77.60	0.50	0.49
TPI:+/- sulfur supply	3	1538.10	512.70	3.29	0.06

### First run: standard deviation and statistical data of glucosinolates

Depend on limited plant material three extracts each sample were prepared for the GSL analysis for approximately half of the samples. **Table 6.7** (IGSLs), **Table 6.12** (AGSLs) and **Table 6.20** (BGSL) show the calculated standard derivations with the corresponding GSL value based on the dependent technical replicates.

**Table 6.7: First run: values of IGSL content  $\pm$  SD at 14 dpi.** Data were calculated in nmol g<sup>-1</sup> DW and based on three dependent technical replicates.

IGSLs	Control +S	VL-infected +S	Control -S	VL-infected -S
<b>Glucobrassicin</b>				
TPI I	89.41 $\pm$ 4.86	94.49 $\pm$ 2.67	-	-
TPI II	-	-	0.17 $\pm$ 0.02	4.02 $\pm$ 0.33
TPI III	111.84 $\pm$ 7.85	-	-	-
TPI IV	-	128.79 $\pm$ 2.33	-	4.02 $\pm$ 0.18
<b>Neoglucobrassicin</b>				
TPI I	18.52 $\pm$ 1.79	18.72 $\pm$ 1.30	-	-
TPI II	-	-	2.86 $\pm$ 0.84	5.11 $\pm$ 0.68
TPI III	22.83 $\pm$ 0.45	-	-	-
TPI IV	-	24.57 $\pm$ 1.75	-	3.53 $\pm$ 0.19
<b>4-Hydroxy-glucobrassicin</b>				
TPI I	11.33 $\pm$ 1.96	10.69 $\pm$ 3.95	-	-
TPI II	-	-	0.15 $\pm$ 0.03	0.30 $\pm$ 0.03
TPI III	22.61 $\pm$ 2.67	-	-	-
TPI IV	-	21.10 $\pm$ 1.09	-	0.19 $\pm$ 0.03

## Appendix

**Table 6.8: First run: statistical analysis of IGSLs compared with different effects.** Df: degrees of freedom in the source; Sum seq: sum of squares due to the source; Mean seq: mean squares; F value: F ratio of two mean square value; P value: level of marginal significance within a statistical hypothesis test representing the probability of the occurrence of a given event: significant codes.

Effect	Df	Sum Sq	Mean Sq	F value	P value
dpi	1	5.11	5.11	355.15	0.00013
control.VL-infected	1	0.01	0.01	0.7	0.42
TPI	3	0.21	0.07	4.82	0.02
+/- sulfur supply	1	4.90	4.90	340.30	0.00005
dpi:control.VL-infected	1	0.01	0.01	0.86	0.37194
dpi:TPI	3	0.04	0.01	0.85	0.49
dpi:+/- sulfur supply	1	2.84	2.84	197.75	0.00038
control.VL-infected:TPI	3	0.20	0.07	4.53	0.02
control.VL-infected:+/-sulfur supply	1	0.01	0.01	0.70	0.42
TPI:+/- sulfur supply	3	0.07	0.02	1.69	0.22

**Table 6.9: First run: statistical analysis of glucobrassicin compared with different effects.** Df: degrees of freedom in the source; Sum seq: sum of squares due to the source; Mean seq: mean squares; F value: F ratio of two mean square value; P value: level of marginal significance within a statistical hypothesis test representing the probability of the occurrence of a given event.

Effect	Df	Sum Sq	Mean Sq	F value	P value
dpi	1	9.63	9.63	128.41	0.00139
control.VL-infected	1	0.20	0.20	2.71	0.46
TPI	3	0.58	0.19	2.60	0.097
+/- sulfur supply	1	9.31	9.31	124.11	0.00170
dpi:control.VL-infected	1	0.01	0.01	0.18	0.68
dpi:TPI	3	0.21	0.07	0.95	0.45
dpi:+/- sulfur supply	1	5.91	5.91	78.74	0.00645
control.VL-infected:TPI	3	0.552	0.184	2.45	0.11
control.VL-infected:+/- sulfur supply	1	0.03	0.02	0.33	0.58
TPI:+/- sulfur supply	3	0.32	0.11	1.42	0.28

**Table 6.10: First run: statistical analysis of neoglucobrassicin compared with different effects.** Df: degrees of freedom in the source; Sum seq: sum of squares due to the source; Mean seq: mean squares; F value: F ratio of two mean square value; P value: level of marginal significance within a statistical hypothesis test representing the probability of the occurrence of a given event.

Effect	Df	Sum Sq	Mean Sq	F value	P value
dpi	1	1.83	1.83	111.82	0.00314
control.VL-infected	1	0.16	0.16	9.70	0.00821
TPI	3	0.06	0.020	1.22	0.34
+/- sulfur supply	1	1.20	1.20	73.07	0.00266
dpi:control.VL-infected	1	0.01	0.01	0.53	0.48
dpi:TPI	3	0.05	0.02	1.11	0.38
dpi:+/- sulfur supply	1	0.88	0.88	53.96	0.01393
control.VL-infected:TPI	3	0.07	0.02	1.32	0.31
control.VL-infected:+/- sulfur supply	1	0.01	0.01	0.31	0.59
TPI:+/- sulfur supply	3	0.03	0.01	0.70	0.57

## Appendix

**Table 6.11: First run: statistical analysis of 4-hydroxyglucobrassicin compared with different effects.** Df: degrees of freedom in the source; Sum seq: sum of squares due to the source; Mean seq: mean squares; F value: F ratio of two mean square value; P value: level of marginal significance within a statistical hypothesis test representing the probability of the occurrence of a given event.

Effect	Df	Sum Sq	Mean Sq	F value	P value
dpi	1	4.78	4.78	69.87	0.00342
control.VL-infected	1	0.01	0.01	0.07	0.79
TPI	3	0.37	0.12	1.79	0.20
+/- sulfur supply	1	7.89	7.89	115.21	0.00264
dpi:control.VL-infected	1	0.09	0.09	1.28	0.28
dpi:TPI	3	0.08	0.03	0.37	0.78
dpi:+/- sulfur supply	1	5.72	5.72	83.48	0.00463
control.VL-infected:TPI	3	0.11	0.04	0.55	0.66
control.VL-infected:+/- sulfur supply	1	0.07	0.07	0.99	0.34
TPI:+/- sulfur supply	3	0.06	0.02	0.29	0.83

**Table 6.12: First run: values of AGSL content  $\pm$  SD at 14 dpi.** Data were calculated in nmol g<sup>-1</sup> DW and based on three dependent technical replicates.

AGSLs	Control +S	VL-infected +S	Control -S	VL-infected -S
<b>Progoitrin</b>				
TPI I	75.73 $\pm$ 5.39	81.23 $\pm$ 8.60	-	-
TPI II	-	-	1.12 $\pm$ 0.39	0.94 $\pm$ 0.23
TPI III	144.08 $\pm$ 13.49	-	-	-
TPI IV	-	115.09 $\pm$ 3.81	-	0.39 $\pm$ 0.03
<b>Glucoalyssin</b>				
TPI I	62.20 $\pm$ 3.60	62.70 $\pm$ 5.49	-	-
TPI II	-	-	4.75 $\pm$ 1.39	4.66 $\pm$ 0.33
TPI III	121.51 $\pm$ 15.68	-	-	-
TPI IV	-	76.85 $\pm$ 4.06	-	3.62 $\pm$ 0.31
<b>Glucoraphanin</b>				
TPI I	13.59 $\pm$ 0.70	10.89 $\pm$ 0.80	-	-
TPI II	-	-	1.77 $\pm$ 0.46	4.31 $\pm$ 1.27
TPI III	15.05 $\pm$ 1.26	-	-	-
TPI IV	-	12.52 $\pm$ 0.87	-	4.96 $\pm$ 0.56
<b>Glucobrassicinapin</b>				
TPI I	40.08 $\pm$ 2.41	42.39 $\pm$ 3.19	-	-
TPI II	-	-	0.05 $\pm$ 0.02	0.18 $\pm$ 0.09
TPI III	72.11 $\pm$ 5.51	-	-	-
TPI IV	-	63.94 $\pm$ 1.25	-	0.44 $\pm$ 0.14
<b>Gluconapin</b>				
TPI I	33.28 $\pm$ 2.52	34.28 $\pm$ 2.91	-	-
TPI II	-	-	0.23 $\pm$ 0.03	1.07 $\pm$ 0.29
TPI III	57.39 $\pm$ 4.87	-	-	-
TPI IV	-	48.91 $\pm$ 2.56	-	1.52 $\pm$ 0.30

**Table 6.13: First run: statistical analysis of AGSLs compared with different effects.** Df: degrees of freedom in the source; Sum seq: sum of squares due to the source; Mean seq: mean squares; F value: F ratio of two mean square value; P value: level of marginal significance within a statistical hypothesis test representing the probability of the occurrence of a given event.

Effect	Df	Sum Sq	Mean Sq	F value	P value
dpi	1	0.99	0.99	104.44	0.00155
control.VL-infected	1	0.70	0.70	73.76	0.00253
TPI	3	0.21	0.07	7.27	0.00415
+/- sulfur supply	1	3.13	3.13	329.89	0.00006
dpi:control.VL-infected	1	0.12	0.12	12.37	0.00379
dpi:TPI	3	0.01	0.003	0.33	0.80
dpi:+/- sulfur supply	1	1.47	1.47	155.37	0.00044
control.VL-infected:TPI	3	0.09	0.03	2.99	0.07
control.VL-infected:+/- sulfur supply	1	0.01	0.01	0.60	0.45
TPI:+/- sulfur supply	3	0.02	0.01	0.70	0.57

## Appendix

**Table 6.14: First run: statistical analysis of progoitrin compared with different effects.** Df: degrees of freedom in the source; Sum seq: sum of squares due to the source; Mean seq: mean squares; F value: F ratio of two mean square value; P value: level of marginal significance within a statistical hypothesis test representing the probability of the occurrence of a given event.

Effect	Df	Sum Sq	Mean Sq	F value	P value
dpi	1	5.30	5.30	146.13	0.00064
control.VL-infected	1	0.21	0.21	5.74	0.03
TPI	3	0.15	0.05	1.36	0.30
+/- sulfur supply	1	11.11	11.11	306.14	0.00009
dpi:control.VL-infected	1	0.24	0.24	6.67	0.023
dpi:TPI	3	0.12	0.04	1.07	0.40
dpi:+/- sulfur supply	1	5.36	5.36	147.81	0.00059
control.VL-infected:TPI	3	0.06	0.02	0.51	0.68
control.VL-infected:+/- sulfur supply	1	0.01	0.01	0.15	0.70
TPI:+/- sulfur supply	3	0.05	0.02	0.49	0.69

**Table 6.15: First run: statistical analysis of glucoalyssin compared with different effects.** Df: degrees of freedom in the source; Sum seq: sum of squares due to the source; Mean seq: mean squares; F value: F ratio of two mean square value; P value: level of marginal significance within a statistical hypothesis test representing the probability of the occurrence of a given event: significant codes.

Effect	Df	Sum Sq	Mean Sq	F value	P value
dpi	1	0.04	0.04	1.03	0.33
control.VL-infected	1	0.21	0.21	5.39	0.04
TPI	3	0.12	0.04	0.9618	0.44
+/- sulfur supply	1	5.55	5.55	139.93	0.00150
dpi:control.VL-infected	1	0.24	0.24	6.05	0.03
dpi:TPI	3	0.09	0.03	0.77	0.53
dpi:+/- sulfur supply	1	0.92	0.92	23.24	0.00034
control.VL-infected:TPI	3	0.13	0.04	1.08	0.39
control.VL-infected:+/- sulfur supply	1	0.04	0.04	0.90	0.36
TPI:+/- sulfur supply	3	0.03	0.01	0.22	0.88

**Table 6.16: First run: statistical analysis of glucoraphanin compared with different effects.** Df: degrees of freedom in the source; Sum seq: sum of squares due to the source; Mean seq: mean squares; F value: F ratio of two mean square value; P value: level of marginal significance within a statistical hypothesis test representing the probability of the occurrence of a given event.

Effect	Df	Sum Sq	Mean Sq	F value	P value
dpi	1	0.58	0.58	18.36	0.00089
control.VL-infected	1	0.49	0.49	15.61	0.00166
TPI	3	0.15	0.05	1.61	0.24
+/- sulfur supply	1	2.38	2.38	75.31	0.00828
dpi:control.VL-infected	1	0.27	0.27	8.52	0.01199
dpi:TPI	3	0.06	0.02	0.58	0.64
dpi:+/- sulfur supply	1	0.09	0.09	2.72	0.12
control.VL-infected:TPI	3	0.18	0.06	1.93	0.18
control.VL-infected:+/- sulfur supply	1	0.001	0.001	0.02	0.88
TPI:+/- sulfur supply	3	0.10	0.04	1.10	0.38

## Appendix

**Table 6.17: First run: statistical analysis of glucobrassicinapin compared with different effects.** Df: degrees of freedom in the source; Sum seq: sum of squares due to the source; Mean seq: mean squares; F value: F ratio of two mean square value; P value: level of marginal significance within a statistical hypothesis test representing the probability of the occurrence of a given event.

Effect	Df	Sum Sq	Mean Sq	F value	P value
dpi	1	4.43	4.43	29.35	0.00012
control.VL-infected	1	0.99	0.99	6.61	0.02322
TPI	3	0.10	0.03	0.21	0.89
+/- sulfur supply	1	23.14	23.14	153.32	0.00048
dpi:control.VL-infected	1	0.001	0.002	0.01	0.92
dpi:TPI	3	0.4	0.15	0.97	0.44
dpi:+/- sulfur supply	1	9.36	9.36	62.04	0.00657
control.VL-infected:TPI	3	0.26	0.09	0.5733	0.64
control.VL-infected:+/- sulfur supply	1	0.19	0.19	1.26	0.28
TPI:+/- sulfur supply	3	0.07	0.02	0.16	0.92

**Table 6.18: First run: statistical analysis of gluconapin compared with different effects.** Df: degrees of freedom in the source; Sum seq: sum of squares due to the source; Mean seq: mean squares; F value: F ratio of two mean square value; P value: level of marginal significance within a statistical hypothesis test representing the probability of the occurrence of a given event.

Effect	Df	Sum Sq	Mean Sq	F value	P value
dpi	1	1.31	1.31	36.76	0.02703
control.VL-infected	1	0.92	0.92	25.83	0.00021
TPI	3	0.39	0.13	3.64	0.04205
+/- sulfur supply	1	10.82	10.82	302.92	0.00009
dpi:control.VL-infected	1	0.10	0.10	2.70	0.12
dpi:TPI	3	0.06	0.02	0.51	0.68
dpi:+/- sulfur supply	1	3.25	3.25	90.86	0.00285
control.VL-infected:TPI	3	0.20	0.06	1.80	0.20
control.VL-infected:+/- sulfur supply	1	0.05	0.05	1.46	0.25
TPI:+/- sulfur supply	3	0.14	0.05	1.28	0.32

**Table 6.19: First run: values of BGSL content  $\pm$  SD at 14 dpi.** Data were calculated in nmol g<sup>-1</sup> DW and based on three dependent technical replicates.

BGSL	Control +S	VL-infected +S	Control -S	VL-infected -S
<b>Gluconasturtiin</b>				
TPI I	50.96 $\pm$ 3.72	74.83 $\pm$ 4.18	-	-
TPI II	-	-	7.51 $\pm$ 1.87	41.63 $\pm$ 3.26
TPI III	58.02 $\pm$ 4.61	-	-	-
TPI IV	-	108.50 $\pm$ 3.44	-	39.03 $\pm$ 0.08

### First run: statistical data of cysteine and glutathione

**Table 6.21: First run: statistical analysis of cysteine compared with different effects.** Df: degrees of freedom in the source; Sum seq: sum of squares due to the source; Mean seq: mean squares; F value: F ratio of two mean square value; P value: level of marginal significance within a statistical hypothesis test representing the probability of the occurrence of a given event.

Effect	Df	Sum Sq	Mean Sq	F value	P value
dpi	1	0.89	0.89	70.67	0.00322
control.VL-infected	1	0.004	0.004	0.29	0.60
TPI	3	0.05	0.02	1.45	0.27
+/- sulfur supply	1	2.37	2.37	188.52	0.0005
dpi:control.VL-infected	1	0.04	0.04	3.09	0.10
dpi:TPI	3	0.07	0.02	1.84	0.19
dpi:+/- sulfur supply	1	0.32	0.32	25.75	0.00021
control.VL-infected:TPI	3	0.03	0.01	0.89	0.47
control.VL-infected:+/- sulfur supply	1	0.001	0.001	0.10	0.76
TPI:+/- sulfur supply	3	0.04	0.01	0.95	0.45

## Appendix

**Table 6.22: First run: statistical analysis of glutathione compared with different effects.**

Df: degrees of freedom in the source; Sum seq: sum of squares due to the source; Mean seq: mean squares; F value: F ratio of two mean square value; P value: level of marginal significance within a statistical hypothesis test representing the probability of the occurrence of a given event.

Effect	Df	Sum Sq	Mean Sq	F value	P value
dpi	1	0.68	0.68	87.31	0.00358
control.VL-infected	1	0.02	0.02	2.14	0.17
TPI	3	0.14	0.05	6.17	0.00770
+/- sulfur supply	1	3.15	3.15	406.26	0.00006
dpi:control.VL-infected	1	0.002	0.002	0.31	0.59
dpi:TPI	3	0.04	0.01	1.75	0.21
dpi:+/- sulfur supply	1	0.54	0.54	69.89	0.00342
control.VL-infected:TPI	3	0.05	0.02	2.29	0.13
control.VL-infected:+/- sulfur supply	1	0.002	0.002	0.25	0.62
TPI:+/- sulfur supply	3	0.08	0.03	3.62	0.04248

### Second run: Statistical data of qPCR analysis

**Table 6.23: Second run: statistical analysis of VL-DNA (ITS primers) compared with different effects.**

Df: degrees of freedom in the source; Sum seq: sum of squares due to the source; Mean seq: mean squares; F value: F ratio of two mean square value; P value: level of marginal significance within a statistical hypothesis test representing the probability of the occurrence of a given event: significant codes.

Effect	Df	Sum Sq	Mean Sq	F value	P value
dpi	2	4.49	2.25	104.44	0.00182
TPI	3	0.08	0.03	1.16	0.37
dpi:TPI	6	0.67	0.11	5.21	0.01118
dpi:+/- sulfur supply	2	1.75	0.88	40.81	0.01044

**Table 6.24: Second run: statistical analysis of VL-DNA ( $\beta$ -tubulin primers) compared with different effects.**

Df: degrees of freedom in the source; Sum seq: sum of squares due to the source; Mean seq: mean squares; F value: F ratio of two mean square value; P value: level of marginal significance within a statistical hypothesis test representing the probability of the occurrence of a given event: significant codes: extremely significant.

Effect	Df	Sum Sq	Mean Sq	F value	P value
dpi	2	5.63	2.82	92.27	0.00327
TPI	3	0.07	0.02	0.73	0.56
dpi:TPI	6	0.63	0.11	3.43	0.04169
dpi:+/- sulfur supply	2	1.31	0.65	21.44	0.00024



## Appendix

**Second run: images of control and VL-infected plants under sufficient and deficient sulfur supply at 7 dpi**

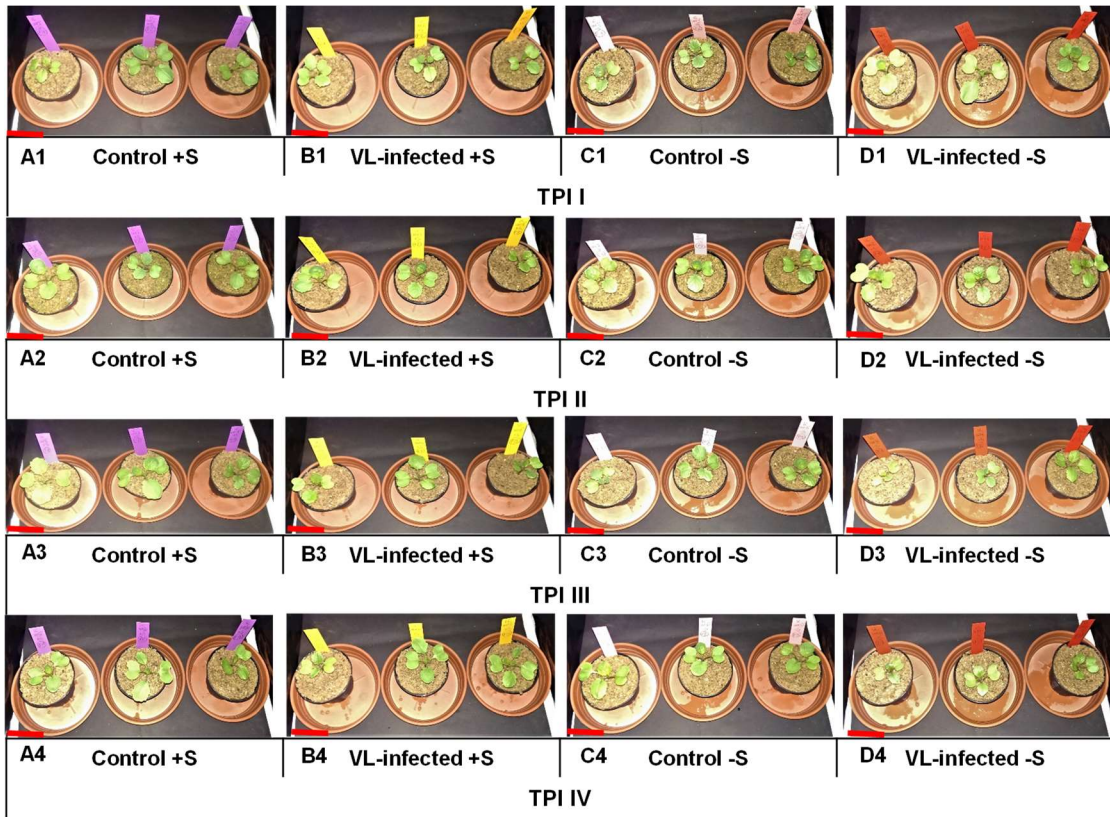


**Figure 6.3: Second run of main experiment: control and VL-infected plants under sufficient and deficient sulfur supply at 7 dpi. A1-A4: control +S at TPI I-IV; B1-B4: VL-infected +S at TPI I-IV; C1-C4: control -S at TPI I-IV; D1-D4: VL-infected -S at TPI I-IV; red scale bar 5 cm.**

### **Second run: cross sections of hypocotyls of control plants**

Toluidine blue stained cross sections of hypocotyls of control plants under sufficient and deficient sulfur supply were occlusions-free (**Fig. 6.4**). They occasionally showed occlusions in the peripheral area.

## Appendix

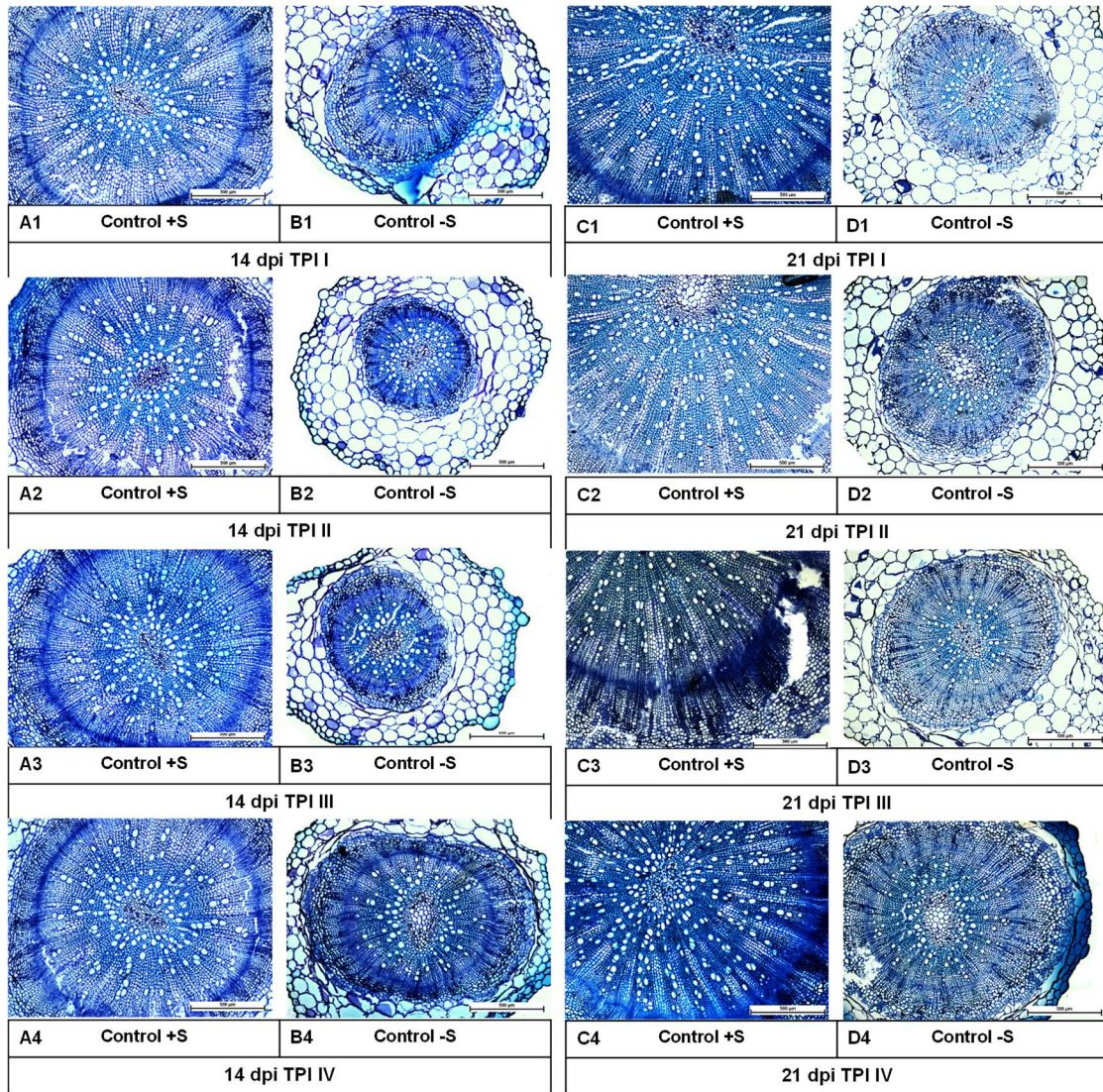


**Figure 6.4: Second run of main experiment: cross sections of hypocotyls of control plants at 14 and 21 dpi.** Cross-sections were stained with toluidine blue; **14 dpi: A1-A4:** control +S at TPI I-IV; **B1-B4:** control -S at TPI I-IV; **21 dpi: C1-C4:** control +S at TPI I-IV; **D1-D4:** control -S at TPI I-IV; scale bar 500  $\mu\text{m}$ .

### Second run: statistical data of the occurrence of occlusions

**Table 6.25: Second run: statistical analysis of occlusions in the xylem compared with different effects.** Df: degrees of freedom in the source; Resid.: Residues; Dev: Deviance; F value: F ratio of two mean square value; P value: level of marginal significance within a statistical hypothesis test representing the probability of the occurrence of a given event.

Effect	Df	Deviance Resid.	Df	Resid. Dev	F value	P value
dpi	1	989.10	14	1294.00	25.21	0.00052
TPI	3	527.00	11	767.00	4.48	0.03074
+/- sulfur supply	1	364.93	10	402.07	9.30	0.01226

## Appendix

### Second run: statistical data of sulfur, calcium, potassium and iron

**Table 6.26: Second run: statistical analysis of sulfur compared with different effects.** Df: degrees of freedom in the source; Sum seq: sum of squares due to the source; Mean seq: mean squares; F value: F ratio of two mean square value; P value: level of marginal significance within a statistical hypothesis test representing the probability of the occurrence of a given event.

Effect	Df	Sum Sq	Mean Sq	F value	P value
dpi	1	39.62	39.62	103.69	0.00133
control.VL-infected	1	0.001	0.001	0.002	0.96
TPI	3	2.95	0.98	2.57	0.10
+/- sulfur supply	1	287.99	287.98	753.82	0.00002
dpi:control.VL-infected	1	0.17	0.17	0.44	0.52
dpi:TPI	3	1.09	0.37	0.96	0.44
dpi:+/- sulfur supply	1	3.79	3.79	9.92	0.00767
control.VL-infected:TPI	3	0.01	0.005	0.01	0.99
control.VL-infected:+/- sulfur supply	1	2.07	2.07	5.41	0.03689
TPI:+/- sulfur supply	3	1.74	0.58	1.51	0.256

**Table 6.27: Second run: statistical analysis of calcium compared with different effects.** Df: degrees of freedom in the source; Sum seq: sum of squares due to the source; Mean seq: mean squares; F value: F ratio of two mean square value; P value: level of marginal significance within a statistical hypothesis test representing the probability of the occurrence of a given event: significant codes: extremely significant.

Effect	Df	Sum Sq	Mean Sq	F value	P value
dpi	1	0.01	0.01	0.002	0.97
control.VL-infected	1	16.64	16.64	2.42	0.14
TPI	3	71.19	23.73	3.44	0.04869
+/- sulfur supply	1	2.34	2.34	0.34	0.57
dpi:control.VL-infected	1	0.09	0.09	0.01	0.91
dpi:TPI	3	10.27	3.42	0.49	0.69
dpi:+/- sulfur supply	1	7.95	7.95	1.15	0.30
control.VL-infected:TPI	3	26.84	8.95	1.29	0.31
control.VL-infected:+/- sulfur supply	1	0.28	0.28	0.04	0.84
TPI:+/- sulfur supply	3	6.49	2.16	0.31	0.81

**Table 6.28: Second run: statistical analysis of potassium compared with different effects.** Df: degrees of freedom in the source; Sum seq: sum of squares due to the source; Mean seq: mean squares; F value: F ratio of two mean square value; P value: level of marginal significance within a statistical hypothesis test representing the probability of the occurrence of a given event: significant codes: extremely significant.

Effect	Df	Sum Sq	Mean Sq	F value	P value
dpi	1	1657.59	1657.59	12.75	0.00341
control.VL-infected	1	272.30	272.30	2.09	0.17
TPI	3	26.83	8.94	0.07	0.98
+/- sulfur supply	1	89.32	89.32	0.69	0.42
dpi:control.VL-infected	1	25.73	25.73	0.19	0.66
dpi:TPI	3	117.44	39.15	0.30	0.82
dpi:+/- sulfur supply	1	623.16	623.16	4.79	0.04739
control.VL-infected:TPI	3	167.11	55.70	0.43	0.74
control.VL-infected:+/- sulfur supply	1	21.76	21.76	0.17	0.69
TPI:+/- sulfur supply	3	103.10	34.37	0.26	0.85

## Appendix

**Table 6.29: Second run: statistical analysis of iron compared with different effects.** Df: degrees of freedom in the source; Sum seq: sum of squares due to the source; Mean seq: mean squares; F value: F ratio of two mean square value; P value: level of marginal significance within a statistical hypothesis test representing the probability of the occurrence of a given event: significant codes: extremely significant.

Effect	Df	Sum Sq	Mean Sq	F value	P value
dpi	1	8286.8	8286.8	69.34	0.00356
control.VL-infected	1	508.4	508.4	4.25	0.06
TPI	3	1548.1	516.0	4.32	0.03
+/- sulfur supply	1	2.9	2.9	0.02	0.88
dpi:control.VL-infected	1	1300.6	1300.6	10.88	0.00575
dpi:TPI	3	279.0	93.0	0.7783	0.53
dpi:+/- sulfur supply	1	805.8	805.8	6.74	0.02215
control.VL-infected:TPI	3	174.7	58.2	0.49	0.69
control.VL-infected:+/- sulfur supply	1	192.8	192.8	1.61	0.23
TPI:+/- sulfur supply	3	211.8	70.6	0.59	0.63

### Second run: standard deviation and statistical data of glucosinolates

Depend on limited plant material three extracts each sample were prepared for the GSL analysis for approximately half of the samples. **Table 6.30** (IGSLs), **Table 6.35** (AGSLs) and **Table 6.42** (BGSL) show the calculated standard derivations with the corresponding GSL value based on the dependent technical replicates.

**Table 6.30: Second run: values of IGSL content  $\pm$  SD at 14 dpi.** Data were calculated in nmol g<sup>-1</sup> DW and based on three dependent technical replicates.

IGSLs	Control +S	VL-infected +S	Control -S	VL-infected -S
<b>Glucobrassicin</b>				
TPI I	92.52 $\pm$ 4.30	158.54 $\pm$ 7.70	-	-
TPI II	-	-	0.06 $\pm$ 0.02	2.75 $\pm$ 0.78
TPI III	97.09 $\pm$ 9.92	-	-	-
TPI IV	-	139.87 $\pm$ 3.86	-	12.31 $\pm$ 0.84
<b>Neoglucobrassicin</b>				
TPI I	20.71 $\pm$ 3.58	17.77 $\pm$ 1.30	-	-
TPI II	-	-	2.60 $\pm$ 0.23	6.20 $\pm$ 1.45
TPI III	19.05 $\pm$ 2.78	-	-	-
TPI IV	-	23.62 $\pm$ 1.64	-	8.27 $\pm$ 0.82
<b>4-Hydroxy-glucobrassicin</b>				
TPI I	14.94 $\pm$ 1.42	19.80 $\pm$ 5.84	-	-
TPI II	-	-	0.29 $\pm$ 0.02	0.22 $\pm$ 0.03
TPI III	14.76 $\pm$ 2.87	-	-	-
TPI IV	-	9.16 $\pm$ 4.34	-	0.31 $\pm$ 0.04

**Table 6.31: Second run: statistical analysis of IGSLs compared with different effects.** Df: degrees of freedom in the source; Sum seq: sum of squares due to the source; Mean seq: mean squares; F value: F ratio of two mean square value; P value: level of marginal significance within a statistical hypothesis test representing the probability of the occurrence of a given event: significant codes: extremely significant.

Effect	Df	Sum Sq	Mean Sq	F value	P value
dpi	1	6.89	6.89	588.31	0.00002
control.VL-infected	1	0.47	0.47	40.46	0.01679
TPI	3	0.09	0.03	2.70	0.09
+/- sulfur supply	1	3.99	3.99	340.18	0.00005
dpi:control.VL-infected	1	0.06	0.06	5.47	0.03597
dpi:TPI	3	0.02	0.01	0.56	0.65
dpi:+/- sulfur supply	1	2.65	2.65	226.13	0.00017
control.VL-infected:TPI	3	0.03	0.01	0.85	0.49
control.VL-infected:+/- sulfur supply	1	0.12	0.12	10.23	0.00699
TPI:+/- sulfur supply	3	0.03	0.01	0.70	0.57

## Appendix

**Table 6.32: Second run: statistical analysis of glucobrassicin compared with different effects.** Df: degrees of freedom in the source; Sum seq: sum of squares due to the source; Mean seq: mean squares; F value: F ratio of two mean square value; P value: level of marginal significance within a statistical hypothesis test representing the probability of the occurrence of a given event: significant codes: extremely significant.

Effect	Df	Sum Sq	Mean Sq	F value	P value
dpi	1	12.99	12.99	153.62	0.00048
control.VL-infected	1	1.88	1.88	22.27	0.00040
TPI	3	0.40	0.13	1.57	0.24
+/- sulfur supply	1	8.21	8.21	97.07	0.00195
dpi:control.VL-infected	1	0.76	0.76	9.02	0.01018
dpi:TPI	3	0.19	0.06	0.76	0.54
dpi:+/- sulfur supply	1	6.14	6.14	72.66	0.00275
control.VL-infected:TPI	3	0.06	0.02	0.22	0.88
control.VL-infected:+/- sulfur supply	1	0.86	0.86	10.22	0.00701
TPI:+/- sulfur supply	3	0.25	0.08	0.98	0.43

**Table 6.33: Second run: statistical analysis of neoglucobrassicin compared with different effects.** Df: degrees of freedom in the source; Sum seq: sum of squares due to the source; Mean seq: mean squares; F value: F ratio of two mean square value; P value: level of marginal significance within a statistical hypothesis test representing the probability of the occurrence of a given event: significant codes: extremely significant.

Effect	Df	Sum Sq	Mean Sq	F value	P value
dpi	1	2.09	2.09	277.65	0.00017
control.VL-infected	1	0.05	0.05	7.20	0.01879
TPI	3	0.07	0.02	3.17	0.06
+/- sulfur supply	1	0.97	0.97	128.41	0.00139
dpi:control.VL-infected	1	0.02	0.02	2.07	0.17
dpi:TPI	3	0.03	0.01	1.35	0.30
dpi:+/- sulfur supply	1	0.62	0.62	82.59	0.00492
control.VL-infected:TPI	3	0.03	0.01	1.16	0.36
control.VL-infected:+/- sulfur supply	1	0.08	0.08	10.85	0.00581
TPI:+/- sulfur supply	3	0.002	0.001	0.10	0.96

**Table 6.34: Second run: statistical analysis of 4-hydroxyglucobrassicin compared with different effects.** Df: degrees of freedom in the source; Sum seq: sum of squares due to the source; Mean seq: mean squares; F value: F ratio of two mean square value; P value: level of marginal significance within a statistical hypothesis test representing the probability of the occurrence of a given event.

Effect	Df	Sum Sq	Mean Sq	F value	P value
dpi	1	3.003	3.003	25.52	0.00022
control.VL-infected	1	0.24	0.24	2.06	0.18
TPI	3	0.18	0.06	0.52	0.68
+/- sulfur supply	1	8.81	8.81	74.80	0.00859
dpi:control.VL-infected	1	0.01	0.01	0.04	0.84
dpi:TPI	3	0.06	0.02	0.18	0.91
dpi:+/- sulfur supply	1	2.72	2.72	23.12	0.00034
control.VL-infected:TPI	3	0.30	0.10	0.84	0.50
control.VL-infected:+/- sulfur supply	1	0.21	0.21	1.77	0.21
TPI:+/- sulfur supply	3	0.05	0.02	0.14	0.93

## Appendix

**Table 6.35: Second run: values of AGSL content  $\pm$  SD at 14 dpi.** Data were calculated in nmol g<sup>-1</sup> DW and based on three dependent technical replicates.

AGSLs	Control +S	VL-infected +S	Control -S	VL-infected -S
<b>Progointrin</b>				
TPI I	58.06 $\pm$ 1.60	104.17 $\pm$ 9.41	-	-
TPI II	-	-	1.43 $\pm$ 0.42	0.90 $\pm$ 0.25
TPI III	105.96 $\pm$ 12.33	-	-	-
TPI IV	-	107.59 $\pm$ 8.89	-	1.04 $\pm$ 0.05
<b>Glucoalyssin</b>				
TPI I	54.31 $\pm$ 1.73	95.48 $\pm$ 11.29	-	-
TPI II	-	-	6.51 $\pm$ 0.66	2.98 $\pm$ 0.33
TPI III	91.62 $\pm$ 10.66	-	-	-
TPI IV	-	87.88 $\pm$ 11.79	-	3.28 $\pm$ 0.34
<b>Glucoraphanin</b>				
TPI I	9.93 $\pm$ 0.34	14.83 $\pm$ 1.61	-	-
TPI II	-	-	2.91 $\pm$ 0.70	3.54 $\pm$ 0.19
TPI III	11.81 $\pm$ 2.10	-	-	-
TPI IV	-	8.52 $\pm$ 2.38	-	7.54 $\pm$ 1.14
<b>Glucobrassicinapin</b>				
TPI I	27.13 $\pm$ 1.30	43.00 $\pm$ 3.90	-	-
TPI II	-	-	0.30 $\pm$ 0.03	0.32 $\pm$ 0.27
TPI III	56.59 $\pm$ 6.94	-	-	-
TPI IV	-	62.48 $\pm$ 3.26	-	0.33 $\pm$ 0.13
<b>Gluconapin</b>				
TPI I	22.13 $\pm$ 0.93	38.01 $\pm$ 2.25	-	-
TPI II	-	-	1.60 $\pm$ 0.38	0.34 $\pm$ 0.09
TPI III	55.56 $\pm$ 7.99	-	-	-
TPI IV	-	29.43 $\pm$ 2.94	-	0.37 $\pm$ 0.09

**Table 6.36: Second run: statistical analysis of AGSLs compared with different effects.** Df: degrees of freedom in the source; Sum seq: sum of squares due to the source; Mean seq: mean squares; F value: F ratio of two mean square value; P value: level of marginal significance within a statistical hypothesis test representing the probability of the occurrence of a given event.

Effect	Df	Sum Sq	Mean Sq	F value	P value
dpi	1	3.76	3.76	200.21	0.00035
control.VL-infected	1	0.14	0.14	7.31	0.01806
TPI	3	0.10	0.03	1.79	0.20
+/- sulfur supply	1	5.97	5.97	318.11	0.00007
dpi:control.VL-infected	1	0.10	0.10	5.35	0.03777
dpi:TPI	3	0.09	0.03	1.53	0.25
dpi:+/- sulfur supply	1	2.94	2.94	156.73	0.00042
control.VL-infected:TPI	3	0.09	0.03	1.54	0.25
control.VL-infected:+/- sulfur supply	1	0.02	0.02	1.15	0.30
TPI:+/- sulfur supply	3	0.03	0.01	0.44	0.73

**Table 6.37: Second run: statistical analysis of progointrin compared with different effects.** Df: degrees of freedom in the source; Sum seq: sum of squares due to the source; Mean seq: mean squares; F value: F ratio of two mean square value; P value: level of marginal significance within a statistical hypothesis test representing the probability of the occurrence of a given event.

Effect	Df	Sum Sq	Mean Sq	F value	P value
dpi	1	9.75	9.75	732.61	0.00002
control.VL-infected	1	0.19	0.19	13.95	0.00249
TPI	3	0.12	0.04	2.93	0.07
+/- sulfur supply	1	9.71	9.71	729.69	0.00002
dpi:control.VL-infected	1	0.07	0.07	4.97	0.04
dpi:TPI	3	0.04	0.01	1.11	0.38
dpi:+/- sulfur supply	1	7.08	7.08	532.13	0.00004
control.VL-infected:TPI	3	0.11	0.04	2.68	0.09
control.VL-infected:+/- sulfur supply	1	0.02	0.02	1.14	0.31
TPI:+/- sulfur supply	3	0.05	0.02	1.33	0.31

## Appendix

**Table 6.38: Second run: statistical analysis of glucoalyssin compared with different effects.** Df: degrees of freedom in the source; Sum seq: sum of squares due to the source; Mean seq: mean squares; F value: F ratio of two mean square value; P value: level of marginal significance within a statistical hypothesis test representing the probability of the occurrence of a given event: significant codes.

Effect	Df	Sum Sq	Mean Sq	F value	P value
dpi	1	3.0012	3.001	70.38	0.00327
control.VL-infected	1	0.02	0.04	0.83	0.38
TPI	3	0.19	0.06	1.50	0.26
+/- sulfur supply	1	6.21	6.21	145.54	0.00066
dpi:control.VL-infected	1	0.39	0.39	9.16	0.00973
dpi:TPI	3	0.16	0.05	1.24	0.33
dpi:+/- sulfur supply	1	2.52	2.52	59.07	0.00856
control.VL-infected:TPI	3	0.07	0.02	0.54	0.66
control.VL-infected:+/- sulfur supply	1	0.13	0.13	3.02	0.11
TPI:+/- sulfur supply	3	0.05	0.02	0.40	0.76

**Table 6.39: Second run: statistical analysis of glucoraphanin compared with different effects.** Df: degrees of freedom in the source; Sum seq: sum of squares due to the source; Mean seq: mean squares; F value: F ratio of two mean square value; P value: level of marginal significance within a statistical hypothesis test representing the probability of the occurrence of a given event: significant codes.

Effect	Df	Sum Sq	Mean Sq	F value	P value
dpi	1	0.004	0.004	0.04	0.84
control.VL-infected	1	0.42	0.42	4.20	0.06
TPI	3	0.44	0.15	1.45	0.27
+/- sulfur supply	1	2.21	2.21	22.01	0.00042
dpi:control.VL-infected	1	0.04	0.04	0.37	0.56
dpi:TPI	3	0.15	0.05	0.49	0.70
dpi:+/- sulfur supply	1	0.01	0.010	0.10	0.756
control.VL-infected:TPI	3	0.21	0.07	0.70	0.57
control.VL-infected:+/- sulfur supply	1	0.002	0.002	0.02	0.88
TPI:+/- sulfur supply	3	0.02	0.01	0.05	0.98

**Table 6.40: Second run: statistical analysis of glucobrassicinapin compared with different effects.** Df: degrees of freedom in the source; Sum seq: sum of squares due to the source; Mean seq: mean squares; F value: F ratio of two mean square value; P value: level of marginal significance within a statistical hypothesis test representing the probability of the occurrence of a given event.

Effect	Df	Sum Sq	Mean Sq	F value	P value
dpi	1	5.53	5.53	254.59	0.00029
control.VL-infected	1	0.04	0.04	1.72	0.21
TPI	3	0.04	0.01	0.59	0.632
+/- sulfur supply	1	10.95	10.95	504.08	0.00005
dpi:control.VL-infected	1	0.04	0.04	1.85	0.20
dpi:TPI	3	0.04	0.02	0.67	0.58
dpi:+/- sulfur supply	1	7.14	7.14	328.75	0.00006
control.VL-infected:TPI	3	0.16	0.05	2.4419	0.11
control.VL-infected:+/- sulfur supply	1	0.06	0.06	2.89	0.11
TPI:+/- sulfur supply	3	0.15	0.05	2.25	0.13

## Appendix

**Table 6.41: Second run: statistical analysis of gluconapin compared with different effects.** Df: degrees of freedom in the source; Sum seq: sum of squares due to the source; Mean seq: mean squares; F value: F ratio of two mean square value; P value: level of marginal significance within a statistical hypothesis test representing the probability of the occurrence of a given event.

Effect	Df	Sum Sq	Mean Sq	F value	P value
dpi	1	3.57	3.57	138.97	0.00087
control.VL-infected	1	0.05	0.05	1.80	0.20
TPI	3	0.12	0.04	1.56	0.25
+/- sulfur supply	1	8.80	8.80	342.72	0.00005
dpi:control.VL-infected	1	0.60	0.60	23.405	0.00032
dpi:TPI	3	0.16	0.05	2.08	0.16
dpi:+/- sulfur supply	1	2.46	2.46	95.789	0.00210
control.VL-infected:TPI	3	0.26	0.086	3.33	0.053
control.VL-infected:+/- sulfur supply	1	0.39	0.39	15.06	0.00189
TPI:+/- sulfur supply	3	0.07	0.02	0.89	0.47

**Table 6.42: Second run: values of BGSL content  $\pm$  SD at 14 dpi.** Data were calculated in nmol g<sup>-1</sup> DW and based on three dependent technical replicates.

BGSL	Control +S	VL-infected +S	Control -S	VL-infected -S
<b>Gluconasturtiin</b>				
TPI I	52.05 $\pm$ 1.43	125.92 $\pm$ 8.14	-	-
TPI II	-	-	5.69 $\pm$ 0.09	35.56 $\pm$ 6.55
TPI III	51.71 $\pm$ 4.09	-	-	-
TPI IV	-	109.09 $\pm$ 2.78	-	45.62 $\pm$ 1.56

**Table 6.43: Second run: statistical analysis of the BGSL gluconasturtiin compared with different effects.** Df: degrees of freedom in the source; Sum seq: sum of squares due to the source; Mean seq: mean squares; F value: F ratio of two mean square value; P value: level of marginal significance within a statistical hypothesis test representing the probability of the occurrence of a given event.

Effect	Df	Sum Sq	Mean Sq	F value	P value
dpi	1	2.42	2.42	157.69	0.00041
control.VL-infected	1	1.69	1.69	110.65	0.00334
TPI	3	0.08	0.03	1.715	0.21
+/- sulfur supply	1	0.73	0.73	47.34	0.00753
dpi:control.VL-infected	1	0.07	0.07	4.36	0.06
dpi:TPI	3	0.04	0.01	0.77	0.53
dpi:+/- sulfur supply	1	0.71	0.71	46.55	0.00821
control.VL-infected:TPI	3	0.03	0.01	0.76	0.534
control.VL-infected:+/- sulfur supply	1	0.04	0.04	2.59	0.13
TPI:+/- sulfur supply	3	0.002	0.00085	0.06	0.98

**Table 6.44: Second run: statistical analysis of cysteine compared with different effects.** Df: degrees of freedom in the source; Sum seq: sum of squares due to the source; Mean seq: mean squares; F value: F ratio of two mean square value; P value: level of marginal significance within a statistical hypothesis test representing the probability of the occurrence of a given event.

Effect	Df	Sum Sq	Mean Sq	F value	P value
dpi	1	1.09	1.09	58.56	0.00898
control.VL-infected	1	0.03	0.04	1.96	0.19
TPI	3	0.01	0.003	0.20	0.89
+/- sulfur supply	1	2.97	2.97	159.13	0.00038
dpi:control.VL-infected	1	0.01	0.01	0.35	0.56
dpi:TPI	3	0.02	0.01	0.35	0.79
dpi:+/- sulfur supply	1	0.61	0.61	32.68	0.04776
control.VL-infected:TPI	3	0.02	0.01	0.35	0.78
control.VL-infected:+/- sulfur supply	1	0.01	0.01	0.49	0.49
TPI:+/- sulfur supply	3	0.02	0.01	0.31	0.82



## Appendix

**Table 6.45: Second run: statistical analysis of glutathione compared with different effects.** Df: degrees of freedom in the source; Sum seq: sum of squares due to the source; Mean seq: mean squares; F value: F ratio of two mean square value; P value: level of marginal significance within a statistical hypothesis test representing the probability of the occurrence of a given event.

<b>Effect</b>	<b>Df</b>	<b>Sum Sq</b>	<b>Mean Sq</b>	<b>F value</b>	<b>P value</b>
<b>dpi</b>	1	0.60	0.60	133.97	0.00108
<b>control.VL-infected</b>	1	0.06	0.06	14.26	0.00230
<b>TPI</b>	3	0.01	0.002	0.53	0.66
<b>+/- sulfur supply</b>	1	2.67	2.67	593.27	0.00002
<b>dpi:control.VL-infected</b>	1	0.00007	0.00007	0.0158	0.90
<b>dpi:TPI</b>	3	0.01	0.005	1.08	0.39
<b>dpi:+/- sulfur supply</b>	1	1.15	1.15	255.57	0.00028
<b>control.VL-infected:TPI</b>	3	0.01	0.002	0.55	0.65
<b>control.VL-infected:+/- sulfur supply</b>	1	0.05	0.05	11.78	0.00445
<b>TPI:+/- sulfur supply</b>	3	0.03	0.01	2.40	0.11

## Danksagung

Diese Arbeit wurde von vielen wichtigen und lieben Menschen unterstützt und begleitet, bei denen ich mich nachfolgend herzlich bedanken möchte.

Ich möchte mich ganz herzlich bei **Prof. Dr. Jutta Papenbrock** für dieses unendlich spannende Thema und die Chance, daran zu forschen, bedanken. Darüber hinaus für die stetige Unterstützung, wenn es um neue Ideen und Ansätze ging, aber auch bei Problemen. Herzlichen Dank auch dafür, dass es immer Zeit gab, Dinge zu besprechen, egal, ob wissenschaftlicher oder persönlicher Natur und für die stetige Förderung der persönlichen Stärken und Potenziale.

Bei **Prof. Dr. Edgar Maiß** möchte ich mich für die Übernahme des Korreferats bedanken sowie bei **Dr. Sascha Offermann** für die Übernahme des Vorsitzes der Promotionskommission.

**Dr. Annekathrin Rumlow** möchte ich für die tolle Unterstützung bei den ersten Experimenten danken und für die vielen wertvollen Tipps. Bei den Gärtnern **Yvonne Leye** und **Fabian Söffker** bedanke ich mich herzlich für die vielen Säcke gedämpften Sandes und für die Unterstützung bei der Pflanzenanzucht.

Ein großer Dank geht an **Dr. Ina Horst-Nießen**, die sich um die qPCR-Messungen gekümmert hat und zudem das System für den Nachweis von VL in Bn etabliert hat. Herzlichen Dank an **Julia Volker** für die vielen Proben-Extrakte und nachfolgenden Thiol-Messungen. Lieben Dank an **Birgit Lippmann**, die immer einen guten Rat rund um die Laborarbeit hatte.

Herzlichen Dank an **Dr. Frank Schaarschmidt**, der sich um die statistische Auswertung meiner Daten gekümmert hat und mir das Ganze verständlich erläutert hat.

Bei **Johann Hornbacher** möchte ich mich ganz besonders bedanken, nicht nur für die Glucosinolat-Messungen, die labormäßige Unterstützung, das „Aufpassen“ bei meinen Nacht-Experimenten und die vielen inspirierenden wissenschaftlichen Gespräche, sondern vor allem für die Freundschaft, die Unterstützung in allen Lebenslagen und die vielen wunderbaren und kostbaren Augenblicke. Ich hab' Dich lieb!

Vielen Dank an **Olaf Viktorin**, meinem Lieblings-Techniker, der mir einige Male bei den Reparaturen der Klimakammern geholfen hat. Hier auch nochmal Danke an **Dr. Sascha Offermann**, der auch am Wochenende bei Klimakammern-Ausfällen gekommen ist.

Ein riesiger Dank geht an **Dr. Linda Hink**, die für mich einer der wichtigsten Menschen in den letzten Monaten geworden ist. Unendlich liebsten Dank für die ganzen Nachtschichten, das Auseinandersetzen mit meiner Arbeit, die Unterstützung, wenn meine Gedanken hingen und meine Nerven am Ende waren. Liebsten Dank auch für die tollen Abende außerhalb der Uni und Deine Freundschaft - hab' Dich lieb mein Lindalein☺.


Ich möchte mich außerdem bei allen Mitarbeitenden der Arbeitsgruppe, besonders **Maria Del Mar Rosales**, **Elia Klitschkus** und **Dr. Ariel Turcios** und den früheren Mitarbeitenden **Lisa**

## Danksagung

**Rierner, Rebecca Herth, Dr. Yvana Glasenapp, Dr. Christian Boestfleisch** und **Dr. Felix Hirschmann** für eine tolle Arbeitsatmosphäre und die Unterstützung bedanken.

Herzlichen Dank an **Dr. Meike Huntebrinker** und **Dr. Tanja Michler-Cieluch**, die mich im Prozess der Stipendiums-Vergabe der Graduiertenakademie beraten und begleitet haben.

Danke auch an die Doktoranden **Anna-Maria Heise** und **Philipp Bohnhorst** von „oben“ für Schoki und gedanklichen Austausch.

Schließlich möchte ich aus tiefstem Herzen **meinen Eltern** und **meiner Schwester** für die Liebe und Unterstützung danken - ohne Euch, wäre das hier nicht möglich gewesen! PUSS PUSS 

# Lebenslauf

Sofia Isabell Rupp  
geb. 25.12.1981, Bad Segeberg

## Studium

06/2016 - dato

### Promotionsstudentin

Naturwissenschaftliche Fakultät, Leibniz Universität  
Hannover, Institut für Botanik, AG Prof. Dr. Papenbrock

04/2006 - 02/2015

### Biologie-Diplomstudium

Johannes Gutenberg-Universität Mainz

Grundstudium: 8 Vordiplome (schriftlich: Zoologie, Botanik,  
Mikrobiologie, Genetik; mündlich: Zoologie, Mathematik,  
Chemie, Physik)

Schwerpunkte Hauptstudium und Diplom-Prüfungen:  
Zoologie, Botanik, Mikrobiologie

05/2014 - 02/2015

### Diplomarbeit

Naturwissenschaftliche Fakultät, Institut für Botanik, AG Prof.  
Dr. Gudrun Kadereit

**Arbeitstitel:** Vergleichende Anatomie von Kotyledonen und  
adulten Blättern in Chenopodiaceae und Amaranthaceae

## Stipendium

06/2019 - 11/2019

### Vergabe durch die Graduiertenakademie LUH

## Studienbegleitende

### Berufserfahrung

12/2019 – 03/2020

### Wissenschaftliche Hilfskraft

Naturwissenschaftliche Fakultät, Leibniz Universität  
Hannover, Institut für Botanik, AG Prof. Dr. Papenbrock

06/2016 - 05/2019

### Wissenschaftliche Mitarbeiterin

Naturwissenschaftliche Fakultät, Leibniz Universität  
Hannover, Institut für Botanik, AG Prof. Dr. Papenbrock

06/2015 - 05/2016

### Wissenschaftliche Hilfskraft

Naturwissenschaftliche Fakultät, Leibniz Universität  
Hannover, Institut für Botanik, AG Prof. Dr. Papenbrock

07/2015 - 05/2016

### Medizinische Aushilfe

amedes MVZ wagnerstibbe für Laboratoriumsmedizin,  
Hämostaseologie, Humangenetik und Mikrobiologie  
Hannover

10/2014 - 11/2014

### Wissenschaftliche Hilfskraft

Johannes Gutenberg-Universität Mainz,  
Naturwissenschaftliche Fakultät,  
Institut für Mikrobiologie und Weinforschung, AG Prof. Dr.  
Helmut König

## Workshops

02/2019 - 03/2019

### Berufseinstieg mit System: Das bin ich! Das biete ich! Dort will ich hin!

GRANAT Leibniz Universität Hannover

06/2018

### Meine Zukunft Existenzgründung?!

GRANAT Leibniz Universität Hannover

## Lebenslauf

07/2017	<b>Image Processing and Analysis for Scientific Publications</b> GRANAT Leibniz Universität Hannover
11/2016	<b>ThermoFisher Scientific</b> Anwendertreffen ICP-OES, Leibniz Universität Hannover
<b>Praktika</b>	
09/2013 - 10/2013	<b>Mikrobiologisches Projekt</b> Hochschule Geisenheim University, Institut für Mikrobiologie und Biochemie, AG Prof. Dr. Manfred Großmann <b>Arbeitstitel:</b> Vergleich der proteolytischen Enzymaktivitäten in <i>Saccharomyces</i> -Hefen und Nichtsaccharomyceten während und nach alkoholischen Gärungen
<b>Publikation</b>	
2018	Nguyen, X.V., Kletschkus, E., Rupp-Schröder, S.I., El Shaffai, A. and Papenbrock, J. (2018): rDNA analysis of the Red Sea seagrass species <i>Halophila ovalis</i> reveals the vicariant evolutionary diversification, <i>Systematics &amp; Biodiversity</i> , 16: 668–679
<b>Konferenz</b>	
09/2015	<b>Caryophyllales 2015</b> , Freie Universität Berlin, Botanischer Garten und Botanisches Museum Berlin-Dahlem <b>Poster-Präsentation:</b> What's inside? - Four anatomical leaf types in the Amaranthaceae s.s.
<b>Sonstige Erfahrungen</b>	
10/2003 - 03/2006	<b>Magister-Studium</b> (ohne Abschluss), Christian-Albrecht-Universität Kiel Fächer: Neuere Deutsche Literatur- und Medienwissenschaften, Allgemeine Sprachwissenschaften, Öffentliches Recht und Psychologie
09/2005	<b>Truppenbesuch BW</b> , Sanitätskommando I, Department 1.5 Kiel-Kronshagen
<b>Ausbildung &amp; Praktika</b>	
05/2005	<b>Praktikum</b> Groß- und Kleintierklinik Wahlstedt, Dr. med. vet. M. Kuhn, Wiesenweg 2-8, 23812 Wahlstedt
1999 - 2000	<b>Ausbildung zur Tierarzhelferin</b> (Abbruch wegen Arbeitsunfall) Groß- und Kleintierklinik Wahlstedt, Dr. med. vet. Lothar Köhler, Wiesenweg 2-8, 23812 Wahlstedt
1998 - 1999	<b>Jahrespraktikum</b> im Bereich Bürokauffrau für Kommunikation Mem-O-Matic GmbH Elektronische Displaysysteme, Jasminstr. 4, 23795 Bad Segeberg
<b>Schule</b>	
2000 - 2003	<b>Allgemeine Hochschulreife</b> Integrierte Gesamtschule Bad Oldesloe
1992 - 1998	<b>Mittlere Reife</b> Realschule am Seminarweg, Bad Segeberg
1988 - 1992	<b>Primarschule</b> Grund- und Hauptschule Leezen